HYPERTENSION AND CHRONIC KIDNEY INJURY OR FAILURE

EDITED BY: Jennifer Sullivan, Zhengrong Guan, Oleg Palygin and Suttira Intapad
PUBLISHED IN: Frontiers in Physiology and Frontiers in Medicine

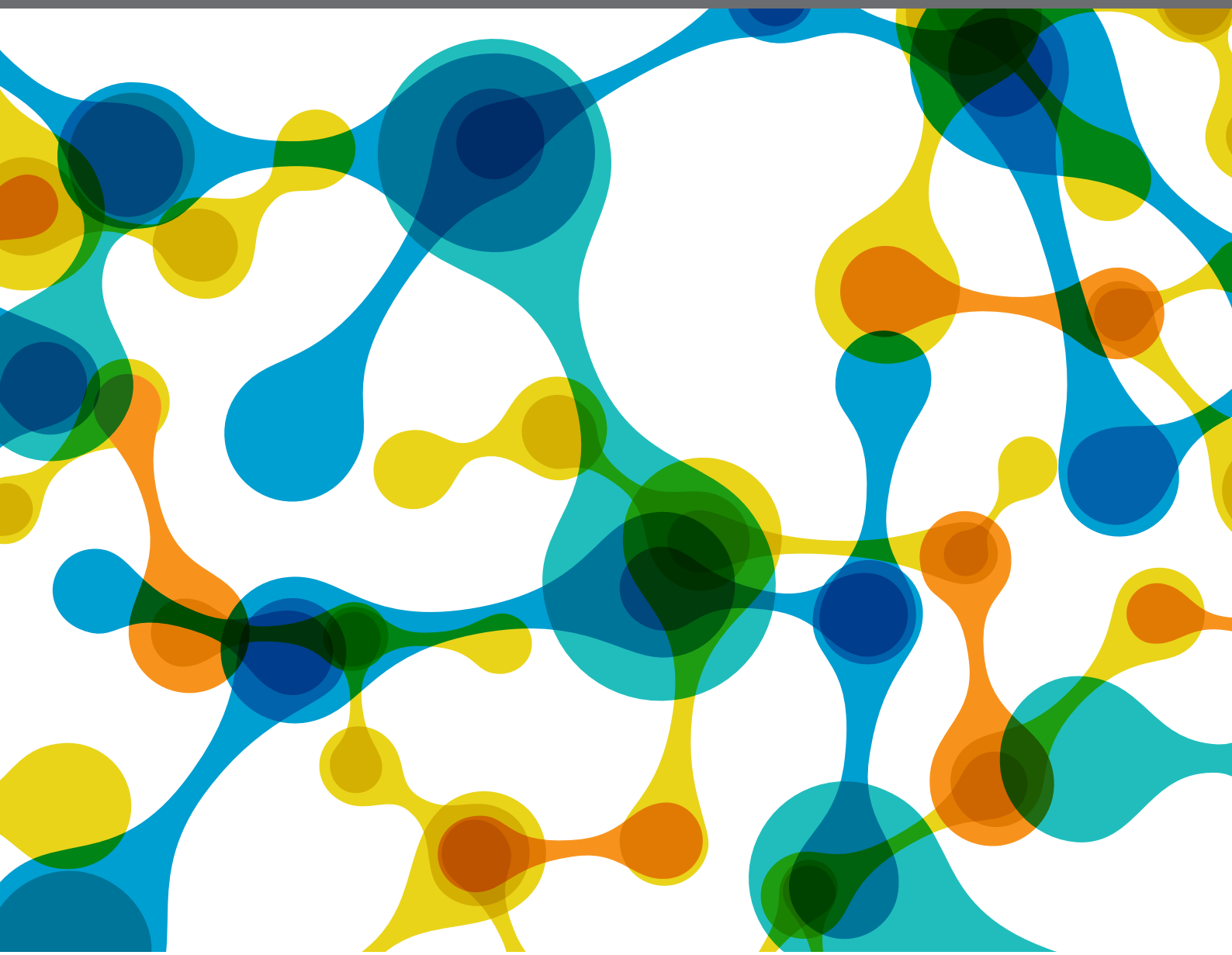

frontiers Research Topics

frontiers

ISSN 1664-8714
ISBN 978-2-88966-728-4
DOI 10.3389/978-2-88966-728-4

About Frontiers

Frontiers is more than just an open-access publisher of scholarly articles: it is a pioneering approach to the world of academia, radically improving the way scholarly research is managed. The grand vision of Frontiers is a world where all people have an equal opportunity to seek, share and generate knowledge. Frontiers provides immediate and permanent online open access to all its publications, but this alone is not enough to realize our grand goals.

Frontiers Journal Series

The Frontiers Journal Series is a multi-tier and interdisciplinary set of open-access, online journals, promising a paradigm shift from the current review, selection and dissemination processes in academic publishing. All Frontiers journals are driven by researchers for researchers; therefore, they constitute a service to the scholarly community. At the same time, the Frontiers Journal Series operates on a revolutionary invention, the tiered publishing system, initially addressing specific communities of scholars, and gradually climbing up to broader public understanding, thus serving the interests of the lay society, too.

Dedication to Quality

Each Frontiers article is a landmark of the highest quality, thanks to genuinely collaborative interactions between authors and review editors, who include some of the world's best academicians. Research must be certified by peers before entering a stream of knowledge that may eventually reach the public - and shape society; therefore, Frontiers only applies the most rigorous and unbiased reviews.
Frontiers revolutionizes research publishing by freely delivering the most outstanding research, evaluated with no bias from both the academic and social point of view. By applying the most advanced information technologies, Frontiers is catapulting scholarly publishing into a new generation.

What are Frontiers Research Topics?

Frontiers Research Topics are very popular trademarks of the Frontiers Journals Series: they are collections of at least ten articles, all centered on a particular subject. With their unique mix of varied contributions from Original Research to Review Articles, Frontiers Research Topics unify the most influential researchers, the latest key findings and historical advances in a hot research area! Find out more on how to host your own Frontiers Research Topic or contribute to one as an author by contacting the Frontiers Editorial Office: frontiersin.org/about/contact

HYPERTENSION AND CHRONIC KIDNEY INJURY OR FAILURE

Topic Editors:
Jennifer Sullivan, Augusta University, United States
Zhengrong Guan, University of Alabama at Birmingham, United States
Oleg Palygin, Medical College of Wisconsin, United States
Suttira Intapad, Tulane University, United States

Citation: Sullivan, J., Guan, Z., Palygin, O., Intapad, S., eds. (2021). Hypertension and Chronic Kidney Injury or Failure. Lausanne: Frontiers Media SA.
doi: 10.3389/978-2-88966-728-4

Table of Contents

frontiers in Physiology

EDITORIAL
published: 11 March 2021
doi: 10.3389/fphys.2021.662737

Editorial: Hypertension and Chronic Kidney Injury or Failure

Oleg Palygin[1]*, *Zhengrong Guan*[2], *Suttira Intapad*[3] and *Jennifer C. Sullivan*[4]

[1] Medical College of Wisconsin, Milwaukee, WI, United States, [2] Division of Nephrology, Department of Medicine, University of Alabama at Birmingham, Birmingham, AL, United States, [3] School of Medicine, Tulane University, New Orleans, LA, United States, [4] Department of Physiology, Medical College of Georgia, Augusta University, Augusta, GA, United States

Keywords: hypertension, renal damage, chronic kidney diseases, therapeutic treatment, clinical studies

Editorial on the Research Topic

Hypertension and Chronic Kidney Injury or Failure

INTRODUCTION

Chronic kidney disease (CKD) negatively impacts long-term health consequences by increasing the risk of cardiovascular pathologies and hastening the progression of kidney failure. As a result, CKD is overall recognized as a significant medical problem, and despite the improvements in renal based therapy to treat high blood pressure, glomerulonephritis, and diabetes, the burden and incidents of CKD are increasing worldwide (Haileamlak, 2018). The underlying disease processes responsible for the multiple pathological changes in the kidney are likely influenced by several different factors including, but not limited to, genetics, the side effects of prescription medication, social and environmental stressors, sex/gender, aging, and the severity of cardiorenal pathologies like hypertension. Thus, it is vital to unravel the mechanisms causing renal injury and subsequently develop more effective and targeted therapeutic interventions to prevent and hopefully delay or even reverse the progressive renal dysfunction. A Research Topic focused on hypertension and chronic kidney injury or failure is thus timely and essential, adding to a growing body of renal research, and providing a foundation for building more effective treatments for cardiorenal abnormalities.

REVIEWS

The Research Topic contains two review articles that addressed hypertension-associated renal dysfunction. The first article provides an important overview on compensatory adaptations to a solitary functioning kidney (SFK), and outlines how these adaptations may contribute to renal damage and hypertension later in life (McArdle et al.). Among the main factors that determine greater risk for developing hypertension and kidney injury in SFK patients are alterations in the renal sympathetic nerves, the renal Renin-Angiotensin System (RAS), and the nitric oxide system. The authors suggest that these systems can potentially be targeted in SFK to reduce the progression of disease. The second review article explores the physiological and pathophysiological conditions manifested primarily by the α2-adrenoceptors activation on renal sodium transporters, vascular tone, and on immune cells in the context of hypertension (Hering et al.). The activation of adrenoceptors promotes interaction between the non-adrenergic cells in the kidney and immune system, critically modulating vascular tone and sodium balance. Further investigation is needed to clarify the pathophysiological role of α2-adrenoceptors in the complex mechanism of renal

OPEN ACCESS

Edited by:
Carolyn Mary Ecelbarger, Georgetown University, United States

Reviewed by:
Fan Fan, University of Mississippi Medical Center, United States

***Correspondence:**
Oleg Palygin
opalygin@mcw.edu

Specialty section:
This article was submitted to Renal and Epithelial Physiology, a section of the journal Frontiers in Physiology

Received: *01 February 2021*
Accepted: *22 February 2021*
Published: *11 March 2021*

Citation:
Palygin O, Guan Z, Intapad S and Sullivan JC (2021) Editorial: Hypertension and Chronic Kidney Injury or Failure. Front. Physiol. 12:662737. doi: 10.3389/fphys.2021.662737

sympathetic nerve activity in hypertension. Together, these reviews provide valuable insights on the mechanisms responsible for the blood pressure regulation and the progression of CKD.

PHARMACOLOGICAL MANAGEMENT OF CHRONIC KIDNEY DISEASE

New strategies for an effective intervention to prevent or slow progressive kidney disease have the potential impact in clinical practice. A trio of original research studies utilized well-established rat models to evaluate new treatments to slow dyslipidemia- or hypertension-induced renal injury. The effects of gemfibrozil treatment, a lipid-regulating medication also known as fibrates, was examined on the progression of renal injury in the obese Dahl salt-sensitive (SS) leptin receptor mutant (SS^{LepR}mutant) rat (Shields et al.). Both male and female rats develop dyslipidemia, progressive proteinuria, and glomerular injury. Treatment with gemfibrozil significantly reduced glomerular pathology and lipid accumulation, and improved renal function, indicating that reductions in cholesterol and triglyceride levels in the bloodstream may successfully inhibit the development of obesity-induced hypertension and renal damage. Next, the therapeutic potential for the novel selective phosphodiesterase 1 inhibitor (PDE_1) BTTQ was tested in spontaneously hypertensive and Dahl SS rats (Dey et al.). PDE_1 inhibition induced vasodilation that was accompanied by a significant reduction of blood pressure in both experimental models. The vasodilatory properties and reduction of peripheral vascular resistance proposed to underlie the benefits of PDE_1 inhibitors could be effective for the treatment of arterial hypertension and CKD. Another article assessed alterations in glomerular density and renal fibrosis following the use of ivabradine, hyperpolarization-activated cyclic nucleotide-gated channel blocker, in experimental rat models of hypertension (Stanko et al.). Ivabradine attenuated kidney alterations induced by L-NAME treatment in hypertensive Wistar rats. Overall, these studies provide new knowledge regarding the therapeutic applications which may be used in the treatment of hypertension and CKD.

EARLY LIFE STRESS AND INTRARENAL RAS IMBALANCE

An original research article by Dalmasso et al. described the impact of maternal separation (MatSep), a chronic behavioral model that mimics the effects of early life stress, on the intrarenal RAS. The study suggests that male Wistar Kyoto rats exposed to MatSep display permanent changes in the renal microvascular architecture in response to intrarenal RAS imbalance. The authors conclude that chronic behavioral stress during childhood may promote changes in renal hemodynamics and will be critical determinant for the hormonal regulation of fluid and electrolyte balance and promote the development of renal diseases in adulthood.

CLINICAL STUDIES

This Research Topic includes a clinical report focused on the use of a combination of unenhanced computed tomography (CT) and texture analysis (CTTA) for the assessment of differential renal function without radioisotope renography in patients with chronic unilateral obstructive upper urinary tract stones (Li et al.). The findings of this study revealed the advantages of the utilization of CTTA as a non-invasive method to identify and characterize renal parenchymal volume for the estimation of renal function. Overall, this method may help urologists determine optimal treatment strategies using unenhanced CT. The impact of the gut microbiome (GM) on hypertensive patients was the focus of another clinical report (Nagase et al.). Using cross-sectional data of the Shika population-based study (Karashima et al., 2018), authors found a correlation between specific gut bacteria composition and the prevalence of hypertension. Moreover, changing dietary habits to low salt in individuals with a particular GM was ineffective in preventing hypertension. Authors conclude that the treatment for gut dysbiosis and restoration of GM homeostasis might be essential to precede the rise in blood pressure and the development of hypertension.

CONCLUSION

The Research Topic Hypertension and Chronic Kidney Injury or Failure highlight recent studies and summarize new insights on the mechanisms contributing to kidney injury progression. This collection of 8 articles includes basic and clinical research demonstrating the importance of understanding physiological function, the use of recently developed therapeutic agents, and implementing novel clinical approaches for the treatment of hypertension and chronic kidney diseases.

AUTHOR CONTRIBUTIONS

OP conceived the content and drafted the manuscript. JS, ZG, and SI revised and approved the final manuscript. All authors contributed to the article and approved the submitted version.

FUNDING

This work was supported by the NIH NIDDK DK126720 (OP), DK106500 (ZG), and NIGMS 5P20GM109036 (SI).

REFERENCES

Haileamlak, A. (2018). Chronic kidney disease is on the rise. *Ethiop. J. Health Sci.* 28, 681–682. doi: 10.4314/ejhs.v28i6.1

Karashima, S., Kometani, M., Tsujiguchi, H., Asakura, H., Nakano, S., Usukura, M., et al. (2018). Prevalence of primary aldosteronism without hypertension in the general population: results in Shika study. *Clin. Exp. Hypertens* 40, 118–125. doi: 10.1080/10641963.2017.1339072

Conflict of Interest: The authors declare that the research was conducted in the absence of any commercial or financial relationships that could be construed as a potential conflict of interest.

frontiers in Physiology

REVIEW
published: 26 June 2020
doi: 10.3389/fphys.2020.00725

Physiology and Pathophysiology of Compensatory Adaptations of a Solitary Functioning Kidney

Zoe McArdle[1], Michiel F. Schreuder[2], Karen M. Moritz[3], Kate M. Denton[1] and Reetu R. Singh[1]*

[1] Cardiovascular Program, Monash Biomedicine Discovery Institute and Department of Physiology, Monash University, Melbourne, VIC, Australia, [2] Department of Pediatric Nephrology, Amalia Children's Hospital, Radboud University Medical Center, Nijmegen, Netherlands, [3] Child Health Research Centre and School of Biomedical Sciences, University of Queensland, Brisbane, QLD, Australia

Children born with a solitary functioning kidney (SFK) have an increased risk of hypertension and kidney disease from early in adulthood. In response to a reduction in kidney mass, the remaining kidney undergoes compensatory kidney growth. This is associated with both an increase in size of the kidney tubules and the glomeruli and an increase in single nephron glomerular filtration rate (SNGFR). The compensatory hypertrophy and increase in filtration at the level of the individual nephron results in normalization of total glomerular filtration rate (GFR). However, over time these same compensatory mechanisms may contribute to kidney injury and hypertension. Indeed, approximately 50% of children born with a SFK develop hypertension by the age of 18 and 20–40% require dialysis by the age of 30. The mechanisms that result in kidney injury are only partly understood, and early biomarkers that distinguish those at an elevated risk of kidney injury are needed. This review will outline the compensatory adaptations to a SFK, and outline how these adaptations may contribute to kidney injury and hypertension later in life. These will be based largely on the mechanisms we have identified from our studies in an ovine model of SFK, that implicate the renal nitric oxide system, the renin angiotensin system and the renal nerves to kidney disease and hypertension associated with SFK. This discussion will also evaluate current, and speculate on next generation, prognostic factors that may predict those children at a higher risk of future kidney disease and hypertension.

Keywords: solitary functioning kidney, compensatory hypertrophy, glomerular hyperfiltration, renal sympathetic nerves, renin angiotensin system, nitric oxide

OPEN ACCESS

Edited by:
Oleg Palygin, Medical College of Wisconsin, United States

Reviewed by:
Tengis Pavlov, Henry Ford Health System, United States
Matthew Aaron Sparks, Duke University, United States
Blythe D. Shepard, Georgetown University Medical Center, United States

****Correspondence:***
Kate M. Denton
Kate.Denton@monash.edu

Specialty section:
This article was submitted to Renal and Epithelial Physiology, a section of the journal Frontiers in Physiology

Received: *29 April 2020*
Accepted: *03 June 2020*
Published: *26 June 2020*

Citation:
McArdle Z, Schreuder MF, Moritz KM, Denton KM and Singh RR (2020) Physiology and Pathophysiology of Compensatory Adaptations of a Solitary Functioning Kidney. Front. Physiol. 11:725. doi: 10.3389/fphys.2020.00725

INTRODUCTION

Congenital anomalies of the kidney and urinary tract (CAKUT) represent the primary cause of chronic kidney disease (CKD) in the pediatric population, accounting for approximately 50% of cases (Becherucci et al., 2016). A solitary functioning kidney (SFK) is a common abnormality in the spectrum of CAKUT and is characterized by a reduction in kidney mass and nephron number. For children born with a SFK, or who undergo unilateral nephrectomy early in life, the risk of hypertension, kidney injury and CKD is increased from early in life. As such, approximately 50% of children born with a SFK develop hypertension as early as the age of 18 years and 20–40% require dialysis by the age of 30 years (Sanna-Cherchi et al., 2009; Westland et al., 2013a). In contrast, in long-term studies it has been demonstrated that kidney function is well preserved

following donation of a kidney in adulthood (Kasiske et al., 1995; Fehrman-Ekholm et al., 2001; Ibrahim et al., 2009). However, recent studies have reported that kidney donation can result in a small increase in the risk of kidney failure compared with healthy non-donors (Muzaale et al., 2014). Additionally, an increase in risk of kidney disease after donation is also observed in kidneys donors with pre-existing conditions such as obesity (Niemi and Mandelbrot, 2014). The mechanisms that underlie the differences in prognosis for loss of a kidney early in life compared with adulthood are not well understood but may be associated with differences in compensatory adaptations to loss of kidney mass. Following a reduction in kidney mass, the remaining kidney undergoes adaptive compensatory hypertrophy, of both the tubules and the glomeruli, and compensatory glomerular hyperfiltration to maintain kidney function. However, the mechanisms that facilitate these compensatory adaptations following a reduction in kidney mass may in the long-term contribute to the onset of hypertension and kidney injury. Although common prognostic indicators of kidney injury [hypertension, proteinuria, estimated GFR (eGFR) $<$ 60 ml/min/1.73 m^2] have been observed in children born with an SFK from as early as 10 years of age, early markers at time of diagnosis of SFK, that distinguish those at an elevated risk of kidney injury are needed (Schreuder et al., 2008; Westland et al., 2011, 2013a).

PREVALENCE OF A SFK

Unilateral renal agenesis (URA) and multicystic dysplastic kidney (MCDK) are the two main abnormalities in the spectrum of CAKUT that result in a SFK (Schreuder et al., 2009; Westland et al., 2013b). There is a higher incidence of CAKUT in males compared with females (Kummer et al., 2012; Tain et al., 2016; Li et al., 2019). In a Taiwanese study, males had a 1.83 greater risk of CAKUT compared with females (Tain et al., 2016). Additionally, males with CAKUT advance to renal replacement therapy earlier than their female counterparts (Wuhl et al., 2013). URA is estimated to occur in 1 in ∼2000 births (Westland et al., 2013b). MCDK is a severe form of renal dysplasia that can result in a non-functioning kidney and has an estimated incidence of 1 in ∼4300 births (Schreuder et al., 2009). Both URA and MCDK are conditions of SFK that are congenital in origin. However, a SFK can also be acquired early in life following unilateral nephrectomy, which can be due to oncological (e.g., Wilm's tumor) or non-oncological causes (e.g., CAKUT such as pelviureteric junction obstruction, posterior urethral valves or vesicoureteral reflux) (Westland et al., 2013a; Mavinkurve-Groothuis et al., 2016).

CLINICAL OUTCOMES

The clinical outcomes of children with a congenital SFK or early-acquired SFK remain contentious. Data on the long-term cardiovascular and renal consequences of a congenital SFK are limited (summarized in **Table 1**) (Argueso et al., 1992; Sanna-Cherchi et al., 2009; Wang et al., 2010; Xu et al., 2019). In a longitudinal study it was observed that of 71 patients with a congenital SFK ∼20–40% had begun dialysis by the age of 30 years (Sanna-Cherchi et al., 2009). In a Chinese study of 48 adults with a congenital SFK, 38.5% had reduced GFR ($<$60 ml/min/1.73 m^2), 35.4% had proteinuria and two individuals had begun dialysis by a mean age of ∼37 years (Wang et al., 2010). Similarly, Xu et al. (2019) found that of 118 patients with URA, 43% had proteinuria and 25% had a reduced GFR ($<$60 ml/min/1.73 m^2) at a median age of 32 years. These studies indicate that there is a progressive loss of kidney function in individuals with a congenital SFK throughout adulthood, and in some individuals results in progression to kidney failure by 30–40 years of age.

The Kidney of MONofunctional Origin (KIMONO) longitudinal study is currently the largest cohort, with over 400 children with both congenital and early-acquired SFK, based in The Netherlands (Schreuder et al., 2008; Westland et al., 2011, 2013a). It was designed to study the prognosis of a SFK of different origins in childhood (Schreuder et al., 2008; Westland et al., 2011, 2013a). The KIMONO cohort comprised of patients with a 'primary' SFK of congenital origin, including both URA and MCDK, and a 'secondary' SFK of early-acquired origin following unilateral nephrectomy due to obstructive or reflux nephropathy (Westland et al., 2011, 2013a). These groups were further subdivided into those with and without ipsilateral CAKUT (in the remnant kidney) (Westland et al., 2011, 2013a). In this study kidney injury was defined as hypertension, proteinuria, reduced eGFR and/or the use of kidney protective medication [e.g., Angiotensin converting enzyme inhibitor (ACEi) or Angiotensin II receptor blockers (ARB)] and kidney length was measured by ultrasound (Westland et al., 2011, 2013a). The KIMONO study showed that approximately one in three children with a SFK had signs of kidney injury at a mean age of 6.4 years (Westland et al., 2013a). Moreover, 26% of children with a SFK developed hypertension as early as 5 years of age, and 19% had proteinuria by 10 years of age (Westland et al., 2013a). In a small portion of children (6%) GFR had begun to decline at a mean age of 6.4 years (Westland et al., 2013a). Kaplan–Meier analysis showed that the median age to develop kidney injury in children with a SFK was ∼15 years (Westland et al., 2013a). Furthermore, children with ipsilateral CAKUT (34% of all children with SFK) had a significantly higher incidence of kidney injury and a younger median age to develop kidney injury (12.8 years) compared with children without ipsilateral CAKUT (Westland et al., 2013a). In the KIMONO cohort a higher proportion of children with a SFK were boys (65%), but no clear influence of gender on the development of kidney injury in SFK was found (Westland et al., 2013a; Westland and Schreuder, 2014).

In other studies the prognosis for children with a congenital SFK is suggested to be more favorable. Indeed, in a recent retrospective study of ∼300 children prenatally diagnosed with a congenital SFK, only 3.9% had signs of kidney injury by a median age of 7 years (Marzuillo et al., 2017). Similarly, La Scola et al. (2016) observed that in a cohort of 146 children with a congenital SFK, only 5% of patients had hypertension at a mean

TABLE 1 | Summary of clinical outcomes in patients with a congenital or early-acquired SFK.

References	Total number of patients	Gender (M/F)	Type of patients included	Age (years)	Kidney injury	Kidney length as a predictor of kidney injury
Sanna-Cherchi et al. (2009)	71	52/19	URA or empty renal fossa upon imaging	Mean age 21 (SD 13.6)	20–40% dialysis	NR
Wang et al. (2010)	65	36/29	48 with URA 17 with severe unilateral kidney dysplasia	Mean age 36.7 (SD 13.1)	38.5% reduced GFR (<60 ml/min/1.73 m^2) 35.4% proteinuria 3% dialysis 36.9% hypertension	Kidney length < 120 mm five-fold greater risk reduced GFR
Xu et al. (2019)	118	62/56	URA	Median age 32	25.4% reduced GFR (<60 ml/min/1.73 m^2) 43% proteinuria 32.2% hypertension	Patients with reduced GFR had a shorter kidney length
Westland et al. (2011, 2013a)	407	265/142	223 congenital SFK (URA or MDCK) 184 early acquired SFK	Mean age 6.4 (SD 5.7) Mean age 9.8 (SD 5.6) Mean age 4.9 (SD 5.4)	6% reduced GFR (<60 ml/min/1.73 m^2) 19% proteinuria 26% hypertension	Patients with a smaller SFK had a greater incidence of kidney injury
Marzuillo et al. (2017, 2019)	306	Not specified	Prenatally diagnosed (URA and MCDK)	Mean age of kidney injury onset 8.2 (SD 5.6)	1.3% reduced GFR (<90 ml/min/1.73 m^2) 3.6% proteinuria 0.6% hypertension	In 162 of the 306 patients - kidney length < 2-SDS in the neonate period had a greater risk of reduced GFR at 15 years of age irrespective of postnatal kidney hypertrophy
La Scola et al. (2016)	146	95/51	URA, aplasia and MCDK	Median age 2.2 Mean age 5.6 ± (4.4 SD) Mean age 12.2 (3.1 SD)	12% reduced GFR (<90 ml/min/1.73 m^2) 4% proteinuria 5% hypertension	Kidney length < 10% expected for a congenital SFK was the strongest predictor of reduced GFR by 10 years of age

NR, not recorded; SD, standard deviation; URA, unilateral renal agenesis; MCDK, multicystic dysplastic kidney; GFR, glomerular filtration rate; eGFR, estimated glomerular filtration rate.

age of 12 years and only 4% presented with proteinuria at a mean age of 6 years. However, a more recent study by La Scola et al. (2020) found that 33% of SFK patients were hypertensive. This was based on ambulatory blood pressure measurement, which did show many cases of masked hypertension, similar to the KIMONO study (Westland et al., 2014; La Scola et al., 2020). The inconsistencies in cardiovascular and renal outcomes observed between studies may therefore reflect differences in study parameters such as inclusion criteria, selection bias, age of follow-up, and methods used to determine blood pressure, GFR and proteinuria. Despite these discrepancies, collectively in these studies it was shown that a congenital SFK does incur a greater predisposition for hypertension and kidney dysfunction later in life. However, there is a need for large long-term follow up studies beyond adolescence in individuals with a congenital SFK, as kidney dysfunction may develop later in life (Kolvek et al., 2014; Schreuder, 2017). It would be highly desirable to determine at diagnosis of SFK, which children have a poor prognosis and for this, accurate and sensitive biomarkers need to be identified.

CONGENITAL SFK VERSUS EARLY ACQUIRED SFK

Although data is limited, there appears to be differences in the renal outcomes associated with the origin of SFK. In the KIMONO cohort those individuals with an early-acquired SFK had a greater incidence of kidney injury compared with those with a congenital SFK (Westland et al., 2011, 2013a). Consistent with these data, Abou Jaoudé et al. (2011) reported an ∼11% lower GFR in children with an early-acquired SFK (n = 53) compared with a congenital SFK (n = 44). A caveat to the finding of the KIMONO study is that those with an early-acquired SFK were older at follow-up and had greater incidence of ipsilateral CAKUT compared with a congenital SFK (Westland et al., 2011, 2013a). As both older age and ipsilateral CAKUT were independent risk factors for kidney injury in the KIMONO cohort, these may account for the greater incidence of kidney injury in individuals with an early-acquired SFK.

PRECLINICAL MODEL SYSTEMS

Over the last 20 years our group has characterized the phenotype of a congenital SFK in sheep. This model is generated by removal of a kidney from the sheep fetus at gestation day 100, during the period of nephrogenesis in the sheep (term = 150 days). There are various advantages of using the sheep as a model of SFK; (1) the development of the kidney in sheep is similar to that in humans with nephrogenesis reaching completion prior to birth in both species; (2) the size of the sheep and blood pressure and kidney function parameters are similar to that in humans making

TABLE 2 | Comparison of the features in human and ovine fetal SFK.

Characteristics	Congenital SFK					
	Children	Age at onset	References	Ovine (males only)	Age at measurement	References
Elevated blood pressure	√	Mean 4.9 years	Westland et al. (2013a)	√ (7–15 mmHg)	6 months	Singh et al. (2010)
Reduced GFR	√	Mean 6.4 years	Westland et al. (2013a)	√ (30% decrease)	6 months	Singh et al. (2010)
Albuminuria	√	Mean 9.8 years	Westland et al. (2013a)	√	6 months	Singh et al. (2009)
Kidney hypertrophy	√	20–36 weeks gestation	Van Vuuren et al. (2012b)	√	130 days gestation	Douglas-Denton et al. (2002)

GFR, glomerular filtration rate.

it an important preclinical model to examine the alterations in mechanisms regulating glomerular and tubular function and how these may underlie kidney injury in children with SFK (**Table 2**) (Moritz et al., 2008). Male and female rat pups that underwent unilateral nephrectomy in the first 24 h of postnatal life, a time when nephrogenesis is ongoing, have elevated blood pressure and lower GFR at the age of 20–22 weeks when compared with controls. In these uninephrectomized males, the elevation in blood pressure was greater than counterpart females and proteinuria and glomerular pathology was only observed in the males (Woods, 1999; Woods et al., 2001b). Similarly, in adult rats compensatory kidney hypertrophy of the remaining kidney 8 weeks after unilateral nephrectomy was two times greater in males compared with females and glomerular hypertrophy and damage were only observed in males but not in females (Mulroney et al., 1999). These observations suggest that SFK may increase disease severity in males more than females but these need to be confirmed in studies in humans.

ADAPTATIONS TO A SFK

It is well established that following a reduction in kidney mass whether it is congenital in origin or following unilateral nephrectomy in the child or the adult, there is marked compensatory kidney growth that is comprised of hypertrophy of both the kidney tubules and the glomerulus (Moritz et al., 2002, 2005; Singh et al., 2010; Fong et al., 2014; Chen et al., 2016; Wang et al., 2019; Zambaiti et al., 2019). In humans, compensatory kidney hypertrophy of the SFK begins as early as 20 weeks into gestation and by 36 weeks into gestation there is an ∼11% mean enlargement of the SFK compared with age matched controls (Van Vuuren et al., 2012b). Compensatory nephrogenesis is a characteristic adaptation to loss of kidney mass *in utero* but this is not always accompanied with compensatory increases in size of glomeruli. In a single human case study of a congenital SFK autopsied from a healthy 27-year-old male, it was observed that the congenital SFK weighed twice as much and had twice as many nephrons as a single kidney from an age-matched control (Maluf, 1997). In a study in 26-week-old pigs born with a congenital SFK, an 80% increase in kidney weight and using stereology, a 50% increase in nephron number in the SFK compared with a single control kidney was observed but individual glomerular volumes were similar to that of control (Van Vuuren et al., 2012a). In our ovine model of congenital SFK, fetal unilateral nephrectomy at 100 days of a 150-day gestation, resulted in a ∼45% greater nephron number in the SFK compared with a single kidney of a sham operated control sheep at 130 days of gestation but individual glomerular volumes were lower in the SFK compared with control at this age (Douglas-Denton et al., 2002). In contrast, unilateral nephrectomy after birth has been shown to result in increase in glomerular size in the rat and the mouse (MacKay et al., 1990; Nyengaard, 1993; Mulroney et al., 1999; Woods, 1999; Woods et al., 2001b).

In addition to the compensatory increase in size of glomeruli, an increase in single nephron filtration (glomerular hyperfiltration), and increases in size and function of kidney tubules are also characteristic responses to loss of kidney mass (Layton et al., 2017). These include increases in the diameter and length of the proximal and distal tubules and density of sodium transporters, all of which facilitate a greater reabsorption of the increased filtered load (Celsi et al., 1986; Shirley and Walter, 1991; Pollock et al., 1992) (see **Table 3**). These have been reviewed in detail elsewhere (Fong et al., 2014; Lankadeva et al., 2014) and will be discussed briefly here. The increase in filtration and increase in function of the kidney tubules facilitates compensation of total GFR such that GFR of a single kidney is relatively the same as that of two kidneys. In landmark studies, originally in 5/6th nephrectomized rats, Brenner hypothesized that a reduction in kidney mass and thus nephron number result in adaptive increases in glomerular capillary pressure and glomerular hypertrophy facilitated glomerular hyperfiltration (increases in single nephron GFR; SNGFR), thus maintaining GFR within normal levels (Brenner et al., 1988). The age at which reduction in kidney mass occurs may strongly influence these compensatory responses with evidence that the compensation is more robust when kidney mass is reduced in the young compared with the adult (Larsson et al., 1980). Indeed, following donation of a kidney in adult humans, GFR recovers to ∼70% of pre-donation values (Krohn et al., 1966; Fesler et al., 2015). In contrast, in children (∼9 years old) with a congenital or early-acquired SFK, GFR is preserved at a normal two-kidney level (100% increase in GFR) (Abou Jaoudé et al., 2011). These observations are also supported by various studies in animals in which GFR and kidney size have been shown to increase more in the young after loss of a kidney compared with the adult (Galla et al., 1974; Larsson et al., 1980; Shirley and Walter, 1991) (see **Table 3**).

TABLE 3 | Summary of compensatory adaptations to reduction in kidney mass.

Species	Variable	Age at nephrectomy	Age at measurement	Outcomes	References
Rat	Kidney weight	5 days 12 days 40 days	60 days old	72% increase 65% increase 36% increase	Larsson et al. (1980)
		Weanling Young adult	4 weeks post-unilateral nephrectomy	144% increase 66% increase	Galla et al. (1974)
Rat	Glomerular volume	3 days 120 days	540 days	59% increase 20% increase	Nyengaard (1993)
Human	Total GFR	Congenital 20–60 years	9 years old 1–18 days post-unilateral nephrectomy	100% increase 70% increase	Abou Jaoudé et al. (2011) Krohn et al. (1966)
Rat	SNGFR	5 days 12 days 40 days	60 days old	115% increase 74% increase 47% increase	Larsson et al. (1980)
Rat	Proximal tubule length	Adult	2–4 weeks post-unilateral nephrectomy	35% increase	Hayslett et al. (1968)
		Adult	4–6 post-unilateral nephrectomy	71% increase	Pollock et al. (1992)
		5 days old	8 weeks	160%	Celsi et al. (1986)
Rat	Sodium reabsorption	Adult	4–6 weeks post-unilateral nephrectomy	50% increase	Pollock et al. (1992)
	Fractional proximal reabsorption	Adult	30 days post-unilateral nephrectomy	40% increase	Shirley and Walter (1991)
Rat	Sodium transporter density	5 days old	2 weeks post-unilateral nephrectomy	168% increase	Celsi et al. (1986)

GFR, glomerular filtration rate; SNGFR, single nephron glomerular filtration rate.

MECHANISMS FACILITATING ADAPTATIONS AND POTENTIATING KIDNEY DYSFUNCTION

Increases in SNGFR facilitate adaptations compensating for loss of functioning nephrons but may also drive glomerular injury and contribute to progressive loss of kidney function (Brenner et al., 1988). Direct measurements of SNGFR are not possible in humans. Total GFR (the sum of all SNGFR) is currently the best prognostic indicator of kidney function in humans (Denic et al., 2017). SNGFR is influenced by various intrarenal mechanisms including glomerular capillary pressure, single nephron plasma flow, and tubuloglomerular feedback (TGF) (Blantz and Pelayo, 1984). The rise in SNGFR and glomerular capillary pressure following reduction in kidney mass has been associated with a reduction in afferent arteriole resistance and a right-ward shift in TGF (Müller-Suur et al., 1980; Salmond and Seney, 1991; Brown et al., 2011; Monu et al., 2018). It has been suggested that the right-ward shift results in blunting (resetting) of TGF where significantly higher fluid flow rates are required to cause a TGF mediated inhibition of SNGFR (Salmond and Seney, 1991). Thus, this resetting of TGF permits the increase in SNGFR and increase in glomerular capillary pressure in the remaining nephrons following nephron loss. In the rat, resetting of TGF 24 h after unilateral nephrectomy is mediated by enhanced connecting tubule glomerular feedback (a feedback system that influences afferent arteriole dilatation and is associated with epithelial sodium transporter; ENaC) (Monu et al., 2018). This resetting of TGF also sustains the increase in glomerular capillary pressure observed following 5/6th and unilateral nephrectomy in the rat (Salmond and Seney, 1991). Since increases in glomerular capillary pressure can increase injury to the glomeruli it can be suggested that resetting of TGF may contribute to glomerular injury following loss of nephrons (Hostetter et al., 1981).

The age-related differences in glomerular hyperfiltration following a reduction in kidney mass may also be associated with differences in the glomerular hemodynamic responses driving glomerular hyperfiltration. In an adult rat model of 5/6th nephrectomy with a two and a half fold increase in SNGFR compared with controls, glomerular capillary pressure was only increased by 10% (Bidani et al., 1990). In contrast, guinea pigs subjected to unilateral nephrectomy at birth had a 30% increase in glomerular capillary pressure at 10–21 days of age (Chevalier, 1983). Interestingly, Celsi et al. (1989) observed that in 20-day-old rats, subjected to unilateral nephrectomy at 5 days of age, the two-fold increase in SNGFR was maintained by an increase in glomerular ultrafiltration pressure. However, by 60 days of age, this increase in SNGFR was maintained by both an increase in glomerular ultrafiltration pressure and increase in the filtering surface area (Celsi et al., 1989). These data suggest that a nephron loss in the young may favor a compensatory increase in glomerular capillary pressure to maintain GFR in the short-term (Celsi et al., 1989). In contrast, in a long-term study of glomerular hemodynamics in adult kidney donors, Lenihan et al. (2015) inferred that following kidney donation compensatory glomerular hyperfiltration was maintained predominantly by glomerular hypertrophy rather than an increase in glomerular capillary pressure. In a Japanese cohort consisting of normotensives, hypertensives and subjects with CKD, Kanzaki et al. (2017) reported that individuals with

a history of CKD had half as many nephrons per kidney (55%) as age matched normotensive individuals and 30% fewer nephrons per kidney than hypertensive individuals. In hypertensive subjects the volume of individual non-sclerosed glomeruli were greater than that of normotensive subjects but volume of non-sclerosed glomeruli was greatest in subjects with CKD. Estimated SNGFR was similar between subjects with hypertension and CKD but greater than that of normotensive subjects (Kanzaki et al., 2017). This suggested that increases in glomerular size supported GFR in the presence of low nephron number. Compensatory adaptations in size and function of kidney tubules facilitate a greater reabsorption of the increased filtered load (Celsi et al., 1986; Shirley and Walter, 1991; Pollock et al., 1992) (see **Table 3**). An increase in sodium transporter expression has been reported following reduction in kidney mass (Amaral et al., 2009; Kim et al., 2010; Singh et al., 2010). In our ovine model of congenital SFK, associated with elevated blood pressure and reduced GFR we have shown increased expression of Na+/K+ATPase β1, Na+/K+ATPase γ subunits and type 3 sodium hydrogen exchanger (NHE3) at 6 months of age (Singh et al., 2010). Moreover, following subtotal nephrectomy in the rat, at 4 weeks of age elevation in expression of Na-K-2Cl cotransporter and Na-Cl cotransporter was observed but these declined in expression by 12 weeks of age and this change in expression was associated with elevation in sodium excretion and increased kidney damage (Kim et al., 2010). This suggests there may be an association between changes in renal sodium transporter expression and severity of kidney injury. A greater reabsorption of certain components of the filtered load may also predispose the tubules to injury. For example, excessive proximal tubular reabsorption of filtered proteins or protein-bound substances in disease states with proteinuria has been shown to cause accumulation of inflammatory cells and macrophages in the tubular interstitium which may in turn enhance synthesis of extracellular matrix and proliferation of interstitial fibroblasts resulting in tubular injury (Eddy, 1994; Kees-Folts et al., 1994; Benigni and Remuzzi, 1996).

The underlying stimulus and mechanisms mediating kidney hypertrophy remain unclear. In the pig, compensatory nephrogenesis resulting in 50% increase in nephron number was associated with 1.4-fold increase in the number of medullary papillae (Van Vuuren et al., 2012a). Using ultrasound, a similar 1.3-fold increase in number of medullary papillae has also been observed in human fetuses with a congenital SFK (24 weeks gestation) compared with control fetuses (Snoek et al., 2018). Increase in number of medullary papillae indicates an increase in ureteric bud arborization, a process that determines final nephron complement suggesting that enhanced ureteric branching morphogenesis facilitates compensatory nephrogenesis in congenital SFK. These findings also suggest that the total nephron endowment in congenital SFK will amount to ∼70–75% rather than 50% of full nephron complement.

Other factors such as the nitric oxide system, the renal sympathetic nerves and the renin angiotensin system (RAS) have been implicated in the compensatory adaptations to reduction in kidney mass (Rojas-Canales et al., 2019). Nitric oxide (NO), released by the endothelium, is an important vasodilator of the vasculature. NO and the by-product L-citrulline, is formed from the precursor L-arginine by NO synthase (NOS), of which there are three isoforms, neuronal NOS (nNOS), inducible NOS (iNOS), and endothelial (eNOS) (Mount and Power, 2006). The expression of all three NOS isoforms have been observed in the kidney, and as such NO plays an important role in the modulation of renal glomerular hemodynamics, tubular function, fluid composition and volume and thus arterial pressure (Denton and Anderson, 1994; Mount and Power, 2006). The kidney hypertrophic response following unilateral nephrectomy in the rat has been suggested to be mediated by an elevation in production of NO and increase in renal blood flow (RBF) (Sigmon et al., 2004). The increased RBF following unilateral nephrectomy has also been proposed to increase the delivery of free amino acids to the remaining kidney stimulating the mTORC1 pathway which induces protein synthesis and cell proliferation leading to kidney hypertrophy (Chen et al., 2015). Blockade of NO with L-NAME prevents this increase in RBF and kidney hypertrophy (Sigmon et al., 2004). In endothelial nitric oxide (eNOS) knockout mice, an increase in kidney weight and increase in RBF were not observed after unilateral nephrectomy whereas in eNOS transgenic mice with targeted overexpression of eNOS to the vascular endothelium, an increase in compensatory kidney growth was observed after unilateral nephrectomy compared with the sham procedure (Nagasu et al., 2012). These collectively suggest that eNOS facilitated increase in RBF and enhanced expression of eNOS promotes compensatory kidney hypertrophy. Conversely, a reduction in NO has also been observed in animal models of reduced kidney mass and in humans with kidney failure and CKD (Blum et al., 1998; Schmidt and Baylis, 2000). At 15 weeks after 5/6th nephrectomy in rats, accompanying decreases in creatinine clearance, increases in proteinuria and glomerulosclerosis, total NO production and renal cortical nNOS were reduced (Tain et al., 2007). In our ovine model of SFK, we have demonstrated a reduced contribution of NO to kidney function in both aged and young sheep (Lankadeva et al., 2015; Singh et al., 2016). In sheep with congenital SFK, the renal responses to systemic blockade of NOS, via the administration of L-NAME, were attenuated compared with sham-operated sheep despite increased expression of renal eNOS (Lankadeva et al., 2015). The increase in expression of eNOS suggested that the kidneys could produce NO but further studies identified that increased oxidative stress maybe contributing to the reduction in bioavailability of NO and reducing the contribution of NO to kidney function in the sheep with SFK (Lankadeva et al., 2015). In addition to the reduced contribution of NO to kidney function, we have demonstrated reduced total urinary nitrate/nitrite levels in sheep with SFK (Singh et al., 2016). From these collective observations, we speculate that increases in eNOS may promote increases in RBF and promote the renal hypertrophic adaptation to SFK in the short-term but that reduction in bioavailability of NO, probably associated with increased oxidative stress may contribute to kidney dysfunction and hypertension in SFK.

Indirect evidence has also implicated renal sympathetic nerve activity (RSNA) in the kidney hypertrophic response (Furukawa et al., 1997). Following unilateral nephrectomy in

the rat, relative mean RSNA increased by 78% at 28 days after nephrectomy, and this was associated with a 62% increase in kidney weight (Furukawa et al., 1997). Although we do not have direct evidence that elevations in RSNA drive compensatory hypertrophy, we do have evidence of renal hyperinnervation in our ovine model of SFK (Singh et al., 2017, 2019). In our recent studies, we have demonstrated sheep with a congenital SFK have a greater proportion of both sympathetic renal nerves and sensory renal nerves than sham animals demonstrating renal nerve hyperinnervation in SFK (Singh et al., 2019). The spontaneously hypertensive rat (SHR) model is a genetic model of hypertension and there is evidence that the kidneys of the SHR have less nephrons than normotensive Wistar Kyoto (WKY) control counterparts (Skov et al., 1994). In this model, accelerated development of renal innervation has been observed from newborn to postnatal week 6 compared with WKY controls and sympathetic innervation induced changes in kidney function in the neonate contribute to development of hypertension in SHR (Gattone et al., 1990; Grisk et al., 2002). Evidence for contribution of overactivity of the renal nerves to hypertension and kidney failure has also been documented in humans (Converse et al., 1992; Grassi et al., 2011; Symplicity, 2011; Krum et al., 2014; Mauriello et al., 2015). Collectively these findings suggest that renal hyperinnervation may have a role in promoting renal and cardiovascular dysfunction in models of reduced nephron number and as such have implications for SFK.

The RAS is a potent modulator of blood pressure, glomerular hemodynamics and fluid and electrolyte homeostasis and is also an important modulator of kidney development and maturation in the fetus and the neonate (Chen et al., 2004). Considerable evidence has also established the role of the RAS in the pathophysiology of hypertension and kidney disease (Hall et al., 1978; Johnson et al., 1992; Woods et al., 2001a; Grigore et al., 2007; Cuffe et al., 2016; Walton et al., 2017). Our ovine model of SFK is a model of low-renin hypertension, where we have reported lower levels of plasma renin in sheep with SFK from 6 months of age in both males and females (Moritz et al., 2002; Singh et al., 2009). This reduction in renin is likely a normal response to the rise in blood pressure that is observed in the sheep with SFK from 6 months of age (Singh et al., 2009). Additionally, we have also demonstrated that regulation of glomerular hemodynamics by the RAS is impaired in sheep with SFK, suggesting that this may potentially be a system that can be targeted to improve renal outcomes in SFK (Singh et al., 2011). Postnatal adaptive maturation of both blood pressure and glomerular filtration rate (GFR) is associated with the RAS (Robillard et al., 1983; Prevot et al., 2002; Vinturache and Smith, 2016). In conscious lambs, blood pressure is low at birth and plasma renin activity is elevated but during the first 3 months of post-natal maturation, plasma renin activity decreases as blood pressure increases (Monument and Smith, 2003; Velaphi et al., 2007). Additionally, in the early postnatal period in conscious lambs angiotensin II activation of AT1R regulates GFR and kidney injury associated with glomerular hyperfiltration and hypertrophy may be underpinned by RAS activation (Babić et al., 2007; Vinturache and Smith, 2016).

BIOMARKERS AND AREAS OF FUTURE STUDY

Classic biomarkers of CKD (albuminuria, reduced eGFR) occur at advanced stages of disease progression. Therefore, advancements in genetic testing, proteomics, metabolomics and imaging techniques may offer prognostic markers to predict CKD risk and disease progression before decline in kidney function occurs, allowing for the possibility of earlier intervention in SFK (**Table 4**) (Greenberg et al., 2018; Bennett et al., 2020).

Nephron Number

A deficiency of nephrons is a risk factor for kidney disease but the threshold of nephron number that predisposes to kidney disease is currently not known (Bertram et al., 2011). Harnessing this knowledge has been limited to-date given that nephron number cannot be determined *in vivo* in living subjects. Magnetic resonance imaging (MRI) in combination with cationized ferritin labeling of glomeruli using both *ex vivo* and *in vivo* approaches has been established as a reliable determinant of nephron number in rodents (Geraci et al., 2017; Baldelomar et al., 2018). Similarly, MRI in combination with cationized ferritin has been utilized to determine nephron number *ex vivo* in the whole kidney of the human (Beeman et al., 2014). Continued progress in this field resulting in determination of nephron number in the living human kidney will improve our ability to identify individuals at risk of developing kidney disease and track the progression of disease. This approach may also assist us in differentiating the long-term cardiovascular and renal outcomes between early-acquired SFK and a congenital SFK. It is known that the kidney of the human does not have the capacity to form new nephrons after birth (Moritz and Wintour, 1999). Thus, the degree of nephron deficit may be more severe in an early-acquired SFK than a congenital SFK, and this may potentially underpin the greater risk for kidney injury in the early-acquired SFK group (Westland et al., 2014; Schreuder, 2017). The ability to determine a threshold for nephron number that predisposes to disease will enable is to devise better treatment strategies in individuals with different origins of SFK.

Kidney Size

In the absence of direct measurements of nephron number and limited information on validity of biomarkers for predicting kidney injury/disease in SFK, kidney size remains an important predictor of kidney injury in SFK. Inadequate kidney growth indicative of reduced nephron hyperplasia and/or hypertrophy has become an important predictive index of kidney dysfunction in children with a SFK (Westland et al., 2013a; Marzuillo et al., 2019; Poggiali et al., 2019). In a small cohort of Chinese adults with a congenital SFK, it was observed that individuals with a kidney length less than 120 mm had a five-fold greater risk for impaired GFR (<60 ml/min/1.73 m^2) (Wang et al., 2010). In the KIMONO cohort, it was demonstrated that a smaller SFK compared with a larger SFK was associated with a greater risk of developing kidney injury (Westland et al., 2013a). Similarly, La Scola et al. (2016) observed that a kidney length less than

TABLE 4 | Current and next generation prognostic biomarkers for progression of kidney injury in children with SFK.

Biomarker	Access	Cost	Prognostic utility	References
Kidney mass and kidney length Ultrasound	Freely accessible	Inexpensive	Children with a smaller SFK are at a greater risk for kidney injury	Wang et al. (2010); Westland et al. (2013a)
Nephron number MRI	Under development-research testing in animals only	Expensive	May assist in differentiating those with a reduced nephron number early in life	Beeman et al. (2014); Baldelomar et al. (2018)
Hyperfiltration eGFR SNGFR Urinary prostaglandin E2 Urinary nitrates	Freely accessible	Inexpensive	Early changes in markers could predict risk of kidney disease	Westland et al. (2013a); Singh et al. (2016); Srivastava et al. (2020)
Plasma Creatinine Cystatin C KIM-1 MCP-1	Freely accessible	Inexpensive	Kidney dysfunction and tubular injury	Wasilewska et al. (2006); Greenberg et al. (2020)
Urine Creatinine eGFR Albuminuria *N*-Acetyl-beta-D-glucosaminidase (NAG) *N*-Acetyl-β-hexosaminidase (HEX)	Freely accessible	Inexpensive	Glomerular and tubular injury Predict risk of kidney injury	Gadalean et al. (2013); Westland et al. (2013a); Taranta-Janusz et al. (2014)

MRI, magnetic resonance imaging; GFR, glomerular filtration rate; eGFR, estimated glomerular filtration rate; SNGFR, single nephron glomerular filtration rate; KIM-1, kidney injury molecular-1; MCP-1, monocyte chemoattractant protein-1.

10% expected for a congenital SFK was the strongest predictor of reduced eGFR by 10 years of age. Conversely, Marzuillo et al. (2019) found that children who were diagnosed prenatally with SFK and had a greater than two standard deviation score (+2-SDS) kidney length in the neonatal period (within 60 days of life) were at a reduced risk of having lower eGFR at the age of 15 years compared with those with a kidney length less than + 2-SDS. Importantly, in this study, it was demonstrated that the risk for low eGFR in children with a kidney length < 2-SDS presenting with postnatal compensatory kidney hypertrophy was similar to those with kidney length < 2-SDS but without postnatal compensatory kidney hypertrophy. Based on these findings the authors concluded that nephron hyperplasia resulting in a greater kidney length likely provided protection against loss of kidney function in the long-term but nephron hypertrophy did not offer this protection (Marzuillo et al., 2019). The importance of kidney length as a predictor of kidney function in SFK has been further highlighted by a study by Wang et al. (2019) who demonstrated that every 1 cm increase in kidney length predicted a 7.8 ml/min/1.73 m^2 increase in GFR in children with a SFK. Together these studies suggest that insufficient compensatory kidney growth; perhaps lack of nephron hyperplasia more so than nephron hypertrophy, may increase the susceptibility to kidney dysfunction. However, it has been found that kidney size estimations in adults (with two kidneys) has poor predictive value in estimating nephron number, with only 5% of the variation in nephron number explained by the variation in kidney size (Bueters et al., 2013). This again highlights the need for determining nephron number together with kidney size in the living human, as these may be important predictive markers that can be utilized to identify those at an elevated risk for future kidney injury.

Glomerular Injury

Mechanisms pertaining to glomerulosclerosis associated with reduction in kidney mass are under investigation and implicate a role for podocyte loss in glomerular injury and dysfunction. During glomerular hypertrophy/hyperfiltration, associated increases in glomerular capillary pressure, exposes podocytes to stretch, tensile stress and fluid flow shear stress (FFSS), which may overtime decrease the integrity of the glomerular filtration barrier, resulting in podocyte damage and loss (Nagata et al., 1992; Srivastava et al., 2014b, 2017; Mallipattu and He, 2016). Following unilateral nephrectomy in young rats it has been observed that increases in SNGFR mediate a 1.5- to 2-fold increase in FFSS over podocytes and isolated glomeruli exposed to FFSS for 2 h have increased permeability to albumin indicating damage to the glomerular filtration barrier (Srivastava et al., 2014a,b). Additionally, in *in vitro* studies, applying FFSS to cultured podocytes has been demonstrated to increase levels of prostaglandins (PGE_2) from as early as 30 min after induction of FFSS and has been demonstrated to cause a reduction in the actin cytoskeleton of the podocytes (Srivastava et al., 2010). This suggests that PGE_2 levels may serve as a marker of hyperfiltration mediated FFSS and glomerular filtration barrier dysfunction. In a recent study in children with SFK, it was shown that urinary PGE_2 and albumin levels were elevated in children with a SFK ($n = 57$), at a mean age of 8.5 years, compared with children with two kidneys but it was also demonstrated that albuminuria was preceded by elevations in urinary PGE_2 (Srivastava et al., 2020).

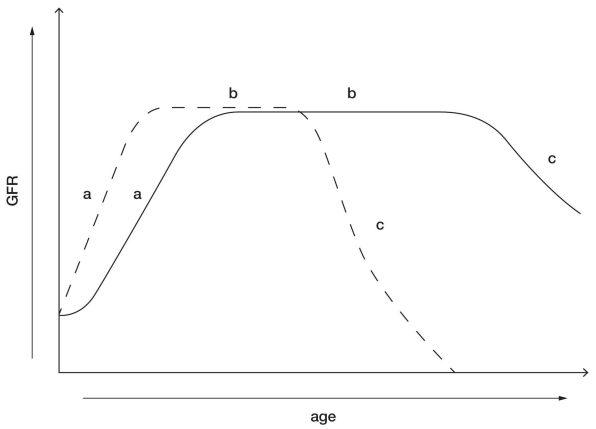

FIGURE 1 | Postnatal maturation of kidney function in healthy individuals with two kidneys (solid line) and maturation of kidney function in children with a congenital SFK (dotted line). (a) The phase after birth when GFR increases. This phase is likely enhanced in children who lose a kidney early in life. (b) GFR reaches its peak and is maintained within normal range for most of life in the absence of a "second hit" such as obesity, hypertension, and diabetes. This phase is likely to be shorter in children with SFK, possibly due to enhanced compensatory adaptations increasing the risk of kidney dysfunction. (c) Age-related decline in GFR in kidneys. This phase may be accelerated in individuals with SFK with kidney dysfunction and in some cases may result in kidney failure.

Therefore, elevated urinary PGE_2 may be a potential biomarker for FFSS associated with hyperfiltration and may predict risk of kidney injury in children with a SFK (Srivastava et al., 2020). Moreover, since the increase in SNGFR after reduction in kidney mass are greater in the young compared with the adult (**Table 2**), these data suggest that adaptive glomerular hyperfiltration and associated increases in FFSS sustained from a younger age may cause degradation of the glomerular filtration barrier earlier in life, resulting in podocyte loss and may account for the greater incidence of kidney injury in children with a SFK compared with adult kidney donors (**Figure 1**).

Tubular Injury

In the CKD in Children (CKiD) multicenter cohort center, plasma concentrations of proximal tubular injury (kidney injury molecular-1, KIM-1), pro-inflammatory markers (monocyte chemoattractant protein-1, MCP-1) and receptors for proinflammatory markers (tumor necrosis factor alpha; TNFR1 and TNFR2) in the highest quartile identified children at greater risk of CKD progression compared with those with concentrations in the lowest quartile (Greenberg et al., 2020). Gadalean et al. (2013) observed that in adult patients with an acquired and congenital SFK there was a ∼52–60% increase in urinary *N*-acetyl-beta-D-glucosaminidase, a marker of proximal tubule dysfunction. Similarly, in children with both a congenital SFK and acquired SFK, urinary *N*-acetyl-β-hexosaminidase (HEX), an indicator of proximal tubular damage, was elevated compared with age-matched healthy individuals (Taranta-Janusz et al., 2014). Moreover, estimated urinary HEX was a good diagnostic indicator of kidney injury (presence of albuminuria) in children with a SFK (Taranta-Janusz et al., 2014). Interestingly, it has been observed that children with URA excrete higher levels of β2 -microglobulin indicating proximal tubular damage, compared with children with an early-acquired SFK (unilateral nephrectomy due to Wilm's tumor) (Stefanowicz et al., 2012). These data indicate that a greater reabsorption of filtered load may increase tubulointerstitial inflammation resulting in tubular injury and that urinary markers of proximal tubular injury are elevated in children with a SFK and may be diagnostic indicators of kidney damage.

Endothelial Dysfunction

Asymmetrical dimethylarginine (ADMA), a competitive NOS inhibitor that causes reduced NO production, and its enantiomer symmetric dimethylarginine (SDMA) have been observed to accumulate in the early stages of CKD and kidney failure (Zoccali et al., 2001; Kielstein et al., 2002; Fleck et al., 2003; Busch et al., 2006; Brooks et al., 2008; El-Sadek et al., 2016). Ravani et al. (2005) demonstrated that plasma ADMA is a strong independent risk factor for progression to kidney failure and death in patients with CKD. Brooks et al. (2008) observed reduced plasma arginine and elevated ADMA and SDMA in pediatric/adolescent CKD (stage 2–3) patients, with SDMA demonstrated to be a strong indicator of reduced GFR. Importantly, in a small cohort of 51 children with a SFK at a mean age of ∼10 years, plasma SDMA was significantly elevated and negatively correlated with GFR, suggesting that plasma SDMA may serve as a marker of endothelial dysfunction in children with a SFK (Taranta-Janusz et al., 2012).

POTENTIAL TREATMENT OPTIONS

Increasing NO Bioavailability

Nitric oxide has an important role in the renal hypertrophic and hemodynamic adaptation in SFK. However, reductions in bioavailability of NO may be associated with increases in oxidative stress in SFK (Lankadeva et al., 2015). Increasing bioavailability of NO by dietary supplementation with L-arginine in rats subjected to subtotal nephrectomy has been shown to prevent glomerular hypertension and preserve kidney function and has been shown to prevent glomerular hyperfiltration and proteinuria in diabetic rats (Reyes et al., 1993; Katoh et al., 1994). In hypertensive patients with micro-vascular angina, oral L-arginine treatment for 4 weeks was shown to improve systolic blood pressure and quality of life (Palloshi et al., 2004). The therapeutic value of oral-L-arginine treatment needs to be further explored in SFK.

Renal Denervation

In our recent studies, we have demonstrated that renal denervation in sheep with SFK resulted in long-term lowering of blood pressure, improvement of GFR and reduction in albuminuria compared with animals with SFK that underwent a sham denervation procedure (Singh et al., 2019). This suggests that hyperinnervation of the renal nerves may potentially be contributing to the elevation in blood pressure and kidney disease

in SFK and has implications for children with SFK. A role for renal sympathetic overactivity in promoting hypertension is also evident in other models of reduced kidney mass, such as the developmental programming models (maternal glucocorticoid exposure) and genetic models (SHR) (Gattone et al., 1990; Alexander et al., 2005; Dagan et al., 2008; Kett and Denton, 2011; Mansuri et al., 2017). Prenatal exposure to dexamethasone is well known to cause a reduction in nephron number and elevation in blood pressure in studies in various species (Singh et al., 2012). In the rat, the elevation in blood pressure in the offspring that results from prenatal exposure to dexamethasone was ameliorated by renal denervation (Dagan et al., 2008). Moreover, renal denervation in SHR reduces blood pressure long-term and attenuates the kidney injury associated with proteinuria and glomerulosclerosis (Wang et al., 2018). Combined with clinical evidence of the association of CKD with sympathetic hyperinnervation, markers of sympathetic activity in young children may serve as a prognostic indicator of future disease severity in children with a SFK. Indeed, noradrenaline can be detected in urine, the levels of which have previously been shown to correlate with the level of sympathetic activity (Lappe et al., 1982). Further studies examining the role of RSNA in models of reduced kidney mass are warranted in the future and may provide evidence to advance this to clinical studies.

RAS Blockade

Pharmacological inhibition of the RAS with either an ACEi or an ARB may be effective in preventing hyperfiltration-mediated injury associated with SFK (Lewis et al., 1993; Romero et al., 2015). Indeed, in patients with diabetic nephropathy, in which hyperfiltration is a hallmark response, ACE inhibition prevents the decline in kidney function independent of its antihypertensive effects (Lewis et al., 1993). There is growing evidence that pharmacologically targeting the RAS during early postnatal maturation may provide long-lasting cardiovascular and renal benefits. Brief and early treatment with ACEi from 6 to 10 weeks of age in the SHR reduced blood pressure by ∼20–30 mm Hg until approximately 82 weeks of age (Harrap et al., 1994). Consistently, in models of maternal low protein diet or calorie restriction, treatment with ACEi or ARB's for a brief period early in postnatal life prevented hypertension into early adulthood (Sherman and Langley-Evans, 1998, 2000; Manning and Vehaskari, 2005; Hsu et al., 2015). Interestingly, Hsu et al. (2015) observed that rat offspring exposed to maternal calorie restriction but treated with aliskiren, a renin inhibitor, from 2 to 4 weeks of age did not develop hypertension at 12 weeks of age. These improvements were associated with a reduction in angiotensinogen expression and improved bioavailability of NO. This suggests that the balance between NO bioavailability and RAS activity may influence regulation of blood pressure. Blockade of RAS in children with CKD and hypertension not only improves control of blood pressure but improves renal outcomes as well. Indeed, in the ESCAPE trial in children with CKD and hypertension, who received a high dose of an ACEi, blood pressure control was intensified and was associated with a 35% reduction in relative risk of loss of kidney function (50%) or kidney failure within the 5-year follow-up (Wuhl et al., 2009). In addition, a higher degree of early anti-proteinuric effects of ACEi predicted a lower risk of renal functional decline in these children with CKD (Van Den Belt et al., 2018). However, following 3 years of ongoing ACEi the proteinuria rebounded in the ESCAPE trial (Wuhl et al., 2009). The improvements in kidney outcomes associated with RAS blockade maybe associated with RAS control of glomerular hemodynamics. Anderson et al. (1985) observed that treatment with ACEi in a rat model of 5/6th nephrectomy controlled systemic and glomerular capillary pressure via efferent arteriole dilation which in turn prevented proteinuria and glomerular injury. Together this evidence indicates that RAS inhibition may prevent the rise in blood pressure and also alter glomerular hemodynamics in a manner that can reduce kidney injury in children with SFK.

CONCLUSION

Children born with a SFK are at a greater risk for developing hypertension, kidney injury and CKD. This predisposition is likely associated with the greater degree of compensatory adaptations early in life that include compensatory increases in GFR, glomerular size and function and size of the kidney tubules following a reduction in kidney mass in young children or in fetuses. Our extensive studies in an ovine model of congenital SFK, along with work in other models of a reduction in kidney mass have demonstrated that alterations in the renal sympathetic nerves, the renal RAS and the nitric oxide system may be strong contributing factors to the development of disease associated with SFK. These studies have provided the foundation suggesting that these systems can potentially be targeted in SFK to reduce the progression of disease. Currently, common prognostic indicators such as hypertension, proteinuria and reduced GFR are available to detect kidney injury/failure in children with a SFK, but these emerge at later stages of disease progression. Emerging indicators such as kidney length and urinary markers of tubular injury and glomerular hyperfiltration may be beneficial in identifying those at an elevated risk of kidney injury earlier in life. However, markers that distinguish those at an elevated risk of kidney injury as opposed to those with a lower risk, before overt kidney injury occur, are needed. Ideally, this would occur during the neonatal period when the SFK was identified.

AUTHOR CONTRIBUTIONS

All authors assisted with drafting the manuscript, searching the literature and proofreading the document. All authors contributed to the article and approved the submitted version.

FUNDING

MS was supported by a grant from The Netherlands Organization for Health Research and Development (ZonMW Vidi 016.156.454). KD (APP1041844) and KM (APP1078164) are supported by Senior Research Fellowships from the National Health and Medical Council of Australia.

REFERENCES

Abou Jaoudé, P., Dubourg, L., Bacchetta, J., Berthiller, J., Ranchin, B., and Cochat, P. (2011). Congenital versus acquired solitary kidney: is the difference relevant? *Nephrol. Dial. Transpl.* 26, 2188–2194. doi: 10.1093/ndt/gfq659

Alexander, B. T., Hendon, A. E., Ferril, G., and Dwyer, T. M. (2005). Renal denervation abolishes hypertension in low-birth-weight offspring from pregnant rats with reduced uterine perfusion. *Hypertension* 45, 754–758. doi: 10.1161/01.hyp.0000153319.20340.2a

Amaral, J. S., Pinho, M. J., and Soares-Da-Silva, P. (2009). Regulation of amino acid transporters in the rat remnant kidney. *Nephrol. Dial. Transpl.* 24, 2058–2067. doi: 10.1093/ndt/gfn752

Anderson, S., Meyer, T. W., Rennke, H. G., and Brenner, B. M. (1985). Control of glomerular hypertension limits glomerular injury in rats with reduced renal mass. *J. Clin. Invest.* 76, 612–619. doi: 10.1172/jci112013

Argueso, L. R., Ritchey, M. L., Boyle, E. T. Jr., Milliner, D. S., Bergstralh, E. J., and Kramer, S. A. (1992). Prognosis of patients with unilateral renal agenesis. *Pediatr. Nephrol.* 6, 412–416. doi: 10.1007/bf00873996

Babić, N., Huskić, J., and Nakas-Ićindić, E. (2007). Angiotensin converting enzyme activity in compensatory renal hypertrophy. *Bosnian J. Basic Med. Sci.* 7, 79–83. doi: 10.17305/bjbms.2007.3098

Baldelomar, E. J., Charlton, J. R., Beeman, S. C., and Bennett, K. M. (2018). Measuring rat kidney glomerular number and size in vivo with MRI. *Am. J .Physiol Renal Physiol.* 314, F399–F406.

Becherucci, F., Roperto, R. M., Materassi, M., and Romagnani, P. (2016). Chronic kidney disease in children. *Clin. Kidney J.* 9, 583–591.

Beeman, S. C., Cullen-Mcewen, L. A., Puelles, V. G., Zhang, M., Wu, T., Baldelomar, E. J., et al. (2014). MRI-based glomerular morphology and pathology in whole human kidneys. *Am. J. Physiol. Renal Physiol.* 306, F1381–F1390.

Benigni, A., and Remuzzi, G. (1996). Glomerular protein trafficking and progression of renal disease to terminal uremia. *Semin. Nephrol.* 16, 151–159.

Bennett, K. M., Baldelomar, E. J., Morozov, D., Chevalier, R. L., and Charlton, J. R. (2020). New imaging tools to measure nephron number : opportunities for developmental nephrology. *J. Dev. Origin. Health Dis.* [Epub ahead of print].

Bertram, J. F., Douglas-Denton, R. N., Diouf, B., Hughson, M. D., and Hoy, W. E. (2011). Human nephron number: implications for health and disease. *Pediatr. Nephrol.* 26, 1529–1533. doi: 10.1007/s00467-011-1843-8

Bidani, A. K., Mitchell, K. D., Schwartz, M. M., Navar, L. G., and Lewis, E. J. (1990). Absence of glomerular injury or nephron loss in a normotensive rat remnant kidney model. *Kidney Int.* 38, 28–38. doi: 10.1038/ki.1990.163

Blantz, R. C., and Pelayo, J. C. (1984). A functional role for the tubuloglomerular feedback mechanism. *Kidney Int.* 25, 739–746. doi: 10.1038/ki.1984.84

Blum, M., Yachnin, T., Wollman, Y., Chernihovsky, T., Peer, G., Grosskopf, I., et al. (1998). Low nitric oxide production in patients with chronic renal failure. *Nephron* 79, 265–268. doi: 10.1159/000045047

Brenner, B. M., Garcia, D. L., and Anderson, S. (1988). Glomeruli and blood pressure. Less of one, more the other? *Am. J. Hypertens.* 1, 335–347. doi: 10.1093/ajh/1.4.335

Brooks, E. R., Langman, C. B., Wang, S., Price, H. E., Hodges, A. L., Darling, L., et al. (2008). Methylated arginine derivatives in children and adolescents with chronic kidney disease. *Pediatr. Nephrol.* 24:129. doi: 10.1007/s00467-008-0972-1

Brown, R. D., Turner, A. J., Carlström, M., Persson, A. E., and Gibson, K. J. (2011). Tubuloglomerular feedback response in the prenatal and postnatal ovine kidney. *Am. J. Physiol. Renal Physiol.* 300, F1368–F1374.

Bueters, R. R., Van De Kar, N. C., and Schreuder, M. F. (2013). Adult renal size is not a suitable marker for nephron numbers: an individual patient data meta-analysis. *Kidney Blood Press. Res.* 37, 540–546. doi: 10.1159/000355734

Busch, M., Fleck, C., Wolf, G., and Stein, G. (2006). Asymmetrical (ADMA) and symmetrical dimethylarginine (SDMA) as potential risk factors for cardiovascular and renal outcome in chronic kidney disease - possible candidates for paradoxical epidemiology? *Amino Acids* 30, 225–232. doi: 10.1007/s00726-005-0268-8

Celsi, G., Larsson, L., and Aperia, A. (1986). Proximal tubular reabsorption and Na-K-ATPase activity in remnant kidney of young rats. *Am. J. Physiol.* 251, F588–F593.

Celsi, G., Larsson, L., Seri, I., Savin, V., and Aperia, A. (1989). Glomerular adaptation in uninephrectomized young rats. *Pediatr. Nephrol.* 3, 280–285. doi: 10.1007/bf00858530

Chen, J. K., Nagai, K., Chen, J., Plieth, D., Hino, M., Xu, J., et al. (2015). Phosphatidylinositol 3-kinase signaling determines kidney size. *J. Clin. Invest.* 125, 2429–2444. doi: 10.1172/jci78945

Chen, K. W., Wu, M. W., Chen, Z., Tai, B. C., Goh, Y. S., Lata, R., et al. (2016). Compensatory hypertrophy after living donor nephrectomy. *Transplant. Proc.* 48, 716–719. doi: 10.1016/j.transproceed.2015.12.082

Chen, Y., Lasaitiene, D., and Friberg, P. (2004). The renin–angiotensin system in kidney development. *Acta Physiol. Scand.* 181, 529–535.

Chevalier, R. L. (1983). Reduced renal mass in early postnatal development. *Neonatology* 44, 158–165. doi: 10.1159/000241710

Converse, R. L. Jr., Jacobsen, T. N., Toto, R. D., Jost, C. M., Cosentino, F., Fouad-Tarazi, F., et al. (1992). Sympathetic overactivity in patients with chronic renal failure. *N. Engl. J. Med.* 327, 1912–1918. doi: 10.1056/nejm199212313272704

Cuffe, J. S. M., Burgess, D. J., O'sullivan, L., Singh, R. R., and Moritz, K. M. (2016). Maternal corticosterone exposure in the mouse programs sex-specific renal adaptations in the renin–angiotensin–aldosterone system in 6-month offspring. *Physiol. Rep.* 4:e12754. doi: 10.14814/phy2.12754

Dagan, A., Kwon, H. M., Dwarakanath, V., and Baum, M. (2008). Effect of renal denervation on prenatal programming of hypertension and renal tubular transporter abundance. *Am. J. Physiol. Renal Physiol.* 295, F29–F34.

Denic, A., Mathew, J., Lerman, L. O., Lieske, J. C., Larson, J. J., Alexander, M. P., et al. (2017). Single-nephron glomerular filtration rate in healthy adults. *N. Engl. J. Med.* 376, 2349–2357.

Denton, K. M., and Anderson, W. P. (1994). Intrarenal haemodynamic and glomerular responses to inhibition of nitric oxide formation in rabbits. *J. Physiol.* 475, 159–167. doi: 10.1113/jphysiol.1994.sp020057

Douglas-Denton, R., Moritz, K. M., Bertram, J. F., and Wintour, E. M. (2002). Compensatory renal growth after unilateral nephrectomy in the ovine fetus. *J. Am. Soc. Nephrol.* 13, 406–410.

Eddy, A. A. (1994). Experimental insights into the tubulointerstitial disease accompanying primary glomerular lesions. *J. Am. Soc. Nephrol.* 5, 1273–1287.

El-Sadek, A. E., Behery, E. G., Azab, A. A., Kamal, N. M., Salama, M. A., Abdulghany, W. E., et al. (2016). Arginine dimethylation products in pediatric patients with chronic kidney disease. *Ann. Med. Surg.* 9, 22–27. doi: 10.1016/j.amsu.2016.05.017

Fehrman-Ekholm, I., Duner, F., Brink, B., Tyden, G., and Elinder, C. G. (2001). No evidence of accelerated loss of kidney function in living kidney donors: results from a cross-sectional follow-up. *Transplantation* 72, 444–449. doi: 10.1097/00007890-200108150-00015

Fesler, P., Mourad, G., Cailar, G. D., Ribstein, J., and Mimran, A. (2015). Arterial stiffness: an independent determinant of adaptive glomerular hyperfiltration after kidney donation. *Am. J. Physiol. Renal Physiol.* 308, F567–F571.

Fleck, C., Schweitzer, F., Karge, E., Busch, M., and Stein, G. (2003). Serum concentrations of asymmetric (ADMA) and symmetric (SDMA) dimethylarginine in patients with chronic kidney diseases. *Clin. Chim. Acta* 336, 1–12. doi: 10.1016/s0009-8981(03)00338-3

Fong, D., Denton, K. M., Moritz, K. M., Evans, R., and Singh, R. R. (2014). Compensatory responses to nephron deficiency: adaptive or maladaptive? *Nephrology* 19, 119–128. doi: 10.1111/nep.12198

Furukawa, K., Ninomiya, I., Shimizu, J., Wada, T., and Matsuura, Y. (1997). Renal sympathetic nerve activity and the weight of the remaining kidney in unilateral nephrectomized rats. *J. Auton. Nerv. Syst.* 63, 91–100. doi: 10.1016/s0165-1838(96)00137-3

Gadalean, F., Kaycsa, A., Gluhovschi, G., Velciov, S., Gluhovschi, C., Bob, F., et al. (2013). Is the urinary biomarkers assessment a non-invasive approach to tubular lesions of the solitary kidney? *Renal Failure* 35, 1358–1364. doi: 10.3109/0886022x.2013.828367

Galla, J. H., Klein-Robbenhaar, T., and Hayslett, J. P. (1974). Influence of age on the compensatory response in growth and function to unilateral nephrectomy. *Yale J. Biol. Med.* 47, 218–226.

Gattone, V. H., Evan, A. P., Overhage, J. M., and Severs, W. B. (1990). Developing renal innervation in the spontaneously hypertensive rat: evidence for a role of the sympathetic nervous system in renal damage. *J. Hypertens.* 8:423. doi: 10.1097/00004872-199005000-00005

Geraci, S., Chacon-Caldera, J., Cullen-Mcewen, L., Schad, L. R., Sticht, C., Puelles, V. G., et al. (2017). Combining new tools to assess renal function and morphology: a holistic approach to study the effects of aging and a congenital nephron deficit. *Am. J. Physiol. Renal Physiol.* 313, F576–F584.

Grassi, G., Quarti-Trevano, F., Seravalle, G., Arenare, F., Volpe, M., Furiani, S., et al. (2011). Early sympathetic activation in the initial clinical stages of chronic renal failure. *Hypertension* 57, 846–851. doi: 10.1161/hypertensionaha.110.164780

Greenberg, J. H., Abraham, A. G., Xu, Y., Schelling, J. R., Feldman, H. I., Sabbisetti, V. S., et al. (2020). Plasma biomarkers of tubular injury and inflammation are associated with chronic kidney disease progression in children. *J. Am. Soc. Nephrol.* 31, 1067–1077.

Greenberg, J. H., Kakajiwala, A., Parikh, C. R., and Furth, S. (2018). Emerging biomarkers of chronic kidney disease in children. *Pediatr. Nephrol.* 33, 925–933. doi: 10.1007/s00467-017-3701-9

Grigore, D., Ojeda, N. B., Robertson, E. B., Dawson, A. S., Huffman, C. A., Bourassa, E. A., et al. (2007). Placental insufficiency results in temporal alterations in the renin angiotensin system in male hypertensive growth restricted offspring. *Am. J. Physiol. Regul. Integr. Comp. Physiol.* 293, R804–R811.

Grisk, O., Rose, H.-J., Lorenz, G., and Rettig, R. (2002). Sympathetic-renal interaction in chronic arterial pressure control. *Am. J. Physiol. Regul. Integr. Comp. Physiol.* 283, R441–R450.

Hall, J. E., Guyton, A. C., Salgado, H. C., Mccaa, R. E., and Balfe, J. W. (1978). Renal hemodynamics in acute and chronic angiotensin II hypertension. *Am. J. Physiol. Renal Physiol.* 235, F174–F179.

Harrap, S. B., Mirakian, C., Datodi, S. R., and Lever, A. F. (1994). Blood pressure and lifespan following brief ACE inhibitor treatment in young spontaneously hypertensive rats. *Clin. Exp. Pharmacol. Physiol.* 21, 125–127. doi: 10.1111/j.1440-1681.1994.tb02479.x

Hayslett, J. P., Kashgarian, M., and Epstein, F. H. (1968). Functional correlates of compensatory renal hypertrophy. *J. Clin. Investig.* 47, 774–782. doi: 10.1172/jci105772

Hostetter, T. H., Olson, J. L., Rennke, H. G., Venkatachalam, M. A., and Brenner, B. M. (1981). Hyperfiltration in remnant nephrons: a potentially adverse response to renal ablation. *Am. J. Physiol.* 241, F85–F93.

Hsu, C. N., Lee, C. T., Huang, L. T., and Tain, Y. L. (2015). Aliskiren in early postnatal life prevents hypertension and reduces asymmetric dimethylarginine in offspring exposed to maternal caloric restriction. *J. Renin. Angiotensin. Aldosterone Syst.* 16, 506–513. doi: 10.1177/1470320313514123

Ibrahim, H. N., Foley, R., Tan, L., Rogers, T., Bailey, R. F., Guo, H., et al. (2009). Long-term consequences of kidney donation. *N. Engl. J. Med.* 360, 459–469.

Johnson, R. J., Alpers, C. E., Yoshimura, A., Lombardi, D., Pritzl, P., Floege, J., et al. (1992). Renal injury from angiotensin II-mediated hypertension. *Hypertension* 19, 464–474. doi: 10.1161/01.hyp.19.5.464

Kanzaki, G., Puelles, V. G., Cullen-Mcewen, L. A., Hoy, W. E., Okabayashi, Y., Tsuboi, N., et al. (2017). New insights on glomerular hyperfiltration: a Japanese autopsy study. *JCI Insight* 2:e94334.

Kasiske, B. L., Ma, J. Z., Louis, T. A., and Swan, S. K. (1995). Long-term effects of reduced renal mass in humans. *Kidney Int.* 48, 814–819. doi: 10.1038/ki.1995.355

Katoh, T., Takahashi, K., Klahr, S., Reyes, A. A., and Badr, K. F. (1994). Dietary supplementation with L-arginine ameliorates glomerular hypertension in rats with subtotal nephrectomy. *J. Am. Soc. Nephrol.* 4, 1690–1694.

Kees-Folts, D., Sadow, J. L., and Schreiner, G. F. (1994). Tubular catabolism of albumin is associated with the release of an inflammatory lipid. *Kidney Int.* 45, 1697–1709. doi: 10.1038/ki.1994.222

Kett, M. M., and Denton, K. M. (2011). Renal programming: cause for concern? *Am. J. Physiol. Regul. Integr. Comp. Physiol.* 300, R791–R803.

Kielstein, J. T., Boger, R. H., Bode-Boger, S. M., Frolich, J. C., Haller, H., Ritz, E., et al. (2002). Marked increase of asymmetric dimethylarginine in patients with incipient primary chronic renal disease. *J. Am. Soc. Nephrol.* 13, 170–176.

Kim, S., Heo, N. J., Jung, J. Y., Son, M. J., Jang, H. R., Lee, J. W., et al. (2010). Changes in the sodium and potassium transporters in the course of chronic renal failure. *Nephron Physiol.* 115, 31–41.

Kolvek, G., Podracka, L., Rosenberger, J., Stewart, R. E., Van Dijk, J. P., and Reijneveld, S. A. (2014). Solitary functioning kidney in children - a follow-up study. *Kidney Blood Press. Res.* 39, 272–278. doi: 10.1159/000355804

Krohn, A. G., Ogden, D. A., and Holmes, J. H. (1966). Renal function in 29 healthy adults before and after nephrectomy. *JAMA* 196, 322–324. doi: 10.1001/jama.196.4.322

Krum, H., Schlaich, M. P., Sobotka, P. A., Böhm, M., Mahfoud, F., Rocha-Singh, K., et al. (2014). Percutaneous renal denervation in patients with treatment-resistant hypertension: final 3-year report of the Symplicity HTN-1 study. *Lancet* 383, 622–629. doi: 10.1016/s0140-6736(13)62192-3

Kummer, S., Von Gersdorff, G., Kemper, M. J., and Oh, J. (2012). The influence of gender and sexual hormones on incidence and outcome of chronic kidney disease. *Pediatr. Nephrol.* 27, 1213–1219. doi: 10.1007/s00467-011-1963-1

La Scola, C., Ammenti, A., Puccio, G., Lega, M. V., De Mutiis, C., Guiducci, C., et al. (2016). Congenital solitary kidney in children: size matters. *J. Urol.* 196, 1250–1256. doi: 10.1016/j.juro.2016.03.173

La Scola, C., Marra, G., Ammenti, A., Pasini, A., Taroni, F., Bertulli, C., et al. (2020). Born with a solitary kidney: at risk of hypertension. *Pediatr. Nephrol.* [Epub ahead of print].

Lankadeva, Y. R., Singh, R. R., Moritz, K. M., Parkington, H. C., Denton, K. M., and Tare, M. (2015). Renal dysfunction is associated with a reduced contribution of nitric oxide and enhanced vasoconstriction after a congenital renal mass reduction in sheep. *Circulation* 131, 280–288. doi: 10.1161/circulationaha.114.013930

Lankadeva, Y. R., Singh, R. R., Tare, M., Moritz, K. M., and Denton, K. M. (2014). Loss of a kidney during fetal life: long-term consequences and lessons learned. *Am. J. Physiol. Renal Physiol.* 306, F791–F800.

Lappe, R. W., Henry, D. P., and Willis, L. R. (1982). Contribution of renal sympathetic nerves to the urinary excretion of norepinephrine. *Can. J. Physiol. Pharmacol.* 60, 1067–1072. doi: 10.1139/y82-153

Larsson, L., Aperia, A., and Wilton, P. (1980). Effect of normal development on compensatory renal growth. *Kidney Int.* 18, 29–35. doi: 10.1038/ki.1980.107

Layton, A. T., Edwards, A., and Vallon, V. (2017). Adaptive changes in GFR, tubular morphology, and transport in subtotal nephrectomized kidneys: modeling and analysis. *Am. J. Physiol. Renal Physiol.* 313, F199–F209.

Lenihan, C. R., Busque, S., Derby, G., Blouch, K., Myers, B. D., and Tan, J. C. (2015). Longitudinal study of living kidney donor glomerular dynamics after nephrectomy. *J. Clin. Investig.* 125, 1311–1318. doi: 10.1172/jci78885

Lewis, E. J., Hunsicker, L. G., Bain, R. P., and Rohde, R. D. (1993). The effect of angiotensin-converting-enzyme inhibition on diabetic nephropathy. *N. Engl. J. Med.* 329, 1456–1462.

Li, Z. Y., Chen, Y. M., Qiu, L. Q., Chen, D. Q., Hu, C. G., Xu, J. Y., et al. (2019). Prevalence, types, and malformations in congenital anomalies of the kidney and urinary tract in newborns: a retrospective hospital-based study. *Ital. J. Pediatr.* 45:50.

MacKay, K., Striker, L. J., Stauffer, J. W., Agodoa, L. Y., and Striker, G. E. (1990). Relationship of glomerular hypertrophy and sclerosis: studies in SV40 transgenic mice. *Kidney Int.* 37, 741–748. doi: 10.1038/ki.1990.41

Mallipattu, S. K., and He, J. C. (2016). The podocyte as a direct target for treatment of glomerular disease? *Am. J. Physiol. Renal Physiol.* 311, F46–F51.

Maluf, N. S. R. (1997). On the enlargement of the normal congenitally solitary kidney. *Br. J. Urol.* 79, 836–841. doi: 10.1046/j.1464-410x.1997.00215.x

Manning, J., and Vehaskari, V. M. (2005). Postnatal modulation of prenatally programmed hypertension by dietary Na and ACE inhibition. *Am. J. Physiol. Regul. Integr. Comp. Physiol.* 288, R80–R84.

Mansuri, A., Legan, S. K., Jain, J., Alhamoud, I., Gattineni, J., and Baum, M. (2017). Effect of renal denervation on urine angiotensinogen excretion in prenatally programmed rats. *Physiol. Rep.* 5:e13482. doi: 10.14814/phy2.13482

Marzuillo, P., Guarino, S., Grandone, A., Di Somma, A., Della Vecchia, N., Esposito, T., et al. (2017). Outcomes of a cohort of prenatally diagnosed and early enrolled patients with congenital solitary functioning kidney. *J. Urol.* 198, 1153–1158. doi: 10.1016/j.juro.2017.05.076

Marzuillo, P., Guarino, S., Grandone, A., Di Somma, A., Diplomatico, M., Rambaldi, P. F., et al. (2019). Congenital solitary kidney size at birth could predict reduced eGFR levels later in life. *J. Perinatol.* 39, 129–134. doi: 10.1038/s41372-018-0260-2

Mauriello, A., Rovella, V., Anemona, L., Servadei, F., Giannini, E., Bove, P., et al. (2015). Increased sympathetic renal innervation in hemodialysis patients is the anatomical substrate of sympathetic hyperactivity in end-stage renal disease. *J. Am. Heart Assoc. Cardiovasc. Cerebrovasc. Dis.* 4:e002426.

Mavinkurve-Groothuis, A. M., Van De Kracht, F., Westland, R., Van Wijk, J. A., Loonen, J. J., and Schreuder, M. F. (2016). Long-term follow-up of blood pressure and glomerular filtration rate in patients with a solitary functioning kidney: a comparison between Wilms tumor survivors and nephrectomy for other reasons. *Pediatr. Nephrol.* 31, 435–441. doi: 10.1007/s00467-015-3215-2

Monu, S. R., Ren, Y., Masjoan-Juncos, J. X., Kutskill, K., Wang, H., Kumar, N., et al. (2018). Connecting tubule glomerular feedback mediates tubuloglomerular feedback resetting after unilateral nephrectomy. *Am. J. Physiol. Renal Physiol.* 315, F806–F811.

Monument, M. J., and Smith, F. G. (2003). Age-dependent effects of captopril on the arterial baroreflex control of heart rate in conscious lambs. *Exp. Physiol.* 88, 761–768. doi: 10.1113/eph8802602

Moritz, K. M., Jefferies, A., Wong, J., Marelyn Wintour, E., and Dodic, M. (2005). Reduced renal reserve and increased cardiac output in adult female sheep uninephrectomized as fetuses. *Kidney Int.* 67, 822–828. doi: 10.1111/j.1523-1755.2005.00147.x

Moritz, K. M., Wintour, E. M., Black, M. J., Bertram, J. F., and Caruana, G. (2008). Factors influencing mammalian kidney development: implications for health in adult life. *Adv. Anat. Embryol. Cell. Biol.* 196, 1–78.

Moritz, K. M., and Wintour, E. M. (1999). Funtional development of the meso- and the metanephros. *Pediatr. Nephrol.* 13, 171–178. doi: 10.1007/s004670050587

Moritz, K. M., Wintour, E. M., and Dodic, M. (2002). Fetal uninephrectomy leads to postnatal hypertension and compromised renal function. *Hypertension* 39, 1071–1076. doi: 10.1161/01.hyp.0000019131.77075.54

Mount, P. F., and Power, D. A. (2006). Nitric oxide in the kidney: functions and regulation of synthesis. *Acta Physiol.* 187, 433–446. doi: 10.1111/j.1748-1716.2006.01582.x

Müller-Suur, R., Norlén, B.-J., Erik, A., Persson, G., Müller-Suur, C., and Forsmark, B. (1980). Resetting of tubuloglomerular feedback in rat kidneys after unilateral nephrectomy. *Kidney Int.* 18, 48–57. doi: 10.1038/ki.1980.109

Mulroney, S. E., Woda, C., Johnson, M., and Pesce, C. (1999). Gender differences in renal growth and function after uninephrectomy in adult rats. *Kidney Int.* 56, 944–953. doi: 10.1046/j.1523-1755.1999.00647.x

Muzaale, A. D., Massie, A. B., Wang, M. C., Montgomery, R. A., Mcbride, M. A., Wainright, J. L., et al. (2014). Risk of end-stage renal disease following live kidney donation. *JAMA* 311, 579–586.

Nagasu, H., Satoh, M., Kidokoro, K., Nishi, Y., Channon, K. M., Sasaki, T., et al. (2012). Endothelial dysfunction promotes the transition from compensatory renal hypertrophy to kidney injury after unilateral nephrectomy in mice. *Am. J. Physiol. Renal Physiol.* 302, F1402–F1408.

Nagata, M., Schärer, K., and Kriz, W. (1992). Glomerular damage after uninephrectomy in young rats. I. Hypertrophy and distortion of capillary architecture. *Kidney Int.* 42, 136–147. doi: 10.1038/ki.1992.271

Niemi, M., and Mandelbrot, D. A. (2014). The outcomes of living kidney donation from medically complex donors: implications for the donor and the recipient. *Curr. Transpl. Rep.* 1, 1–9. doi: 10.1007/s40472-013-0001-6

Nyengaard, J. R. (1993). Number and dimensions of rat glomerular capillaries in normal development and after nephrectomy. *Kidney Int.* 43, 1049–1057. doi: 10.1038/ki.1993.147

Palloshi, A., Fragasso, G., Piatti, P., Monti, L. D., Setola, E., Valsecchi, G., et al. (2004). Effect of oral l-arginine on blood pressure and symptoms and endothelial function in patients with systemic hypertension, positive exercise tests, and normal coronary arteries. *Am. J. Cardiol.* 93, 933–935. doi: 10.1016/j.amjcard.2003.12.040

Poggiali, I. V., Simões, E., Silva, A. C., Vasconcelos, M. A., Dias, C. S., Gomes, I. R., et al. (2019). A clinical predictive model of renal injury in children with congenital solitary functioning kidney. *Pediatr. Nephrol.* 34, 465–474. doi: 10.1007/s00467-018-4111-3

Pollock, C. A., Bostrom, T. E., Dyne, M., Gyory, A. Z., and Field, M. J. (1992). Tubular sodium handling and tubuloglomerular feedback in compensatory renal hypertrophy. *Pflug. Arch.* 420, 159–166. doi: 10.1007/bf00374985

Prevot, A., Mosig, D., and Guignard, J. P. (2002). The effects of losartan on renal function in the newborn rabbit. *Pediatr. Res.* 51, 728–732. doi: 10.1203/01.pdr.0000015103.96800.88

Ravani, P., Tripepi, G., Malberti, F., Testa, S., Mallamaci, F., and Zoccali, C. (2005). Asymmetrical dimethylarginine predicts progression to dialysis and death in patients with chronic kidney disease: a competing risks modeling approach. *J. Am. Soc. Nephrol.* 16, 2449–2455. doi: 10.1681/asn.2005010076

Reyes, A. A., Karl, I. E., Kissane, J., and Klahr, S. (1993). L-arginine administration prevents glomerular hyperfiltration and decreases proteinuria in diabetic rats. *J. Am. Soc. Nephrol.* 4, 1039–1045.

Robillard, J. E., Weismann, D. N., Gomez, R. A., Ayres, N. A., Lawton, W. J., and Vanorden, D. E. (1983). Renal and adrenal responses to converting-enzyme inhibition in fetal and newborn life. *Am. J. Physiol.* 244, R249–R256.

Rojas-Canales, D. M., Li, J. Y., Makuei, L., and Gleadle, J. M. (2019). Compensatory renal hypertrophy following nephrectomy: when and how? *Nephrology* 24, 1225–1232. doi: 10.1111/nep.13578

Romero, C. A., Orias, M., and Weir, M. R. (2015). Novel RAAS agonists and antagonists: clinical applications and controversies. *Nat. Rev. Endocrinol.* 11, 242–252. doi: 10.1038/nrendo.2015.6

Salmond, R., and Seney, F. D. Jr. (1991). Reset tubuloglomerular feedback permits and sustains glomerular hyperfunction after extensive renal ablation. *Am. J. Physiol.* 260, F395–F401.

Sanna-Cherchi, S., Ravani, P., Corbani, V., Parodi, S., Haupt, R., Piaggio, G., et al. (2009). Renal outcome in patients with congenital anomalies of the kidney and urinary tract. *Kidney Int.* 76, 528–533.

Schmidt, R. J., and Baylis, C. (2000). Total nitric oxide production is low in patients with chronic renal disease. *Kidney Int.* 58, 1261–1266. doi: 10.1046/j.1523-1755.2000.00281.x

Schreuder, M. F. (2017). Life with one kidney. *Pediatr. Nephrol.* 33, 595–604. doi: 10.1007/s00467-017-3686-4

Schreuder, M. F., Langemeijer, M. E., Bokenkamp, A., Delemarre-Van De Waal, H. A., and Van Wijk, J. A. (2008). Hypertension and microalbuminuria in children with congenital solitary kidneys. *J. Paediatr. Child Health* 44, 363–368. doi: 10.1111/j.1440-1754.2008.01315.x

Schreuder, M. F., Westland, R., and Van Wijk, J. A. (2009). Unilateral multicystic dysplastic kidney: a meta-analysis of observational studies on the incidence, associated urinary tract malformations and the contralateral kidney. *Nephrol. Dial. Transplant.* 24, 1810–1818. doi: 10.1093/ndt/gfn777

Sherman, R. C., and Langley-Evans, S. C. (1998). Early administration of angiotensin-converting enzyme inhibitor captopril, prevents the development of hypertension programmed by intrauterine exposure to a maternal low-protein diet in the rat. *Clin. Sci.* 94, 373–381. doi: 10.1042/cs0940373

Sherman, R. C., and Langley-Evans, S. C. (2000). Antihypertensive treatment in early postnatal life modulates prenatal dietary influences upon blood pressure in the rat. *Clin. Sci.* 98, 269–275. doi: 10.1042/cs0980269

Shirley, D. G., and Walter, S. J. (1991). Acute and chronic changes in renal function following unilateral nephrectomy. *Kidney Int.* 40, 62–68. doi: 10.1038/ki.1991.180

Sigmon, D. H., Gonzalez-Feldman, E., Cavasin, M. A., Potter, D. L., and Beierwaltes, W. H. (2004). Role of nitric oxide in the renal hemodynamic response to unilateral nephrectomy. *J. Am. Soc. Nephrol.* 15, 1413–1420. doi: 10.1097/01.asn.0000130563.67384.81

Singh, R. R., Cuffe, J. S., and Moritz, K. M. (2012). Short- and long-term effects of exposure to natural and synthetic glucocorticoids during development. *Clin. Exp. Pharmacol. Physiol.* 39, 979–989. doi: 10.1111/1440-1681.12009

Singh, R. R., Denton, K. M., Bertram, J. F., Jefferies, A. J., Head, G. A., Lombardo, P., et al. (2009). Development of cardiovascular disease due to renal insufficiency in male sheep following fetal unilateral nephrectomy. *J. Hypertens.* 27, 386–396. doi: 10.1097/hjh.0b013e32831bc778

Singh, R. R., Denton, K. M., Bertram, J. F., Jefferies, A. J., and Moritz, K. M. (2010). Reduced nephron endowment due to fetal uninephrectomy impairs renal sodium handling in male sheep. *Clin. Sci.* 118, 669–680. doi: 10.1042/cs20090479

Singh, R. R., Easton, L. K., Booth, L. C., Schlaich, M. P., Head, G. A., Moritz, K. M., et al. (2016). Renal nitric oxide deficiency and chronic kidney disease in young sheep born with a solitary functioning kidney. *Sci. Rep.* 6:26777.

Singh, R. R., Mcardle, Z. M., Iudica, M., Easton, L. K., Booth, L. C., May, C. N., et al. (2019). Sustained decrease in blood pressure and reduced anatomical and functional reinnervation of renal nerves in hypertensive sheep 30 months after catheter-based renal denervation. *Hypertension* 73, 718–727. doi: 10.1161/hypertensionaha.118.12250

Singh, R. R., Moritz, K. M., Wintour, E. M., Jefferies, A. J., Iqbal, J., Bertram, J. F., et al. (2011). Fetal uninephrectomy in male sheep alters the systemic and renal responses to angiotensin II infusion and AT1R blockade. *Am. J. Physiol. Renal Physiol.* 301, F319–F326.

Singh, R. R., Sajeesh, V., Booth, L. C., Mcardle, Z., May, C. N., Head, G. A., et al. (2017). Catheter-based renal denervation exacerbates blood pressure fall during hemorrhage. *J. Am. Coll. Cardiol.* 69, 951–964. doi: 10.1016/j.jacc.2016.12.014

Skov, K., Nyengaard, J. R., Korsgaard, N., and Mulvany, M. J. (1994). Number and size of renal glomeruli in spontaneously hypertensive rats. *J. Hypertens.* 12, 1373–1376.

Snoek, R., De Heus, R., De Mooij, K. J., Pistorius, L. R., Lilien, M. R., Lely, A. T., et al. (2018). Assessing nephron hyperplasia in fetal congenital solitary functioning kidneys by measuring renal papilla number. *Am. J. Kidney Dis.* 72, 465–467. doi: 10.1053/j.ajkd.2018.03.018

Srivastava, T., Alon, U. S., Cudmore, P. A., Tarakji, B., Kats, A., Garola, R. E., et al. (2014a). Cyclooxygenase-2, prostaglandin E2, and prostanoid receptor EP2 in fluid flow shear stress-mediated injury in the solitary kidney. *Am. J. Physiol. Renal Physiol.* 307, F1323–F1333.

Srivastava, T., Celsi, G. E., Sharma, M., Dai, H., Mccarthy, E. T., Ruiz, M., et al. (2014b). Fluid flow shear stress over podocytes is increased in the solitary kidney. *Nephrol. Dial. Transplant.* 29, 65–72. doi: 10.1093/ndt/gft387

Srivastava, T., Ju, W., Milne, G. L., Rezaiekhaligh, M. H., Staggs, V. S., Alon, U. S., et al. (2020). Urinary prostaglandin E2 is a biomarker of early adaptive hyperfiltration in solitary functioning kidney. *Prostaglandins Other Lipid Mediat.* 146:106403. doi: 10.1016/j.prostaglandins.2019.106403

Srivastava, T., Mccarthy, E. T., Sharma, R., Cudmore, P. A., Sharma, M., Johnson, M. L., et al. (2010). Prostaglandin E(2) is crucial in the response of podocytes to fluid flow shear stress. *J. Cell Commun. Signal.* 4, 79–90. doi: 10.1007/s12079-010-0088-9

Srivastava, T., Thiagarajan, G., Alon, U. S., Sharma, R., El-Meanawy, A., Mccarthy, E. T., et al. (2017). Role of biomechanical forces in hyperfiltration-mediated glomerular injury in congenital anomalies of the kidney and urinary tract. *Nephrol. Dial. Transplant.* 32, 759–765. doi: 10.1093/ndt/gfw430

Stefanowicz, J., Owczuk, R., Kaluzynska, B., Aleksandrowicz, E., Owczarzak, A., Adamkiewicz-Drozynska, E., et al. (2012). Renal function and solitary kidney disease: wilms tumour survivors versus patients with unilateral renal agenesis. *Kidney Blood Press. Res.* 35, 174–181. doi: 10.1159/000332083

Symplicity, H. T. N. I. (2011). Catheter-based renal sympathetic denervation for resistant hypertension: durability of blood pressure reduction out to 24 months. *Hypertension* 57, 911–917. doi: 10.1161/hypertensionaha.110.163014

Tain, Y.-L., Freshour, G., Dikalova, A., Griendling, K., and Baylis, C. (2007). Vitamin E reduces glomerulosclerosis, restores renal neuronal NOS, and suppresses oxidative stress in the 5/6 nephrectomized rat. *Am. J. Physiol. Renal Physiol.* 292, F1404–F1410.

Tain, Y. L., Luh, H., Lin, C. Y., and Hsu, C. N. (2016). Incidence and risks of congenital anomalies of kidney and urinary tract in newborns: a population-based case-control study in Taiwan. *Medicine* 95:e2659. doi: 10.1097/md.0000000000002659

Taranta-Janusz, K., Wasilewska, A., Stypulkowska, J., and Sutula, M. (2012). Osteopontin and symmetric dimethylarginine plasma levels in solitary functioning kidney in children. *Acta Paediatr.* 101, e369–e372. doi: 10.1111/j.1651-2227.2012.02690.x

Taranta-Janusz, K., Zalewska-Szajda, B., Gościk, E., Chojnowska, S., Dmochowska, M., Pszczółkowska, M., et al. (2014). New tubular injury markers in children with a solitary functioning kidney. *Pediatr. Nephrol.* 29, 1599–1605. doi: 10.1007/s00467-014-2802-y

Van Den Belt, S. M., Heerspink, H. J. L., Gracchi, V., De Zeeuw, D., Wuhl, E., Schaefer, F., et al. (2018). Early proteinuria lowering by angiotensin-converting enzyme inhibition predicts renal survival in children with CKD. *J. Am. Soc. Nephrol.* 29, 2225–2233. doi: 10.1681/asn.2018010036

Van Vuuren, S. H., Sol, C. M., Broekhuizen, R., Lilien, M. R., Oosterveld, M. J. S., Nguyen, T. Q., et al. (2012a). Compensatory growth of congenital solitary kidneys in pigs reflects increased nephron numbers rather than hypertrophy. *PLoS One* 7:e49735. doi: 10.1371/journal.pone.0049735

Van Vuuren, S. H., Van Der Doef, R., Cohen-Overbeek, T. E., Goldschmeding, R., Pistorius, L. R., and De Jong, T. P. (2012b). Compensatory enlargement of a solitary functioning kidney during fetal development. *Ultrasound Obstet. Gynecol.* 40, 665–668. doi: 10.1002/uog.11168

Velaphi, S. C., Despain, K., Roy, T., and Rosenfeld, C. R. (2007). The renin-angiotensin system in conscious newborn sheep: metabolic clearance rate and activity. *Pediatr. Res.* 61, 681–686. doi: 10.1203/pdr.0b013e3180534252

Vinturache, A. E., and Smith, F. G. (2016). Renal effects of angiotensin II in the newborn period: role of type 1 and type 2 receptors. *BMC Physiol.* 16:3. doi: 10.1186/s12899-016-0022-3

Walton, S. L., Bielefeldt-Ohmann, H., Singh, R. R., Li, J., Paravicini, T. M., Little, M. H., et al. (2017). Prenatal hypoxia leads to hypertension, renal renin-angiotensin system activation and exacerbates salt-induced pathology in a sex-specific manner. *Sci. Rep.* 7:8241.

Wang, M., Han, W., Zhang, M., Fang, W., Zhai, X., Guan, S., et al. (2018). Long-term renal sympathetic denervation ameliorates renal fibrosis and delays the onset of hypertension in spontaneously hypertensive rats. *Am. J. Transl. Res.* 10, 4042–4053.

Wang, M. K., Gaither, T., Phelps, A., Cohen, R., and Baskin, L. (2019). The incidence and durability of compensatory hypertrophy in pediatric patients with solitary kidneys. *Urology* 129, 188–193. doi: 10.1016/j.urology.2019.04.003

Wang, Y., Wang, Z., Wang, W., Ren, H., Zhang, W., and Chen, N. (2010). Analysis of factors associated with renal function in chinese adults with congenital solitary kidney. *Intern. Med.* 49, 2203–2209. doi: 10.2169/internalmedicine.49.3742

Wasilewska, A., Zoch-Zwierz, W., Jadeszko, I., Porowski, T., Biernacka, A., Niewiarowska, A., et al. (2006). Assessment of serum cystatin C in children with congenital solitary kidney. *Pediatr. Nephrol.* 21, 688–693. doi: 10.1007/s00467-006-0065-y

Westland, R., Kurvers, R. A., Van Wijk, J. A., and Schreuder, M. F. (2013a). Risk factors for renal injury in children with a solitary functioning kidney. *Pediatrics* 131, e478–e485. doi: 10.1542/peds.2012-2088

Westland, R., and Schreuder, M. F. (2014). Gender differences in solitary functioning kidney: do they affect renal outcome? *Pediatr. Nephrol.* 29, 2243–2244. doi: 10.1007/s00467-013-2473-0

Westland, R., Schreuder, M. F., Bokenkamp, A., Spreeuwenberg, M. D., and Van Wijk, J. A. (2011). Renal injury in children with a solitary functioning kidney–the KIMONO study. *Nephrol. Dial. Transplant.* 26, 1533–1541. doi: 10.1093/ndt/gfq844

Westland, R., Schreuder, M. F., Ket, J. C., and Van Wijk, J. A. (2013b). Unilateral renal agenesis: a systematic review on associated anomalies and renal injury. *Nephrol. Dial. Transplant.* 28, 1844–1855. doi: 10.1093/ndt/gft012

Westland, R., Schreuder, M. F., Van Der Lof, D. F., Vermeulen, A., Dekker-Van Der Meer, I. M., Bokenkamp, A., et al. (2014). Ambulatory blood pressure monitoring is recommended in the clinical management of children with a solitary functioning kidney. *Pediatr. Nephrol.* 29, 2205–2211. doi: 10.1007/s00467-014-2853-0

Woods, L. L. (1999). Neonatal uninephrectomy causes hypertension in adult rats. *Am. J. Physiol.* 276, R974–R978.

Woods, L. L., Ingelfinger, J. R., Nyengaard, J. R., and Rasch, R. (2001a). Maternal protein restriction suppresses the newborn renin-angiotensin system and programs adult hypertension in rats. *Pediatr. Res.* 49, 460–467. doi: 10.1203/00006450-200104000-00005

Woods, L. L., Weeks, D. A., and Rasch, R. (2001b). Hypertension after neonatal uninephrectomy in rats precedes glomerular damage. *Hypertension* 38, 337–342. doi: 10.1161/01.hyp.38.3.337

Wuhl, E., Trivelli, A., Picca, S., Litwin, M., Peco-Antic, A., Zurowska, A., et al. (2009). Strict blood-pressure control and progression of renal failure in children. *N. Engl. J. Med.* 361, 1639–1650. doi: 10.1056/nejmoa0902066

Wuhl, E., Van Stralen, K. J., Verrina, E., Bjerre, A., Wanner, C., Heaf, J. G., et al. (2013). Timing and outcome of renal replacement therapy in patients with congenital malformations of the kidney and urinary tract. *Clin. J. Am. Soc. Nephrol.* 8, 67–74. doi: 10.2215/cjn.03310412

Xu, Q., Wu, H., Zhou, L., Xie, J., Zhang, W., Yu, H., et al. (2019). The clinical characteristics of Chinese patients with unilateral renal agenesis. *Clin. Exp. Nephrol.* 23, 792–798. doi: 10.1007/s10157-019-01704-x

Zambaiti, E., Sergio, M., Baldanza, F., Corrado, C., Di Pace, M. R., and Cimador, M. (2019). Correlation between hypertrophy and risk of hypertension in congenital solitary functioning kidney. *Pediatr. Surg. Int.* 35, 167–174. doi: 10.1007/s00383-018-4389-z

Zoccali, C., Bode-Boger, S., Mallamaci, F., Benedetto, F., Tripepi, G., Malatino, L., et al. (2001). Plasma concentration of asymmetrical dimethylarginine and mortality in patients with end-stage renal disease: a prospective study. *Lancet* 358, 2113–2117. doi: 10.1016/s0140-6736(01)07217-8

Conflict of Interest: The authors declare that the research was conducted in the absence of any commercial or financial relationships that could be construed as a potential conflict of interest.

frontiers in Medicine

ORIGINAL RESEARCH
published: 03 July 2020
doi: 10.3389/fmed.2020.00309

Estimation of Renal Function Using Unenhanced Computed Tomography in Upper Urinary Tract Stones Patients

Jiali Li[1†], Yang Xun[2†], Cong Li[2], Yunfeng Han[3], Yaqi Shen[1], Xuemei Hu[1], Daoyu Hu[1], Zheng Liu[2], Shaogang Wang[2*] and Zhen Li[1*]*

[1] Department of Radiology, Tongji Hospital, Tongji Medical College, Huazhong University of Science and Technology, Wuhan, China, [2] Department of Urology, Tongji Hospital, Tongji Medical College, Huazhong University of Science and Technology, Wuhan, China, [3] Department of Radiology and Nuclear Medicine, Tongji Hospital, Tongji Medical College, Huazhong University of Science and Technology, Wuhan, China

OPEN ACCESS

Edited by:
Jennifer Sullivan,
Augusta University, United States

Reviewed by:
Florian Grahammer,
University Medical Center Hamburg-Eppendorf, Germany
Ahmed A. Elmarakby,
Augusta University, United States

***Correspondence:**
Zheng Liu
lz2013tj@163.com
Shaogang Wang
sgwangtjm@163.com
Zhen Li
zhenli@hust.edu.cn

[†] These authors have contributed equally to this work and share first authorship

Specialty section:
This article was submitted to Nephrology, a section of the journal Frontiers in Medicine

Received: 17 January 2020
Accepted: 28 May 2020
Published: 03 July 2020

Citation:
Li J, Xun Y, Li C, Han Y, Shen Y, Hu X, Hu D, Liu Z, Wang S and Li Z (2020) Estimation of Renal Function Using Unenhanced Computed Tomography in Upper Urinary Tract Stones Patients. Front. Med. 7:309. doi: 10.3389/fmed.2020.00309

Objectives: The aim of this study was to determine whether unenhanced computed tomography (CT) imaging can estimate differential renal function (DRF) in patients with chronic unilateral obstructive upper urinary tract stones.

Materials and Methods: This was a single-center retrospective study of 76 patients. All the patients underwent unenhanced CT and nuclear renography (RG) at an interval of 4 to 6 weeks due to chronic unilateral obstructive urinary stones. Renal CT measurements (RCMs), including residual parenchymal volume (RPV) and volumetric CT texture analysis parameters, were obtained through a semiautomatic method. Percent RCMs were calculated and compared with renal function determined by RG.

Results: The strongest Pearson coefficient between percent RCM and DRF was reflected by RPV ($r = 0.957$, $P < 0.001$). Combinations of RPV and other parameters did not significantly improve the correlation compared with RPV alone ($r = 0.957$ vs. $r = 0.957$, 0.957, 0.887, 0.815, and 0.956 for combination with Hounsfield unit, parenchymal voxel, skewness, kurtosis, and entropy, respectively; all $P < 0.001$). Percent RPV was subsequently introduced into linear regression, and the equation $y = -2.66 + 1.07^* \times$ ($P < 0.001$) was derived to calculate predicted DRF. No statistically difference was found between predicted DRF using the equation and observed DRF according to RG ($P = 0.959$).

Conclusion: Unenhanced CT imaging can estimate DRF in patients with chronic unilateral obstructive upper urinary tract stones, and RG might not be necessary as a conventional method in clinical.

Keywords: unenhanced CT, differential renal function, residual parenchymal volume, CT texture analysis, upper urinary tract stones

INTRODUCTION

Urolithiasis is the most common disease that encountered in urology departments, and affects 1–20% of the adult population. In developed countries, such as Canada, Sweden and the United States, the prevalence of urolithiasis is greater than 10% (1). In developing countries, take China for example, kidney stones affect approximately one in 17 adults, corresponding to the prevalence of 5.8–6.5% in men and 5.1% in women (2). Owing to the lack of periodic physical examination, a large number of patients experience acute or chronic obstruction and renal failure. Estimation of differential renal function (DRF), which reflects the contribution of a single kidney to overall renal function, of the obstructed kidney is vital to decide whether it is worth saving. A cut-off value of 15% split DRF is commonly used by urologists when counseling patients to undergo lithotripsy vs. nephrectomy (3).

Nuclear renography (RG) is seen as the standard imaging modality for evaluating differential renal function. However, its clinical applications are limited due to some disadvantages (4, 5), including exposure to radiation, operator dependence, high costs, and prolonged examination time. In contrast, wide popularity and short acquisition time of unenhanced computed tomography (CT) make it a first-line examination method for imaging patients with ureteral stones (6, 7). Hence, exploring the relationship between renal CT measurements (RCM) and DRF has been an active area. Nevertheless, the results of previous research may not be applicable to the populations with upper urinary tract stones, given that previous studies primarily focused on patients with ureteropelvic junction obstruction (UPJO) or included heterogeneous population with a wide range of causes of stones (8, 9). Furthermore, some studies may exposed patients to the risk for contrast nephropathy due to the use of iodinated contrast medium (10, 11). Therefore, the research that only focused on patients with upper urinary tract stones and based on unenhanced CT is valuable and urgently needed.

A major emerging trend in medical imaging research is CT texture analysis (CTTA), which is a novel technique used to assess internal structural heterogeneity by processing existing CT images (12). To our knowledge, few studies exploring the relevance of CTTA and DRF have been published. In the present study, residual parenchymal volume (RPV) and CTTA parameters were obtained very readily and accurately by common software and techniques.

Therefore, this study, which focused on patients with chronic unilateral obstructive upper urinary tract stones, first aimed to correlate percent RPV measured by unenhanced CT with DRF estimated by RG, and second aimed to explore applications of volumetric CTTA in estimating DRF.

MATERIALS AND METHODS

Patients

This retrospective study was conducted under the approval of the Ethics Committee of Tongji Medical College, Huazhong University of Science and Technology (2019S1035) and the informed consent was waived. Data from 112 patients with upper urinary tract stones, who underwent unenhanced multi-detector CT (MDCT) and nuclear RG at an interval of 4–6 weeks between April 2016 and May 2018, were reviewed. Inclusion criteria were as follows: (a) the age was more than 18 years; (b) patients had chronic unilateral obstructive upper urinary tract stones but with a normal contralateral kidney; (c) the stone history was more than 2 months. Exclusion criteria were as follows: (a) patents with a solitary kidney; (b) males with a serum creatinine level $>$ 104 μmoI/L, females with a serum creatinine level $>$ 84 μmoI/L; (c) patients with acute obstruction which were found on contrast-enhanced CT; (d) patents with serious urinary infection; (e) patents with obstruction due to ureteral stricture or ureteropelvic junction obstruction (UPJO). According to the inclusion and exclusion criteria, 76 patients were ultimately included in this study.

Unenhanced CT

All patients underwent abdominal and pelvic CT examinations (Discovery CT 750, GE Medical Systems, USA; or Aquilion One, Toshiba, Japan). The imaging parameters were as follows: slice thickness, 0.625 mm; pitch, 0.984; gantry rotation time, 0.5 s; tube voltage, 120 kV; and automatic tube current modulation, 100–200 mA. A 5-mm interval was used for CT image reconstruction.

All patients' CT Digital Imaging and Communications in Medicine (DICOM) images were transferred to a dedicated image analysis workstation equipped with an open source software (Fire Voxel, New York University, NY, USA), and then processed by an abdominal radiologist in a double-blinded manner. First, renal parenchyma of two sides were drawn on the superior and inferior layers of the axial kidney image. The software automatically filled the entire kidney according to the Hounsfield unit (HU) threshold to obtain a volume of interest (VOI), including the renal cortex and medulla. Second, the VOI was magnified, and the edges were manually modified to ensure that all functional renal parenchyma was contained while hydronephrosis, calculi, and cysts were avoided (**Figure 1**). Third, RCMs (morphological and CTTA parameters) were automatically calculated based on

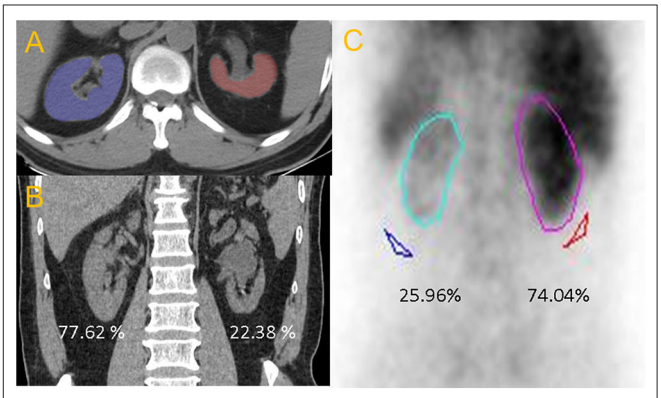

FIGURE 1 | (A) Axial non-enhanced CT image. **(B)** The percentage of CT renal volume for right and left kidney were 77.62 and 22.38%, respectively. **(C)** The differential renal function from RG of right and left kidney were 74.04 and 25.96%, respectively.

the final VOI, including RPV, HU, parenchymal voxel, skewness, kurtosis, and entropy.

Nuclear RG

RG values were recorded based on the reports compiled by a professional radiologist. All DRF on RG data were blindly obtained from an observer and processed using the Discovery NM670 SPECT/CT platform (GE Healthcare, USA).

RCM Analysis

RCMs were evaluated for their power of correlation to DRF. The percent RCM were calculated using the general format "100* [Left RCM / (Left RCM + Right RCM)]" as previously reported (8, 13). All percent RCMs used the left kidney, regardless of whether it was obstructed. The contralateral side can always be determined by assigning the remaining percentage because the two sides total 100. The percent RCM were then compared with the DRF, as determined by RG.

Statistical Analysis

Continuous variables were expressed as mean ± standard variation. Pearson's correlation coefficient and linear regression were used to evaluate correlations between percent RCM and DRF on RG. A p value < 0.05 was considered to indicate a statistically significant difference. SPSS version 24 (IBM Corporation, Armonk, NY, USA) was used to perform the statistical analyses. The difference in correlation coefficient between men and women was calculated using MedCalc (version 12.7, Mariakerke, Belgium).

TABLE 1 | Baseline cohort characteristics, $n = 76$.

Characteristic	
Age in years–mean ± SD	51.14 ± 10.61
Serum creatinine–mean ± SD	76.05 ± 15.4
Gender–no. (%)	
Male	31 (40.8%)
Female	45 (59.2%)
Preoperative drainage–no. (%)	
Yes	13 (17.1%)
No	63 (82.9%)
Drainage type–no. (%)	
Drainage type	6 (46.2%)
Double J ureteral stents	4 (30.8%)
Drainage type + double J ureteral stents	3 (23.0%)
Stone side–no. (%)	
Right	45 (59.2%)
Left	31 (40.8%)
Hypertension–no. (%)	
Yes	8 (10.5%)
No	68 (80.5%)
Diabetes–no. (%)	
Yes	5 (6.6%)
No	71 (93.4%)
Operation for stone–no. (%)	
Ureteroscopic lithotripsy	16 (21.1%)
Percutaneous nephrolithotomy	33 (43.4%)
Laparoscopic nephrectomy	27 (35.5%)

SD, standard deviation.

RESULTS

A total of 31 men and 45 women, who underwent unenhanced CT and nuclear RG, were included in the analysis. Baseline patient characteristics were summarized in **Table 1**. The mean age of the patients was 51.14 ± 10.61 years, and the mean serum creatinine level was 76.05 ± 15.4 μmoI/L. There were 45 cases of right-sided stones and 31 cases of left-sided stones. Eight patients had hypertension and five patients had diabetes, but all of them were well controlled. Ureteroscopic lithotripsy was performed in 16 cases, and percutaneous nephrolithotomy was performed in 33 cases, the remaining 27 patients underwent laparoscopic nephrectomy.

The percent RPV, HU, parenchymal voxel, skewness, kurtosis, and entropy were separately evaluated for their strength of correlation to DRF on RG. In addition, multiple combinations of these RCMs were also used to evaluate the correlation with DRF. For each RCM, a Pearson's correlation coefficient between the percent RCM and the DRF was calculated (**Table 2**). The strongest correlation between RCM and DRF was achieved with RPV ($r = 0.957$, $P < 0.001$). However, RPV multiplied by HU, and parenchymal voxel multiplied by HU, also achieved the same correlation ($r = 0.957$, $P < 0.001$). Moreover, there was a relatively high correlation between the percent RPV multiplied by entropy and DRF ($r = 0.956$, $P < 0.001$). The results of gender-based subgroup analysis were shown in **Table 3**. Whether in men or women, RPV has still achieved the strongest correlation between RCM and DRF ($r = 0.962$ for female, $r = 0.950$ for male). Although the correlation coefficient of women is slightly larger than that of men, the difference is not statistically significant ($P = 0.565$).

Linear regression produced an equation for estimating DRF: y = −2.66+1.07* x" ($P < 0.001$), in which "x" is the left percent RPV, and "y" is the equation-estimated DRF (**Figure 2**). The numerical values comparing the percent RPV, equation-estimated DRF, and actual reported DRF from RG were provided in **Supplementary Table S1**. No statistically significant difference was observed between equation-estimated DRF and actual reported DRF ($P = 0.959$).

DISCUSSION

Chronic urinary tract obstruction caused by stone often leads to renal impairment of the affected unit, and DRF of the obstructed kidney can impact the surgical decision. Urologists usually determine split DRF by nuclear RG. However, high cost of nuclear RG precludes some hospitals from performing this examination. Therefore, given increases in morbidity of urolithiasis (1), the need of using unenhanced CT (basic examination) to avoid nuclear RG is also on the rise. In this preliminary study, the percent RPV from unenhanced CT

TABLE 2 | Evaluating differential CT measurements and their correlation to DRF on RG.

Measurement/Calculation	Pearson correlation	*p*-value
CT Texture:		
Skewness*	0.282	0.013
Kurtosis**	0.297	0.009
Entrophy	−0.22	0.849
HU	0.198	0.086
Parenchymal Voxel***	0.956	<0.001
Volume		
Parenchymal Volume***	0.957	<0.001
Combinations		
Parenchymal Volume × HU***	0.957	<0.001
Parenchymal Volume × skewness***	0.887	<0.001
Parenchymal Volume × Kurtosis***	0.815	<0.001
Parenchymal Volume × Entropy***	0.956	<0.001
Parenchymal Voxel x HU***	0.957	<0.001
Parenchymal Volume × Parenchymal Voxel x HU***	0.951	<0.001

*Parenchyma defined as both renal cortex and medulla. HU, Hounsfield Units. *P < 0.05, **P < 0.01, ***P < 0.001.*

TABLE 3 | Gender subgroup analysis of the correlation between differential CT measurements and DRF on RG.

	Male ($n = 31$)		Female ($n = 45$)	
Measurement/ Calculation	Pearson correlation	*p*-value	Pearson correlation	*p*-value
HU	0.673	<0.001	0.249	0.099
Parenchymal Voxel	0.948	<0.001	0.962	<0.001
Parenchymal Volume	0.950	<0.001	0.962	<0.001
Parenchymal Volume × HU	0.950	<0.001	0.962	<0.001
Parenchymal Voxel × HU	0.949	<0.001	0.962	<0.001
Parenchymal Volume × Parenchymal Voxel × HU	0.941	<0.001	0.958	<0.001

Parenchyma defined as both renal cortex and medulla. HU, Hounsfield Units.

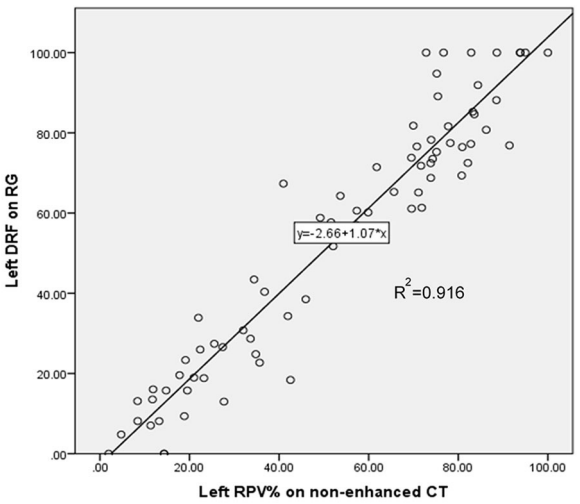

FIGURE 2 | Linear regression of unenhanced computerized tomography (CT) percent left residual parenchymal volume (RPV) estimating left differential renal function (DRF) on nuclear renography (RG).

demonstrated a strong correlation with DRF from RG ($r = 0.957$). Moreover, DRF was easily and precisely evaluated using the equation from unenhanced CT.

In 2016, Jacob et al. (8) investigated 49 patients with UPJO and reported a strong correlation between percent cortical area multiplied by HU on CT and DRF of RG. Studies in 2014 by Hamed et al. (10) and in 2012 by Sarma et al. (14), including 42 and 21 patients, respectively, found that percent RPV on CT strongly correlated with DRF using 99mTc-DTPA renal scan. As mentioned above, multiple studies have indicated that DRF can be adequately assessed using percent RCM, and previous results were compatible with those of this study. However, enhanced CT was used most frequently in previous studies. Despite the strong correlation, enhanced CT as a tool for assessing DRF is not without limitations, primarily because the exposure to contrast medium adversely affects renal function (15). Enhanced CT is prohibited in patients with worsening renal function (16) or allergy to contrast media. Furthermore, some studies (8, 17, 18) have applied HU to calculate CT-based DRF; however, it is difficult to standardize the data because tissue attenuation derived from enhanced CT is affected by a variety of factors (19, 20), including contrast medium type, injection concentration and rate, and image acquisition time. However, these disadvantages do not apply in unenhanced CT. Hence, a reasonable assumption could be drawn that the results of this study may be more easily adopted and validated by other medical centers, and easier to be generalized into clinical practice.

In 2010 Morrisroe et al. (13) and in 2015 Martinez-Suarez et al. (21), compared percent RPV on unenhanced CT with DRF on nuclear renal scan. The common limitation of their research, however, was the rather small sample size (10 and 19 patients, respectively). A relatively larger sample ($n = 72$) was studied by Feder et al. (9), and their results indicated a strong correlation between percent renal parenchymal area from unenhanced CT and DRF from renal scintigraphy, similar to the results of the present study (Pearson's $r = 0.967$ vs. $r = 0.957$). However, the 72 patients had a wide range of disease types (and included kidney donors). In contrast, the inclusion criteria for this study were strictly controlled (only including patients with chronic unilateral obstruction upper urinary tract stones). Therefore, the statistical power of the results from the present study may be stronger, especially in patients with upper urinary tract stones. In addition to the classic morphological indicator (RPV), relatively novel CTTA parameters were also introduced to this study.

Numerous studies have demonstrated that CTTA can reflect heterogeneity in the microstructure (12, 22, 23). Given that it is not unusual for chronic renal obstruction to undergo the changes in kidney texture during functional impairment, this study sought to ascertain whether CTTA could accurately reflect

DRF. This research demonstrated a strong correlation between percent CTTA parameters multiplied by RPV and DRF. Although the combinations did not significantly improve the correlation compared with individual RPV, this result still reflected a certain value. First, this study and its findings may provide a reference for researchers who are committed to studying the relationship between renal function and CTTA. Second, it could be reasonably inferred that CTTA parameters may be more helpful in situations for which RPV does not accurately reflect renal function. For example, the expanded interstitial spaces caused by active infection or acute obstruction can lead to enlarged renal volume (13), further reducing the correlation between renal volume and function. Whereas microenvironmental changes may be recognized by CTTA parameters, the use of CTTA to detect acute myocardial infarction supports this hypothesis (24, 25). Hence, the contribution of CTTA may exceed the renal volume in such situations, although further verification is needed.

Although this research verified a correlation between CT measurements and DRF, it helped only a little in clinical practice; therefore, this study further introduced RPV into the equation from linear regression to obtain a CT equation-estimated DRF. Importantly, the difference between equation-estimated DRF and reported DRF according to RG did not fulfill formal statistical criteria. Consequently, this equation may be used as a method to prospectively screen patients for further validation, at least in this single medical center.

There were several limitations to this investigation. First, although previous studies (9, 13) have reported that the correlations were weakened in patients with worse renal function, this study did not perform subgroup analysis based on renal function due to the relatively small sample size. Interestingly, the correlation between percent RPV and DRF in this study may be stronger theoretically if patients with a split renal function of zero are excluded. In future, larger-sample studies, subgroup analysis based on renal function will be considered more cautiously and comprehensively. Second, postoperative renal function was not analyzed in this study due to the lack of follow-up data. Although this is not inconsistent with the purpose of this study (focusing on preoperative patients), it is necessary to include postoperative renal function assessment in further studies. Third, reproducibility was not evaluated, given that previous studies (26, 27) have demonstrated excellent intra-class correlation coefficient (ICC) values for RCM (>0.9). If the ICC test was performed, the results of this study using three-dimensional volume software should be at least as good as those of previous studies.

CONCLUSION

In conclusion, for patients with chronic unilateral obstructive upper urinary tract stones, unenhanced CT enabled preoperative DRF to be rapidly and accurately estimated, and the role of RPV is more important than CTTA parameters. Measuring RPV on unenhanced CT images may assist urologists in determining optimal treatment strategies. Probably in most chronic unilateral obstructive upper urinary tract stones patients, measuring RPV on unenhanced CT may be sufficient to evaluate renal function, and RG may not be necessary as a conventional method in clinical.

DATA AVAILABILITY STATEMENT

All datasets generated for this study are included in the article/**Supplementary Material**.

ETHICS STATEMENT

The studies involving human participants were reviewed and approved by Ethics Committee in Tongji Medical College. Written informed consent for participation was not required for this study in accordance with the national legislation and the institutional requirements.

AUTHOR CONTRIBUTIONS

JL and YX: writing original draft and acquisition of data. CL and YH: data analysis and interpretation. YS, XH, and DH: literature research. ZLiu, ZLi, and SW: revising article and study supervision. All authors contributed to the article and approved the submitted version.

FUNDING

This study was supported by grants from National Natural Science Foundation of China (81771801, 81701657, 81801695, and 81571642).

SUPPLEMENTARY MATERIAL

The Supplementary Material for this article can be found online at: https://www.frontiersin.org/articles/10.3389/fmed.2020.00309/full#supplementary-material

REFERENCES

1. Turk C, Petrik A, Sarica K, Seitz C, Skolarikos A, Straub M, et al. EAU guidelines on diagnosis and conservative management of urolithiasis. *European urology.* (2016) 69:468–74. doi: 10.1016/j.eururo.2015.07.040
2. Zeng G, Mai Z, Xia S, Wang Z, Zhang K, Wang L, et al. Prevalence of kidney stones in China: an ultrasonography based cross-sectional study. *BJU Int.* (2017) 120:109–16. doi: 10.1111/bju.13828
3. Wein AJ, Kavoussi LR, Novick AC, Partin AW, Peters CA. *Campbell-Walsh Urology, Tenth Edition*. Philadelphia, PA: Saunders (2012). doi: 10.1016/B978-1-4160-6911-9.00147-X
4. Folks RD, Garcia EV, Taylor AT. Development and prospective evaluation of an automated software system for quality control of quantitative 99mTc-MAG3 renal studies. *J Nucl Med Technol.* (2007) 35:27–33.
5. Brolin G, Edenbrandt L, Granerus G, Olsson A, Afzelius D, Gustafsson A, et al. The accuracy of quantitative parameters in (99m) Tc-MAG3 dynamic

renography: a national audit based on virtual image data. *Clin Physiol Funct Imag.* (2016) 36:146–54. doi: 10.1111/cpf.12208
6. Shine S. Urinary calculus: IVU vs CT renal stone? A critically appraised topic. *Abdom Imag.* (2008) 33:41–3. doi: 10.1007/s00261-007-9307-0
7. Goldman SM, Faintuch S, Ajzen SA, Christofalo DM, Araujo MP, Ortiz V, et al. Diagnostic value of attenuation measurements of the kidney on unenhanced helical CT of obstructive ureterolithiasis. *Am J Roentgenol.* (2004) 182:1251–4. doi: 10.2214/ajr.182.5.1821251
8. Ark JT, Mitchell CR, Marien TP, Herrell SD. Use of contrasted computerized tomography as a surrogate for nuclear medicine renogram to categorize renal function in the setting of ureteropelvic junction obstruction. *Urology.* (2016) 97:238–44. doi: 10.1016/j.urology.2016.04.068
9. Feder MT, Blitstein J, Mason B, Hoenig DM. Predicting differential renal function using computerized tomography measurements of renal parenchymal area. *J Urol.* (2008) 180:2110–5. doi: 10.1016/j.juro.2008.07.057
10. Hamed MA. New advances in assessment of the individual renal function in chronic unilateral renal obstruction using functional CT compared to 99mTc-DTPA renal scan. *Nucl Med Rev Cent East Europe.* (2014) 17:59–64. doi: 10.5603/NMR.2014.0018
11. Funahashi Y, Hattori R, Yamamoto T, Kamihira O, Sassa N, Gotoh M. Relationship between renal parenchymal volume and single kidney glomerular filtration rate before and after unilateral nephrectomy. *Urology.* (2011) 77:1404–8. doi: 10.1016/j.urology.2010.03.063
12. Lubner MG, Smith AD, Sandrasegaran K, Sahani DV, Pickhardt PJ. CT texture analysis: definitions, applications, biologic correlates, and challenges. *Radiographics.* (2017) 37:1483–503. doi: 10.1148/rg.2017170056
13. Morrisroe SN, Su RR, Bae KT, Eisner BH, Hong C, Lahey S, et al. Differential renal function estimation using computerized tomography based renal parenchymal volume measurement. *J Urol.* (2010) 183:2289–93. doi: 10.1016/j.juro.2010.02.024
14. Sarma D, Barua SK, Rajeev TP, Baruah SJ. Correlation between differential renal function estimation using CT-based functional renal parenchymal volume and (99m)Tc - DTPA renal scan. *Indian J Urol.* (2012) 28:414–7. doi: 10.4103/0970-1591.105753
15. Nyman U, Ahlkvist J, Aspelin P, Brismar T, Frid A, Hellstrom M, et al. Preventing contrast medium-induced acute kidney injury : Side-by-side comparison of Swedish-ESUR guidelines. *Eur Radiol.* (2018) 28:5384–95. doi: 10.1007/s00330-018-5678-6
16. Santos RO, Malvar B, Silva R, Ramalho V, Pessegueiro P, Amoedo M, et al. [Contrast-induced nephropathy]. *Acta Med Port.* (2011) 24:809–20.
17. El-Ghar ME, Shokeir AA, El-Diasty TA, Refaie HF, Gad HM, El-Dein AB. Contrast enhanced spiral computerized tomography in patients with chronic obstructive uropathy and normal serum creatinine: a single session for anatomical and functional assessment. *J Urol.* (2004) 172:985–8. doi: 10.1097/01.ju.0000135368.77589.7c
18. Kwon SH, Saad A, Herrmann SM, Textor SC, Lerman LO. Determination of single-kidney glomerular filtration rate in human subjects by using CT. *Radiology.* (2015) 276:490–8. doi: 10.1148/radiol.2015141892
19. Han JK, Kim AY, Lee KY, Seo JB, Kim TK, Choi BI, et al. Factors influencing vascular and hepatic enhancement at CT: experimental study on injection protocol using a canine model. *J Comp Assist Tomogr.* (2000) 24:400–6. doi: 10.1097/00004728-200005000-00008
20. Choi SY, Lee I, Seo JW, Park HY, Choi HJ, Lee YW. Optimal scan delay depending on contrast material injection duration in abdominal multi-phase computed tomography of pancreas and liver in normal Beagle dogs. *J Vet Sci.* (2016) 17:555–61. doi: 10.4142/jvs.2016.17.4.555
21. Martinez-Suarez HJ, Durso T, Kadlec AO, Gupta GN, Farooq AV, Turk T. Three-dimensional renal parenchymal volume as a surrogate for renal function estimation in obstructed kidneys undergoing surgical repair. *J Endourol.* (2015) 29:630–3. doi: 10.1089/end.2014.0232
22. Chilamkurthy S, Ghosh R, Tanamala S, Biviji M, Campeau NG, Venugopal VK, et al. Deep learning algorithms for detection of critical findings in head CT scans: a retrospective study. *Lancet.* (2018) 392:2388–96. doi: 10.1016/S0140-6736(18)31645-3
23. Dekkers T, Prejbisz A, Kool LJS, Groenewoud H, Velema M, Spiering W, et al. Adrenal vein sampling versus CT scan to determine treatment in primary aldosteronism: an outcome-based randomised diagnostic trial. *Lancet Diab Endocrinol.* (2016) 4:739–46. doi: 10.1016/S2213-8587(16)30100-0
24. Mannil M, von Spiczak J, Manka R, Alkadhi H. Texture analysis and machine learning for detecting myocardial infarction in noncontrast low-dose computed tomography: unveiling the invisible. *Invest Radiol.* (2018) 53:338–43. doi: 10.1097/RLI.0000000000000448
25. Hinzpeter R, Wagner MW, Wurnig MC, Seifert B, Manka R, Alkadhi H. Texture analysis of acute myocardial infarction with CT: First experience study. *PLoS ONE.* (2017) 12:e0186876. doi: 10.1371/journal.pone.0186876
26. Ramaswamy K, Marien T, Mass A, Stifelman M, Shah O. Simplified approach to estimating renal function based on computerized tomography. *Canadian J Urol.* (2013) 20:6833–9.
27. Breau RH, Clark E, Bruner B, Cervini P, Atwell T, Knoll G, et al. A simple method to estimate renal volume from computed tomography. *Canad Urol Assoc J.* (2013) 7:189–92. doi: 10.5489/cuaj.1338

Conflict of Interest: The authors declare that the research was conducted in the absence of any commercial or financial relationships that could be construed as a potential conflict of interest.

frontiers in Medicine

BRIEF RESEARCH REPORT
published: 10 July 2020
doi: 10.3389/fmed.2020.00325

Ivabradine Ameliorates Kidney Fibrosis in L-NAME-Induced Hypertension

Peter Stanko[1†], Tomas Baka[1†], Kristina Repova[1], Silvia Aziriova[1], Kristina Krajcirovicova[1], Andrej Barta[2], Pavol Janega[2,3], Michaela Adamcova[4], Ludovit Paulis[1,2] and Fedor Simko[1,5,6]*

[1] Institute of Pathophysiology, Faculty of Medicine, Comenius University, Bratislava, Slovakia, [2] Institute of Normal and Pathological Physiology, Centre of Experimental Medicine, Slovak Academy of Sciences, Bratislava, Slovakia, [3] Institute of Pathological Anatomy, Faculty of Medicine, Comenius University, Bratislava, Slovakia, [4] Department of Physiology, School of Medicine, Charles University, Prague, Czechia, [5] 3rd Department of Internal Medicine, Faculty of Medicine, Comenius University, Bratislava, Slovakia, [6] Institute of Experimental Endocrinology, Biomedical Research Center, Slovak Academy of Sciences, Bratislava, Slovakia

OPEN ACCESS

Edited by:
Jennifer Sullivan, Augusta University, United States

Reviewed by:
Hee-Seong Jang, University of Nebraska Medical Center, United States
Swastika Sur, University of California San Francisco, United States

***Correspondence:**
Fedor Simko
fedor.simko@fmed.uniba.sk

[†] *These authors have contributed equally to this work*

Specialty section:
This article was submitted to Nephrology, a section of the journal Frontiers in Medicine

Received: *06 March 2020*
Accepted: *03 June 2020*
Published: *10 July 2020*

Citation:
Stanko P, Baka T, Repova K, Aziriova S, Krajcirovicova K, Barta A, Janega P, Adamcova M, Paulis L and Simko F (2020) Ivabradine Ameliorates Kidney Fibrosis in L-NAME-Induced Hypertension. Front. Med. 7:325. doi: 10.3389/fmed.2020.00325

Hypertension-induced renal injury is characterized by structural kidney alterations and function deterioration. Therapeutics for kidney protection are limited, thus novel renoprotectives in hypertension are being continuously sought out. Ivabradine, an inhibitor of the I_f current in the sinoatrial node reducing heart rate (HR), was shown to be of benefit in various cardiovascular pathologies. Yet, data regarding potential renoprotection by ivabradine in hypertension are sparse. Thirty-six adult male Wistar rats were divided into non-diseased controls and rats with N^G-nitro-L-arginine methyl ester (L-NAME)-induced hypertension to assess ivabradine's site-specific effect on kidney fibrosis. After 4 weeks of treatment, L-NAME increased the average systolic blood pressure (SBP) (by 27%), decreased glomerular density (by 28%) and increased glomerular tuft area (by 44%). Moreover, L-NAME induced glomerular, tubulointerstitial, and vascular/perivascular fibrosis by enhancing type I collagen volume (16-, 19- and 25-fold, respectively). L-NAME also increased the glomerular type IV collagen volume and the tubular injury score (3- and 8-fold, respectively). Ivabradine decreased average SBP and HR (by 8 and 12%, respectively), increased glomerular density (by 57%) and reduced glomerular tuft area (by 30%). Importantly, ivabradine decreased type I collagen volume at all three of the investigated sites (by 33, 38, and 72%, respectively) and enhanced vascular/perivascular type III collagen volume (by 67%). Furthermore, ivabradine decreased the glomerular type IV collagen volume and the tubular injury score (by 63 and 34%, respectively). We conclude that ivabradine attenuated the alterations of glomerular density and tuft area and modified renal fibrosis in a site-specific manner in L-NAME-hypertension. It is suggested that ivabradine may be renoprotective in hypertensive kidney disease.

Keywords: ivabradine, L-NAME, hypertension, fibrosis, nephroprotection

INTRODUCTION

Chronic kidney disease (CKD), determined by a decline of total glomerular filtration rate and albuminuria persisting >3 months, is a severe health and social problem. CKD afflicts almost 15% of the global population and significantly worsens life expectancy (1). Although a considerable number of etiologic factors may come into force, diabetes mellitus, and arterial hypertension clearly dominate (2). CKD in hypertension is characterized by a persistent systemic blood pressure overload gradually exceeding auto-regulatory mechanisms for maintaining adequate glomerular filtration pressure. Glomerular hypertension and hyperfiltration are associated with compensatory glomerular hypertrophy, albuminuria, and persistent inflammation (3). Progressive necrotic or apoptotic cell death is followed by glomerulosclerosis, tubular atrophy, and tubulointerstitial fibrosis representing the principle pathologic components and therapeutic targets of CKD (4).

Ivabradine, the heart rate (HR)-reducing selective inhibitor of the sinoatrial I_f current, was proved to attenuate morbidity in heart failure (5). The HR-reducing effect of ivabradine was declared the principle mechanism of its therapeutic benefit. However, several of ivabradine's pleiotropic effects have recently emerged, which suggests the possibility of using ivabradine in yet off-label indications such as endothelial dysfunction (6), hypertensive heart disease (7), and hypertension with elevated or non-dipping HR (8, 9).

This study aimed to show whether ivabradine is able to modify kidney alterations in N^G-nitro-L-arginine methyl ester (L-NAME)-induced hypertension. We investigated ivabradine's potential antifibrotic effect in a site-specific manner as glomerulosclerosis (glomerular fibrosis), tubulointerstitial fibrosis, and arteriosclerosis (vascular fibrosis) with perivascular fibrosis.

MATERIALS AND METHODS

Thirty-six 3-month-old male Wistar rats (Department of Toxicology and Laboratory Animals Breeding, Slovak Academy of Sciences, Dobra Voda, Slovakia) were divided into 4 groups ($n = 9$ animals per group) and treated for 4 weeks as follows: control (C; untreated), ivabradine (Iva; 10 mg/kg/day; Servier, Suresnes, France), L-NAME (LN; 40 mg/kg/day; Sigma-Aldrich Chemie, Munich, Germany) and L-NAME plus ivabradine in corresponding doses (LN+Iva). Both L-NAME and ivabradine were dissolved in drinking water and their concentrations were adjusted to daily water consumption to ensure the correct dosage. The rats were individually housed and maintained under standard laboratory conditions (12:12-h light-dark cycle at 22 ± 2°C temperature and 55 ± 10% humidity) with free access to food and water. The study was conducted in accordance with the Guide for the Care and Use of Laboratory Animals published by the US National Institutes of Health (NIH Publication No. 85-23, revised 1996). The protocol was approved by the ethical committee of the Institute of Pathophysiology, Faculty of Medicine, Comenius University, Bratislava, Slovakia (approval number: 1306/14-221).

Systolic blood pressure (SBP) and heart rate (HR) were measured once a week in each animal by non-invasive tail-cuff plethysmography (Hugo-Sachs Elektronic, Freiburg, Germany). After 4 weeks of treatment, the rats were euthanized by isoflurane inhalation and left kidneys were used for subsequent histopathological analysis. The kidney samples were fixed in 4% formaldehyde for 24 h, embedded in paraffin and cut in 5 μm sections. Three sets of deparaffinized and rehydrated sections were stained with: (i) hematoxylin-eosin (H-E) for glomerular morphometry and tubular injury scoring; (ii) picrosirius red (PSR; 0.1% sirius red F3BA in a saturated water solution of picric acid for 90 min and washed in 0.01 N HCl for 2 min) for a quantitative analysis of kidney fibrosis; and (iii) type IV collagen immunostaining (anti-collagen IV antibody; ab6586; Abcam, Cambridge, UK was used for immunostaining conforming the manufacturer's protocol: a heat-mediated antigen retrieval was followed by overnight incubation with primary anti-collagen IV antibody at 4°C; a horseradish peroxidase-conjugated secondary anti-rabbit IgG antibody with a 3,3′-diaminobenzidine chromogen and hematoxylin counterstain was used for visualization; ab205718; Abcam, Cambridge, UK) to determine type IV collagen volume in glomeruli. Histopathological observations were performed using transmitted or polarized light microscopy on a NIKON Eclipse Ti C2+ microscope (NIKON, Tokyo, Japan). The rendered images were analyzed by NIKON NIS-Elements Analysis software (NIKON, Tokyo, Japan) and ImageJ version 1.52p for Windows (National Institutes of Health, Bethesda, MD, USA). All histopathological analyses were performed by an experienced examiner blinded to the group identity.

For glomerular morphometry, H-E-stained sections were analyzed at 10x magnification using transmitted light microscopy and NIKON NIS-Elements Analysis software as follows: (i) to assess glomerular numerical density per area, well-preserved glomeruli were counted in a digital frame of 1 mm^2 placed over the kidney cortex in 10 microscopic fields per animal (i.e., 90 per group; $n = 9$ animals per group); (ii) to assess glomerular tuft area, perpendicular maximum and minimum diameters (d_{max} and d_{min}, respectively) of 10 random glomerular tufts per animal (i.e., 90 per group; $n = 9$ animals per group) were measured to subsequently calculate tuft ellipse areas by using the formula: glomerular tuft area $= \pi(d_{max}/2)(d_{min}/2)$ (10, 11).

In order to obtain a quantitative analysis of kidney fibrosis, PSR-stained sections were analyzed at 100x magnification using polarized light microscopy and ImageJ software as follows: PSR increases birefringence of collagen fibers type-dependently, thus visualizing thick type I collagen (Col-I, 1.6-2.4 μm in diameter) in red-orange shades and thin type III collagen (Col-III, <0.8 μm in diameter) in green-yellow shades; by setting the appropriate "hue" thresholds of the color spectrum, the red-orange and green-yellow shaded areas were expressed as the percentage of the total area of interest (AOI) by ImageJ processing. To particularly detail kidney fibrosis, three AOIs were determined by employing a method described previously (12): (i) to assess glomerular fibrosis, 50 AOIs per animal (i.e., 450 per group; $n = 9$

animals per group) of 50 × 50 μm each, placed at intraglomerular space were examined (**Figure 2A1**); (ii) to assess tubulointerstitial fibrosis, 50 AOIs per animal (i.e., 450 per group; $n = 9$ animals per group) of 72 × 192 μm each, placed at interstitial cortex space including no glomeruli or vessels were examined (**Figure 2B1**); (iii) to assess vascular/perivascular fibrosis, 5 AOIs per animal (i.e., 45 per group; $n = 9$ animals per group) were selected by the tight-cropping of an artery between 50 and 100 μm in diameter (corresponding to interlobar, arcuate, and interlobular arteries) in each; only cross-sectionally captured arteries were considered (**Figure 2C1**).

In order to determine type IV collagen (Col-IV) volume in glomeruli, anti-Col-IV-immunostained sections were analyzed at 200x magnification using transmitted light microscopy and ImageJ software as follows (13): the anti-Col-IV-immunostain visualizes Col-IV in brown shades (**Figure 3A**); by setting the appropriate "hue" threshold of the color spectrum, the brown shaded area was expressed as the percentage of the total glomerular AOI by ImageJ processing. Ten glomerular AOIs per animal (i.e., 90 per group; $n = 9$ animals per group) of 50 × 50 μm each, placed at intraglomerular space were examined.

Tubular injury was determined as tubular injury score by employing a method described previously (14). Briefly, 20 cortical fields per animal (i.e., 180 per group; $n = 9$ animals per group) in H-E-stained sections were analyzed at 100x magnification using transmitted light microscopy. Tubular injury was defined as tubular dilatation, atrophy, cast formation, sloughing of tubular epithelial cells, or thickening of the tubular basement membrane (**Figure 4A**). The tubular injury was semi-quantitatively scored using the following scoring system: Score 0, no tubular injury; Score 1, <10% of tubules injured; Score 2, 10–25% of tubules injured; Score 3, 26–50% of tubules injured; Score 4, 51–75% of tubules injured; Score 5, >75% of tubules injured.

The results are presented as the mean ± SEM. A Shapiro-Wilk normality test was used to determine data distribution. The one-way two-tailed analysis of variance (ANOVA) followed by a Holm-Sidak *post-hoc* test was used for statistical analysis. A Spearman correlation was used to analyze the relationship between glomerular tuft area and glomerular Col-IV volume, and tubular injury score and tubulointerstitial fibrosis. Statistical significance was defined as $P < 0.05$. The statistical analysis was conducted using GraphPad Prism 8 for Windows (GraphPad Software, La Jolla, CA, USA).

RESULTS

The SBP and HR averaged over the 4-week-course of treatment were 122.6 ± 1.05 mmHg and 356.0 ± 2.75 bpm in controls; L-NAME increased ($P < 0.01$) average SBP by 27% and decreased ($P < 0.01$) average HR by 8%. In the L-NAME group, ivabradine decreased both average SBP and HR by 8% ($P < 0.05$) and 12% ($P < 0.01$), respectively; in controls, ivabradine decreased ($P < 0.01$) average HR by 16% and had no effect on average SBP (**Figures 1A,B**).

The glomerular numerical density per area was 5.43 ± 0.1 per mm^2 in controls and L-NAME decreased ($P < 0.01$) it by 28%. In the L-NAME group, ivabradine increased ($P < 0.01$) the glomerular numerical density per area by 57% (**Figure 1C**). The glomerular tuft area was 5,383 ± 256 μm^2 in controls and L-NAME increased ($P < 0.01$) it by 44%. In the L-NAME group, ivabradine decreased ($P < 0.01$) the glomerular tuft area by 30% (**Figure 1D**).

Quantitative analysis of glomerular fibrosis: in controls, the volume of Col-I and Col-III in intraglomerular AOI were 0.68 ± 0.11 and 2.71 ± 0.38%, respectively; L-NAME increased ($P < 0.0001$) the proportion of Col-I by 1,584%. In the L-NAME group, ivabradine decreased ($P < 0.05$) the proportion of Col-I by 33%. The Col-I:Col-III ratio was 0.29 ± 0.06 in controls and L-NAME increased ($P < 0.05$) it by 3,880%; ivabradine had no effect on the ratio (**Figure 2A**).

Quantitative analysis of tubulointerstitial fibrosis: in controls, the volume of Col-I and Col-III in tubulointerstitial AOI were 0.49 ± 0.11 and 2.01 ± 0.25%, respectively; L-NAME increased ($P < 0.0001$) the proportion of Col-I by 1,894%. In the L-NAME group, ivabradine decreased ($P < 0.01$) the proportion of Col-I by 38%. The Col-I:Col-III ratio was 0.22 ± 0.04 in controls and L-NAME increased ($P < 0.01$) it by 3,734%; ivabradine had no effect on the ratio (**Figure 2B**).

Quantitative analysis of vascular/perivascular fibrosis: in controls, the volume of Col-I and Col-III in vascular/perivascular AOI were 0.21 ± 0.06 and 3.11 ± 0.18%, respectively; L-NAME increased ($P < 0.001$) the proportion of Col-I by 2,487%. In the L-NAME group, ivabradine decreased ($P < 0.01$) the proportion of Col-I by 72% and increased ($P < 0.001$) the proportion of Col-III by 67%. The Col-I:Col-III ratio was 0.07 ± 0.02 in controls and L-NAME increased ($P < 0.0001$) it by 2,796%; ivabradine decreased ($P < 0.0001$) the ratio by 85% (**Figure 2C**).

The volume of Col-IV in glomerular AOI was 2.80 ± 0.90% in controls and L-NAME increased ($P < 0.01$) it by 245%. In the L-NAME group, ivabradine decreased ($P < 0.01$) glomerular Col-IV volume by 63% (**Figures 3A,B**). The glomerular Col-IV volume significantly ($P < 0.001$) correlated with glomerular tuft area (Spearman $r = 0.51$) (**Figure 3C**).

The tubular injury score was 0.45 ± 0.02 in controls and L-NAME increased ($P < 0.001$) it by 754%. In the L-NAME group, ivabradine decreased ($P < 0.01$) the tubular injury score by 34% (**Figures 4A,B**). The tubular injury score significantly ($P < 0.001$) correlated with the sum of Col-I and Col-III volume in tubulointerstitial AOI (Spearman $r = 0.81$) (**Figure 4C**).

DISCUSSION

The increased SBP, induced by a 4-week L-NAME administration, was associated with decreased glomerular density, increased glomerular tuft area, tubular injury, and profound renal fibrosis. Besides reducing the average HR and SBP, ivabradine increased glomerular density and reduced

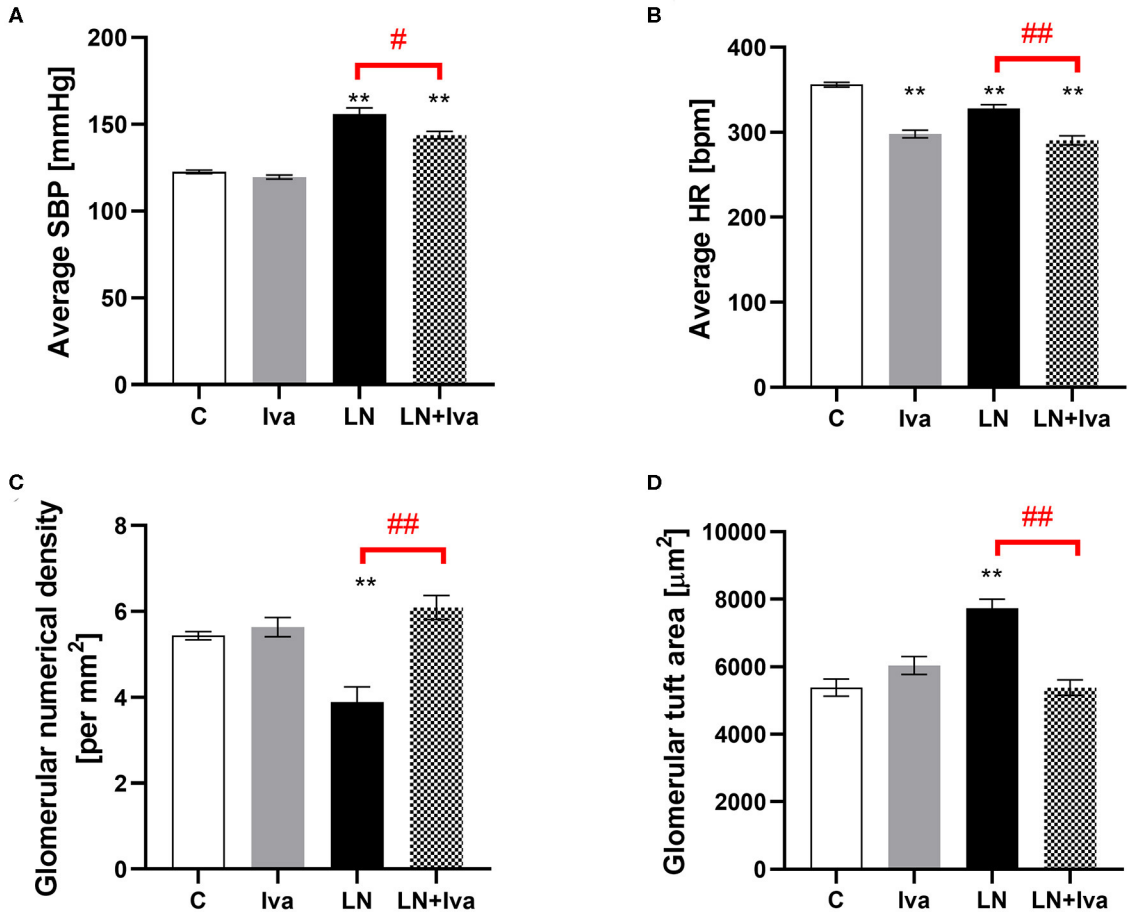

FIGURE 1 | Effect of ivabradine on average systolic blood pressure (SBP) **(A)**, average heart rate (HR) **(B)**, glomerular numerical density per area **(C)**, and glomerular tuft area **(D)** in L-NAME-induced hypertension after 4 weeks of treatment. C, controls; Iva, ivabradine; LN, L-NAME; $n = 9$ animals per group. One-way two-tailed ANOVA followed by Holm–Sidak *post-hoc test*; $^{**}P < 0.01$ vs. C; $^{\#}P < 0.05$ vs. LN; $^{\#\#}P < 0.01$ vs. LN.

glomerular tuft area. Furthermore, ivabradine ameliorated the L-NAME-induced kidney fibrosis site-dependently: it decreased Col-I volume in glomerular, interstitial, and vascular/perivascular fibrosis and increased Col-III volume in vascular/perivascular fibrosis. Ivabradine also mitigated the increase of both the glomerular Col-IV volume and the tubular injury score in L-NAME-hypertension. To the best of our knowledge, this is the first study analysing L-NAME-induced kidney fibrosis and renoprotection by ivabradine in a site-specific manner.

L-NAME inhibits nitric oxide (NO) synthase activity and decreases cyclic guanosine monophosphate (cGMP) concentration shown in various tissues including heart, aorta, brain, and kidney, thus resulting in NO-deficient hypertension (15–19). NO's waning vasodilative and antiproliferative effects associated with concomitant neurohumoral activation (20) were shown to result in target organ damage (7, 18, 19). In kidneys, L-NAME-hypertension induces glomerulosclerosis, tubulointerstitial fibrosis, and tubular atrophy associated with a deteriorated glomerular filtration rate and increased urinary protein excretion (21–23); these alterations are administered by a cluster of pro-inflammatory and pro-proliferative hormones, cytokines and growth factors (24).

The renal antifibrotic effect of ivabradine observed in this study was similar to previous findings within the heart: ivabradine reduced cardiac collagen and improved left ventricular function in post-myocardial infarction (MI) rats (25) and cholesterol-fed rabbits (26). Antiremodeling by ivabradine may be associated with some of its pleiotropic effects. Indeed, ivabradine improved endothelial function in ApoE knockout mice by reducing vascular oxidative stress and preventing endothelial NO synthase uncoupling (27, 28) and in patients with coronary artery disease after complete revascularisation (6). Increased NO-availability by various interventions was previously shown to reduce the L-NAME's proliferative effect not only in the heart and aorta, but also in the brain and kidneys (17, 18, 28). Besides improving NO-availability, ivabradine was shown to reduce serum angiotensin II in both post-MI rats (25) and hypercholesterolemic rabbits (26), and to decrease

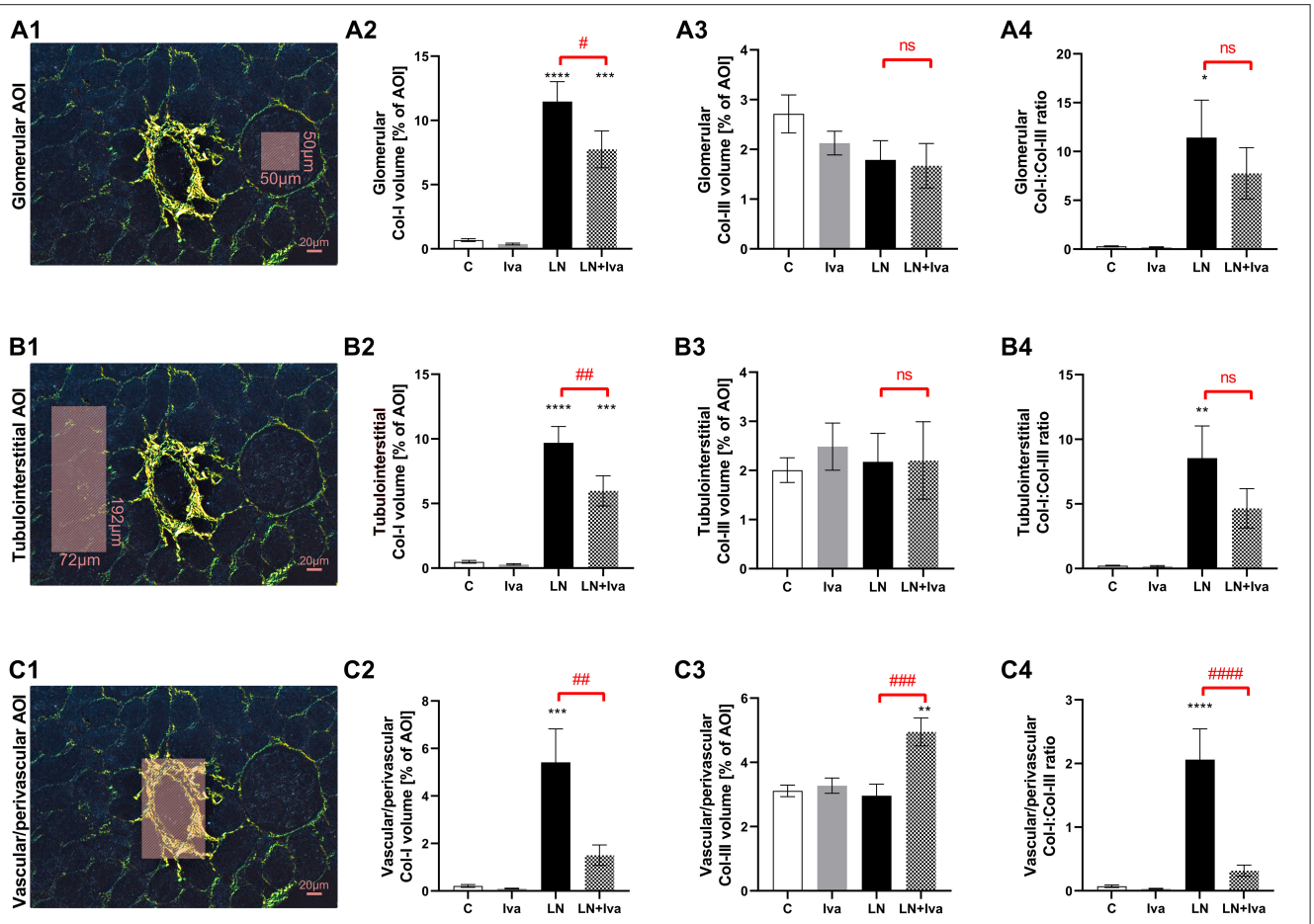

FIGURE 2 | Effect of ivabradine on kidney fibrosis detailed as glomerular **(A)**, tubulointerstitial **(B)**, and vascular/perivascular fibrosis **(C)** in L-NAME-induced hypertension after 4 weeks of treatment. PSR-stained sections at 100x magnification using polarized light microscopy. AOI, area of interest depicted as shaded rectangle; C, controls; Col-I, type I collagen; Col-III, type III collagen; Iva, ivabradine; LN, L-NAME; $n = 9$ animals per group. One-way two-tailed ANOVA followed by Holm–Sidak *post-hoc test*; $^{*}P < 0.05$ vs. C; $^{**}P < 0.01$ vs. C; $^{***}P < 0.001$ vs. C; $^{****}P < 0.0001$ vs. C; $^{\#}P < 0.05$ vs. LN; $^{\#\#}P < 0.01$ vs. LN; $^{\#\#\#}P < 0.001$ vs. LN; $^{\#\#\#\#}P < 0.0001$ vs. LN; ns, non-significant.

serum aldosterone in L-NAME-induced hypertension (7). The potential inhibition of the renin-angiotensin-aldosterone system might contribute to the antiremodeling effect of ivabradine. Indeed, previous data in L-NAME-hypertension indicated an angiotensin converting enzyme inhibitor to mitigate remodeling of the heart, aorta (19, 20, 29–31) and kidneys (21). Furthermore, one of the principle factors of CKD management is the reduction of hemodynamic overload. The recommended target SBP values in hypertensive patients with CKD are below 130 vs. 140 mmHg in hypertensive patients without kidney disease (32). Presumably, HR-reduction by ivabradine may be renoprotective via diminishing the hemodynamic burden by both the rate-pressure working product decline and vascular shear stress modulation (33). Here, in line with our previous experiments (7, 8, 34), ivabradine reduced both the average SBP and HR, which indeed might have contributed to the renoprotection. The HR reduction by L-NAME found in this study is consistent with previous results in L-NAME-hypertension by our laboratory (7, 8, 15) and others (35, 36). Several plausible mechanisms of heart rate reduction in L-NAME-hypertension were suggested, including the baroreceptor-mediated modulation of the autonomic nervous system (37, 38) and the direct effect of NO-deficiency on cardiac function (39, 40). Yet, ivabradine is an open-channel I_f-blocker, i.e., the ivabradine molecule is able to access its binding site in the f-channel only when the channel is open. This can underlie ivabradine's use-dependence, i.e., a blocking action that is more pronounced the more frequently the f-channel is open, implying that the higher the HR the larger the HR-reducing effect of ivabradine (41, 42). This might explain our finding that ivabradine reduced HR in controls by 16%, but only 12% in L-NAME-hypertension, since the HR in L-NAME-hypertension was already decreased by L-NAME below the values seen in controls.

Col-I and Col-III are the most abundant collagen types in the extracellular matrix (43, 44). In kidneys, they were found co-expressed at all three of the investigated sites, i.e., glomeruli, tubulointerstitium and vasculature (45), and gradually

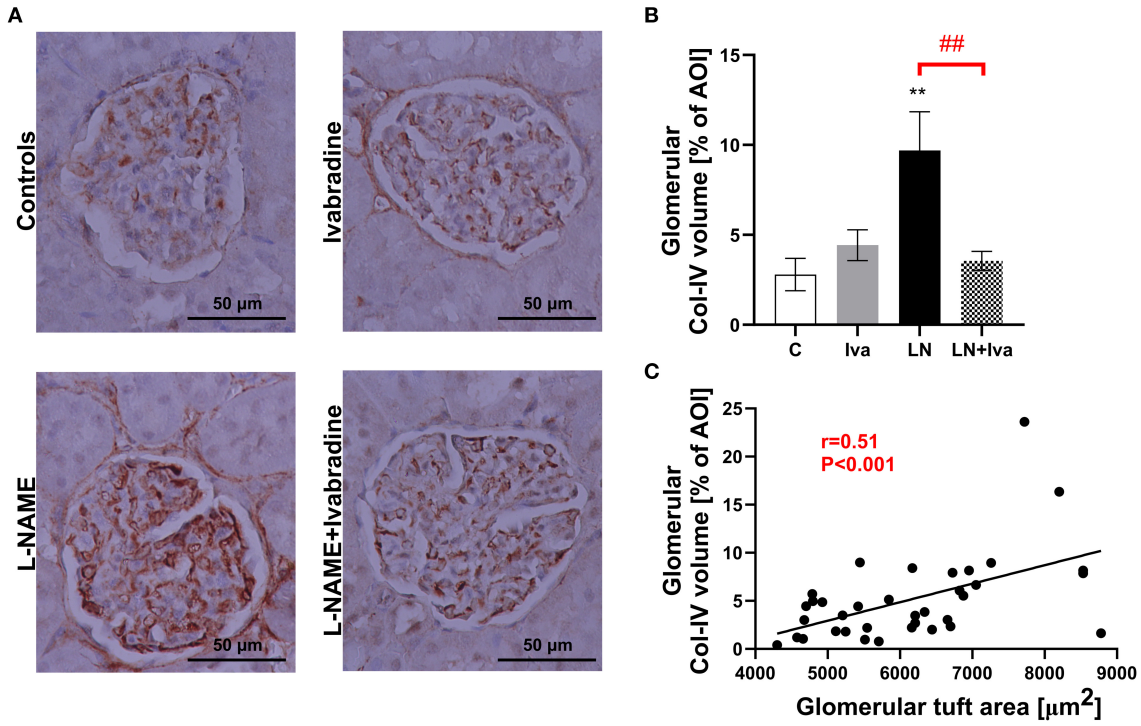

FIGURE 3 | Effect of ivabradine on type IV collagen volume in glomeruli **(A,B)** and the relationship between glomerular tuft area and glomerular type IV collagen volume **(C)** in L-NAME-induced hypertension after 4 weeks of treatment. For **(A)**: anti-collagen IV-immunostained sections at 200x magnification using transmitted light microscopy. For **(B)**: C, controls; Iva, ivabradine; LN, L-NAME; $n = 9$ animals per group. One-way two-tailed ANOVA followed by Holm–Sidak *post-hoc test*; $^{**}P < 0.01$ vs. C; $^{\#\#}P < 0.01$ vs. LN. For **(C)**: AOI, area of interest; Col-IV, type IV collagen. Spearman correlation; $n = 9$ animals per group.

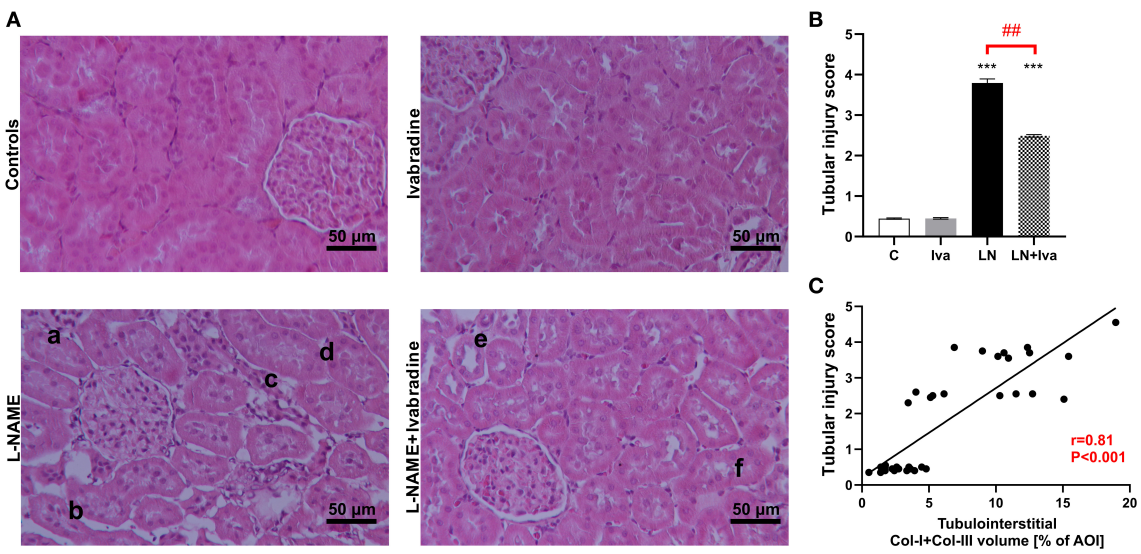

FIGURE 4 | Effect of ivabradine on tubular injury **(A,B)** and the relationship between tubular injury score and tubulointerstitial fibrosis **(C)** in L-NAME-induced hypertension after 4 weeks of treatment. For **(A)**: H-E-stained sections at 100x magnification using transmitted light microscopy; a, tubular cast; b, tubular atrophy and interstitial thickening; c, interstitial cellular infiltration; d, tubular basal membrane thickening; e, tubular dilatation; f, tubular cell sloughing. For **(B)**: C, controls; Iva, ivabradine; LN, L-NAME; $n = 9$ animals per group. One-way two-tailed ANOVA followed by Holm–Sidak *post-hoc* test; $^{***}P < 0.001$ vs. C; $^{\#\#}P < 0.01$ vs. LN. For **(C)**: AOI, area of interest; Col-I, type I collagen; Col-III, type III collagen. Spearman correlation; $n = 9$ animals per group.

deposited from the early stages of kidney fibrosis (45, 46). Col-I and Col-III co-expression is considered to provide a tissue with high tensile strength, but also contribute to its extensile properties (44, 46). Indeed, Col-I exerts high tensile strength and its expression is associated with tissue stiffness, whilst Col-III is more distensible and its expression refers to tissue elasticity, distensibility, and softness (43, 44). Thus, a high Col-I:Col-III ratio was found in tissues with high mechanical stiffness and low elasticity such as bones, and low Col-I:Col-III ratio was found in tissues with high elasticity, distensibility, or softness such as lung, bladder, and blood vessels (44). In cardiovascular remodeling, the Col-I:Col-III ratio is considered a marker of tissue stiffness determining mechanical properties and was shown to be associated with adverse outcomes (47). Indeed, an elevated Col-I:Col-III ratio was associated with increased myocardial stiffness and electrical instability of the myocardium (48), and increased stiffness of vessels including the aorta and arteries (49, 50). Increased stiffness of the remodeled vasculature was shown to be prognostically unfavorable in hypertension (51). We previously found an upward shift of the Col-I:Col-III ratio in a remodeled heart (52) and aorta (49) in a model of continuous light-induced hypertension. Reducing the Col-I:Col-III ratio in vessels was associated with improved hemodynamics in continuous light-induced hypertension (49) and pulmonary arterial hypertension (53). In this study, we dosed L-NAME for only 4 weeks (reaching a moderate increase in 4-week average systolic blood pressure) to assess early hypertensive kidney damage and its potential reversibility with ivabradine. Although Col-I and Col-III are deposited from early stages of kidney fibrosis (45, 46), NO deficiency in L-NAME-hypertension was found to specifically up-regulate collagen I expression in kidneys at an early stage even preceding the increase in blood pressure (54). This might explain the increased Col-I expression (early activation) and unchanged Col-III expression (activation lagging) observed in early hypertensive kidney damage in this study. Furthermore, in L-NAME-treated rats, ivabradine increased Col-III volume solely in the vascular/perivascular fibrosis while a profound drop in Col-I volume prevailed at all three of the investigated sites. Previously, ivabradine was shown to increase aortic compliance in apolipoprotein E-deficient mice (55), improve carotid pulsatile arterial hemodynamics in spontaneously hypertensive rats (56), restore acetylcholine-induced maximal dilatation of renal and cerebral arteries in dyslipidaemic mice (57), and most importantly, improve myocardial perfusion in post-MI rats by ameliorating perivascular fibrosis in small resistant coronary arteries (25). Therefore, by virtue of Col-III's elastic properties, the vascular/perivascular Col-III enhancement associated with the reduction of the Col-I:Col-III ratio by ivabradine observed in our study implies improved arterial compliance and pulsatile hemodynamics (49).

Col-IV, a main component of the glomerular basement membrane, is considered to play a critical role in glomerular pathology (58). Indeed, capillary expansion and mesangial cell stretching by increased intraglomerular pressure, often seen in hypertension, were found to provoke increased mesangial extracellular matrix (including Col-IV) production and deposition (59). Therefore, increased Col-IV protein expression was found in kidneys in various animal models of hypertension such as spontaneously hypertensive rats (60), angiotensin II-induced hypertension (61) or 2 kidneys, 1 clip model of hypertension (62), and also in patients with preeclampsia or other hypertensive syndromes in pregnancy (63). In L-NAME-hypertension, in particular, an exaggerated Col-IV gene and protein expression within the renal vasculature associated with glomerulosclerosis was found (64). Nonetheless, to the best of our knowledge, this is the first study determining Col-IV volume specifically in glomeruli in L-NAME-hypertension, where ivabradine mitigated the L-NAME-induced increase of glomerular Col-IV volume, thus supporting ivabradine's beneficial effect on glomerulosclerosis in L-NAME-hypertension.

Furthermore, in this study, L-NAME-hypertension induced tubular injury that correlated with tubulointerstitial fibrosis. This is in line with findings from other animal models of hypertension such as spontaneously hypertensive rats (65), angiotensin II-induced hypertension (66), and the Dahl salt-sensitive rat model of hypertension (67). Yet, mechanisms underlying tubular injury in hypertension are puzzling. Indeed, there were suggested (i) hemodynamics-dependent mechanisms, including tubular atrophy following glomerulotubular disconnection associated with glomerular injury (68), and (ii) hemodynamics-independent mechanisms, including renal oxidative stress and inflammation (69). In this study, ivabradine mitigated tubular injury and decreased tubulointerstitial fibrosis in L-NAME-hypertension, which were presumably associated with ivabradine's effects on both hemodynamics-dependent and independent mechanisms of tubular injury.

Recently, the plasma and urinary markers of Col-III (70), Col-IV and Col-VI (43) turnover have been shown to be a proxy for kidney fibrosis correlating with kidney function deterioration, and severity and the prognosis of CKD, thus holding promise as a novel, non-invasive diagnostic and prognostic tool to monitor kidney fibrosis in CKD (70, 71). This histopathological study was designed to directly and site-specifically determine collagen volumes in L-NAME-induced kidney fibrosis. It may be of interest to correlate histopathology and plasma or urinary markers of kidney fibrosis and function. Yet, this was beyond the scope and possibilities of the present histopathological study.

We conclude that ivabradine mitigated alterations to glomerular density and tuft area and site-specifically modified renal fibrosis in L-NAME-hypertension. These results suggest that ivabradine may be renoprotective in hypertensive kidney disease.

DATA AVAILABILITY STATEMENT

The datasets generated for this study are available on request to the corresponding author.

ETHICS STATEMENT

The animal study was reviewed and approved by The Ethical Committee of the Institute of Pathophysiology, Faculty of Medicine, Comenius University, Bratislava, Slovakia.

AUTHOR CONTRIBUTIONS

FS and TB conceived and designed the study and drafted the manuscript. PS, TB, KR, SA, and KK carried out animal experiments. PS, AB, PJ, MA, and LP conducted histopathological analysis. All authors participated in data analysis and interpretation, manuscript revision, and approved the submitted version.

FUNDING

This experiment was supported by research Grants VEGA 1/0035/19, VEGA 2/0112/19, UK/45/2020, and Program PROGRES Q40/5.

REFERENCES

1. Mills KT, Xu Y, Zhang W, Bundy JD, Chen CS, Kelly TN, et al. A systematic analysis of worldwide population-based data on the global burden of chronic kidney disease in 2010. *Kidney Int.* (2015) 88:950–7. doi: 10.1038/ki.2015.230
2. Hrenak J, Paulis L, Repova K, Aziriova S, Nagtegaal EJ, Reiter RJ, et al. Melatonin and renal protection: novel perspectives from animal experiments and human studies (review). *Curr Pharm Des.* (2015) 21:936–49. doi: 10.2174/1381612820666140929092929
3. Schlondorff DO. Overview of factors contributing to the pathophysiology of progressive renal disease. *Kidney Int.* (2008) 74:860–6. doi: 10.1038/ki.2008.351
4. Bidani AK, Griffin KA. Pathophysiology of hypertensive renal damage: implications for therapy. *Hypertension.* (2004) 44:595–601. doi: 10.1161/01.HYP.0000145180.38707.84
5. Swedberg K, Komajda M, Böhm M, Borer JS, Ford I, Dubost-Brama A, et al. Ivabradine and outcomes in chronic heart failure (SHIFT): a randomised placebo-controlled study. *Lancet.* (2010) 376:875–85. doi: 10.1016/S0140-6736(10)61198-1
6. Mangiacapra F, Colaiori I, Ricottini E, Balducci F, Creta A, Demartini C, et al. Heart rate reduction by IVabradine for improvement of ENDothELial function in patients with coronary artery disease: the RIVENDEL study. *Clin Res Cardiol.* (2017) 106:69–75. doi: 10.1007/s00392-016-1024-7
7. Simko F, Baka T, Poglitsch M, Repova K, Aziriova S, Krajcirovicova K, et al. Effect of ivabradine on a hypertensive heart and the renin-angiotensin-aldosterone system in L-NAME-induced hypertension. *Int J Mol Sci.* (2018) 19:E3017. doi: 10.3390/ijms19103017
8. Baka T, Simko F. Ivabradine reversed nondipping heart rate in rats with l-NAME-induced hypertension. *Clin Exp Pharmacol Physiol.* (2019) 46:607–10. doi: 10.1111/1440-1681.13075
9. Simko F, Baka T. Chronotherapy as a potential approach to hypertensive patients with elevated heart rate? *Br J Clin Pharmacol.* (2019) 85:1861–2. doi: 10.1111/bcp.14020
10. Hrenak J, Arendasova K, Rajkovicova R, Aziriova S, Repova K, Krajcirovicova K, et al. Protective effect of captopril, olmesartan, melatonin and compound 21 on doxorubicin-induced nephrotoxicity in rats. *Physiol Res.* (2013) 62 (Suppl. 1):S181–9.
11. Pechanova O, Matuskova J, Capikova D, Jendekova L, Paulis L, Simko F. Effect of spironolactone and captopril on nitric oxide and S-nitrosothiol formation in kidney of L-NAME-treated rats. *Kidney Int.* (2006) 70:170–6. doi: 10.1038/sj.ki.5001513
12. Seccia TM, Maniero C, Belloni AS, Guidolin D, Pothen P, Pessina AC, et al. Role of angiotensin II, endothelin-1 and L-type calcium channel in the development of glomerular, tubulointerstitial and perivascular fibrosis. *J Hypertens.* (2008) 26:2022–9. doi: 10.1097/HJH.0b013e328309f00a
13. Hartig SM. Basic image analysis and manipulation in ImageJ. *Curr Protoc Mol Biol.* (2013) Chapter 14:Unit14.15. doi: 10.1002/0471142727.mb1415s102
14. Pichler RH, Franceschini N, Young BA, Hugo C, Andoh TF, Burdmann EA, et al. Pathogenesis of cyclosporine nephropathy: roles of angiotensin II and osteopontin. *J Am Soc Nephrol.* (1995) 6:1186–96.
15. Simko F, Baka T, Krajcirovicova K, Repova K, Aziriova S, Zorad S, et al. Effect of melatonin on the renin-angiotensin-aldosterone system in l-NAME-induced hypertension. *Molecules.* (2018) 23:E265. doi: 10.3390/molecules23020265
16. Bernatova I, Pechanova O, Simko F. Captopril prevents NO-deficient hypertension and left ventricular hypertrophy without affecting nitric oxide synthase activity in rats. *Physiol Res.* (1996) 45:311–6.
17. Pechanova O, Bernatova I, Pelouch V, Simko F. Protein remodelling of the heart in NO-deficient hypertension: the effect of captopril. *J Mol Cell Cardiol.* (1997) 29:3365–74. doi: 10.1006/jmcc.1997.0566
18. Bernatova I, Pechanova O, Simko F. Effect of captopril in L-NAME-induced hypertension on the rat myocardium, aorta, brain and kidney. *Exp Physiol.* (1999) 84:1095–105. doi: 10.1111/j.1469-445X.1999.01890.x
19. Simko F, Matuskova J, Luptak I, Krajcirovicova K, Kucharska J, Gvozdjakova A, et al. Effect of simvastatin on remodeling of the left ventricle and aorta in L-NAME-induced hypertension. *Life Sci.* (2004) 74:1211–24. doi: 10.1016/j.lfs.2003.07.032
20. Simko F, Simko J. The potential role of nitric oxide in the hypertrophic growth of the left ventricle. *Physiol Res.* (2000) 49:37–46.
21. Hropot M, Grötsch H, Klaus E, Langer KH, Linz W, Wiemer G, et al. Ramipril prevents the detrimental sequels of chronic NO synthase inhibition in rats: hypertension, cardiac hypertrophy and renal insufficiency. *Naunyn Schmiedebergs Arch Pharmacol.* (1994) 350:646–52. doi: 10.1007/BF00169370
22. Ndisang JF, Chibbar R. Heme oxygenase improves renal function by potentiating podocyte-associated proteins in Nω-nitro-l-arginine-methyl ester (l-NAME)-induced hypertension. *Am J Hypertens.* (2015) 28:930–42. doi: 10.1093/ajh/hpu240
23. Ikeda H, Tsuruya K, Toyonaga J, Masutani K, Hayashida H, Hirakata H, et al. Spironolactone suppresses inflammation and prevents L-NAME-induced renal injury in rats. *Kidney Int.* (2009) 75:147–55. doi: 10.1038/ki.2008.507
24. Suehiro T, Tsuruya K, Ikeda H, Toyonaga J, Yamada S, Noguchi H, et al. Systemic aldosterone, but not angiotensin II, plays a pivotal role in the pathogenesis of renal injury in chronic nitric oxide-deficient male rats. *Endocrinology.* (2015) 156:2657–66. doi: 10.1210/en.2014-1369
25. Dedkov EI, Zheng W, Christensen LP, Weiss RM, Mahlberg-Gaudin F, Tomanek RJ. Preservation of coronary reserve by ivabradine-induced reduction in heart rate in infarcted rats is associated with decrease in perivascular collagen. *Am J Physiol Heart Circ Physiol.* (2007) 293:H590–8. doi: 10.1152/ajpheart.00047.2007
26. Busseuil D, Shi Y, Mecteau M, Brand G, Gillis MA, Thorin E, et al. Heart rate reduction by ivabradine reduces diastolic dysfunction and cardiac fibrosis. *Cardiology.* (2010) 117:234–42. doi: 10.1159/000322905
27. Custodis F, Baumhäkel M, Schlimmer N, List F, Gensch C, Böhm M, et al. Heart rate reduction by ivabradine reduces oxidative stress, improves endothelial function, and prevents atherosclerosis in apolipoprotein E-deficient mice. *Circulation.* (2008) 117:2377–87. doi: 10.1161/CIRCULATIONAHA.107.746537
28. Kröller-Schön S, Schulz E, Wenzel P, Kleschyov AL, Hortmann M, Torzewski M, et al. Differential effects of heart rate reduction with ivabradine in two models of endothelial dysfunction and oxidative stress. *Basic Res Cardiol.* (2011) 106:1147–58. doi: 10.1007/s00395-011-0227-3
29. Simko F, Pechanova O, Pelouch V, Krajcirovicova K, Mullerova M, Bednarova K, et al. Effect of melatonin, captopril, spironolactone and simvastatin on blood pressure and left ventricular remodelling in

spontaneously hypertensive rats. *J Hypertens Suppl.* (2009) 27:S5–10. doi: 10.1097/01.hjh.0000358830.95439.e8
30. Simko F, Pechanova O, Pelouch V, Krajcirovicova K, Celec P, Palffy R, et al. Continuous light and L-NAME-induced left ventricular remodelling: different protection with melatonin and captopril. *J Hypertens.* (2010) 28 (Suppl. 1):S13–8. doi: 10.1097/01.hjh.0000388489.28213.08
31. Simko F, Pechanova O, Repova K, Aziriova S, Krajcirovicova K, Celec P, et al. Lactacystin-induced model of hypertension in rats: effects of melatonin and captopril. *Int J Mol Sci.* (2017) 18:E1612. doi: 10.3390/ijms18081612
32. Williams B, Mancia G, Spiering W, Agabiti Rosei E, Azizi M, Burnier M, et al. 2018 ESC/ESH guidelines for the management of arterial hypertension. *Eur Heart J*. (2018) 39:3021–104. doi: 10.1097/HJH.0000000000001940
33. Luong L, Duckles H, Schenkel T, Mahmoud M, Tremoleda JL, Wylezinska-Arridge M, et al. Heart rate reduction with ivabradine promotes shear stress-dependent anti-inflammatory mechanisms in arteries. *Thromb Haemost*. (2016) 116:181–90. doi: 10.1160/TH16-03-0214
34. Aziriova S, Repova K, Krajcirovicova K, Baka T, Zorad S, Mojto V, et al. Effect of ivabradine, captopril and melatonin on the behaviour of rats in L-nitro-arginine methyl ester-induced hypertension. *J Physiol Pharmacol*. (2016) 67:895–902.
35. Küng CF, Moreau P, Takase H, Lüscher TF. L-NAME hypertension alters endothelial and smooth muscle function in rat aorta. Prevention by trandolapril and verapamil. *Hypertension*. (1995) 26:744–51. doi: 10.1161/01.HYP.26.5.744
36. Jones AM, Wilkerson DP, Campbell IT. Nitric oxide synthase inhibition with L-NAME reduces maximal oxygen uptake but not gas exchange threshold during incremental cycle exercise in man. *J Physiol*. (2004) 560:329–38. doi: 10.1113/jphysiol.2004.065664
37. Scrogin KE, Hatton DC, Chi Y, Luft FC. Chronic nitric oxide inhibition with L-NAME: effects on autonomic control of the cardiovascular system. *Am J Physiol.* (1998) 274:R367–74. doi: 10.1152/ajpregu.1998.274.2.R367
38. Vasquez EC, Cunha RS, Cabral AM. Baroreceptor reflex function in rats submitted to chronic inhibition of nitric oxide synthesis. *Braz J Med Biol Res*. (1994) 27:767–74.
39. Sherman AJ, Davis CA III, Klocke FJ, Harris KR, Srinivasan G, Yaacoub AS, et al. Blockade of nitric oxide synthesis reduces myocardial oxygen consumption *in vivo*. *Circulation*. (1997) 95:1328–34. doi: 10.1161/01.CIR.95.5.1328
40. Shesely EG, Maeda N, Kim HS, Desai KM, Krege JH, Laubach VE, et al. Elevated blood pressures in mice lacking endothelial nitric oxide synthase. *Proc Natl Acad Sci USA*. (1996) 93:13176–81. doi: 10.1073/pnas.93.23.13176
41. DiFrancesco D. Cardiac pacemaker I(f) current and its inhibition by heart rate-reducing agents. *Curr Med Res Opin*. (2005) 21:1115–22. doi: 10.1185/030079905X50543
42. Bucchi A, Baruscotti M, DiFrancesco D. Current-dependent block of rabbit sino-atrial node I(f) channels by ivabradine. *J Gen Physiol*. (2002) 120:1–13. doi: 10.1085/jgp.20028593
43. Rasmussen DGK, Boesby L, Nielsen SH, Tepel M, Birot S, Karsdal MA, et al. Collagen turnover profiles in chronic kidney disease. *Sci Rep*. (2019) 9:16062. doi: 10.1038/s41598-019-51905-3
44. Asgari M, Latifi N, Heris HK, Vali H, Mongeau L. *In vitro* fibrillogenesis of tropocollagen type III in collagen type I affects its relative fibrillar topology and mechanics. *Sci Rep*. (2017) 7:1392. doi: 10.1038/s41598-017-01476-y
45. Bülow RD, Boor P. Extracellular matrix in kidney fibrosis: more than just a scaffold. *J Histochem Cytochem*. (2019) 67:643–61. doi: 10.1369/0022155419849388
46. Genovese F, Manresa AA, Leeming DJ, Karsdal MA, Boor P. The extracellular matrix in the kidney: a source of novel non-invasive biomarkers of kidney fibrosis? *Fibrogenesis Tissue Repair*. (2014) 7:4. doi: 10.1186/1755-1536-7-4
47. Weber KT. Targeting pathological remodeling: concepts of cardioprotection and reparation. *Circulation*. (2000) 102:1342–5. doi: 10.1161/01.CIR.102.12.1342
48. Xu J, Cui G, Esmailian F, Plunkett M, Marelli D, Ardehali A, et al. Atrial extracellular matrix remodeling and the maintenance of atrial fibrillation. *Circulation*. (2004) 109:363–8. doi: 10.1161/01.CIR.0000109495.02213.52
49. Repova-Bednarova K, Aziriova S, Hrenak J, Krajcirovicova K, Adamcova M, Paulis L, et al. Effect of captopril and melatonin on fibrotic rebuilding of the aorta in 24 hour light-induced hypertension. *Physiol Res.* (2013) 62 (Suppl. 1):S135–41.
50. Dobrin PB, Mrkvicka R. Failure of elastin or collagen as possible critical connective tissue alterations underlying aneurysmal dilatation. *Cardiovasc Surg*. (1994) 2:484–8.
51. Schiffrin EL. Vascular remodeling in hypertension: mechanisms and treatment. *Hypertension*. (2012) 59:367–74. doi: 10.1161/HYPERTENSIONAHA.111.187021
52. Paulis L, Vazan R, Simko F, Pechanova O, Styk J, Babal P, et al. Morphological alterations and NO-synthase expression in the heart after continuous light exposure of rats. *Physiol Res*. (2007) 56(Suppl. 2):S71–6.
53. Liu P, Yan S, Chen M, Chen A, Yao D, Xu X, et al. Effects of baicalin on collagen I and collagen III expression in pulmonary arteries of rats with hypoxic pulmonary hypertension. *Int J Mol Med*. (2015) 35:901–8. doi: 10.3892/ijmm.2015.2110
54. Chatziantoniou C, Boffa JJ, Ardaillou R, Dussaule JC. Nitric oxide inhibition induces early activation of type I collagen gene in renal resistance vessels and glomeruli in transgenic mice. Role of endothelin. *J Clin Invest*. (1998) 101:2780–9. doi: 10.1172/JCI2132
55. Custodis F, Fries P, Müller A, Stamm C, Grube M, Kroemer HK, et al. Heart rate reduction by ivabradine improves aortic compliance in apolipoprotein E-deficient mice. *J Vasc Res.* (2012) 49:432–40. doi: 10.1159/000339547
56. Albaladejo P, Carusi A, Apartian A, Lacolley P, Safar ME, Bénétos A. Effect of chronic heart rate reduction with ivabradine on carotid and aortic structure and function in normotensive and hypertensive rats. *J Vasc Res.* (2003) 40:320–8. doi: 10.1159/000072696
57. Drouin A, Gendron ME, Thorin E, Gillis MA, Mahlberg-Gaudin F, Tardif JC. Chronic heart rate reduction by ivabradine prevents endothelial dysfunction in dyslipidaemic mice. *Br J Pharmacol.* (2008) 154:749–57. doi: 10.1038/bjp.2008.116
58. Miner JH. The glomerular basement membrane. *Exp Cell Res*. (2012) 318:973–8. doi: 10.1016/j.yexcr.2012.02.031
59. Riser BL, Cortes P, Zhao X, Bernstein J, Dumler F, Narins RG. Intraglomerular pressure and mesangial stretching stimulate extracellular matrix formation in the rat. *J Clin Invest*. (1992) 90:1932–43. doi: 10.1172/JCI116071
60. Guo Z, Sun H, Zhang H, Zhang Y. Anti-hypertensive and renoprotective effects of berberine in spontaneously hypertensive rats. *Clin Exp Hypertens*. (2015) 37:332–9. doi: 10.3109/10641963.2014.972560
61. Castoldi G, Carletti R, Ippolito S, Colzani M, Barzaghi F, Stella A, et al. Renal anti-fibrotic effect of sodium glucose cotransporter 2 inhibition in angiotensin II-dependent hypertension. *Am J Nephrol*. (2020) 51:119–29. doi: 10.1159/000505144
62. Li L, Wang C, Gu Y. Collagen IV, a promising serum biomarker for evaluating the prognosis of revascularization in a 2-kidney, 1-clip hypertensive rat model. *Interact Cardiovasc Thorac Surg*. (2020) 30:483–90. doi: 10.1093/icvts/ivz275
63. Foidart JM, Nochy D, Nusgens B, Foidart JB, Mahieu PR, Lapiere CM, et al. Accumulation of several basement membrane proteins in glomeruli of patients with preeclampsia and other hypertensive syndromes of pregnancy. possible role of renal prostaglandins and fibronectin. *Lab Invest*. (1983) 49:250–9.
64. Boffa JJ, Lu Y, Placier S, Stefanski A, Dussaule JC, Chatziantoniou C. Regression of renal vascular and glomerular fibrosis: role of angiotensin II receptor antagonism and matrix metalloproteinases. *J Am Soc Nephrol*. (2003) 14:1132–44. doi: 10.1097/01.ASN.0000060574.38107.3B
65. Ofstad J, Iversen BM. Glomerular and tubular damage in normotensive and hypertensive rats. *Am J Physiol Renal Physiol*. (2005) 288:F665–72. doi: 10.1152/ajprenal.00226.2004
66. Polichnowski AJ, Cowley AW Jr. Pressure-induced renal injury in angiotensin II versus norepinephrine-induced hypertensive rats. *Hypertension*. (2009) 54:1269–77. doi: 10.1161/HYPERTENSIONAHA.109.139287
67. Wei SY, Wang YX, Zhang QF, Zhao SL, Diao TT, Li JS, et al. Multiple mechanisms are involved in salt-sensitive hypertension-induced renal injury and interstitial fibrosis. *Sci Rep*. (2017) 7:45952. doi: 10.1038/srep45952
68. Chevalier RL, Forbes MS. Generation and evolution of atubular glomeruli in the progression of renal disorders. *J Am Soc Nephrol*. (2008) 19:197–206. doi: 10.1681/ASN.2007080862

69. Polichnowski AJ, Lu L, Cowley AW Jr. Renal injury in angiotensin II+L-NAME-induced hypertensive rats is independent of elevated blood pressure. *Am J Physiol Renal Physiol*. (2011) 300:F1008–16. doi: 10.1152/ajprenal.00354.2010
70. Genovese F, Boor P, Papasotiriou M, Leeming DJ, Karsdal MA, Floege J. Turnover of type III collagen reflects disease severity and is associated with progression and microinflammation in patients with IgA nephropathy. *Nephrol Dial Transplant*. (2016) 31:472–9. doi: 10.1093/ndt/gfv301
71. Papasotiriou M, Genovese F, Klinkhammer BM, Kunter U, Nielsen SH, Karsdal MA, et al. Serum and urine markers of collagen degradation reflect renal fibrosis in experimental kidney diseases. *Nephrol Dial Transplant*. (2015) 30:1112–21. doi: 10.1093/ndt/gfv063

Conflict of Interest: The authors declare that the research was conducted in the absence of any commercial or financial relationships that could be construed as a potential conflict of interest.

frontiers in Physiology

ORIGINAL RESEARCH
published: 01 September 2020
doi: 10.3389/fphys.2020.01046

Intrarenal Renin Angiotensin System Imbalance During Postnatal Life Is Associated With Increased Microvascular Density in the Mature Kidney

*Carolina Dalmasso[1], Alejandro R. Chade[2], Mariela Mendez[3], Jorge F. Giani[4], Gregory J. Bix[5], Kuey C. Chen[1] and Analia S. Loria[1]**

[1] Department of Pharmacology and Nutritional Sciences, University of Kentucky, Lexington, KY, United States, [2] Department of Physiology and Biophysics, Medicine, and Radiology, University of Mississippi Medical Center, Jackson, MS, United States, [3] Department of Internal Medicine, Hypertension and Vascular Research Division, Henry Ford Hospital, Detroit, MI, United States, [4] Departments of Biomedical Sciences and Pathology, Cedars-Sinai Medical Center, Los Angeles, CA, United States, [5] Clinical Neuroscience Research Center, Tulane University, New Orleans, LA, United States

OPEN ACCESS

Edited by:
Suttira Intapad, Tulane University School of Medicine, United States

Reviewed by:
Dulce Elena Casarini, Federal University of São Paulo Paulista School of Medicine, Brazil
Adrien Flahault, CHU Sainte-Justine Research Center, Canada
Ryousuke Satou, Tulane Medical Center, United States
Sarah Walton, Monash University, Australia

***Correspondence:**
Analia S. Loria
analia.loria@uky.edu

Specialty section:
This article was submitted to Renal and Epithelial Physiology, a section of the journal Frontiers in Physiology

Received: *12 May 2020*
Accepted: *30 July 2020*
Published: *01 September 2020*

Citation:
Dalmasso C, Chade AR, Mendez M, Giani JF, Bix GJ, Chen KC and Loria AS (2020) Intrarenal Renin Angiotensin System Imbalance During Postnatal Life Is Associated With Increased Microvascular Density in the Mature Kidney. Front. Physiol. 11:1046. doi: 10.3389/fphys.2020.01046

Environmental stress during early life is an important factor that affects the postnatal renal development. We have previously shown that male rats exposed to maternal separation (MatSep), a model of early life stress, are normotensive but display a sex-specific reduced renal function and exacerbated angiotensin II (AngII)-mediated vascular responses as adults. Since optimal AngII levels during postnatal life are required for normal maturation of the kidney, this study was designed to investigate both short- and long-term effect of MatSep on (1) the renal vascular architecture and function, (2) the intrarenal renin-angiotensin system (RAS) components status, and (3) the genome-wide expression of genes in isolated renal vasculature. Renal tissue and plasma were collected from male rats at different postnatal days (P) for intrarenal RAS components mRNA and protein expression measurements at P2, 6, 10, 14, 21, and 90 and microCT analysis at P21 and 90. Although with similar body weight and renal mass trajectories from P2 to P90, MatSep rats displayed decreased renal filtration capacity at P90, while increased microvascular density at both P21 and P90 ($p < 0.05$). MatSep increased renal expression of renin, and angiotensin type 1 (AT1) and type 2 (AT2) receptors ($p < 0.05$), but reduced ACE2 mRNA expression and activity from P2-14 compared to controls. However, intrarenal levels of AngII peptide were reduced ($p < 0.05$) possible due to the increased degradation to AngIII by aminopeptidase A. In isolated renal vasculature from neonates, Enriched Biological Pathways functional clusters (EBPfc) from genes changed by MatSep reported to modulate extracellular structure organization, inflammation, and pro-angiogenic transcription factors. Our data suggest that male neonates exposed to MatSep could display permanent changes in the renal microvascular architecture in response to intrarenal RAS imbalance in the context of the atypical upregulation of angiogenic factors.

Keywords: maternal separation, kidney, renin-angiotensin system, microvascular density, renal transcriptome

INTRODUCTION

Recent statistics show that nearly 40 million adults in the United States are estimated to have chronic kidney disease (CKD), while around 250 deaths per day are a consequence of end-stage renal disease (Centers for Disease Control Prevention, 2019). The majority of patients with CKD develop hypertension, a risk factor for cardiovascular disease (Ku et al., 2019). A healthy renal function is determined by genetic and environmental factors including low birth weight and intrauterine growth restriction (Franco et al., 2012; Ponzio et al., 2012; Souza et al., 2017). Particularly, both *in utero* and early life are periods of high tissue plasticity, susceptible to stressors and insults that impair the normal development of neuroendocrine, inflammatory, hormonal and autonomic responses (Zandi-Nejad et al., 2006; Hershkovitz et al., 2007; Stangenberg et al., 2015). From birth to age 4, congenital abnormalities and hereditary diseases are the leading causes of kidney disease (US Renal Data System, 2010). However, there is limited understanding of the pathophysiology by which psychosocial factors contribute to kidney disease.

Early life stress (ELS), or chronic behavioral stress during childhood, has been established as an independent cardiovascular disease risk factor (Su et al., 2015; Murphy et al., 2017). Overall, models of fetal programming of cardiovascular disease have been designed to test the effect of environmental stressors including perinatal low-protein diet, growth restriction or beta-dexamethasone exposure (Hershkovitz et al., 2007). These approaches induce a dramatic reduction in glomerular number, with a subsequent renal damage and development of hypertension. The human kidney is functional beginning at week 10 of gestation, and diuresis rate is 10 ml/hr at 32 weeks of gestation (Campbell et al., 1973); however, its maturation is completed during the next several years. In rodents, the developing kidney is particularly vulnerable to adverse perinatal environments affecting both the early and the late nephrogenic period, which will result in impaired renal excretory capacity later in life (Chen et al., 2004; Singh et al., 2013; Walton et al., 2018). Moreover, a hallmark of these models is the well-defined role of the intrarenal renin-angiotensin system (RAS) as a prerequisite for a normal nephron endowment (Guron and Friberg, 2000; Lasaitiene et al., 2003). Conversely, the pharmacological blockade of either angiotensin converting enzyme (ACE) or angiotensin II (AngII) type 1 (AT1) receptor during late nephrogenesis (postnatal days 2–14) impair renal maturation and is associated with the development of hypertension later in life (Loria et al., 2007; Saez et al., 2007).

Maternal separation (MatSep) is a chronic behavioral stress model that mimics the effects of ELS on behavioral, neuroendocrine, metabolic and cardiovascular responses (Loria et al., 2010; De Miguel et al., 2018). In previous studies, we have reported that adult male rats exposed to MatSep are normotensive and display reduced glomerular filtration rate (GFR) (Loria et al., 2013a; Loria and Osborn, 2017) and enhanced sensitivity to *in vitro* and *in vivo* AngII-mediated responses (Loria et al., 2010, 2011). On the other hand, adult female MatSep rats are normotensive but do not undergo impaired GFR or signs of proteinuria (Loria et al., 2013b). Furthermore, female MatSep rats show exacerbated AngII-induced hypertension independent of any significant worsening of the renal function compared to control littermates. In this regard, several studies have shown that hypersensitization to AngII after *in utero* exposure to low pressor doses of AngII occurs in adult male rats only (Johnson and Xue, 2018). This phenomenon can be reversed by renal denervation or ACE inhibitors (Xue et al., 2017). Thus, postnatal stress may exert the sensitization of the renal system via alteration of neuroendocrine, sympathetic and/or immune responses in a sex-specific manner.

As AngII has been shown to play a crucial role in the stimulation of vasculogenesis and angiogenesis during renal development (Sequeira Lopez and Gomez, 2004), MatSep-induced intrarenal imbalance of RAS components during postnatal life could result in permanent structural and/or functional alterations on male rats' kidneys. Therefore, we investigated the effect of MatSep at different timepoints from neonatal to adult life, in order to determine (1) the renal vascular architecture and function, (2) the intrarenal renin-angiotensin system (RAS) components status, and (3) the genome-wide expression of genes in isolated renal vasculature, with the goal to create an integrative view of underlying mechanisms by which MatSep impact the normal renal structure and function in male rats.

MATERIALS AND METHODS

Maternal Separation (MatSep) Protocol

All experiments were conducted per the National Institutes of Health Guide for the Care and Use of Laboratory Animals, approved and monitored by the University of Kentucky Institutional Animal Care and Use Committee. MatSep was performed using offspring from Wistar Kyoto breeders. All pups were removed from their dam's cage from postnatal days 2 to 14 of life at the same time of day by transferring the pups to a clean cage in an incubator ($30 \pm 1°C$) for 3 h. The control group was the non-handled litters that remained with their mother (Loria et al., 2010; De Miguel et al., 2017). Different samples were taken under light isoflurane anesthesia at postnatal day 2 (P2), P6, P10, P14, P21, P90, and P180. Female littermates were kept for sampling or included in other studies.

Experimental Design

Groups were comprised of male rats from at least 4 different litters. Littermates were randomized at different time points. In a first subset, body weight, and kidney weights were recorded while plasma and renal tissue were collected at different timepoints and kidney gene and protein expression in frozen tissue were determined at different timepoints. The whole kidney for P2–P21 and renal cortex for P90 time points were used in the experiments. In this subset, the glomerular filtration rate (GFR) was determined at P21 and P90 in randomized littermates. In a second subset, kidneys were collected in neonates (P10) and adults (P180) to isolate the renal vasculature and perform a genome-wide transcriptome assays using Affymetrix GeneChip

microarrays. In the third subset of offspring, male rats were perfused at P21 and P90 with a silicone polymer, and kidneys were collected to measure the microvascular density.

Micro-Computerized Tomography

A saline-filled cannula was placed in the aorta, the aorta was ligated below and above the renal arteries, and infusion of 0.9% saline (containing 10 units/mL heparin) was initiated under physiological perfusion pressure at a rate of 2 mL/min (Syringe Infusion Pump 22; Harvard Apparatus, Holliston, MA, United States). A small incision was performed in the inferior vena cava to allow the saline infusion to drain. After 10–15 min of saline infusion and when it drained freely from the vein, it was immediately replaced with an infusion of intravascular contrast agent (2 mL/min), which was a freshly mixed radio-opaque silicone polymer contrast containing lead chromate (SkyScan 1076, Bruker Biospin Corp., MA, United States) until the polymer drained freely from the vein as previously reported (Flynn et al., 2013; Tullos et al., 2015). Then, the polymer-filled kidneys were left at 4°C overnight and then immersed in 10% buffered formalin for 72 h before scanning. The kidney samples were scanned at 0.3° increments using a micro-CT scanner (SkyScan 1076 system; Micro Photonics, Inc., Allentown, PA, United States), and the X-ray transmission images were acquired in each angle of view at a resolution of 18 μm and digitized to 16 bits grayscale. Three-dimensional (3D) volume images were reconstructed using a filtered back-projection algorithm and displayed on a computer workstation by volume rendering for display and analysis of renal MV using the Analyze software package (Biomedical Imaging Resource; Mayo Clinic, Rochester, MN, United States).

Western Blot

The whole kidney at P21 was homogenized and protein concentration was determined using the Bradford assay (Bio-Rad), and then samples containing 30 μg protein/well were loaded in 10% SDS-PAGE and transferred onto PVDF membranes. Membranes were incubating in blocking buffer (5% non-fat dry milk/TBS) for 1 h at room temperature, followed by overnight incubation at 4°C in the presence of antibodies directed against Perlecan primary antibody 1:250 (#sc-25848, Santa Cruz, CA, United States), and GAPDH primary antibody 1:10,000 (#GTX100118, GeneTex). Membranes were washed with TBS–0.1% Tween 20 and incubated in the presence of HRP-conjugated secondary antibody 1:20,000 (#926-32211, 926-68020). Band detection was performed by the LiCor Odyssey imaging system. Blot quantification was performed using NIH ImageJ software.

Immunohistochemistry

Whole kidneys were collected at P21 and frozen in OCT. Tissue was cut in 20 μm sections using a cryostat and directly mounted onto slides. Sections were fixed with ice-cold acetone/methanol (50:50 mixture) prior to incubating in blocking buffer (5% BSA in 1xPBS with 0.1% Triton X-100) for 1 h at room temperature. The sections were then incubated overnight at 4°C with FITC-conjugated tomato-lectin (1:200; Vector Laboratories, Burlingame, CA, United States). Slides were then washed and coverslipped with fluorescent mounting media (Vector Laboratories, Burlingame, CA, United States) and images were captured using Eclipse Ti microscope/DS-Ri1 CCD color camera and NIS analysis software (Nikon Instruments). Five images per animal were then analyzed for the number of stain-specific positive pixels using Adobe Photoshop (Adobe Inc.). Briefly, images were converted to grayscale, adjusted to a set threshold equal to the antibody staining and the number of pixels calculated. The data were averaged per group and are presented a number of positive pixels.

Transcutaneous Glomerular Filtration Rate (tGFR)

Renal function was evaluated by transcutaneous measurement of the elimination kinetics of fluorescein isothiocyanate (FITC)-sinistrin (Mannheim Pharma & Diagnostics). Rats were placed under light anesthesia (isoflurane) and the flank area was depilated to apply the transcutaneous receiver on top (NIC-kidney device). The receiver was secured around the body with 3M surgical tape. After the animal awakened from anesthesia, a 5-min baseline trace was recorded. Then, they were injected with 30 μl of FITC-sinistrin (5 mg/100 g BW in 0.9% saline, retroorbital, Fresenius Kabi, Linz, Austria) under light isoflurane using microneedles. After 90 min of measurement, the device was removed. The probe was read to determine $t_{1/2}$ in minutes. Renal function was evaluated by the elimination kinetics (three-compartmental model) using the following formula = $21.33/(t_{1/2})$ = GFR (μl/min/100 g BW).

Intrarenal RAS Components Trajectory

Renal Gene Expression by RT-qPCR

RNA was extracted from kidneys using RNeasy mini kit (Qiagen, CA). Briefly, total mRNA was extracted from tissues using TRIZOL reagent (Invitrogen Life Technologies, Carlsbad, CA, United States) according to the manufacturer's protocol. Rat forward (sense) and reverse (antisense) QuantiTect primers for GAPDH (Entrez ID: 35728), AGT (Entrez ID: 24179), renin (Entrez ID: 24715), AT_1 receptor (Entrez ID: 24182), AT_2 receptor (Entrez ID: 24180), ACE (Entrez ID: 24310), ACE2 (Entrez ID: 302668), MAS-1 (Entrez ID: 24180), Neprilysin (Entrez ID: 24590) and aminopeptidase A (Entrez ID: 64017) were analyzed by quantitative real-time RT-PCR as previously reported (Loria et al., 2011). GAPDH was used as a housekeeper gene. Ct values from each sample were normalized to GAPDH expression within the sample (ΔCt) followed by normalization to ΔCt values for AT2 control samples at P2 (ΔΔCt) prior to calculation of relative gene expression ($2^{-\Delta\Delta Ct}$) as previously described (Loria et al., 2011).

Renal AGT Protein Content

Renal tissue was homogenized in ELISA buffer (∼100 mg tissue/500 μl) and diluted 1:200 following the manufacturer's protocol (Immuno-Biological Laboratories America, Minneapolis, MN, United States) (Dalmasso et al., 2019).

Renal AngII Peptide Content

Kidneys were excised, drained, weighed, and homogenized in chilled inhibitor cocktail (EDTA 200 mM, PMSF 1 mM, 1,10 phenanthroline 125 mM, Pepstatin A 2 mM, Enalapril 1 mM) and 1 ml of methanol, centrifuged at 4°C for 10 min. The supernatants were dried overnight in a vacuum centrifuge (Savant, Hicksville, NY, United States). The dried residue was kept at −20°C until AngII peptide was determined by radioimmunoassays as described previously (Mitchell et al., 1997).

Plasma Renin Concentration (PRC)

Whole blood was collected in pre-chilled EDTA-coated tubes, centrifuged at 4°C and rapidly snap-frozen in liquid nitrogen. Immediately after thawing the samples, a protease inhibitor (PMSF) was added to the sample to prevent angiotensin I (AngI) cleavage by other proteases. PRC was determined as the amount of AngI synthesized after incubation with excess of angiotensinogen as previously described (Peng et al., 2001; Mendez et al., 2011). The assay relies on the fact that as long as the concentration of substrate is not limiting, the production of AngI by renin is constant. Substrate consumption is never greater than 3% of total AngI, and therefore assures linearity over time. Thus, plasma samples were incubated with excess rat angiotensinogen at 37°C for 1.5 h, boiled for 10 min, followed by centrifugation at 16,100 *g*. Supernatants were collected and generated AngI was measured using an ELISA kit (Immuno-Biological Laboratories, Minneapolis, MN, United States). Values were expressed as ng AngI/ml, generated per hour of incubation.

Renal Vasculature Isolation

Following euthanasia, kidneys from neonates (P10) or adults (P180) were removed and immediately placed into a petri dish with cold physiological saline solution (PSS). After removal of the renal capsule, the kidney was placed between a circle sieve of 70-μm pore size for neonates and 100-μm pore size for adult rats (Biodesign, Carmel, NY, United States) as previously reported (Loria and Osborn, 2017). Kidney vessels were immediately isolated by rapid and gentle grating. The kidney vessels were subsequently frozen in liquid nitrogen and stored at −80°C.

ACE and ACE2 Activity in Neonatal Kidneys

Both ACE and ACE2 activities were measured using fluorescence assays, as previously described (Eriguchi et al., 2018). Briefly, whole snap-frozen kidneys were gently homogenized in 20 mM HEPES (pH 7.3) and centrifuged at 3,000 *g* for 15 min at 4°C. The supernatant was discarded, and the pellets were vigorously re-homogenized in 20 mM HEPES with 0.5% Triton X-100 (pH 7.3). After a second centrifugation at 20,000 *g* for 20 min at 4°C, the supernatant was collected and the protein concentration was determined using a Pierce BCA protein assay kit (Thermo Scientific, Rockford, IL, United States). The ACE activity was measured using 2 μg of protein extract and 10 μM of the fluorescent substrate (Mca-Arg-Pro-Pro-Gly-Phe-Ser-Ala-Phe-Lys(Dnp)-OH (R&D Systems, Minneapolis, MN, United States) with and without the 2 μM ACE inhibitor captopril. ACE2 activity was measured using 3 μg of protein extract and 50 μM of the fluorescent substrate Mca-Ala-Pro-Lys(Dnp)-OH (Anaspec, Fremont, CA, United States) with and without 1 μM of the ACE2 inhibitor DX600. The degradation of the fluorogenic peptides (fluorescence) was measured over time in a spectrophotometer (FLUOstar Omega, BMG LABTECH) at 320 nm excitation and 405 nm emissions. Only the hydrolytic activity inhibited by the specific inhibitors was considered for calculations.

Microarray

Frozen renal tissue was used to extract and assess RNA purity and integrity. Tissue RNA was isolated from neonates and adults MatSep rats and their control littermates (P10 and P180, respectively; $n = 5$ per group). The genome-wide analysis was performed using rat GeneChip expression RaGene2.0_st arrays (Affymetrix, Thermo Fisher Scientific, United States). The microarray assays were run in the Microarray Core Facility at the University of Kentucky. Briefly, tissue RNA was labeled using WT-IVT whole transcriptome amplification procedure (following Affymetrix rat array protocol). For each sample, the labeled probes were applied on a rat Gene2.0 ST array for hybridization overnight, followed by array scanning to obtain probe signal intensity data file. The array data files of tissue samples were further processed to obtain signal intensity for each gene transcript. Enriched Biological Pathways functional clusters (EBPfc) affected by MatSep were analyzed by gene over-representation analysis using DAVID Functional Annotation Bioinformatics Microarray Analysis v6.8[1]. Data are available at https://www.ncbi.nlm.nih.gov/geo/query/acc.cgi?acc=GSE151402. Extended microarray findings including a general validation can be found in the **Supplementary Material**.

Statistical Analysis

Analysis was performed using the GraphPad Prism version 7.00 (Macintosh, GraphPad Software, La Jolla, CA, United States[2]). Data are reported as means ± SE. The criterion for significance was $p < 0.05$. Differences between control and MatSep groups between more than two-timepoints (P2-P90) were determined by two-way ANOVA. Differences in means among groups for non-repeated variables were compared by *t*-test when normality was verified.

For the statistical analysis of the microarray data, gene specific analysis (GSA) model implemented in Partek Genomics Suite (Partek, Inc., MO) was used to assess differential expression among the four experimental groups. Each RNA transcript signal intensity was first normalized to its mean value across all samples from the four experimental groups. Differentially expressed genes affected by MatSep in neonates and adult rats were identified by *post hoc* pair-wise comparisons.

[1] http://david.ncifcrf.gov

[2] www.graphpad.com

RESULTS

Effect of MatSep on Renal Mass and Function

Exposure to maternal separation did not affect the body weight trajectory from P2 to P90 in male rats (**Figure 1A**). In addition, MatSep and control rats displayed similar kidney weights at the same time points (**Figure 1B**). MatSep and control weanlings showed similar GFR. However, although older animals showed increased renal filtration capacity was increased in older rats, MatSep reduced GFR when compared with control littermates. These data indicate that MatSep induces long-term changes in renal function that are not caused by low birth weight or reduced renal mass (**Figure 1C**).

Effect of MatSep on Renal Microvascular Architecture

In response to MatSep, the number of vessels in the 0–200 and 0–500 μM range in kidneys from 21-day-old weanlings was significantly increased in both medulla and cortex areas (**Figure 2A**). Similarly, microvascular density was increased in kidneys from MatSep rats at P90 (**Figure 2B**), suggesting that MatSep exerts early, long-lasting effects on the density of the renal microvasculature. **Figures 2C,D** show representative images of the renal vascular tree at P21 and P90, respectively.

Furthermore, we determined perlecan (a marker of basement membrane) and tomato-Lectin (a marker of vascular endothelium) in kidneys from P21 rats. While perlecan protein expression was similar between groups (1.1 ± 0.1 vs. 0.9 ± 0.2 AU, **Figure 3A**), tomato-Lectin staining was reduced in kidneys from MatSep compared to control (32687 ± 4185 vs. 52578 ± 5988 positive pixels, $p < 0.05$, **Figure 3B**). Thus, MatSep induces a mismatch between increased microvasculature and cells expressing vascular endothelium in kidneys.

Effect of MatSep on Intrarenal RAS Trajectory

In the neonatal kidney, angiotensinogen (AGT) mRNA expression was not statistically different among the groups (**Figure 4A**). Renin (**Figure 4B**), Agtr1 (AT1) receptors (**Figure 4C**) and Agtr2 (AT2) receptors (**Figure 4D**) mRNA expression were higher in MatSep offspring between P6-P14 compared to controls. Renin and AngII receptors mRNA abundance were similar in kidneys from MatSep and control adult rats and significantly reduced compared to neonatal levels.

Notably, ACE mRNA expression was unchanged from P6-14 in MatSep neonates (**Figure 5A**), while ACE activity was increased (**Figure 5B**). However, both ACE2 mRNA and enzymatic activity were significantly reduced in kidneys from MatSep neonates compared to controls. In addition, the ACE/ACE2 ratio at P6 was ∼10 fold increased in MatSep tissue (**Figure 5C**). Furthermore, enpep (aminopeptidase A), another RAS enzyme which converts AngII to AngIII, was increased by MatSep during this postnatal window.

Renal AGT protein content was not significantly different between groups at any age (**Figure 6A**); however, AngII peptide levels were reduced by MatSep at P2, 6, 10, and 14 (**Figure 6B**). Nevertheless, PRC was increased at P6, P10, and P14 (**Figure 6C**).

Age Effect on Gene Expression in Isolated Renal Vasculature From Control Rats

Comparisons were made taking as a reference the changes in gene expression underwent by control samples from neonatal to adult life (P10 and P180). Of a total of 20258 annotated genes RNA transcripts, 12821 genes did not have significant changes in gene expression associated with age ($p < 0.03$ at step-up FDR < 0.05). However, 3745 genes showed a higher expression in neonates compared to adults and called "early life" genes. The 3692 remaining genes showed a higher expression in adults compared to neonates and were classified as "adult life" genes. A total of 489 genes altered by MatSep (FDR < 0.05). In addition, we identified 368 genes in which the expression was affected by the *MatSep x Age* interaction (FDR < 0.4). A detailed description of *MatSep x Age* interactions on isolated renal vasculature gene expression can be found in the **Supplementary Excel Spreadsheet**.

Effect of MatSep on Isolated Renal Vasculature Transcriptomics

Renal vasculature of MatSep neonates showed increased RAS of (**Table 1**), angiogenic (**Table 2**) and inflammatory (**Table 3**) gene expression compared with controls. Ace2 transcript was not included in the rat microarray that was used for this study.

Furthermore, MatSep induced downstream effects in a group of genes, whereas some of them were also linked to inflammation and angiogenesis (**Supplementary Table S2**). These genes were expressed similarly between groups in neonates but significantly changed by MatSep in adult rats. The 25 upregulated genes participate in diverse metabolic processes, embryonic cranium morphogenesis, anatomical structure development, circadian regulation of gene expression as well as ion homeostasis.

Table 4 shows that EBPfc affected by MatSep in neonates and adult rats are mostly related to cell proliferation and immune system activation. Finally, due to the fact that MatSep changes the vascular architecture of the kidney, we validated the tubular contamination and the proportion of vascular vs. non-vascular cells by RT-qPCR in our preparation. Similar to lectin, the vascular endothelium marker PECAM-1 was significantly reduced in both neonate and adult isolated vascular samples; however, the expression of tubular markers remained unchanged between groups (**Supplementary Figure S1**). Similarly, we found that the expression of these and other tubular markers in the microarray was similar amongst the groups (**Supplementary Table S3**).

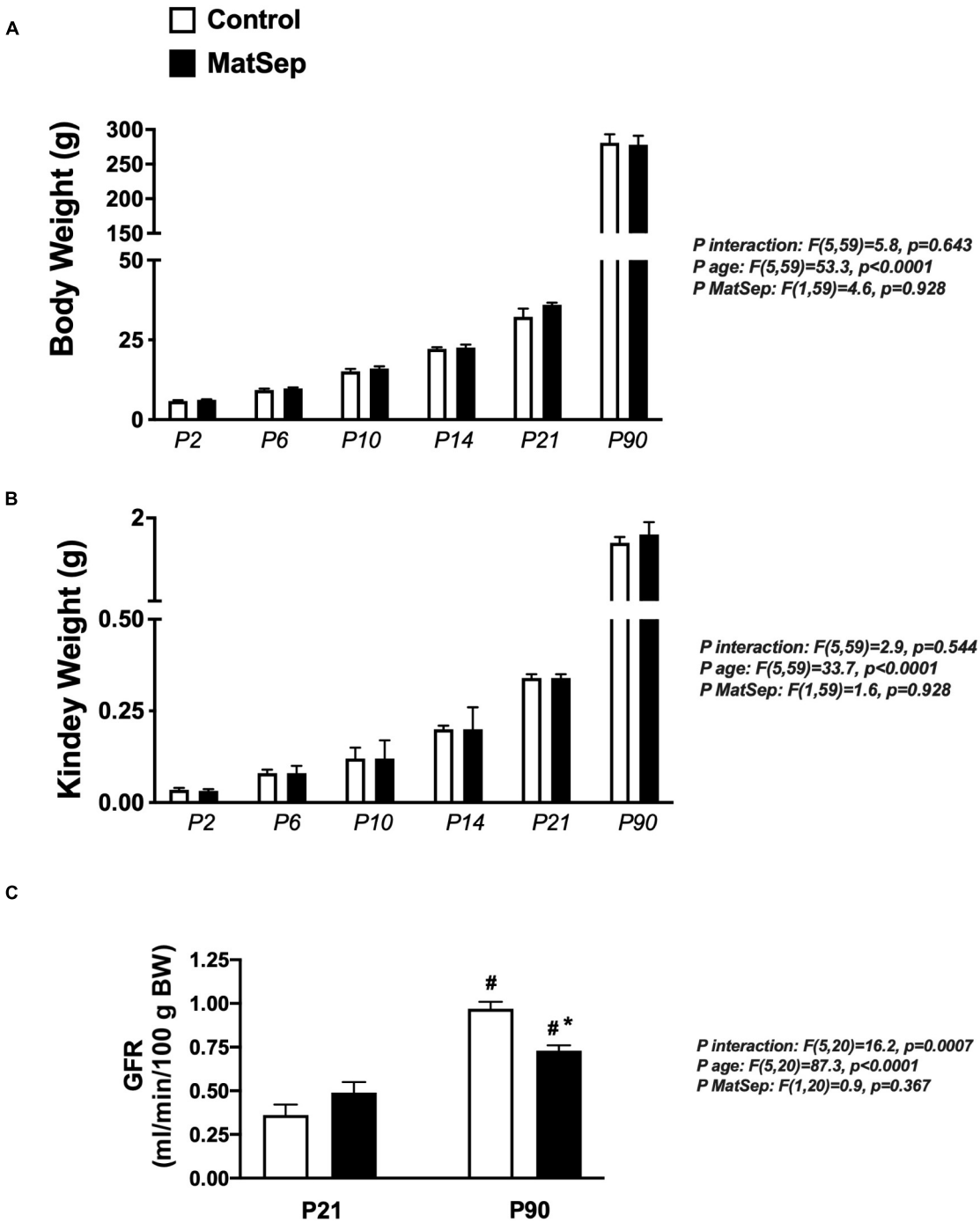

FIGURE 1 | Effect of MatSep on the trajectory from neonatal to adult male rats in: **(A)** body weight, **(B)** Kidney, and **(C)** conscious GFR. #$p < 0.05$ vs. P21, *$p < 0.05$ vs. C. P: postnatal day. $n = 6$–8 per group.

DISCUSSION

This study shows that MatSep, a rat model of early life stress, dysregulates the expression and activity of several components of the RAS, which normal function is required for an optimal nephron and vascular tissue development during early postnatal life (Guron and Friberg, 2000; Lasaitiene et al., 2003; Walton et al., 2018). Surprisingly, intrarenal AngII levels were reduced in neonates, along with reduced ACE2 expression and activity. These data suggest that other AngII-derived peptides, in addition

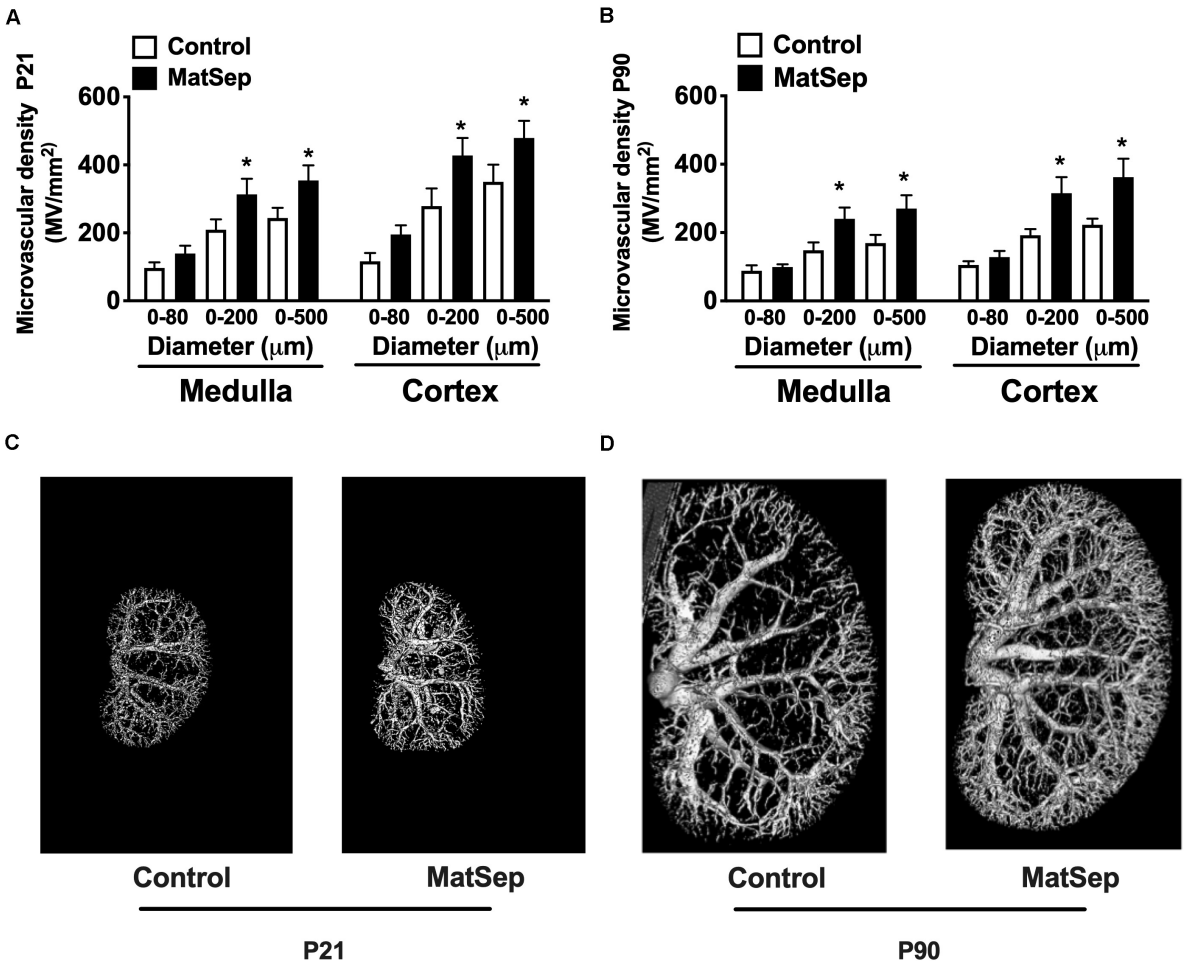

FIGURE 2 | Effect of maternal separation (MatSep) on microvascular density in renal cortex and medulla at **(A)** P21 and **(B)** P90. Renal microphotographs in Control (right) and MatSep (left) at **(C)** P21 and **(D)** P90. P: postnatal day. *$p < 0.05$ vs. C. $n = 5–7$ per group.

to the lack of anti-angiogenic effects elicited by Ang 1–7, could be responsible for the exacerbated microvascular density found in MatSep weanlings and adult rats. Furthermore, our transcriptomic analysis indicates that MatSep induces the upregulation of pro-angiogenic and pro-inflammatory gene expression that may contribute to the permanent alterations of the renal microvascular architecture. Our data support the notion that MatSep serves as a strong stimulus during the early postnatal life capable of inducing temporospatial changes in the intrarenal RAS. Overall, these data imply a potential link between postnatal stress and impaired renal structure and function.

Different models of developmental origins of adult disease are based on the exposure to low protein diet, excess of glucocorticoids, induced intrauterine growth restriction and postnatal blockade of the renin-angiotensin system. A common feature of these models is the development of renal damage and hypertension (Zandi-Nejad et al., 2006; Hershkovitz et al., 2007; Ingelfinger and Nuyt, 2012; Stangenberg et al., 2015; Cuffe et al., 2016; Vieira-Rocha et al., 2019; DuPriest et al., 2020; Lamothe et al., 2020). Conversely, MatSep is a chronic behavioral stress model that induces subtle effects on the cardiovascular system in baseline/unstimulated conditions. However, the sensitization of the autonomic, neuroendocrine and immune system becomes a key feature in the enhanced response to secondary stressors (Sanders and Anticevic, 2007; Trombini et al., 2012; Loria et al., 2015). Renal developmental length is species-specific. The initiation of the nephrogenic involves 1/8 of gestation in the humans, 1/3 of gestation in the sheep and 1/2 of gestation in rats. The permanent kidney formation (Metanephros) begins at day 12 in the rat (Seely, 2017). Thus, rats are born during active nephrogenesis. However, once the metanephros stage is achieved, further development and differentiation of tubular and vascular architecture continues throughout P22 (Sequeira Lopez and Gomez, 2004). Importantly, the generation of microvessels in the kidney is not restricted to *in utero* development and can also be activated in response to renal damage later in life (Sequeira Lopez and Gomez, 2004, 2011). During development, renal vascularization occurs in parallel with nephrogenesis, as blood vessels develop through two

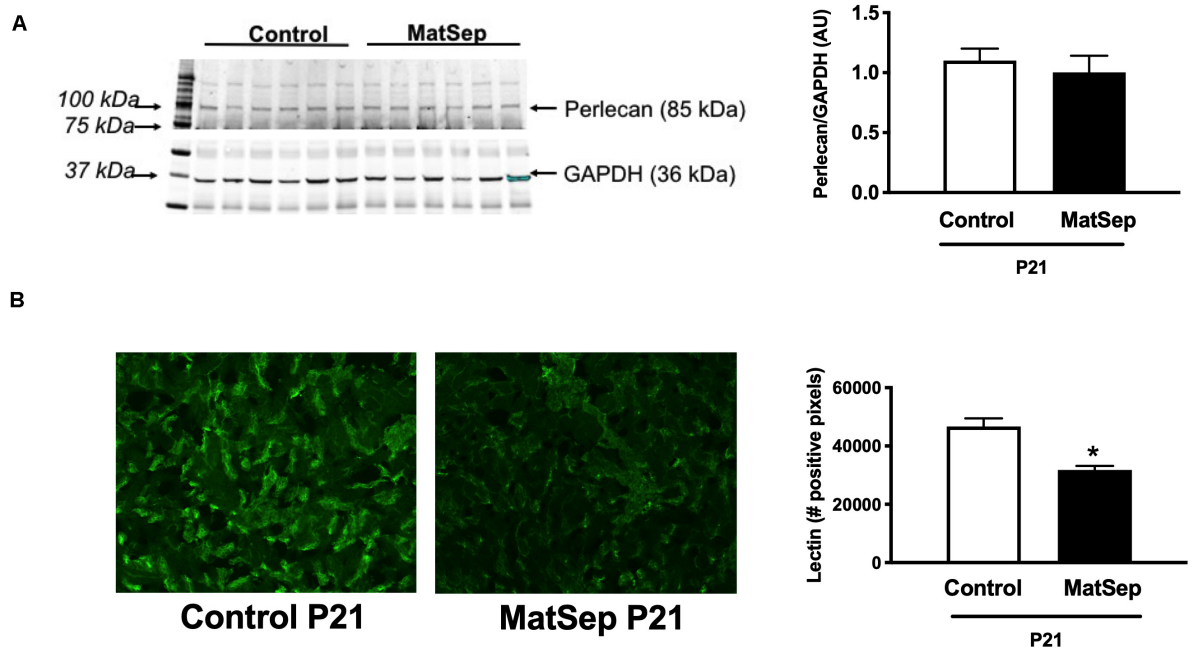

FIGURE 3 | Effect of maternal separation (MatSep) on: **(A)** renal protein expression of perlecan, and **(B)** immunostaining intensity for lectin in 3-week old male weanlings (P21). *$p < 0.05$ vs. C. $n = 5$ per group.

mechanisms: vasculogenesis (neoformation of vessels) and angiogenesis (sprouting and branching from pre-existent vessels) (Sequeira Lopez and Gomez, 2004, 2011). Newborn renal blood flow (RBF), initially low after birth, progressively increases during postnatal maturation until reaching the adult levels. Newborns display low RBF primarily due to the occurrence of elevated renal vascular resistance (RVR). The increase in RBF observed from postnatal to adult life is caused by progressive reduction of RVR given by the concomitant RAS activation (Nada et al., 2017).

One potential explanation describing the connection between MatSep and an upregulation of RAS components is via the actions of the stress hormones. The chronic behavioral stress associated to MatSep induces the dysregulation of the glucocorticoid (Marais et al., 2008; Chen et al., 2012; Roque et al., 2014), which are well-known for upregulating RAS components, including AGT and angiotensin receptors density and binding in vascular smooth muscle cells and blood vessels (Sato et al., 1994; Schelling et al., 1994; Ullian and Walsh, 1995), adrenal gland (Bobrovskaya et al., 2013), liver epithelial cells (Shelat et al., 1999a) and brain (Aguilera et al., 1995; Shelat et al., 1999b). These actions are mediated by the stimulation of the glucocorticoid response element present in regions of both the AGT and angiotensin receptor promoter (Guo et al., 1995; Matsubara, 1998). AngII synthesis rate depends upon the availability of substrate, AGT, renin, and the activity of the ACE/ACE2 enzymes. Our data shows that MatSep lowered AngII intrarenal concentration while most of the RAS components were upregulated during postnatal life. Thus, we investigated potential explanations and found that ACE in kidneys from MatSep neonates is increased while ACE2 expression and activity are reduced. This data suggests that anti-angiogenic effects mediated by Ang 1–7 could be dramatically attenuated, thus promoting further vessel development (van Esch et al., 2008; Pei et al., 2016; Touyz and Montezano, 2018). Furthermore, it has been shown that AngIII pro-angiogenic effects are mediated by both AT1 and AT2 receptors binding (Kawasaki et al., 1988; Cheng et al., 1994; Del Borgo et al., 2015; Alanazi and Clark, 2019, 2020). Therefore, our data suggests that in the context of glucocorticoid stimulation due to chronic stress, the upregulation of several RAS components could be a major player in the increased renal vascular density via the overstimulation of the AT1 and AT2 receptors along with the reduced Ang 1–7 anti-angiogenic effects. Therefore, factors contributing to AngII degradation in this postnatal milieu, such as increased aminopeptidase A (Enpep) need further investigation.

Kidneys from MatSep weanlings show reduced lectin expression, and both neonates and adult rats show reduced PECAM-1 expression. These data indicate that the alterations in the vascular architecture could be linked to a reduced number of endothelial cells and thus microvascular rarefaction. Potential mechanisms by which MatSep increases microvascular density could be given by the capacity of (pro)renin (Yokota et al., 2008; Uraoka et al., 2009; Zhu et al., 2015) and renin cells (Amaral et al., 2001; Rider et al., 2015) to induce the transcription of angiogenic factors; or linked to the fact that the most of the genes upregulated by MatSep in

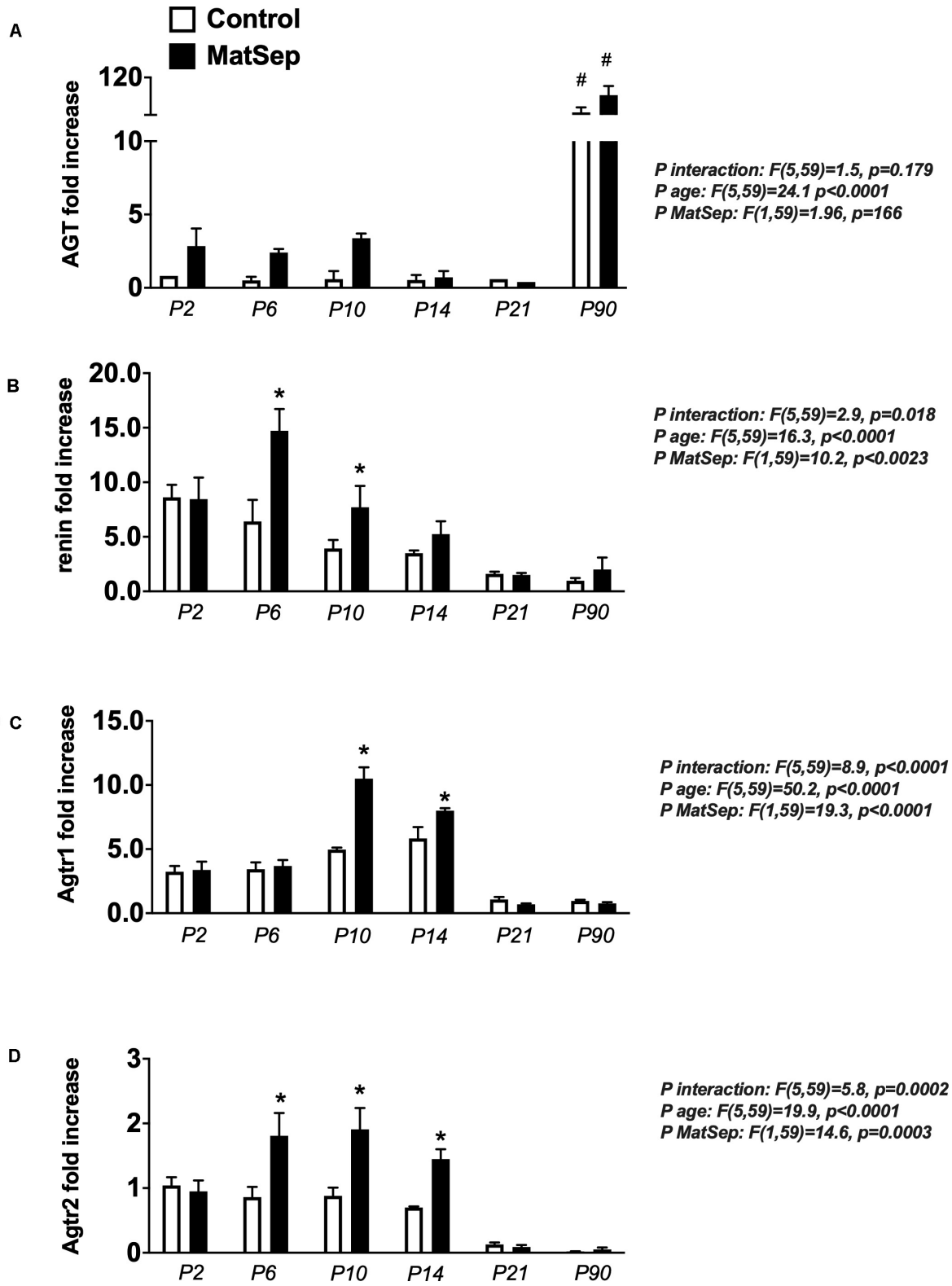

FIGURE 4 | Effect of maternal separation (MatSep) on intrarenal RAS mRNA expression trajectory from P2 to P90: **(A)** Angiotensinogen (Agt), **(B)** renin, **(C)** angiotensin type 1 receptor (Agtr1) and **(D)** angiotensin type 1 receptor (Agtr2). Each RAS component was normalized to Agtr2 receptor control levels at P2. #$p < 0.05$ vs. P2–P21, *$p < 0.05$ vs. C. n = 6–8 per group.

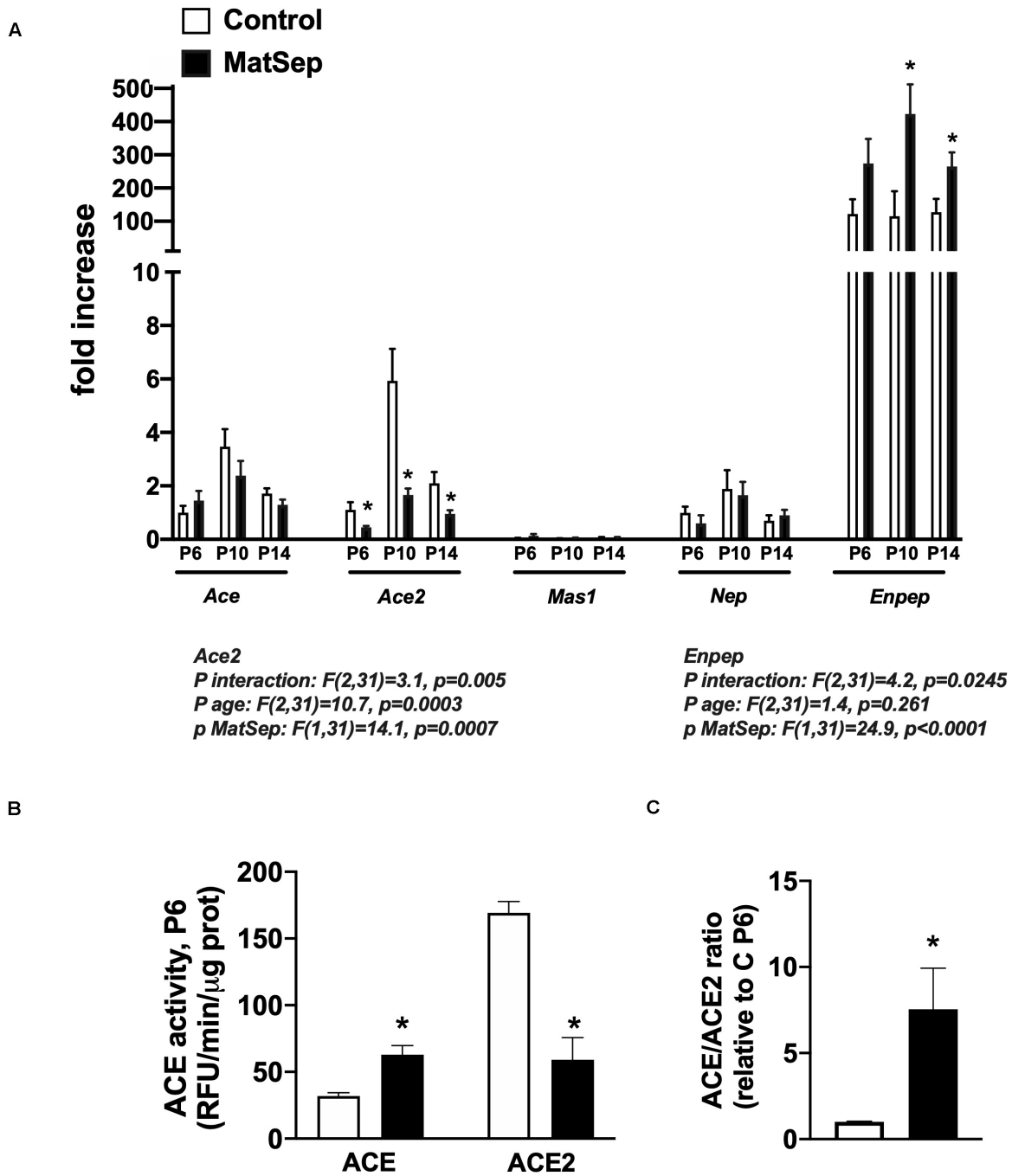

FIGURE 5 | Effect of maternal separation (MatSep) on intrarenal RAS components at postnatal day 6, 10, and 14 in male neonates: **(A)** Ace, Ace2, Mas1, Nep, and Enpep; **(B)** ACE and ACE2 enzymatic activity; **(C)** ACE/ACE2 ratio. *$p < 0.05$ vs. C. $n = 4–8$ per group.

isolated renal vasculature are associated with angiogenesis during pathophysiological processes. One of them is the microfibrillar-associated protein (Mfap5), which is implicated in the regulation of cell proliferation, differentiation, angiogenesis and apoptosis (Choi et al., 2015; Marti et al., 2015; Saikawa et al., 2018; Boopathy and Hong, 2019). Other gene that shows a strong upregulation in neonates is the fatty acid-binding protein 4 (Fabp4). Fabp4 display both pro-angiogenic (Elmasri et al., 2012; Harjes et al., 2017) and pro-inflammatory (Steen et al., 2017; Dou et al., 2020) actions, therefore its upregulation in the context of chronic stress could be implicated with the enhancement of the vascular density. Finally, despite changes in the angiogenesis regulation directly modulated by MatSep,

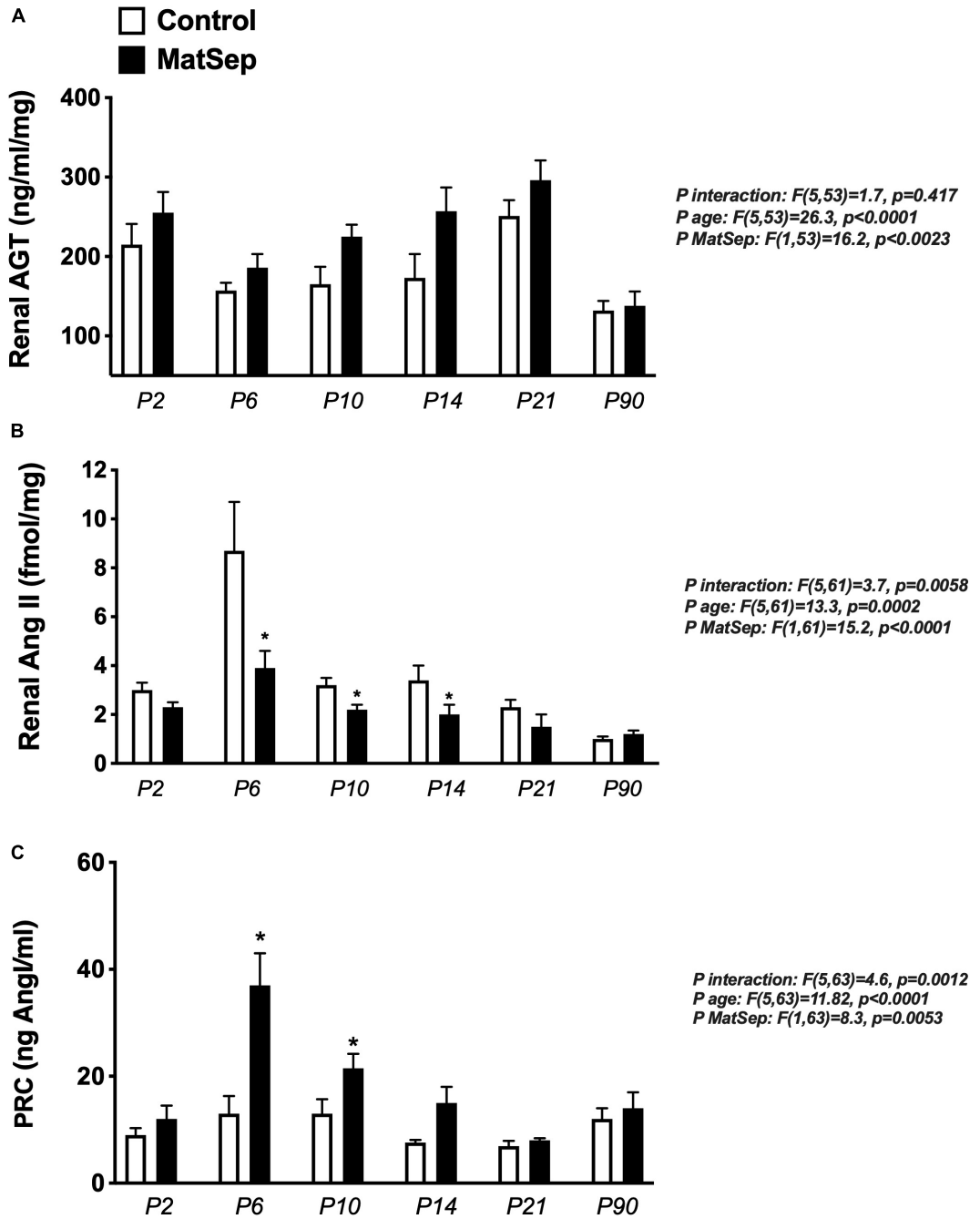

FIGURE 6 | Effect of maternal separation (MatSep) on RAS trajectory from neonatal to adult life in: **(A)** renal angiotensinogen (AGT), **(B)** renal angiotensin II (AngII), and **(C)** plasma renin concentration (PRC) in ng AngI/ml generated per hour of incubation. *$p < 0.05$ vs. C. $n = 6–8$ per group.

we are not able to rule out possible vascular remodeling secondary to stress-induced transient blood pressure increases during postnatal life.

It is important to highlight that reduced renal function in MatSep rats at baseline is associated with a moderate increase in proteinuria and no considerable histological renal damage, in rats that otherwise are normotensive and show similar circulating RAS components. Previously, we have reported that adult male MatSep rats display increased sympathetic outflow to the kidneys (Loria et al., 2013a; Loria and Osborn, 2017), showing a reduced number of alpha-adrenergic receptors in isolated renal vasculature. Furthermore, renal filtration capacity was normalized by renal denervation. Taken together, these data suggest that increased microvascular density could also be interrelated with the effects of a greater sympathetic tone on renal hemodynamics. A summary of the current and previous findings

TABLE 1 | Effect of MatSep on RAS gene expression trajectory from neonate-to-adult life.

RefSeq	Gene	Fold Increase Neonate	*p*-value	Fold Increase adult	*p*-value
	Classical				
NM_030985	**Agtr1a**	**1.14**	**0.020**	−1.080	0.150
NM_012576	**Nr3C1**	**1.11**	**0.004**	1.023	0.482
NM_134432	AGT	−1.07	0.484	−1.135	0.214
NM_012642	REN	−1.02	0.800	1.042	0.657
NM_012544	ACE	1.16	0.239	1.100	0.458
ENSRNOT00000052018	Nr3C2	−1.09	0.169	1.039	0.513
NM_017080	HSD11b1	−1.02	0.717	1.008	0.902
ENSRNOT00000023130	HSD11b2	−1.03	0.738	1.075	0.482
	Non-classical				
NM_012494	**AGTR2**	**1.59**	**0.003**	−1.082	0.563
ENSRNOT00000021840	**IGF2R**	**1.16**	**0.027**	1.039	0.531
NM_012757	MAS1	1.08	0.607	1.214	0.229
NM_001007091	ATP6AP2	−1.06	0.519	1.008	0.925
NM_031012	ANPEP	−1.07	0.253	−1.054	0.398
ENSRNOT00000009198	RNPEP	1.04	0.521	−1.002	0.970
	Related				
ENSRNOT00000014970	**CPA3**	**1.61**	**0.005**	−1.01	0.939
NM_031523	**KLK1**	**1.34**	**0.014**	1.02	0.843
NM_012608	MME	−1.22	0.088	1.04	0.702
ENSRNOT00000010831	CYP11A1	−1.08	0.197	1.04	0.724
NM_012538	CYP11b2	−1.01	0.971	1.07	0.657
NM_012537	CYP11b1	1.21	0.151	−1.22	0.136
NM_012753	CYP17A1	1.13	0.316	1.10	0.106
ENSRNOT00000006087	EGFR	1.07	0.233	−1.07	0.265
NM_001113403	LNPEP	1.02	0.661	1.00	0.926
NM_053748	DPP3	1.01	0.724	1.03	0.329
NM_134334	CTSD	−1.01	0.823	1.08	0.408
NM_001011959	CTSA	−1.02	0.838	1.05	0.634
ENSRNOT00000000360	PREP	1.00	0.951	1.01	0.902

Fold change was calculated from control samples at P10. In bold: genes with significant increases in fold vs. control, n = 5 per group. Noting, ACE2 transcript was not available in the array.

related to circulating, vascular and renal RAS in male MatSep rats across the lifespan can be found in **Supplementary Table S4**.

Nonetheless, this study presents several limitations that may impact the interpretation of the outcomes. First, further studies performing an in-depth characterization of the microvasculature to determine changes in arteriolar alpha SMA actin, ACTA2, MYH11, myosin heavy chain will pinpoint the relationship between increased microvascular density and the vascular wall properties. For instance, it has been shown that postnatal RAS inhibition impairs the development of the microvasculature causing medullary injury. A common characteristic of all these manipulations is the presence of concentric vascular hypertrophy. Thus, determining the effects of MatSep on this type of variables will contribute to the interpretation of the functional consequences of increased renal microvascular density. Second, the isolation of the renal vasculature was performed by the mechanical separation of the vascular from the tubular structures. As such, our samples are enriched in vessels but certainly contains tubular cells. However, we were able to determine that the expression of tubular markers was not different between groups. In addition, this type of procedure is normally associated with a low recovery of the renin cells, which could result in an underestimation of its gene expression. Third, the use of *in situ* hybridization showing whether the increased pro-angiogenic genes are localized on the renal vasculature could address the lack of cell type-specificity. Hence, from all these matters pointed, a single cell analysis will be preferable over the whole vasculature due to the complexity of the sample. The kidney development is based on differential 25-cell type-specific expression of a vast number of genes. Thus, *in situ* hybridization, laser capture microdissection (LCM) and fluorescence-activated cell sorting (FACS) may help to tease the genes specifically involved in the vascular endothelium or vascular wall. Gene expression microarrays provide a powerful tool for studying multifaceted physiological processes. However, implications from microarray data are often impeded by multiple comparisons, small sample sizes, and uncertain relationships to functional endpoints. To date, several genomic studies have been performed in the developing kidney, but fewer have been conducted in the isolated renal vasculature.

TABLE 2 | Effect of MatSep on angiogenic gene expression trajectory from neonate-to-adult life.

RefSeq	Gene	Fold Increase neonate	*p*-value	Fold Increase adult	*p*-value
	Up				
NM_001108644	**Mfap5**	**2.639**	**0.0001**	−1.145	0.484
NM_012494	**Agtr2**	**1.589**	**0.003**	−1.082	0.563
ENSRNOT00000015395	**Rspo3**	**1.545**	**0.003**	−1.117	0.377
NM_001107100	**Col8a1**	**1.536**	**0.017**	−1.153	0.393
NM_031970	**Hspb1**	**1.480**	**0.012**	−1.163	0.293
NM_030868	**Nov**	**1.430**	**0.009**	−1.232	0.105
ENSRNOT00000013093	**Il18**	**1.402**	**0.006**	−1.071	0.532
NM_001109383	**Angptl1**	**1.309**	**0.034**	1.015	0.896
NM_199115	**Angptl4**	**1.281**	**0.035**	−1.247	0.057
ENSRNOT00000038994	**Cybb**	**1.302**	**0.002**	−1.033	0.649
ENSRNOT00000016485	**Fgf10**	**1.273**	**0.006**	1.170	0.055
NM_031054	**Mmp2**	**1.262**	**0.020**	−1.152	0.135
NM_017154	**Xdh**	**1.250**	**0.004**	−1.088	0.215
ENSRNOT00000012216	**C3ar1**	**1.241**	**0.001**	−1.099	0.101
NM_053560	**Chi3l1**	**1.236**	**0.004**	−1.058	0.385
NM_012769	**Gucy1b3**	**1.233**	**0.017**	−1.106	0.218
NM_019185	**Gata6**	**1.230**	**0.014**	−1.110	0.185
NM_001107159	**Mmp19**	**1.214**	**0.041**	−1.069	0.453
NM_133569	**Angptl2**	**1.203**	**0.029**	−1.062	0.450
NM_001109093	**Grb10**	**1.185**	**0.005**	1.006	0.913
NM_017364	**Zfp260**	**1.175**	**0.002**	−1.061	0.181
NM_001106579	**Sema3e**	**1.161**	**0.011**	1.078	0.169
NM_134452	**Col5a1**	**1.152**	**0.005**	−1.010	0.827
NM_031798	**Slc12a2**	**1.135**	**0.017**	1.053	0.290
NM_134454	Angpt2	1.026	0.674	−1.070	0.274
NM_031530	Ccl2	1.203	0.074	−1.511	0.914
ENSRNOT00000003313	Tgfb2	1.179	0.236	1.017	0.900
NM_012802	Pdgfra	1.164	0.108	−1.418	0.001
NM_053394	Klf5	1.118	0.222	1.014	0.878
NM_031525	Pdgfrb	1.080	0.474	−1.211	0.087
XM_002725723	Adam12	1.064	0.413	−1.292	0.003
NM_024400	Adamts1	1.047	0.475	1.007	0.916
ENSRNOT00000001248	Flt1	1.041	0.580	1.032	0.664
NM_053549	Vegfb	1.089	0.310	−1.054	0.525
	Down				
ENSRNOT00000019210	**Col24a1**	**−1.170**	**0.025**	−1.025	0.697
NM_133386	**Sphk1**	**−1.249**	**0.0002**	1.037	0.440
NM_012801	**Pdgfa**	**−1.247**	**0.001**	−1.006	0.908
NR_031903	**Mir185**	**−1.231**	**0.002**	−1.005	0.925
NM_133286	Fgf8	−1.042	0.416	−1.084	0.122
ENSRNOT00000009669	Amot	−1.080	0.097	1.027	0.550

Fold change was calculated from control samples at P10. In bold: genes with significant increases vs. C.

Although this study was performed exclusively in male rats, it has been reported that female MatSep rats also display exacerbated AngII-induced hypertension, yet independent of any significant worsening on renal function compared to control littermates (Loria et al., 2013b). The well-described mechanisms by which female rodents show lower blood pressure and protected renal function compared to males is based in the increased pro-vasodilatory factors and greater number of infiltrating T regulatory cells in combination with reduced sympathetic drive, differences that are most likely stimulated by estradiol (Yanes et al., 2008; Garovic and August, 2016). Thus, postnatal stress may exert the sensitization of the renal system via alteration of neuroendocrine, immune and sympathetic responses in a sex-specific manner. Future studies will determine whether intrarenal RAS in female rats respond to MatSep in a similar fashion, while other compensatory factors may account for an optimal renal function during adult life.

TABLE 3 | Effect of MatSep on inflammatory gene expression trajectory from neonate-to-adult life.

RefSeq	Gene	Fold Increase neonate	*p*-value	Fold Increase adult	*p*-value
	Up				
ENSRNOT00000014701	**Fabp4**	**3.737**	**0.015**	−1.321	0.571
NM_001008513	**Ccl21**	**1.695**	**0.003**	−1.38	0.051
NM_001145366	**Pparg**	**1.585**	**0.040**	−1.015	0.942
ENSRNOT00000000172	**Cdo1**	**1.540**	**0.007**	1.086	0.565
NM_031970	**Hspb1**	**1.480**	**0.012**	−1.163	0.293
NM_013174	**Tgfb3**	**1.465**	**0.003**	−1.182	0.150
NM_031504	**C4a**	**1.464**	**0.002**	−1.123	0.589
NM_030868	**Nov**	**1.430**	**0.009**	−1.232	0.105
ENSRNOT00000021064	**Abcd2**	**1.412**	**0.001**	−1.13	0.181
ENSRNOT00000013093	**Il18**	**1.402**	**0.006**	−1.071	0.532
NM_012705	**Cd4**	**1.401**	**0.002**	−1.038	0.681
ENSRNOT00000037681	**Nfam1**	**1.384**	**0.0003**	−1.087	0.262
NM_053611	**Nupr1**	**1.384**	**0.005**	−1.081	0.447
ENSRNOT00000020265	**Ifitm3**	**1.375**	**0.009**	−1.043	0.703
NM_001013427	**Rarres2**	**1.359**	**0.002**	−1.146	0.109
NM_012870	**Tnfrsf11b**	**1.353**	**0.015**	1.045	0.699
NM_001131001	**Fcer1g**	**1.328**	**0.003**	−1.020	0.809
ENSRNOT00000024110	**Ccdc3**	**1.313**	**0.002**	−1.019	0.802
ENSRNOT00000028131	**Axl**	**1.300**	**0.009**	−1.095	0.324
NM_001134545	**Ssc5d**	**1.291**	**0.0004**	−1.090	0.151
ENSRNOT00000005686	**Irak3**	**1.288**	**0.003**	−1.035	0.639
ENSRNOT00000021397	**Dpep1**	**1.287**	**0.012**	−1.423	0.001
ENSRNOT00000009993	**Casp1**	**1.286**	**0.009**	−1.025	0.247
ENSRNOT00000018328	**Tgm2**	**1.272**	**0.002**	−1.163	0.035
ENSRNOT00000045867	**Ccl6**	**1.257**	**0.014**	1.013	0.880
NM_053560	**Chi3l1**	**1.236**	**0.004**	−1.058	0.385
NM_013110	**Il7**	**1.209**	**0.013**	−1.017	0.813
NM_001008722	**Irf8**	**1.201**	**0.004**	−1.076	0.195
NM_173045	**Ripk2**	**1.196**	**0.002**	−1.062	0.242
NM_001106418	**Il7r**	**1.189**	**0.016**	−1.136	0.067
NM_001257278	**Il31ra**	**1.178**	**0.017**	−1.284	0.001
NM_138879	**Sele**	**1.173**	**0.046**	−1.034	0.659
NM_013185	**Hck**	**1.172**	**0.015**	1.053	0.391
ENSRNOT00000020108	**Il1rl1**	**1.171**	**0.049**	−1.149	0.083
ENSRNOT00000025222	**Csf1**	**1.170**	**0.006**	−1.059	0.703
ENSRNOT00000014560	**Birc2**	**1.150**	**0.002**	1.027	0.474
ENSRNOT00000019673	**Il1r1**	**1.138**	**0.014**	−1.196	0.001
NM_145789	**Il13ra1**	**1.117**	**0.015**	−1.023	0.582
NM_138502	**Mgll**	**1.115**	**0.016**	1.032	0.443
ENSRNOT00000004285	**Gne**	**1.085**	**0.044**	−1.045	0.350
NM_020542	Ccr1	1.578	0.0001	−1.262	0.014
XM_001058423	Eda	1.135	0.095	−1.245	0.007
XM_001056441	C2cd4b	1.071	0.231	−1.032	0.569
ENSRNOT00000002089	Cd80	1.054	0.249	−1.326	0.0001
NM_001109112	Tnfsf13b	1.060	0.391	−1.292	0.001
NM_012675	Tnf	1.067	0.241	−1.143	0.023
NM_001013894	Lilrb4	−1.083	0.262	−1.289	0.002
	Down				
ENSRNOT00000000621	**Mapk13**	**−1.272**	0.004	−1.021	0.779
NM_133386	**Sphk1**	**−1.249**	0.0002	1.037	0.440
NM_012854	Il10	−1.044	0.399	−1.120	0.036
NM_031512	Il1b	−1.066	0.402	−1.197	0.028

Fold change was calculated from control samples at P10. In bold: genes with significant increases in fold vs. control, n = 5 per group.

TABLE 4 | Enriched Biological Pathways functional clusters (EBPfc) affected by MatSep.

Category	Term	Count	%	*p*-value	FE	FDR
Neonates						
GOTERM_CC_DIRECT	GO:0005615~extracellular space	34	17	0.00000	2.49	0.00
GOTERM_BP_DIRECT	GO:0045087~innate immune response	18	9	0.00000	7.20	0.00
GOTERM_BP_DIRECT	GO:0006954~inflammatory response	13	6.5	0.00005	4.34	0.07
GOTERM_BP_DIRECT	GO:0043065~positive regulation of apoptotic process	12	6	0.00091	3.35	1.45
KEGG_PATHWAY	rno04060:Cytokine-cytokine receptor interaction	10	5	0.00065	4.08	0.78
GOTERM_BP_DIRECT	GO:0006955~immune response	10	5	0.00089	4.00	1.43
GOTERM_BP_DIRECT	GO:0006915~apoptotic process	10	5	0.01347	2.64	19.59
GOTERM_BP_DIRECT	GO:0043547~positive regulation of GTPase activity	10	5	0.01722	2.53	24.35
GOTERM_CC_DIRECT	GO:0031012~extracellular matrix	9	12.2	0.00000	9.92	0.00
GOTERM_BP_DIRECT	GO:0008284~positive regulation of cell proliferation	7	9.46	0.00940	3.79	12.84
KEGG_PATHWAY	rno04640:Hematopoietic cell lineage	7	3.5	0.00026	7.68	0.31
KEGG_PATHWAY	rno04015:Rap1 signaling pathway	6	8.11	0.00064	7.97	0.74
GOTERM_MF_DIRECT	GO:0005125~cytokine activity	6	3	0.01663	4.02	20.32
GOTERM_BP_DIRECT	GO:0043123~positive reg I-kappaB kinase/NF-kappaB	6	3	0.02272	3.71	30.87
GOTERM_BP_DIRECT	GO:0050727~regulation of inflammatory response	5	2.5	0.00309	8.22	4.85
GOTERM_BP_DIRECT	GO:0030199~collagen fibril organization	4	5.41	0.00040	27.27	0.58
KEGG_PATHWAY	rno04261:Adrenergic signaling	4	5.41	0.01227	7.87	13.29
GOTERM_BP_DIRECT	GO:0070555~response to interleukin-1	4	2	0.01056	8.72	15.69
GOTERM_BP_DIRECT	GO:0002250~adaptive immune response	4	2	0.03103	5.81	39.74
GOTERM_MF_DIRECT	GO:0005518~collagen binding	3	4.05	0.01396	16.34	15.22
KEGG_PATHWAY	rno04370:VEGF signaling pathway	3	4.05	0.01760	14.05	18.53
GOTERM_BP_DIRECT	GO:0010759~pos regul of macrophage chemotaxis	3	1.5	0.00548	26.15	8.45
Adult						
GOTERM_BP_DIRECT	GO:0070374~positive regulation of ERK1 and ERK2	6	4.17	0.01355	4.23	19.01
GOTERM_MF_DIRECT	GO:0020037~heme binding	5	3.47	0.02451	4.51	27.99
GOTERM_MF_DIRECT	GO:0005506~iron ion binding	5	3.47	0.04604	3.68	46.40
KEGG_PATHWAY	rno04062:Chemokine signaling pathway	5	3.47	0.04885	3.34	51.85
KEGG_PATHWAY	rno04060:Cytokine-cytokine receptor interaction	4	14.3	0.00236	12.75	2.11
GOTERM_BP_DIRECT	GO:0090263~pos regulation of canonical Wnt path	4	2.78	0.01583	7.51	21.87
GOTERM_BP_DIRECT	GO:0042102~pos regulation of T cell proliferation	3	10.7	0.00390	30.63	4.84
KEGG_PATHWAY	rno05323:Rheumatoid arthritis	3	10.7	0.00567	23.42	5.01
GOTERM_BP_DIRECT	GO:0007623~circadian rhythm	3	10.7	0.01247	16.80	14.71
GOTERM_BP_DIRECT	GO:0019221~cytokine-mediated signaling pathway	3	10.7	0.01487	15.31	17.31
GOTERM_BP_DIRECT	GO:0046329~negative regulation of JNK cascade	3	2.08	0.01571	15.44	21.72
KEGG_PATHWAY	rno04330:Notch signaling pathway	3	2.08	0.04698	7.61	50.68
GOTERM_BP_DIRECT	GO:0031295~T cell co-stimulation	2	7.14	0.02834	66.63	30.56

Data was analyzed using DAVID Functional Annotation Bioinformatics Microarray Analysis. FE = Fisher's exact test, FDR = Force discovery rate.

In summary, our data show that MatSep is associated with the temporospatial changes in the expression of a cluster of genes, including several RAS components, expressed in the kidney and the renal vasculature. Our results reveal a molecular context to define the critical pathways mediating growth and developmental aberrations resulting in potential changes of function. Although processes such as vasculogenesis and angiogenesis were initially thought to occur only in the developing kidney, now is more accepted that these processes also occur during (physio)pathologic responses during postnatal life. Thus, vasculogenesis and angiogenesis could be activated during the remodeling of the vasculature in response to environmental insults, including this model of psychosocial stress. The kidney is a highly vascularized organ that normally receives ∼20% of the cardiac output. The unique architectural organization of the kidney vasculature with each nephron is critical for the regulation of renal hemodynamics and water and electrolytes balance. However, mechanisms that govern the development of the kidney vasculature are poorly understood. This study provides insights regarding the endowment of renal vessels, with the potential to benefit children and adults with congenital and acquired kidney diseases, vascular diseases, and hypertension.

DATA AVAILABILITY STATEMENT

The datasets generated for this study are available at https://www.ncbi.nlm.nih.gov/geo/query/acc.cgi?acc=GSE151402.

ETHICS STATEMENT

The animal study was reviewed and approved by Division of Laboratory Animal Resources, IACUC office.

AUTHOR CONTRIBUTIONS

CD, AC, GB, KC, and AL designed the experiments. CD, AC, MM, JG, GB, KC, and AL conducted the experiments, analyzed the data, and edited and approved the final version of the manuscript. All authors contributed to the article and approved the submitted version.

FUNDING

This study was supported by grants from the NIH National Heart, Lung, and Blood Institute (R00 HL111354 to AL, R01135158 to AL, and R01HL142672 to JG), the Kentucky Center of Research on Obesity and Cardiovascular Disease COBRE P20 GM103527, and start-up funds from the University of Kentucky.

ACKNOWLEDGMENTS

We gratefully acknowledge the outstanding technical support from Xiu Xu, Dianne Cohn, Timothy Mahanes, and Jill Roberts at the University of Kentucky. We also acknowledge the expertise of Dr. Gabriel Navar's laboratory for the determination of the AngII peptide in kidney samples. We acknowledge that BLM.

SUPPLEMENTARY MATERIAL

The Supplementary Material for this article can be found online at: https://www.frontiersin.org/articles/10.3389/fphys.2020.01046/full#supplementary-material

REFERENCES

Aguilera, G., Kiss, A., and Luo, X. (1995). Increased expression of type 1 angiotensin II receptors in the hypothalamic paraventricular nucleus following stress and glucocorticoid administration. *J. Neuroendocrinol.* 7, 775–783. doi: 10.1111/j.1365-2826.1995.tb00714.x

Alanazi, A. Z., and Clark, M. A. (2019). Angiotensin III induces JAK2/STAT3 leading to IL-6 production in rat vascular smooth muscle cells. *Int. J. Mol. Sci.* 20:5551. doi: 10.3390/ijms20225551

Alanazi, A. Z., and Clark, M. A. (2020). Angiotensin III induces p38 Mitogen-activated protein kinase leading to proliferation of vascular smooth muscle cells. *Pharmacol. Rep.* 72, 246–253. doi: 10.1007/s43440-019-00035-8

Amaral, S. L., Roman, R. J., and Greene, A. S. (2001). Renin gene transfer restores angiogenesis and vascular endothelial growth factor expression in Dahl S rats. *Hypertension* 37, 386–390. doi: 10.1161/01.hyp.37.2.386

Bobrovskaya, L., Maniam, J., Ong, L. K., Dunkley, P. R., and Morris, M. J. (2013). Early life stress and post-weaning high fat diet alter tyrosine hydroxylase regulation and AT1 receptor expression in the adrenal gland in a sex dependent manner. *Neurochem. Res.* 38, 826–833. doi: 10.1007/s11064-013-0985-4

Boopathy, G. T. K., and Hong, W. (2019). Role of hippo pathway-YAP/TAZ signaling in angiogenesis. *Front. Cell Dev. Biol.* 7:49. doi: 10.3389/fnbeh.2014.00049

Campbell, S., Wladimiroff, J. W., and Dewhurst, C. J. (1973). The antenatal measurement of fetal urine production. *J. Obstet. Gynaecol. Br. Commonw.* 80, 680–686. doi: 10.1111/j.1471-0528.1973.tb16049.x

Centers for Disease Control, and Prevention, (2019). *Chronic Kidney Disease in the United States, 2019*. Atlanta, GA: Centers for Disease Control and Prevention.

Chen, J., Evans, A. N., Liu, Y., Honda, M., Saavedra, J. M., and Aguilera, G. (2012). Maternal deprivation in rats is associated with corticotrophin-releasing hormone (CRH) promoter hypomethylation and enhances CRH transcriptional responses to stress in adulthood. *J. Neuroendocrinol.* 24, 1055–1064. doi: 10.1111/j.1365-2826.2012.02306.x

Chen, Y., Lasaitiene, D., and Friberg, P. (2004). The renin-angiotensin system in kidney development. *Acta Physiol. Scand.* 181, 529–535.

Cheng, D. Y., DeWitt, B. J., McMahon, T. J., and Kadowitz, P. J. (1994). Comparison of pressor responses to angiotensin I, II, and III in pulmonary vascular bed of cats. *Am. J. Physiol.* 266, H2247–H2255.

Choi, H. J., Zhang, H., Park, H., Choi, K. S., Lee, H. W., Agrawal, V., et al. (2015). Yes-associated protein regulates endothelial cell contact-mediated expression of angiopoietin-2. *Nat. Commun.* 6:6943.

Cuffe, J. S., Burgess, D. J., O'Sullivan, L., Singh, R. R., and Moritz, K. M. (2016). Maternal corticosterone exposure in the mouse programs sex-specific renal adaptations in the renin-angiotensin-aldosterone system in 6-month offspring. *Physiol. Rep.* 4:e12754. doi: 10.14814/phy2.12754

Dalmasso, C., Leachman, J. R., Ensor, C. M., Yiannikouris, F. B., Giani, J. F., Cassis, L. A., et al. (2019). Female mice exposed to postnatal neglect display angiotensin II-dependent obesity-induced hypertension. *J. Am. Heart Assoc.* 8:e012309.

De Miguel, C., Obi, I. E., Ho, D. H., Loria, A. S., and Pollock, J. S. (2017). Early life stress induces priming of the immune response in kidneys of adult male rats. *Am. J. Physiol. Renal Physiol.* 314, F343–F355.

De Miguel, C., Obi, I. E., Ho, D. H., Loria, A. S., and Pollock, J. S. (2018). Early life stress induces immune priming in kidneys of adult male rats. *Am. J. Physiol. Renal Physiol.* 314, F343–F355.

Del Borgo, M., Wang, Y., Bosnyak, S., Khan, M., Walters, P., Spizzo, I., et al. (2015). beta-Pro7Ang III is a novel highly selective angiotensin II type 2 receptor (AT2R) agonist, which acts as a vasodepressor agent via the AT2R in conscious spontaneously hypertensive rats. *Clin. Sci.* 129, 505–513. doi: 10.1042/cs20150077

Dou, H. X., Wang, T., Su, H. X., Gao, D. D., Xu, Y. C., Li, Y. X., et al. (2020). Exogenous FABP4 interferes with differentiation, promotes lipolysis and inflammation in adipocytes. *Endocrine* 67, 587–596. doi: 10.1007/s12020-019-02157-8

DuPriest, E., Hebert, J., Morita, M., Marek, N., Meserve, E. E. K., Andeen, N., et al. (2020). Fetal renal DNA Methylation and developmental programming of stress-induced hypertension in growth-restricted male mice. *Reprod. Sci.* 27, 1110–1120. doi: 10.1007/s43032-019-00121-5

Elmasri, H., Ghelfi, E., Yu, C. W., Traphagen, S., Cernadas, M., Cao, H., et al. (2012). Endothelial cell-fatty acid binding protein 4 promotes angiogenesis: role of stem cell factor/c-kit pathway. *Angiogenesis* 15, 457–468. doi: 10.1007/s10456-012-9274-0

Eriguchi, M., Lin, M., Yamashita, M., Zhao, T. V., Khan, Z., Bernstein, E. A., et al. (2018). Renal tubular ACE-mediated tubular injury is the major contributor to microalbuminuria in early diabetic nephropathy. *Am. J. Physiol. Renal Physiol.* 314, F531–F542.

Flynn, E. R., Lee, J., Hutchens, Z. M. Jr., Chade, A. R., and Maric-Bilkan, C. (2013). C-peptide preserves the renal microvascular architecture in the streptozotocin-induced diabetic rat. *J. Diabetes Complicat.* 27, 538–547. doi: 10.1016/j.jdiacomp.2013.07.002

Franco, M. C., Oliveira, V., Ponzio, B., Rangel, M., Palomino, Z., and Gil, F. Z. (2012). Influence of birth weight on the renal development and kidney diseases in adulthood: experimental and clinical evidence. *Int. J. Nephrol.* 2012:608025.

Garovic, V. D., and August, P. (2016). Sex differences and renal protection: keeping in touch with your feminine side. *J. Am. Soc. Nephrol.* 27, 2921–2924. doi: 10.1681/asn.2016040454

Guo, D.-F., Uno, S., Ishihata, A., Nakamura, N., and Inagami, T. (1995). Identification of a cis-acting glucocorticoid responsive element in the rat angiotensin II Type 1A promoter. *Circ. Res.* 77, 249–257. doi: 10.1161/01.res.77.2.249

Guron, G., and Friberg, P. (2000). An intact renin-angiotensin system is a prerequisite for normal renal development. *J. Hypertens.* 18, 123–137. doi: 10.1097/00004872-200018020-00001

Harjes, U., Bridges, E., Gharpure, K. M., Roxanis, I., Sheldon, H., Miranda, F., et al. (2017). Antiangiogenic and tumour inhibitory effects of downregulating tumour endothelial FABP4. *Oncogene* 36, 912–921. doi: 10.1038/onc.2016.256

Hershkovitz, D., Burbea, Z., Skorecki, K., and Brenner, B. M. (2007). Fetal programming of adult kidney disease: cellular and molecular mechanisms. *Clin. J. Am. Soc. Nephrol.* 2, 334–342. doi: 10.2215/cjn.03291006

Ingelfinger, J. R., and Nuyt, A. M. (2012). Impact of fetal programming, birth weight, and infant feeding on later hypertension. *J. Clin. Hypertens.* 14, 365–371. doi: 10.1111/j.1751-7176.2012.00660.x

Johnson, A. K., and Xue, B. (2018). Central nervous system neuroplasticity and the sensitization of hypertension. *Nat. Rev. Nephrol.* 14, 750–766. doi: 10.1038/s41581-018-0068-5

Kawasaki, H., Takasaki, K., Cline, W. H. Jr., and Su, C. (1988). Effect of angiotensin III (des-Asp1-angiotensin II) on the vascular adrenergic neurotransmission in spontaneously hypertensive rats. *Eur. J. Pharmacol.* 147, 125–130. doi: 10.1016/0014-2999(88)90641-3

Ku, E., Lee, B. J., Wei, J., and Weir, M. R. (2019). Hypertension in CKD: core curriculum 2019. *Am. J. Kidney Dis.* 74, 120–131. doi: 10.1053/j.ajkd.2018.12.044

Lamothe, J., Khurana, S., Tharmalingam, S., Williamson, C., Byrne, C. J., Khaper, N., et al. (2020). The role of DNMT and HDACs in the fetal programming of hypertension by glucocorticoids. *Oxid. Med. Cell Longev.* 2020:5751768.

Lasaitiene, D., Chen, Y., Guron, G., Marcussen, N., Tarkowski, A., Telemo, E., et al. (2003). Perturbed medullary tubulogenesis in neonatal rat exposed to renin-angiotensin system inhibition. *Nephrol. Dial. Transplant.* 18, 2534–2541. doi: 10.1093/ndt/gfg447

Loria, A., Reverte, V., Salazar, F., Saez, F., Llinas, M. T., and Salazar, F. J. (2007). Sex and age differences of renal function in rats with reduced ANG II activity during the nephrogenic period. *Am. J. Physiol. Renal Physiol.* 293, F506–F510.

Loria, A. S., Brands, M. W., Pollock, D. M., and Pollock, J. S. (2013a). Early life stress sensitizes the renal and systemic sympathetic system in rats. *Am. J. Physiol. Renal Physiol.* 305, F390–F395.

Loria, A. S., Yamamoto, T., Pollock, D. M., and Pollock, J. S. (2013b). Early life stress induces renal dysfunction in adult male rats but not female rats. *Am. J. Physiol. Regul. Integr. Comp. Physiol.* 304, R121–R129.

Loria, A. S., Kang, K. T., Pollock, D. M., and Pollock, J. S. (2011). Early life stress enhances angiotensin II-mediated vasoconstriction by reduced endothelial nitric oxide buffering capacity. *Hypertension* 58, 619–626. doi: 10.1161/hypertensionaha.110.168674

Loria, A. S., and Osborn, J. L. (2017). Maternal separation diminishes alpha-adrenergic receptor density and function in renal vasculature from male Wistar-Kyoto rats. *Am. J. Physiol. Renal Physiol.* 313, F47–F54.

Loria, A. S., Pollock, D. M., and Pollock, J. S. (2010). Early life stress sensitizes rats to angiotensin II-induced hypertension and vascular inflammation in adult life. *Hypertension* 55, 494–499. doi: 10.1161/hypertensionaha.109.145391

Loria, A. S., Pollock, D. M., and Pollock, J. S. (2015). Angiotensin II is required to induce exaggerated salt sensitivity in Dahl rats exposed to maternal separation. *Physiol. Rep.* 3:e12408. doi: 10.14814/phy2.12408

Marais, L., van Rensburg, S. J., van Zyl, J. M., Stein, D. J., and Daniels, W. M. (2008). Maternal separation of rat pups increases the risk of developing depressive-like behavior after subsequent chronic stress by altering corticosterone and neurotrophin levels in the hippocampus. *Neurosci. Res.* 61, 106–112. doi: 10.1016/j.neures.2008.01.011

Marti, P., Stein, C., Blumer, T., Abraham, Y., Dill, M. T., Pikiolek, M., et al. (2015). YAP promotes proliferation, chemoresistance, and angiogenesis in human cholangiocarcinoma through TEAD transcription factors. *Hepatology* 62, 1497–1510. doi: 10.1002/hep.27992

Matsubara, H. (1998). Pathophysiological role of angiotensin II Type 2 receptor in cardiovascular and renal diseases. *Circ. Res.* 83, 1182–1191. doi: 10.1161/01.res.83.12.1182

Mendez, M., Gross, K. W., Glenn, S. T., Garvin, J. L., and Carretero, O. A. (2011). Vesicle-associated membrane protein-2 (VAMP2) mediates cAMP-stimulated renin release in mouse juxtaglomerular cells. *J. Biol. Chem.* 286, 28608–28618. doi: 10.1074/jbc.m111.225839

Mitchell, K. D., Jacinto, S. M., and Mullins, J. J. (1997). Proximal tubular fluid, kidney, and plasma levels of angiotensin II in hypertensive ren-2 transgenic rats. *Am. J. Physiol.* 273, F246–F253.

Murphy, M. O., Cohn, D. M., and Loria, A. S. (2017). Developmental origins of cardiovascular disease: Impact of early life stress in humans and rodents. *Neurosci. Biobehav. Rev.* 74, 453–465. doi: 10.1016/j.neubiorev.2016.07.018

Nada, A., Bonachea, E. M., and Askenazi, D. J. (2017). Acute kidney injury in the fetus and neonate. *Semin. Fetal Neonatal Med.* 22, 90–97. doi: 10.1016/j.siny.2016.12.001

Pei, N., Wan, R., Chen, X., Li, A., Zhang, Y., Li, J., et al. (2016). Angiotensin-(1-7) decreases cell growth and angiogenesis of human nasopharyngeal carcinoma xenografts. *Mol. Cancer Ther.* 15, 37–47. doi: 10.1158/1535-7163.mct-14-0981

Peng, H., Carretero, O. A., Alfie, M. E., Masura, J. A., and Rhaleb, N. E. (2001). Effects of angiotensin-converting enzyme inhibitor and angiotensin type 1 receptor antagonist in deoxycorticosterone acetate-salt hypertensive mice lacking Ren-2 gene. *Hypertension* 37, 974–980. doi: 10.1161/01.hyp.37.3.974

Ponzio, B. F., Carvalho, M. H., Fortes, Z. B., and do Carmo Franco, M. (2012). Implications of maternal nutrient restriction in transgenerational programming of hypertension and endothelial dysfunction across F1-F3 offspring. *Life Sci.* 90, 571–577. doi: 10.1016/j.lfs.2012.01.017

Rider, S. A., Mullins, L. J., Verdon, R. F., MacRae, C. A., and Mullins, J. J. (2015). Renin expression in developing zebrafish is associated with angiogenesis and requires the Notch pathway and endothelium. *Am. J. Physiol. Renal Physiol.* 309, F531–F539.

Roque, S., Mesquita, A. R., Palha, J. A., Sousa, N., and Correia-Neves, M. (2014). The behavioral and immunological impact of maternal separation: a matter of timing. *Front. Behav. Neurosci.* 8:192. doi: 10.3389/fnbeh.2014.00192

Saez, F., Castells, M. T., Zuasti, A., Salazar, F., Reverte, V., Loria, A., et al. (2007). Sex differences in the renal changes elicited by angiotensin II blockade during the nephrogenic period. *Hypertension* 49, 1429–1435. doi: 10.1161/hypertensionaha.107.087957

Saikawa, S., Kaji, K., Nishimura, N., Seki, K., Sato, S., Nakanishi, K., et al. (2018). Angiotensin receptor blockade attenuates cholangiocarcinoma cell growth by inhibiting the oncogenic activity of Yes-associated protein. *Cancer Lett.* 434, 120–129. doi: 10.1016/j.canlet.2018.07.021

Sanders, B. J., and Anticevic, A. (2007). Maternal separation enhances neuronal activation and cardiovascular responses to acute stress in borderline hypertensive rats. *Behav. Brain Res.* 183, 25–30. doi: 10.1016/j.bbr.2007.05.020

Sato, A., Suzuki, H., Murakami, M., Nakazato, Y., Iwaita, Y., and Saruta, T. (1994). Glucocorticoid increases angiotensin II type 1 receptor and its gene expression. *Hypertension* 23, 25–30. doi: 10.1161/01.hyp.23.1.25

Schelling, J. R., DeLuca, D. J., Konieczkowski, M., Marzec, R., Sedor, J. R., Dubyak, G. R., et al. (1994). Glucocorticoid uncoupling of antiogensin II-dependent phospholipase C activation in rat vascular smooth muscle cells. *Kidney Int.* 46, 675–682. doi: 10.1038/ki.1994.320

Seely, J. C. (2017). A brief review of kidney development, maturation, developmental abnormalities, and drug toxicity: juvenile animal relevancy. *J. Toxicol. Pathol.* 30, 125–133. doi: 10.1293/tox.2017-0006

Sequeira Lopez, M. L., and Gomez, R. A. (2004). The role of angiotensin II in kidney embryogenesis and kidney abnormalities. *Curr. Opin. Nephrol. Hypertens.* 13, 117–122. doi: 10.1097/00041552-200401000-00016

Sequeira Lopez, M. L., and Gomez, R. A. (2011). Development of the renal arterioles. *J. Am. Soc. Nephrol.* 22, 2156–2165. doi: 10.1681/asn.2011080818

Shelat, S. G., Flanagan-Cato, L. M., and Fluharty, S. J. (1999a). Glucocorticoid and mineralocorticoid regulation of angiotensin II type 1 receptor binding and inositol triphosphate formation in WB cells. *J. Endocrinol.* 162, 381–391. doi: 10.1677/joe.0.1620381

Shelat, S. G., King, J. L., Flanagan-Cato, L. M., and Fluharty, S. J. (1999b). Mineralocorticoids and glucocorticoids cooperatively increase salt intake and angiotensin II receptor binding in rat brain. *Neuroendocrinology* 69, 339–351. doi: 10.1159/000054436

Singh, R. R., Lankadeva, Y. R., Denton, K. M., and Moritz, K. M. (2013). Improvement in renal hemodynamics following combined angiotensin

II infusion and AT1R blockade in aged female sheep following fetal unilateral nephrectomy. *PLoS One* 8:e68036. doi: 10.1371/journal.pone.068036

Souza, L. V., Oliveira, V., De Meneck, F., Grotti Clemente, A. P., Strufaldi, M. W., and Franco, M. D. (2017). Birth weight and its relationship with the cardiac autonomic balance in healthy children. *PLoS One* 12:e0167328. doi: 10.1371/journal.pone.0167328

Stangenberg, S., Chen, H., Wong, M. G., Pollock, C. A., and Saad, S. (2015). Fetal programming of chronic kidney disease: the role of maternal smoking, mitochondrial dysfunction, and epigenetic modfification. *Am. J. Physiol. Renal Physiol.* 308, F1189–F1196.

Steen, K. A., Xu, H., and Bernlohr, D. A. (2017). FABP4/aP2 regulates macrophage redox signaling and inflammasome activation via control of UCP2. *Mol. Cell. Biol.* 37:e0282-16.

Su, S., Wang, X., Pollock, J. S., Treiber, F. A., Xu, X., Snieder, H., et al. (2015). Adverse childhood experiences and blood pressure trajectories from childhood to young adulthood: the georgia stress and Heart study. *Circulation* 131, 1674–1681. doi: 10.1161/circulationaha.114.013104

Touyz, R. M., and Montezano, A. C. (2018). Angiotensin-(1-7) and vascular function: the clinical context. *Hypertension* 71, 68–69. doi: 10.1161/hypertensionaha.117.10406

Trombini, M., Hulshof, H. J., Graiani, G., Carnevali, L., Meerlo, P., Quaini, F., et al. (2012). Early maternal separation has mild effects on cardiac autonomic balance and heart structure in adult male rats. *Stress* 15, 457–470. doi: 10.3109/10253890.2011.639414

Tullos, N. A., Stewart, N. J., Davidovich, R., and Chade, A. R. (2015). Chronic blockade of endothelin A and B receptors using macitentan in experimental renovascular disease. *Nephrol. Dial. Transplant.* 30, 584–593. doi: 10.1093/ndt/gfu361

Ullian, M. E., and Walsh, L. G. (1995). Corticosterone metabolism and effects on angiotensin II receptors in vascular smooth muscle. *Circ. Res.* 77, 702–709. doi: 10.1161/01.res.77.4.702

Uraoka, M., Ikeda, K., Nakagawa, Y., Koide, M., Akakabe, Y., Nakano-Kurimoto, R., et al. (2009). Prorenin induces ERK activation in endothelial cells to enhance neovascularization independently of the renin-angiotensin system. *Biochem. Biophys. Res. Commun.* 390, 1202–1207. doi: 10.1016/j.bbrc.2009.10.121

US Renal Data System, (2010). *United States Renal Data System 2010 Annual Data Report: Volume 2: Atlas of End-Stage Renal Disease in the United States*. Washington, DC: US Renal Data System.

van Esch, J. H., Oosterveer, C. R., Batenburg, W. W., van Veghel, R., and Jan Danser, A. H. (2008). Effects of angiotensin II and its metabolites in the rat coronary vascular bed: is angiotensin III the preferred ligand of the angiotensin AT2 receptor? *Eur. J. Pharmacol.* 588, 286–293. doi: 10.1016/j.ejphar.2008.04.042

Vieira-Rocha, M. S., Rodriguez-Rodriguez, P., Sousa, J. B., Gonzalez, M. C., Arribas, S. M., Lopez de Pablo, A. L., et al. (2019). Vascular angiotensin AT1 receptor neuromodulation in fetal programming of hypertension. *Vascul. Pharmacol.* 117, 27–34. doi: 10.1016/j.vph.2018.10.003

Walton, S. L., Mazzuca, M. Q., Tare, M., Parkington, H. C., Wlodek, M. E., Moritz, K. M., et al. (2018). Angiotensin receptor blockade in juvenile male rat offspring: Implications for long-term cardio-renal health. *Pharmacol. Res.* 134, 320–331. doi: 10.1016/j.phrs.2018.06.001

Xue, B., Yin, H., Guo, F., Beltz, T. G., Thunhorst, R. L., and Johnson, A. K. (2017). Maternal gestational hypertension-induced sensitization of angiotensin II hypertension is reversed by renal denervation or angiotensin-converting enzyme inhibition in rat offspring. *Hypertension* 69, 669–677. doi: 10.1161/hypertensionaha.116.08597

Yanes, L. L., Sartori-Valinotti, J. C., and Reckelhoff, J. F. (2008). Sex steroids and renal disease: lessons from animal studies. *Hypertension* 51, 976–981. doi: 10.1161/hypertensionaha.107.105767

Yokota, H., Takamiya, A., Nagaoka, T., Hikichi, T., Ishida, Y., Suzuki, F., et al. (2008). Role of prorenin in the pathogenesis of retinal neovascularization. *Hokkaido Igaku Zasshi* 83, 159–165.

Zandi-Nejad, K., Luyckx, V. A., and Brenner, B. M. (2006). Adult hypertension and kidney disease: the role of fetal programming. *Hypertension* 47, 502–508. doi: 10.1161/01.hyp.0000198544.09909.1a

Zhu, T., Miller, A. G., Deliyanti, D., Berka, D. R., Agrotis, A., Campbell, D. J., et al. (2015). Prorenin stimulates a pro-angiogenic and pro-inflammatory response in retinal endothelial cells and an M1 phenotype in retinal microglia. *Clin. Exp. Pharmacol. Physiol.* 42, 537–548. doi: 10.1111/1440-1681.12376

Conflict of Interest: The authors declare that the research was conducted in the absence of any commercial or financial relationships that could be construed as a potential conflict of interest.

frontiers in Physiology

CORRECTION
published: 16 November 2020
doi: 10.3389/fphys.2020.615022

Corrigendum: Intrarenal Renin Angiotensin System Imbalance During Postnatal Life Is Associated With Increased Microvascular Density in the Mature Kidney

Carolina Dalmasso[1], *Alejandro R. Chade*[2], *Mariela Mendez*[3], *Jorge F. Giani*[4], *Gregory J. Bix*[5], *Kuey C. Chen*[1] *and Analia S. Loria*[1]*

[1] Department of Pharmacology and Nutritional Sciences, University of Kentucky, Lexington, KY, United States, [2] Department of Physiology and Biophysics, Medicine, and Radiology, University of Mississippi Medical Center, Jackson, MS, United States, [3] Department of Internal Medicine, Hypertension and Vascular Research Division, Henry Ford Hospital, Detroit, MI, United States, [4] Departments of Biomedical Sciences and Pathology, Cedars-Sinai Medical Center, Los Angeles, CA, United States, [5] Clinical Neuroscience Research Center, Tulane University, New Orleans, LA, United States

Keywords: maternal separation, kidney, renin-angiotensin system, microvascular density, renal transcriptome

OPEN ACCESS

Edited by:
Bellamkonda K. Kishore, University of Utah Health Care, United States

Reviewed by:
Yufeng Huang, The University of Utah, United States

***Correspondence:**
Analia S. Loria
analia.loria@uky.edu

Specialty section:
This article was submitted to Renal and Epithelial Physiology, a section of the journal Frontiers in Physiology

Received: *07 October 2020*
Accepted: *19 October 2020*
Published: *16 November 2020*

Citation:
Dalmasso C, Chade AR, Mendez M, Giani JF, Bix GJ, Chen KC and Loria AS (2020) Corrigendum: Intrarenal Renin Angiotensin System Imbalance During Postnatal Life Is Associated With Increased Microvascular Density in the Mature Kidney. Front. Physiol. 11:615022. doi: 10.3389/fphys.2020.615022

A Corrigendum on

Intrarenal Renin Angiotensin System Imbalance During Postnatal Life Is Associated With Increased Microvascular Density in the Mature Kidney

by Dalmasso, C., Chade, A. R., Mendez, M., Giani, J. F., Bix, G. J., Chen, K. C., et al. (2020). Front. Physiol. 11:1046. doi: 10.3389/fphys.2020.01046

In the original article, there was a mistake in **Figure 1C** as published. **GFR was labeled as mg/day/100 g BW.** The corrected **Figure 1C, where GFR is labeled as ml/min/100 g BW** appears below.

The authors apologize for this error and state that this does not change the scientific conclusions of the article in any way. The original article has been updated.

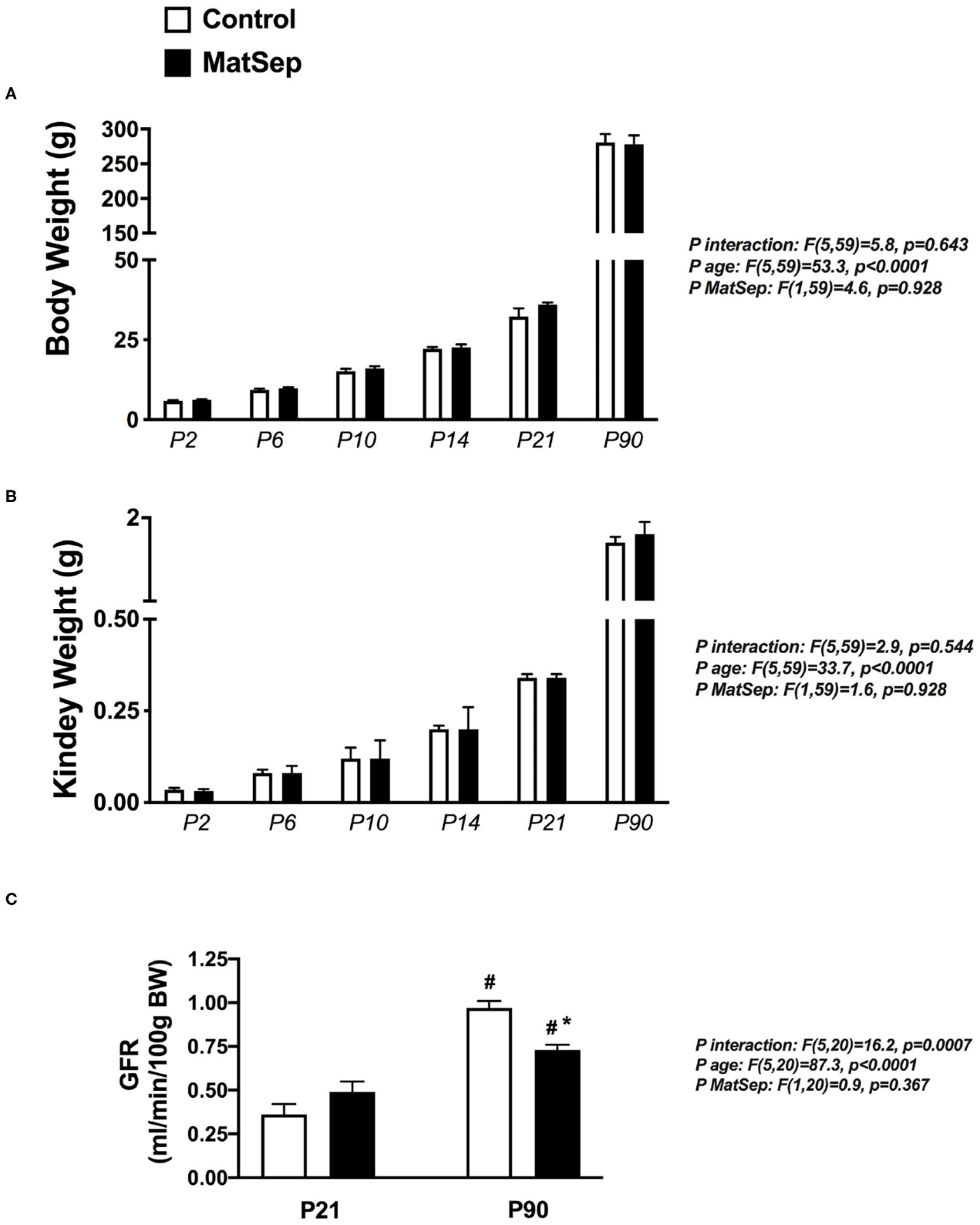

FIGURE 1 | Effect of MatSep on the trajectory from neonatal to adult male rats in: **(A)** body weight, **(B)** Kidney, and **(C)** conscious GFR. $^{\#}p < 0.05$ vs. P21, $^{*}p < 0.05$ vs. C. P: postnatal day. $n = 6$–8 per group.

frontiers in Medicine

ORIGINAL RESEARCH
published: 02 September 2020
doi: 10.3389/fmed.2020.00475

Impact of Gut Microbiome on Hypertensive Patients With Low-Salt Intake: Shika Study Results

Satoshi Nagase[1†], Shigehiro Karashima[2†], Hiromasa Tsujiguchi[3], Hirohito Tsuboi[4], Sakae Miyagi[3], Mitsuhiro Kometani[2], Daisuke Aono[2], Takuya Higashitani[2], Masashi Demura[5], Hiroyuki Sakakibara[6], Akihiro Yoshida[7], Akinori Hara[3], Hiroyuki Nakamura[3], Yoshiyu Takeda[2], Hidetaka Nambo[8], Takashi Yoneda[2,9] and Shigefumi Okamoto[1]**

[1] Department of Laboratory Science, Faculty of Health Sciences, Kanazawa University, Kanazawa, Japan, [2] Department of Endocrinology and Metabolism, Kanazawa University Hospital, Kanazawa, Japan, [3] Department of Environmental and Preventive Medicine, Advanced Preventive Medical Sciences, Kanazawa University, Kanazawa, Japan, [4] Division of Psychosomatic Medicine, Institute of Medical, Pharmaceutical, and Health Sciences, Kanazawa University, Kanazawa, Japan, [5] Department of Hygiene, Kanazawa University Graduate School of Medicine, Kanazawa, Japan, [6] Graduate School of Agriculture, University of Miyazaki, Miyazaki, Japan, [7] Department of Oral Microbiology, Matsumoto Dental University Graduate School of Oral Medicine, Shiojiri, Japan, [8] School of Electrical, Information, and Communication Engineering, College of Science and Engineering, Kanazawa University, Kanazawa, Japan, [9] Department of Health Promotion and Medicine of the Future, Kanazawa University Graduate School of Medicine, Kanazawa, Japan

OPEN ACCESS

Edited by:
Zhengrong Guan,
University of Alabama at Birmingham, United States

Reviewed by:
Wei Chen,
Sun Yat-sen University, China
Elaine Mary Richards,
University of Florida, United States

***Correspondence:**
Takashi Yoneda
endocrin@med.kanazawa-u.ac.jp
Shigefumi Okamoto
sokamoto@mhs.mp.kanazawa-u.ac.jp

[†]These authors have contributed equally to this work

Specialty section:
This article was submitted to Nephrology, a section of the journal Frontiers in Medicine

Received: *04 March 2020*
Accepted: *14 July 2020*
Published: *02 September 2020*

Citation:
Nagase S, Karashima S, Tsujiguchi H, Tsuboi H, Miyagi S, Kometani M, Aono D, Higashitani T, Demura M, Sakakibara H, Yoshida A, Hara A, Nakamura H, Takeda Y, Nambo H, Yoneda T and Okamoto S (2020) Impact of Gut Microbiome on Hypertensive Patients With Low-Salt Intake: Shika Study Results. Front. Med. 7:475. doi: 10.3389/fmed.2020.00475

Salt intake is one of the most important environmental factors impacting hypertension onset. Meanwhile, the potential roles of the gut microbiome (GM) in altering the health status of hosts have drawn considerable attention. Here, we aimed to perform an observational study to investigate the impact of intestinal bacterial flora in hypertensive patients with low-salt or high-salt intake. A total of 239 participants were enrolled, and their gut microbiomes, clinical and demographic details, as well as physiological parameters pertaining to the renin-angiotensin-aldosterone system and inflammatory cytokine profiles, were examined. The participants were classified into four groups based on the presence of different enterotype bacteria, as determined via cluster analysis, and salt intake: low salt/GM enterotype 1, low salt/GM enterotype 2, high salt/GM enterotype 1, and high salt/GM enterotype 2. Results show that the prevalence of hypertension was significantly lower in the low-salt/GM enterotype 2 group (27%) compared to the low salt/GM enterotype 1 group (47%; $p = 0.04$). Alternatively, no significant differences were observed in hypertension prevalence between the two high-salt intake groups (GM enterotype 1 = 50%, GM enterotype 2 = 47%; $p = 0.83$). Furthermore, The low-salt/GM enterotype 2 was higher in the relative abundances of *Blautia*, *Bifidobacterium*, *Escherichia-Shigella*, *Lachnoclostridium*, and *Clostridium sensu stricto than* the low-salt/GM enterotype 1. differed significantly between the GM enterotypes. These results suggested that consumption of a low-salt diet was ineffective in regulating hypertension in individuals with a specific gut bacteria composition. Our findings support the restoration of GM homeostasis as a new strategy for controlling blood pressure and preventing the development of hypertension.

Keywords: gut microbiome, blood pressure, salt-intake, renin-angiotensin-aldosterone system, hypertension

INTRODUCTION

Hypertension has become an important global health issue and is a major risk factor for cardiovascular, cerebrovascular, and kidney diseases (1, 2). It is believed that the etiology of hypertension depends on the complex interplay of both genetic and environmental factors (3, 4). Salt intake is one of the most important environmental factors of hypertension onset. For instance, the Intersalt Cooperative Research Group found significant positive relationships between 24 h urinary sodium excretion and blood pressure (BP) in the study participants (5). In addition, the Dietary Approaches to Stop Hypertension (DASH) interventional study showed that dietary salt-intake patterns may affect BP in the adult population with BP in the high normal range compared to those that are moderately hypertensive (6). Most studies show that excess sodium consumption raises BP in a dose-dependent manner; however, salt sensitivity, that is how BP responds to salt, varies, with less than one-third of normotensive individuals and less than one-half of hypertensive individuals classified as salt sensitive (7–10). Known sources of such variability include genetic polymorphisms of the associated renin-angiotensin-aldosterone system (RAAS), dietary intake, and kidney disease.

In recent decades, the potential roles of the gut microbiome (GM) in altering the health status of hosts have drawn considerable attention. Several lines of evidence suggest a link between GM and lifestyle disease, including diabetes, obesity, and hypertension (11–13). For instance, GM dysbiosis accompanies hypertension in rodents (14, 15). In Dahl rats, distinct differences in metagenomic composition have been identified for salt-sensitive and salt-resistant strains (16). Furthermore, the GM of salt-sensitive rats is suggested to have symbiotic relationships with their hosts (16). This suggests that changes in GM precede the onset of hypertension, which is supported by the findings of Wilck et al., who demonstrated that feeding mice a high-salt diet decreases the proportion of gut *Lactobacillus murinus*, which is associated with increased number and activation of TH17 cells (17). These cells secrete a pro-inflammatory cytokine, interleukin-17 (IL-17), which is believed to promote high BP and accompanying inflammation in artery walls (17). However, most of these studies were performed using animal models, which may not directly translate to human disease. Furthermore, there are only limited human clinical trials that have been performed to decipher the relationships between dietary salt, GM, immunological reactions, and BP. The aim of the current observational study was to, therefore, investigate the impact of the intestinal bacterial flora on hypertensive patients with low-salt intake.

MATERIALS AND METHODS

Study Population

We used cross-sectional data of the Shika study, which is a population-based study that aims to establish a method to prevent lifestyle-related diseases (18, 19). It includes interviews, questionnaires, and health examinations. Health examination data was collected between March 2014 and January 2018 from the residents of Shika, a town with more than 20,000 residents (20), located in a north area of Ishikawa Prefecture, Japan (21). The present study was conducted from December 2017 through January 2018 with four model districts in Shika being selected, including Horimatsu, Higashi-Masuho, Tsuchida, and Togi.

Ethical Considerations

The study was approved by the Ethics Committee for Human Studies at Kanazawa University Hospital (No. 1491) and was performed in accordance with the principles of the Declaration of Helsinki and the Microorganism Safety Management Regulations of Kanazawa University. All participants were provided an explanation of the research and subsequently provided written informed consent prior to the collection of gut microorganisms. Collected microorganisms were processed in a biosafety level-2 laboratory.

Data Collection

Data through the Shika study were collected by participant interviews and included demographics, such as age, sex, underlying diseases, and medications. Height, weight, and BP were measured during study visits. Specifically, BP was measured when the subjects were seated in a chair. A suitably sized cuff was placed on the right upper arm and attached to UM-15P (Paramatech Co., Ltd., Fukuoka, Japan) and HEM-907 (OMRON Co., Ltd., Kyoto, Japan). BP monitors contained automated digital sphygmomanometer based on the oscillometric method (18). Hypertension was defined as sBP of 140 mmHg, dBP of 90 mmHg, or if participants reported use of antihypertensive drugs. Venous blood samples were collected in the mornings after 15 min periods of rest following a 12 h overnight fast.

Daily salt-intake was evaluated by urine sodium levels and creatine ratios in urine samples (22). Estimated glomerular filtration rates (eGFR) were calculated using serum creatinine levels. Plasma renin activity (PRA) and plasma aldosterone concentration (PAC) were measured using radioimmunoassays, as previously reported (23). Serum levels of cytokines, including, granulocyte-macrophage colony-stimulating factor (GM-CSF), interleukin-17a (IL-17a), and tumor necrosis factor alfa (TNF-α) were measured using a MILLIPLEX MAP Human High Sensitivity T Cell Panel-Immunology Multiplex Assay (Merck KGaA, Darmstadt, Germany) and Luminex® 200TM flow cytometry system (Thermo Fisher Scientific, MA, US).

Stool Sample Collection and DNA Extraction

Stool samples were collected from 254 participants. However, 15 of the samples were excluded due to the subjects taking antimicrobial or steroid drugs, resulting in 239 stool samples for analysis. Fecal sample collection was accomplished using clean paper (AS ONE Inc., Osaka Japan) and a clean spatula with plastic tube (AS ONE Inc.). The fecal samples were then transferred to sterile closed plastic tubes the in morning and transported to the laboratory on ice within the day. The samples were stored at −80°C until DNA extraction. Whole DNA was extracted from the fecal samples using NucleoSpin® DNA

Stool (Macherey-Nagel Inc., Düren Germany) according to the manufacturer's instructions.

Next Generation Sequencing (NGS)

The extracted DNA of gut microbiome was processed for 16S rRNA gene sequencing by NGS using methods previously described (24). V3-4 regions of the 16S rRNA gene were amplified using Ex Taq® Hot Start Version polymerase and TaKaRa PCR Thermal Cycler Dice® Gradient (TaKaRa Bio Inc., Shiga, Japan). The PCR products were purified by Agencourt AMPure XP magnetic beads (Beckman Coulter, Inc., CA, USA). The amount of the PCR products were measured by Qubit® dsDNA HS Assay Kit and Qubit® 3.0 fluorometer (Thermo Fisher Scientific, Inc.). All purified PCR products were sent to Hokkaido System Science Co., Ltd. (Hokkaido, Japan) for Illumina MiSeq sequencing. The NGS data were registered in the DNA Data Bank of Japan (DDBJ; accession number PRJDB8820).

Microbiome Analysis

Microbiome analysis was performed according to methods reported in a previous study (24). The pair-end sequences were filtered by Sickle (version 1.33) (25) and assembled by PANDAseq (version 2.11) (26). Removed chimera sequences were used by USEARCH (version 10.0.240_i86linux32) (27) and Silva 16S rRNA database (release 132) (28). From non-chimeric sequences, the "pick_de_novo_otus.py" command in Qiime (version 1.9.1) and the Silva 16S rRNA gene database (release 132) was used to generate operational taxonomic unit (OTU) (97% similarity threshold) (29). Finally, global singletons were removed using the "filter_otus_from_otu_table.py" command in Qiime.

Statistics

R Package (version 3.5.0) software was used for all statistical analyses (30). Box plots showed the median, 1st quartile, 3rd quartile with 1st quartile + 1.5 × interquartile range (IQR), and 3rd quartile – 1.5 × IQR whiskers, and points exhibited outliers. Participant characteristics and relative abundance among each group were compared using one-way analysis of variance (ANOVA) and analysis of covariance (ANCOVA) with adjustment for age, sex, and body mass index (BMI). The relative abundance of each microgram was compared using the DESeq2 package (31). Cluster analysis was performed based on the previous study (32). Principal component analysis (PCA) used Jensen-Shannon divergence values based on the genus level. Cluster analysis was performed used Partitioning Around Medoid (PAM) clustering. The PCA and cluster analysis were performed using "philentropy" and "pamr" package (32, 33). A random forest analysis used the randomForest package of R (34). All microorganisms and participant information [age, sex, BMI, PRA, PAC, eGFR, diabetes mellitus (DM) rate, hyperlipidemia (HL) rate, IL-17a levels, GM-CSF levels, and TNF-α levels] were evaluated with the random forest function using default parameters. Random forest analysis of bacterial genera and participant information contained out of bag error rates of 44.3 and 37.7%, respectively. The similarity of microbiome composition between each participant group was assessed by permutational multivariate analysis of variance (PERMANOVA) using the "adonis" command in the vegan package of R (10,000 simulations) (35).

RESULTS

Enterotype Clustering and Salt Intake

In total, 239 participants were included for analysis. The prevalence of hypertension was 44.8% in the study population. Mean systolic BP (SBP) and diastolic BP (DBP) were 136 ± 17 and 80 ± 11 mmHg, respectively. The mean daily salt-intake was 9.4 ± 1.9 g/day (median 9.6 g/day). The antihypertensive drug usage rate was 11.7% (28/239). Specifically, 25 participants were treated with angiotensin converting enzyme inhibitors and/or angiotensin receptor blockers. There was no participant treated with mineralocorticoid receptor antagonists. There were three patients treated with the other antihypertensives excluding RAAS inhibitors.

To explore the potential differences between hypertension rates with respect to microbiome and salt intake, the participants were separated into four groups based on cluster analysis. First, the GMs of the participants were structured into two enterotypes using the PAM clustering method based on Jensen-Shannon distance (**Figures 1A,B**). There was no significant difference in the participant information between the two enterotypes (**Supplemental Table 1**). Next, two groups were formed based on median salt-intake values, a high-salt group which was defined as higher than 9.6 g/day of daily salt-intake, and a low-salt group which was defined as the lower. There was no significant difference in relative microgram levels of salt between the high-salt and low-salt groups. Finally, we classified the study participants into four groups based on GM enterotype and salt intake. These included a low salt/GM enterotype 1 group, a low salt/GM enterotype 2 group, a high salt/GM enterotype 1 group, and a high salt/GM enterotype 2 group.

Clinical Background

The clinical background information for the four groups of participants based on salt intake and GM are shown in **Table 1**. There were significant differences among the four groups with respect to the prevalence of females ($p = 0.04$), daily salt intake ($p < 0.01$), and PAC ($p < 0.01$). However, no differences were observed for any other clinical parameters including sBP ($p = 0.21$) and dBP ($p = 0.34$). There were, however, significant difference observed between the low-salt groups with respect to the prevalence of females ($p = 0.02$). Meanwhile, the high-salt groups did not exhibit significant differences between enterotype 1 and enterotype 2 (**Supplemental Table 2**).

Prevalence of Hypertension a Random Forest Analysis

Figure 2 shows the prevalence of hypertension in the four groups of participants categorized by enterotype and daily salt-intake. The prevalence of hypertension was significantly different ($p < 0.05$) for the two GM enterotype groups with low-salt intake (enterotype 1, 47%; enterotype 2, 27%). However, there was no significant difference ($p = 0.83$) in hypertension prevalence for

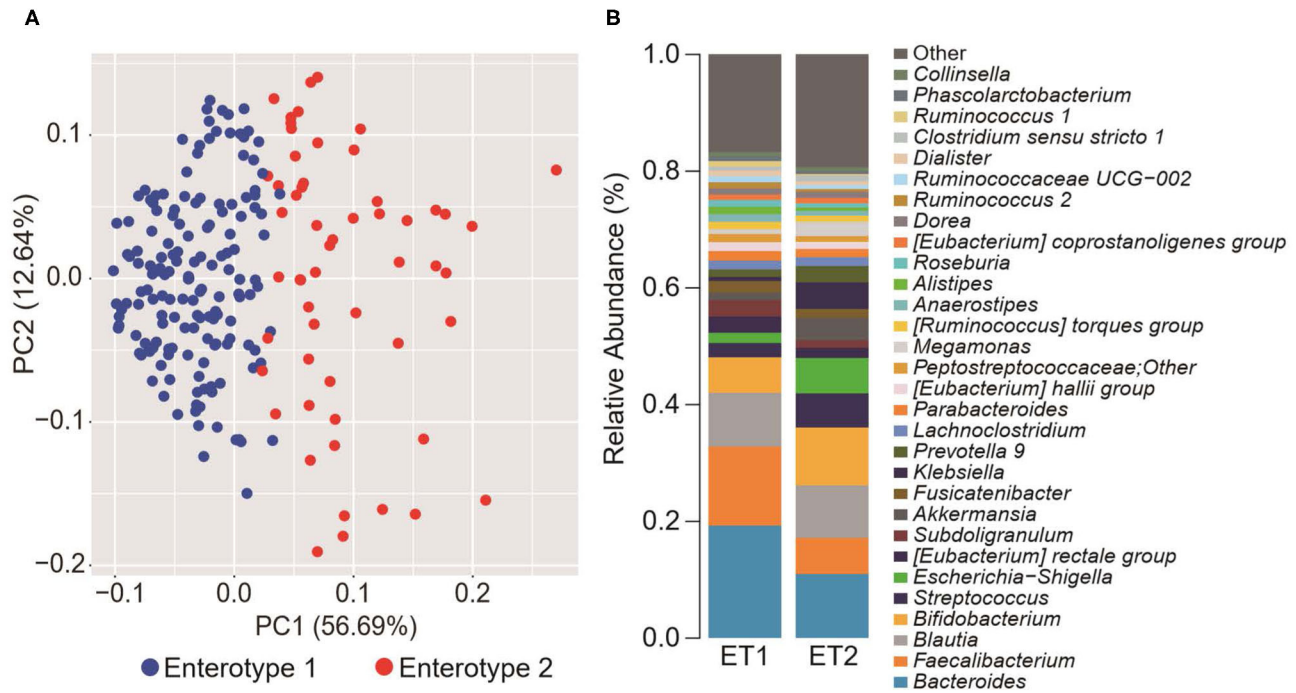

FIGURE 1 | Gut microbiome differences determined by clustering analysis. **(A)** Principal component analysis (PCA) plot generated using the Partitioning Around Medoid (PAM) clustering method based on Jensen-Shannon distance of operational taxonomic unit (OTU) counts. Blue, enterotype 1; Red, enterotype 2. **(B)** Relative abundance of the top 30 microorganisms identified by the gut microbiome cluster.

TABLE 1 | Characteristics of the four groups of study participants categorized by gut microbiome clustering and daily salt-intake.

Characteristics	All	Low salt intake		High salt intake	
	(*n* = 239)	Enterotype 1 (*n* = 83)	Enterotype 2 (*n* = 37)	Enterotype 1 (*n* = 89)	Enterotype 2 (*n* = 30)
Age, y	63 ± 10	64 ± 11	61 ± 11	63 ± 9	63 ± 9
Female, %*	52.3	66.3‡	40.5	47.2	43.3
BMI, kg/m^2	23.3 ± 3.1	23.0 ± 3.7	22.6 ± 2.7	23.7 ± 2.5	23.4 ± 3.3
Hypertension, %	44.8	47.0‡	27.0	49.4	46.7
SBP, mmHg	136 ± 17	135 ± 19	132 ± 17	139 ± 17	138 ± 17
DSP, mmHg	80 ± 11	78 ± 12	78 ± 9	82 ± 10	83 ± 11
Salt intake, g/day †	9.4 ± 1.9	7.9 ± 1.2	7.8 ± 1.3	10.9 ± 1.2	10.8 ± 1.1
eGFR, mL/min/1.73 m^2	68.4 ± 12.1	66.0 ± 12.3	67.5 ± 11.5	69.6 ± 11.1	72.5 ± 12.1
PRA, ng/mL/h	2.4 ± 5.6	2.8 ± 8.4	3.0 ± 5.4	1.9 ± 2.0	1.8 ± 2.2
PAC, pg/mL †	140.6 ± 69.2	155.0 ± 86.9	161.5 ± 57.9	124.5 ± 51.9	122.3 ± 54.1
GM-CSF, pg/mL	8.1 ± 12.6	9.3 ± 15	5.8 ± 4.1	8.9 ± 14.0	5.3 ± 12.6
IL17a, pg/mL	2.0 ± 1.3	2.1 ± 1.2	2.0 ± 1.1	2.1 ± 1.5	1.7 ± 1.3
TNF-α, pg/mL	1.5 ± 0.6	1.5 ± 0.6	1.4 ± 0.4	1.6 ± 0.8	1.3 ± 0.6
Antihypertensive %	11.7	14.5	18.9	5.6	13.3

**P < 0.05 and † P < 0.01 based on analysis of covariance in four groups. ‡P < 0.05 vs. enterotype 2 (ANCOVA).: BMI, body mass index; SBP, systolic blood pressure; DBP, diastolic blood pressure; eGFR, estimated glomerular filtration rate; PAC, plasma aldosterone concentration; PRA, plasma renin activity; GM-CSF, granulocyte-macrophage colony-stimulating factor; IL-17a, interleukin-17a; TNF-α, tumor necrosis factor alpha.*

the two GM enterotype groups with high-salt intake (enterotype 1, 50%; enterotype 2, 47%).

Univariate analysis and multiple logistic regression analysis adjusted for age, sex, and BMI revealed that predictive changes in GM enterotypes were associated with hypertension in the low-salt group (**Supplemental Table 3**). Scatter plots of systolic and diastolic BP vs. salt intake are shown in **Figure 3**. The slopes of the approximate straight lines were greater for enterotype 2

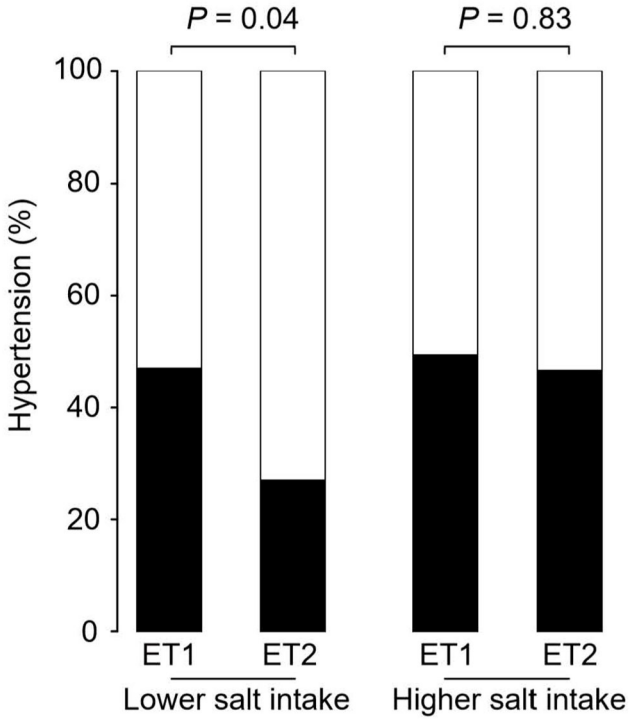

FIGURE 2 | Hypertension prevalence rates for enterotype and salt-intake groups. Hypertension rates are shown based on GM clustering and salt-intake. Black, hypertension rate; White, non-hypertension rate. *P*-values were calculated using Fisher's test.

(SBP = 2.00, DBP = 1.30) than for enterotype 1 (SBP = 1.23, DBP = 1.18).

Significant Intestinal Bacteria Genera

Figure 4 shows the GM compositions of the low-salt groups. The relative abundance of certain microorganisms was significantly different between enterotype 1 and enterotype 2 groups. For instance, the relative abundances of *Blautia*, *Bifidobacterium*, *Escherichia-Shigella*, *Lachnoclostridium*, and *Clostridium. sensu. stricto.* were significantly higher in the enterotype 2 groups. Feature importance ranking indicated that the *Eubacterium rectale* group and *Blautia* were the top two most discriminatory bacteria between enterotype 1 and enterotype 2 groups in the low-salt groups. Also, in high-salt group, *Bifidobacterium* and *Lachnoclostridium* differed significantly between enterotype 1 and enterotype 2 (*Bifidobacterium* $p < 0.01$, *Lachnoclostridium* $p = 0.01$), while, *Escherichia-Shigella, Clostridium sensu stricto.1, and Blautia* did not differ significantly *(Escherichia-Shigella* $p = 0.09$, *Clostridium sensu stricto.1* $p = 0.89$, *Blautia* $p = 0.99$).

The Renin-Angiotensin-Aldosterone System and Inflammatory Cytokines

Enterotype 1 and enterotype 2 were categorized using PCA. The PCA plot included age, sex, BMI, PRA, PAC, eGFR, IL-17a, GM-CSF, and TNF-α, past history of DM, and past history of HL. In the low-salt groups, there was a significant difference in these components between the enterotype 1 and enterotype 2 groups (PERMANOVA; $p < 0.05$). However, in the high-salt group and all-participants group, there were no significant differences between the enterotype 1 and enterotype 2 groups (**Supplemental Figure 1A**). Feature importance ranking revealed that GM-CSF, PRA, TNF-α, PAC, and IL-17a were the most discriminatory factors between the groups (**Supplemental Figure 1B**).

DISCUSSION

We defined two distinct enterotype groups based on the composition of fecal microbial communities in the general Japanese population. There was a significantly higher prevalence of hypertension in the enterotype 1 group with low-salt intake compared to the enterotype 2 group with low-salt intake. Six significant candidate bacterial genera were identified for classifying the two enterotypes with low-salt intake. *Blautia, Bifidobacterium, Escherichia-Shigella, Lachnoclostridium*, and *Clostridium sensu stricto* showed significant differences in their prevalence ratios for fecal bacteria genera and the *Eubacterium rectale* group and *Blautia* had higher feature importance rankings used to define the two enterotype groups with low-salt intake. Further, *Bifidobacterium* and *Lachnoclostridium* differed significantly between the two enterotype groups in both low-salt intake and high-salt intake.

Several previous studies have recently reported evidence that GM and the regulation of BP are linked and have described the potential mechanisms involved (14–16). For instance, the following candidate mechanisms for an association between GM and hypertension have been presented: (1) immunomodulatory function via GM (17, 36); (2) short-chain fatty acids (SCFA)-producing GM (37, 38); (3) trimethylamine N-oxide (TMAO) (39, 40); (4) glucocorticoid metabolism (41); and (5) epigenetic regulation (42–44).

First, GM demonstrates a multitude of physiological functions through the modulation of the host immune system (45). The subtle imbalance of GM composition may play a key role in the onset of hypertension. Wilck et al. showed that high-salt intake also drives autoimmunity by inducing T-helper (Th)17 cells, which then contribute to hypertension by depleting *Lactobacillus murinus* (17). They also demonstrated that a 14-d challenge of a high-salt diet increases BP and the number of circulating IL-$17A^+$/TNF-α^+/$CD4^+$ T-cells while reducing fecal *Lactobacillus* species in humans (17). In our current investigation, there were few *Lactobacillus* and no significant differences in composition between enterotype 1 and enterotype 2. Therefore, *Lactobacillus* composition was not regarded as a contributor to the prevalence of hypertension in our population group. *Bifidobacterium* is reported to induce the development of regulatory T-cells (Treg) and Th17 cell compartments in the intestine and the secretion of IL-17 (46). This suggests that bacteria may play a role in balancing the development of Treg and Th17 cell compartments. This may induce an effector function such as secreting IL-17 or a regulatory

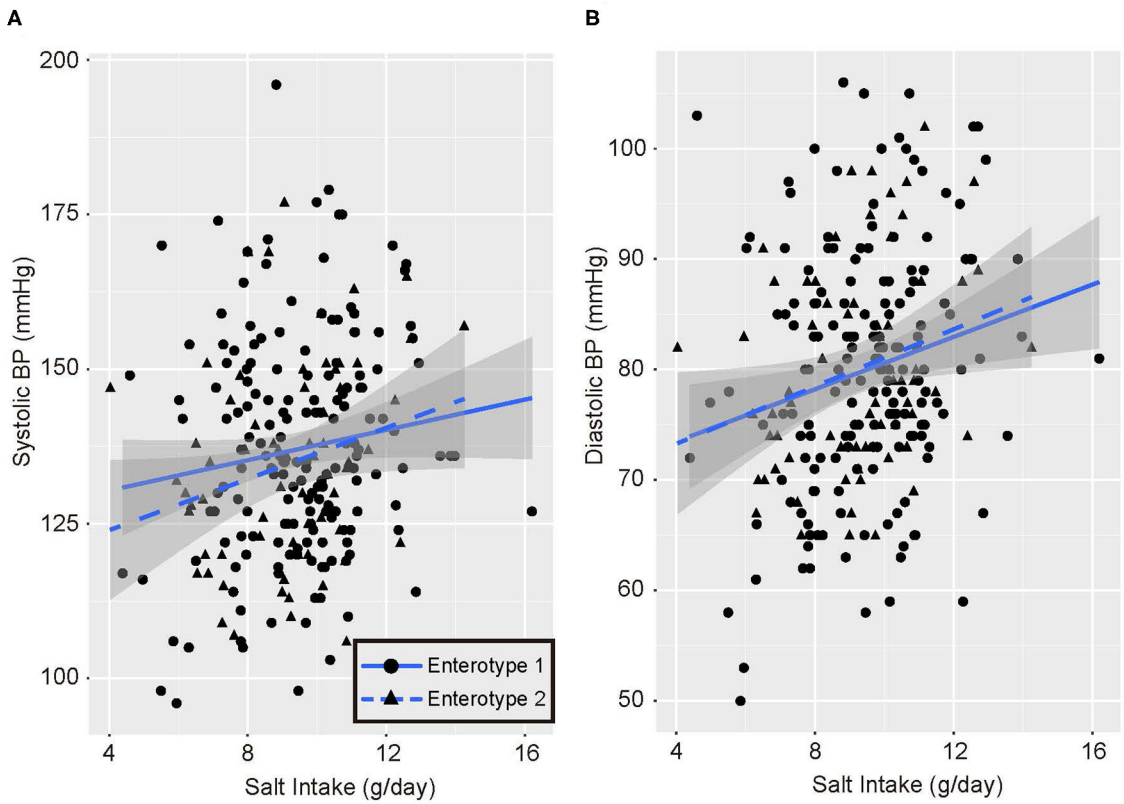

FIGURE 3 | Blood pressure and salt intake scatter plots. **(A)** Systolic blood pressure (BP) and salt intake. **(B)** Diastolic blood pressure and salt intake. Black circles and solid blue line, enterotype 1; Black triangles and broken blue line, enterotype 2.

action such as suppressing the activation of the immune system, depending on the environment and the nature of the stimuli, including high-salt intake (47).

Second, among the six candidate bacterial genera identified for classifying the two enterotypes with low-salt intake, *Blautia*, *Bifidobacterium, Lachnoclostridium*, and the *Eubacterium rectale* group are reported to be SCFA-producing bacteria. SCFAs are the major nutrients produced by bacterial fermentation with the three major SCFAs being acetate, propionate, and butyrate. Acetate was produced by all four of the bacteria genera. In addition, *Blautia obeum* is able to produce both propionate and butyrate (48) whereas *Eubacterium spp.* produces mainly butyrate. SCFAs are known to influence several aspects of host physiology, including the regulation of BP (49). SCFAs can influence host cells by interacting with host G protein-coupled receptor 41 (Gpr41) and olfactory receptor 78 (Olfr78). Intriguingly, Olfr78 null mice are hypotensive (37), whereas Gpr41 null mice are hypertensive (38). SCFAs are known to induce vasorelaxation (50, 51). Thus, SCFAs acting on Gpr41 in the vascular endothelium may help to set the vascular tone. These pathways may be physiologically important links between SCFAs and the control of host BP.

Third, TMAO is a small organic compound derived mainly from choline and is metabolized by the microbiota to produce trimethylamine (TMA). TMAO is a known predictor of prevalent cardiovascular diseases (CVDs) (52) and of future cardiovascular events in clinical cohorts (53). Ge et al. recently performed a systematic review and meta-analysis and found that subjects with high TMAO concentrations have a 12% greater risk of hypertension compared to those with low circulating TMAO concentrations (39). Furthermore, Martin et al. showed that TMAO prolongs the hypertensive effect of angiotensin II in rats (40). Therefore, TMAO may play a key mediator role in the development of hypertension via angiotensin II activation. However, there are currently few reports regarding the association of TMAO with the six genera of bacteria that we identified in the current study. Additional investigation is needed regarding this topic.

Fourth, other investigators have proposed an alternative relationship between hypertension-onset and GM system. Gut bacteria are involved in metabolizing the endogenous glucocorticoids corticosterone and cortisol (41), which are able to bind and activate mineralocorticoid receptors (MR), causing sodium retention, hypertension, and renal injury (54). 21-deoxycortisol is derived from 21-dehydroxylation of corticosterone or cortisol by intestinal bacteria and most notably the inhibition of 11β-hydroxysteroid dehydrogenase (11β-HSD) type 1 and type 2. Plasma levels of 21-deoxycortisol are elevated in humans with hypertension compared with that of normotensive controls (55).

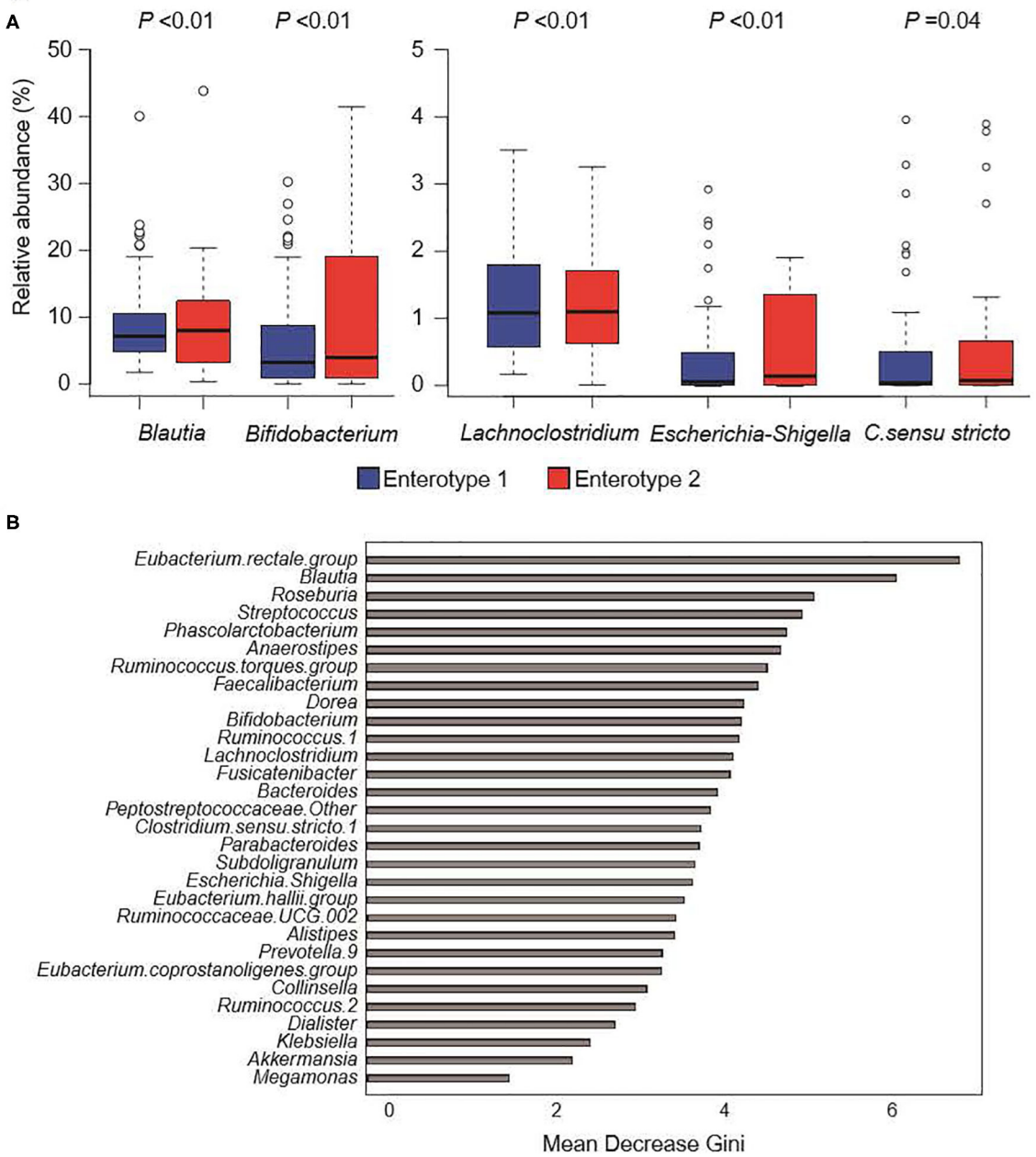

FIGURE 4 | Gut microbiome composition in low-salt groups. **(A)** Relative abundance of gut microorganisms with significant differences between enterotype 1 and enterotype 2. *P*-values were calculated using DESeq2 differential gene expression analysis. **(B)** Random forest model using explanatory variables of gut microorganisms.

Finally, recent studies have provided evidence for gut-derived effector molecules affecting host epigenetics as another mechanism of dynamic interactions between hosts and GM, including histone deacetylation. Diet, including salt intake, and GM can influence epigenetics (56–58). There are several reports on the relevance of Histone deacetylases (HDACs) to the development of hypertension (42–44, 59). In addition, SCFAs generated from SCFA-producing bacteria have histone deacetylase inhibitory activity and alter the expression of specific hypertension-related genes via conformational changes in the active site of HDAC, resulting in HDAC inactivation (60, 61). Pharmacological inhibition of HDACs is expected to be a practical novel therapeutic strategy for the treatment of hypertension.

While our current study provided important new details on the impact of the intestinal bacterial flora on hypertensive patients with high-salt intake, certain limitations should also be addressed. The study design was cross-sectional,

and therefore, the causality of the relationships could not be assessed. Furthermore, although this study includes a relatively large amount of information on the Japanese general population, however, only small sample sizes were included for two of the four final groups, the low-salt/GM enterotype 2 and the high-salt/GM enterotype 2. Regarding the six candidate GM biomarkers we identified, further interventional studies are necessary using both animal- and human-based study designs to investigate the change in GM by salt-intake and the effect on BP by feces transplant, bacteria transplant, or prebiotics. Further, daily salt-intake was estimated by urine sodium levels and creatine ratios in spot urine samples, and not in the 24 h urine samples. However, Huang et al. reported that the estimated daily salt-intake by spot urine testing was unable to detect the differences in sodium excretion measured by 24 h urine samples (62). Spot urine-based methods may be enough to evaluate daily salt-intake.

In conclusion, the current study demonstrated that the prevalence of hypertension is associated with the constitution of fecal bacteria and salt intake, and six microbial genera related to hypertension prevalence were identified in subjects who had low-salt intake. This suggested that there may be individuals with a specific gut bacteria composition for which changing dietary habits to low salt would be ineffective in preventing hypertension. The specific gut bacteria composition may not mean large quantities of a specific bacteria but appropriate population ratio with some bacteria. Physicians could identify the specific GM composition of hypertensive patients on salt diets for whom control of blood pressure has been difficult and could provide them the appropriate advice regarding low salt diets. Furthermore, treatment for gut dysbiosis, such as the administration of probiotics or fecal microbiota transplantation, might be affected by the stability of BP control in patients with hypertension. Our findings indicate a new strategy for controlling BP and the development of hypertension through the restoration of GM homeostasis. However, further studies examining the prospective relationship between the microbiome and hypertension induced by high-salt intake and the detailed mechanisms are still needed.

DATA AVAILABILITY STATEMENT

The result in DDBJ (DRA009074) can be seen in NCBI at the following URL; https://www.ncbi.nlm.nih.gov/sra/?term=DRA009074.

ETHICS STATEMENT

The studies involving human participants were reviewed and approved by the Ethics Committee for Human Studies at Kanazawa University Hospital. The patients/participants provided their written informed consent to participate in this study.

AUTHOR CONTRIBUTIONS

SN, SK, TY, and SO contributed to the study design and conducted the study. SN and SK wrote the manuscript. SN, SK, and HNam analyzed statistically. HTsuj, SM, AH, and HNak prepared the application to the ethics committee. MK, DA, TH, and YT collected the clinical data. SN, AY, and SO performed DNA extraction from stool samples and Next Generation Sequencing. HTsub and HS measured cytokine levels. SK, MD, and YT edited the manuscript. SN and SO are the guarantor of this work and, as such, had full access to all the data in the study and takes responsibility for the integrity of the data and the accuracy of the data analysis. All the authors have read the manuscript and have approved this submission. All authors contributed to the article and approved the submitted version.

FUNDING

This work was supported by a grant from the Ministry of Health, Labor, and Welfare, Japan (Nanbyo-Ippan-046, YT) and JSPS KAKENHI Grant Number JP19K17956 (SK).

ACKNOWLEDGMENTS

We thank Editage (Tokyo, Japan; www.editage.jp) for English language editing. We also thank the entire staff of the Endocrine and Hypertension group at Kanazawa University Hospital for their support in obtaining clinical data: Mikiya Usukura, Ayako Wakayama, Atsushi Hashimoto, Shunsuke Mori, Masashi Ohe, Toshitaka Sawamura, Rika Okuda, Seigo Konishi, Yoshimichi Takeda, Kei Sawada, Kenro Sugiyama, Yusuke Wakabayashi, Koichiro Takakuwa, Yui Soma, Tomomi Kimura, Tomoko Takahashi, Youhei Toyoda, Shohei Yoshikura, Yuya Nishimoto, Eiko Smimizu, and Yukiko Takamiya.

SUPPLEMENTARY MATERIAL

The Supplementary Material for this article can be found online at: https://www.frontiersin.org/articles/10.3389/fmed.2020.00475/full#supplementary-material

REFERENCES

1. Hillege HL, Girbes AR, de Kam PJ, Boomsma F, de Zeeuw D, Charlesworth A, et al. Renal function, neurohormonal activation, and survival in patients with chronic heart failure. *Circulation.* (2000) 102:203–10. doi: 10.1161/01.CIR.102.2.203
2. Pierdomenico SD, Di Nicola M, Esposito AL, Di Mascio R, Ballone E, Lapenna D, et al. Prognostic value of different indices of blood pressure variability in hypertensive patients. *Am J Hypertens.* (2009) 22:842–7. doi: 10.1038/ajh.2009.103
3. He FJ, Li J, Macgregor GA. Effect of longer-term modest salt reduction on blood pressure. *Cochrane Database Syst Rev.* (2013) CD004937. doi: 10.1002/14651858.CD004937.pub2
4. Kato N, Takeuchi F, Tabara Y, Kelly TN, Go MJ, Sim X, et al. Meta-analysis of genome-wide association studies identifies common variants associated

with blood pressure variation in East Asians. *Nat Genet.* (2011) 43:531–8. doi: 10.1038/ng.834
5. Intersalt Cooperative Research Group. Intersalt: an international study of electrolyte excretion and blood pressure. Results for 24-hour urinary sodium and potassium excretion. *BMJ.* (1988) 297:319–28. doi: 10.1136/bmj.297.6644.319
6. Sacks FM, Svetkey LP, Vollmer WM, Appel LJ, Bray GA, Harsha D, et al. DASH-Sodium Collaborative Research Group. Effects on blood pressure of reduced dietary sodium and the Dietary Approaches to Stop Hypertension (DASH) diet. DASH-Sodium Collaborative Research Group. *N Engl J Med.* (2001) 344:3–10. doi: 10.1056/NEJM200101043440101
7. Kotchen TA, Cowley AW Jr., Frohlich ED. Salt in health and disease–a delicate balance. *N Engl J Med.* (2013) 368:1229–37. doi: 10.1056/NEJMra1212606
8. Kawasaki T, Delea CS, Bartter F, Smith H. The effect of high-sodium and low-sodium intakes on blood pressure and other related variables in human subjects with idiopathic hypertension. *Am J Med.* (1978) 64:193–8. doi: 10.1016/0002-9343(78)90045-1
9. Grim CE, Luft FC, Fineberg NS, Weinberger MH. Responses to volume expansion and contraction in categorized hypertensive and normotensive man. *Hypertension.* (1979) 1:476–85. doi: 10.1161/01.HYP.1.5.476
10. Weinberger MH, Miller JZ, Luft FC, Grim CE, Finberg NS. Definitions and characteristics of sodium sensitivity and blood pressure resistance. *Hypertension.* (1986) 8:II127–34. doi: 10.1161/01.HYP.8.6_Pt_2.II127
11. Qin J, Li Y, Cai Z, Li S, Zhu J, Zhang F, et al. A metagenome-wide association study of gut microbiota in type 2 diabetes. *Nature.* (2012) 490:55–60. doi: 10.1038/nature11450
12. Chang CJ, Lin CS, Lu CC, Martel J, Ko YF, Ojcius DM, et al. *Ganoderma lucidum* reduces obesity in mice by modulating the composition of the gut microbiota. *Nat Commun.* (2015) 6:7489. doi: 10.1038/ncomms8489
13. Li J, Zhao F, Wang Y, Chen J, Tao J, Tian G, et al. Gut microbiota dysbiosis contributes to the development of hypertension. *Microbiome.* (2017) 5:14. doi: 10.1186/s40168-016-0222-x
14. Yang T, Santisteban MM, Rodriguez V, Li E, Ahmari N, Carvajal JM, et al. Gut dysbiosis is linked to hypertension. *Hypertension.* (2015) 65:1331–40. doi: 10.1161/HYPERTENSIONAHA.115.05315
15. Santisteban MM, Qi Y, Zubcevic J, Kim S, Yang T, Shenoy V, et al. Hypertension-linked pathophysiological alterations in the gut. *Circ Res.* (2017) 120:312–23. doi: 10.1161/CIRCRESAHA.116.309006
16. Mell B, Jala VR, Mathew AV, Byun J, Waghulde H, Zhang Y, et al. Evidence for a link between gut microbiota and hypertension in the Dahl rat. *Physiol Genomics.* (2015) 47:187–97. doi: 10.1152/physiolgenomics.00136.2014
17. Wilck N, Matus MG, Kearney SM, Olesen SW, Forslund K, Bartolomaeus H, et al. Salt-responsive gut commensal modules T_H17 axis and disease. *Nature.* (2017) 551:585–9. doi: 10.1038/nature24628
18. Nakamura H, Tsujiguchi H, Hara A, Kambayashi Y, Miyagi S, Thu Nguyen TT, et al. Dietary calcium intake and hypertension: importance of serum concentrations of 25-hydroxyvitamin D. *Nutrients.* (2019) 11:E911. doi: 10.3390/nu11040911
19. Karashima S, Kometani M, Tsujiguchi H, Asakura H, Nakano S, Usukura M, et al. Prevalence of primary aldosteronism without hypertension in the general population: results in Shika study. *Clin Exp Hypertens.* (2018) 40:118–25. doi: 10.1080/10641963.2017.1339072
20. *Shika Town Shikatown Population.* Available online at: http://www.town.shika.ishikawa.jp/jyuumin/shika_ town_pop/shika_population.html (accessed March 1, 2019).
21. Nakamura H, Hara A, Tsujiguchi H, Thi Thu Nguyen T, Kambayashi Y, Miyagi S, et al. Relationship between dietary n-6 fatty acid intake and hypertension: e?ect of glycated hemoglobin levels. *Nutrients.* (2018) 10:E1825. doi: 10.3390/nu10121825
22. Umemura S, Arima H, Arima S, Asayama K, Dohi Y, Hirooka Y, et al. The Japanese Society of Hypertension guidelines for the management of hypertension (JSH 2019). *Hypertens Res.* (2019) 42:1235–481. doi: 10.1038/s41440-019-0284-9
23. Karashima S, Yoneda T, Kometani M, Ohe M, Mori S, Sawamura T, et al. Comparison of eplerenone and spironolactone for the treatment of primary aldosteronism. *Hypertens Res.* (2016) 39:133–7. doi: 10.1038/hr.2015.129
24. Ogai K, Nagase S, Mukai K, Iuchi T, Mori Y, Matsue M, et al. A comparison of techniques for collecting skin microbiome samples: swabbing versus tape-stripping. *Front Microbiol.* (2018) 9:2362. doi: 10.3389/fmicb.2018.02362
25. Joshi NA, Fass JN. *Sickle: A Sliding-Window, Adaptive, Quality-Based Trimming Tool for FastQ Files.* (2016). Available online at: https://github.com/najoshi/sickle (accessed November 11, 2016).
26. Masella AP, Bartram AK, Truszkowski JM, Brown DG, Neufeld JD. PANDAseq: paired-end assembler for illumina sequences. *BMC Bioinformatics.* (2012) 13:31. doi: 10.1186/1471-2105-13-31
27. Edgar RC. Search and clustering orders of magnitude faster than BLAST. *Bioinformatics.* (2010) 26:2460–1. doi: 10.1093/bioinformatics/btq461
28. Quast C, Pruesse E, Yilmaz P, Gerken J, Schweer T, Yarza P, et al. The SILVA ribosomal RNA gene database project: improved data processing and web-based tools. *Nucleic Acids Res.* (2013) 41:D590–6. doi: 10.1093/nar/gks1219
29. Caporaso JG, Kuczynski J, Stombaugh J, Bittinger K, Bushman FD, Costello EK, et al. QIIME allows analysis of high-throughput community sequencing data. *Nat Methods.* (2010) 7:335–6. doi: 10.1038/nmeth.f.303
30. R Core Team. *R: A Language and Environment for Statistical Computing.* (2018). Available online at: https://www.r-project.org/ (accessed December 4, 2018).
31. Love MI, Huber W, Anders S. Moderated estimation of fold change and dispersion for RNA-Seq data with DESeq2. *Genome Biol.* (2014) 15:550. doi: 10.1186/s13059-014-0550-8
32. Drost H-G. Philentropy: information theory and distance quantification with R. *J Open Source Softw.* (2018) 3:765. doi: 10.21105/joss.00765
33. Tibshirani R, Hastie T, Narasimhan B, Chu G. Diagnosis of multiple cancer types by shrunken centroids of gene expression. *PNAS.* (2002) 99:6567–72. doi: 10.1073/pnas.082099299
34. Liaw A, Wiener M. Classification and regression by randomForest. *R News.* (2002) 2:18–22.
35. The Comprehensive R Archive Network. *vegan: Community Ecology Package.* (2016). Available online at: https://cran.r-project.org/web/packages/vegan/
36. Norlander AE, Madhur MS, Harrison DG. The immunology of hypertension. *J Exp Med.* (2018) 215:21–33. doi: 10.1084/jem.20171773
37. Pluznick JL, Protzko RJ, Gevorgyan H, Peterlin Z, Sipos A, Han J, et al. Olfactory receptor responding to gut microbiota-derived signals plays a role in renin secretion and blood pressure regulation. *Proc Natl Acad Sci USA.* (2013) 110:4410–5. doi: 10.1073/pnas.1215927110
38. Natarajan N, Hori D, Flavahan S, Steppan J, Flavahan NA, Berkowitz DE, et al. Microbial short chain fatty acid metabolites lower blood pressure via endothelial G-protein coupled receptor 41. *Physiol Genomics.* (2016) 48:826–34. doi: 10.1152/physiolgenomics.00089.2016
39. Ge X, Zheng L, Zhuang R, Yu P, Xu Z, Liu G, et al. The gut microbial metabolite trimethylamine N-oxide and hypertension risk: a systematic review and dose-response meta-analysis. *Adv Nutr.* (2019) 11:66–76. doi: 10.1093/advances/nmz064
40. Ufnal M, Jazwiec R, Dadlez M, Drapala A, Sikora M, Skrzypecki J. Trimethylamine-N-oxide: a carnitine- derived metabolite that prolongs the hypertensive effect of angiotensin II in rats. *Can J Cardiol.* (2014) 30:1700–5. doi: 10.1016/j.cjca.2014.09.010
41. Morris DJ, Brem AS. Role of gut metabolism of adrenal corticosteroids and hypertension: clues gut-cleansing antibiotics give us. *Physiol Genomics.* (2019) 51:83–9. doi: 10.1152/physiolgenomics.00115.2018
42. Choi SY, Kee HJ, Sun S, Seok YM, Ryu Y, Kim GR, et al. Histone deacetylase inhibitor LMK235 attenuates vascular constriction and aortic remodelling in hypertension. *J Cell Mol Med.* (2019) 23:2801–12. doi: 10.1111/jcmm.14188
43. Lemon DD, Horn TR, Cavasin MA, Jeong MY, Haubold KW, Long CS, et al. Cardiac HDAC6 catalytic activity is induced in response to chronic hypertension. *J Mol Cell Cardiol.* (2011) 51:41–50. doi: 10.1016/j.yjmcc.2011.04.005
44. Lee HA, Lee DY, Cho HM, Kim SY, Iwasaki Y, Kim IK. Histone deacetylase inhibition attenuates transcriptional activity of mineralocorticoid receptor through its acetylation and prevents development of hypertension. *Circ Res.* (2013) 112:1004–12. doi: 10.1161/CIRCRESAHA.113.301071
45. Honda K, Littman DR. The microbiota in adaptive immune homeostasis and disease. *Nature.* (2016) 535:75–84. doi: 10.1038/nature18848

46. López P, González-Rodríguez I, Gueimonde M, Margolles A, Suárez A. Immune response to *Bifidobacterium bifidum* strains support Treg/Th17 plasticity. *PLoS ONE.* (2011) 6:e24776. doi: 10.1371/journal.pone.0024776
47. Ivanov II, Frutos Rde L, Manel N, Yoshinaga K, Rifkin DB, Sartor RB, et al. Specific microbiota direct the differentiation of IL-17-producing T-helper cells in the mucosa of the small intestine. *Cell Host Microbe.* (2008) 4:337–49. doi: 10.1016/j.chom.2008.09.009
48. Louis P, Flint HJ. Formation of propionate and butyrate by the human colonic microbiota. *Environ Microbiol.* (2017) 19:29–41. doi: 10.1111/1462-2920.13589
49. Pluznick JL. Microbial short-chain fatty acids and blood pressure regulation. *Curr Hypertens Rep.* (2017) 19:25. doi: 10.1007/s11906-017-0722-5
50. Mortensen FV, Nielsen H, Mulvany MJ, Hessov I. Short chain fatty acids dilate isolated human colonic resistance arteries. *Gut.* (1990) 31:1391–4. doi: 10.1136/gut.31.12.1391
51. Knock G, Psaroudakis D, Abbot S, Aaronson PI. Propionate-induced relaxation in rat mesenteric arteries: a role for endothelium-derived hyperpolarising factor. *J Physiol.* (2002) 538:879–90. doi: 10.1113/jphysiol.2001.013105
52. Wang Z, Klipfell E, Bennett BJ, Koeth R, Levison BS, Dugar B, et al. Gut flora metabolism of phosphatidylcholine promotes cardiovascular disease. *Nature.* (2011) 472:57–63. doi: 10.1038/nature09922
53. Tang WH, Wang Z, Levison BS, Koeth RA, Britt EB, Fu X, et al. Intestinal microbial metabolism of phosphatidylcholine and cardiovascular risk. *N Engl J Med.* (2013) 368:1575–84. doi: 10.1056/NEJMoa1109400
54. Zhu A, Yoneda T, Demura M, Karashima S, Usukura M, Yamagishi M, et al. Effect of mineralocorticoid receptor blockade on the renal renin-angiotensin system in Dahl salt-sensitive hypertensive rats. *J Hypertens.* (2009) 27:800–5. doi: 10.1097/HJH.0b013e328325d861
55. Eisenhofer G, Peitzsch M, Kaden D, Langton K, Pamporaki C, Masjkur J, et al. Reference intervals for plasma concentrations of adrenal steroids measured by LC-MS/MS: impact of gender, age, oral contraceptives, body mass index and blood pressure status. *Clin Chim Acta.* (2017) 470:115–24. doi: 10.1016/j.cca.2017.05.002
56. Schwenk RW, Vogel H, Schürmann A. Genetic and epigenetic control of metabolic health. *Mol Metab.* (2013) 2:337–47. doi: 10.1016/j.molmet.2013.09.002
57. Liu Y, Liu P, Yang C, Cowley AW Jr., Liang M. Base-resolution maps of 5-methylcytosine and 5-hydroxymethylcytosine in Dahl S rats: effect of salt and genomic sequence. *Hypertension.* (2014) 63:827–38. doi: 10.1161/HYPERTENSIONAHA.113.02637
58. Stilling RM, Dinan TG, Cryan JF. Microbial genes, brain & behaviour - epigenetic regulation of the gut-brain axis. *Genes Brain Behav.* (2014) 13:69–86. doi: 10.1111/gbb.12109
59. Kim GW, Gocevski G, Wu CJ, Yang XJ. Dietary, metabolic, and potentially environmental modulation of the lysine acetylation machinery. *Int J Cell Biol.* (2010) 2010:632739. doi: 10.1155/2010/632739
60. Aoyama M, Kotani J, Usami M. Butyrate and propionate induced activated or non-activated neutrophil apoptosis via HDAC inhibitor activity but without activating GPR-41/GPR-43 pathways. *Nutrition.* (2010) 26:653–61. doi: 10.1016/j.nut.2009.07.006
61. Bhat MI, Kapila R. Dietary metabolites derived from gut microbiota: critical modulators of epigenetic changes in mammals. *Nutr Rev.* (2017) 75:374–89. doi: 10.1093/nutrit/nux001
62. Huang L, Woodward M, Stepien S, Tian M, Yin X, Hao Z, et al. Spot urine samples compared with 24-h urine samples for estimating changes in urinary sodium and potassium excretion in the China salt substitute and stroke study. *Int J Epidemiol.* (2018) 47:1811–20. doi: 10.1093/ije/dyy206

Conflict of Interest: The authors declare that the research was conducted in the absence of any commercial or financial relationships that could be construed as a potential conflict of interest.

frontiers in Physiology

ORIGINAL RESEARCH
published: 08 September 2020
doi: 10.3389/fphys.2020.543727

Selective Phosphodiesterase 1 Inhibitor BTTQ Reduces Blood Pressure in Spontaneously Hypertensive and Dahl Salt Sensitive Rats: Role of Peripheral Vasodilation

Asim B. Dey[1†], Sherif Khedr[2,3†], James Bean[1], Leah L. Porras[1], Tamika D. Meredith[1], Francis S. Willard[1], Joseph V. Hass[1], Xin Zhou[1], Maia Terashvili[2], Cynthia D. Jesudason[1], Kevin M. Ruley[1], Michael R. Wiley[1], Mark Kowala[1], Simon J. Atkinson[4‡], Alexander Staruschenko[2,5] and Mark D. Rekhter[1‡]*

[1] Eli Lilly and Company, Indianapolis, IN, United States, [2] Department of Physiology, Medical College of Wisconsin, Milwaukee, WI, United States, [3] Department of Physiology, Faculty of Medicine, Ain Shams University, Cairo, Egypt, [4] Department of Biology, Indiana University – Purdue University Indianapolis, Indianapolis, IN, United States, [5] Clement J. Zablocki VA Medical Center, Milwaukee, WI, United States

Regulation of the peripheral vascular resistance via modulating the vessel diameter has been considered as a main determinant of the arterial blood pressure. Phosphodiesterase enzymes (PDE1-11) hydrolyse cyclic nucleotides, which are key players controlling the vessel diameter and, thus, peripheral resistance. Here, we have tested and reported the effects of a novel selective PDE1 inhibitor (BTTQ) on the cardiovascular system. Normal Sprague Dawley, spontaneously hypertensive (SHR), and Dahl salt-sensitive rats were used to test *in vivo* the efficacy of the compound. Phosphodiesterase radiometric enzyme assay revealed that BTTQ inhibited all three isoforms of PDE1 in nanomolar concentration, while micromolar concentrations were needed to induce effective inhibition for other PDEs. The myography study conducted on mesenteric arteries revealed a potent vasodilatory effect of the drug, which was confirmed *in vivo* by an increase in the blood flow in the rat ear arteriols reflected by the rise in the temperature. Furthermore, BTTQ proved a high efficacy in lowering the blood pressure about 9, 36, and 24 mmHg in normal Sprague Dawley, SHR and, Dahl salt-sensitive rats, respectively, compared to the vehicle-treated group. Moreover, additional blood pressure lowering of about 22 mmHg could be achieved when BTTQ was administered on top of ACE inhibitor lisinopril, a current standard of care in the treatment of hypertension. Therefore, PDE1 inhibition induced efficient vasodilation that was accompanied by a significant reduction of blood pressure in different hypertensive rat models. Administration of BTTQ was also associated with increased heart rate in both models of hypertension as well as in the normotensive rats. Thus, PDE1 appears to be an attractive therapeutic target for the treatment of resistant hypertension, while tachycardia needs to be addressed by further compound structural optimization.

Keywords: phosphodiesterase 1, arterial hypertension, spontaneously hypertensive rat, Dahl salt sensitive rat, vasodilation

OPEN ACCESS

Edited by:
Suttira Intapad, Tulane University School of Medicine, United States

Reviewed by:
Erik Nicolaas Theodorus Petrus Bakker, University of Amsterdam, Netherlands
Ryousuke Satou, Tulane Medical Center, United States

***Correspondence:**
Asim B. Dey
dey_asim_bikash@lilly.com

† These authors have contributed equally to this work

‡Present address:
Simon J. Atkinson, The University of Kansas, Lawrence, KS, United States
Mark D. Rekhter, Integral, Boston, MA, United States

Specialty section:
This article was submitted to Renal and Epithelial Physiology, a section of the journal Frontiers in Physiology

Received: *18 March 2020*
Accepted: *14 August 2020*
Published: *08 September 2020*

Citation:
Dey AB, Khedr S, Bean J, Porras LL, Meredith TD, Willard FS, Hass JV, Zhou X, Terashvili M, Jesudason CD, Ruley KM, Wiley MR, Kowala M, Atkinson SJ, Staruschenko A and Rekhter MD (2020) Selective Phosphodiesterase 1 Inhibitor BTTQ Reduces Blood Pressure in Spontaneously Hypertensive and Dahl Salt Sensitive Rats: Role of Peripheral Vasodilation. Front. Physiol. 11:543727. doi: 10.3389/fphys.2020.543727

INTRODUCTION

Despite the significant improvement in patient care, resistant arterial hypertension remains an unmet medical need (Carey et al., 2018). A number of drugs, including compounds affecting renin-angiotensin-aldosterone system (RAAS), diuretics, beta-blockers, and calcium channel blockers are currently in practice; however, current therapeutic approaches are still limited (Kitt et al., 2019). It is feasible that the drugs targeting RAAS are missing critical RAAS-independent mechanistic nodes. Specifically, vascular smooth muscle cell (SMC) contractility, the focal point defining peripheral vascular resistance, is likely to be partially regulated in RAAS-independent manner (Muñoz-Durango et al., 2016).

Smooth muscle cell relaxation is primarily mediated by 3′, 5′-cyclic guanosine monophosphate (cGMP). cGMP level is determined by the balance between the rate of synthesis, mediated by guanylate cyclases, and degradation, through cyclic nucleotide phosphodiesterases (PDEs). The superfamily of PDEs consists of 11 PDE families (PDE1–PDE11) formed by multiple genes and isoforms. The role of PDE5 and PDE3 is widely explored in this context (Turko et al., 1999; Bellamy and Garthwaite, 2001; Corbin, 2004). PDE1 is highly expressed in SMCs (Giachini et al., 2011; Khammy et al., 2017). However, much less attention has been paid to PDE1. There are three isoforms of PDE1: A, B, and C. PDE1A and PDE1B have a substrate preference for cGMP, and PDE1C has equal affinity for cGMP and 3′, 5′-cyclic adenosine monophosphate (cAMP). PDE1 isozymes are unique among PDEs, in that they are activated by calcium-calmodulin (Maurice et al., 2014), and this may be critical in the context of hypertension featuring enhanced calcium signaling (Pinterova et al., 2011). Finally, genome-wide association studies (GWAS) have reported an association between PDE1A snp and blood pressure (Tragante et al., 2014; Bautista Nino et al., 2015). While the role of PDE1 in vascular reactivity has been highlighted in several papers, systematic research employing potent and selective PDE1 inhibitors in animal models of hypertension is lacking.

In this manuscript, we presented a novel and potent PDE1 inhibitor BTTQ that is highly selective for PDE1 over all other phosphodiesterases, but equipotent for all isoforms of PDE1 (A, B and C). This compound possesses absorption, distribution, metabolism, excretion (ADME) characteristics, allowing its use *in vivo* (**Figure 2C** and **Supplementary Table 3**). BTTQ demonstrated blood pressure (BP) lowering effects in both normotensive rats and animals with hypertension of different genesis (SHR, a high renin model, and Dahl salt-sensitive hypertension, a low renin model) suggesting the pattern of activity independent of the primary mechanisms of hypertension. Moreover, additional BP lowering could be achieved when BTTQ was administered on top of ACE inhibitor lisinopril, a current standard of care in the treatment of hypertension. These anti-hypertensive effects are likely associated with vasodilatory properties of BTTQ that we have demonstrated *in vitro*, using isolated mesenteric arteries, and *in vivo*, using novel PK/PD model.

MATERIALS AND METHODS

Animals

The animal care and experimental protocols in this study were conducted under the supervision of a veterinarian following a protocol reviewed and approved by the Eli Lilly and Company's Animal Care and Use Committees or by the IACUC at the Medical College of Wisconsin. The procedures in this protocol are in compliance with the U.S. Department of Agriculture's (USDA) Animal Welfare Act (9 CFR Parts 1, 2, and 3); the Guide for the Care and Use of Laboratory Animals (Institute for Laboratory Animal Research, The National Academies Press, Washington, DC, United States); and the National Institutes of Health, Office of Laboratory Animal Welfare (for NIH funded studies). Whenever possible, procedures in this study are designed to avoid or minimize discomfort, distress, and pain to animals. All the rats used in this study were between 6 and 8 weeks for the SD, SHR, and Dahl Salt sensitive rats studies.

Generation of PDE Proteins

All PDE proteins were expressed in baculoviral infected insect cells using standard methods [pFastBac, pFastBac Dual (Invitrogen), pIEX4 (Novagen)]. See **Supplementary Table 1** for DNA sequences, construct boundaries, affinity tags, and expression vectors. HIS_6 tagged PDE proteins were purified using Ni-NTA agarose (Qiagen) followed by size exclusion chromatography on a Superdex 200 column (GE Healthcare) in storage buffer (20 mM Tris-HCl, pH 7.5, 150 mM NaCl, 10% Glycerol). FLAG-tagged PDE proteins including the PDE6A/6B heterodimer were purified using anti-FLAG M2-agarose (Sigma-Aldrich), after purification through NiNTA column chromatography and eluted in storage buffer (50 mM Tris-HCl, pH 7.5, 150 mM NaCl, 10% Glycerol, 0.1 mg/ml Flag peptide). All purified proteins were stored at −80°C in small aliquots.

Phosphodiesterase Enzyme Assays

All PDE enzyme activities were measured with a yittrium silicate based scintillation proximity assay that detects radioactive nucleotide monophosphates but not cyclic monophosphates. Assays are conducted in a total volume of 50 μl in 384 well plates (3706, Corning): comprised of 24 μl enzyme, 1 μl compound, and 25 μl of cyclic nucleotide. The general assay buffer consists of 50 mM Tris-HCl (pH 7.5) and 0.1% (w/v) bovine serum albumin (Fatty Acid Free, Sigma-Aldrich). Enzyme concentrations, substrate concentrations, and various PDE-specific buffer additives are described in **Supplementary Table 1**. Compounds to be tested are diluted in pure dimethyl sulfoxide (DMSO) using 10-point concentration-response curves, and 1 μl is acoustically dispensed into assay plates using the Echo555 (LabCyte). Maximal compound concentration in the reaction mixture is either 10 or 100 μM. Compounds at the appropriate concentration are pre-incubated with either of the PDE enzymes for 30 min before the reaction is started by the addition of substrate ([8-^{3}H]-cAMP, 20.7 Ci/mmol or [8-^{3}H]-cGMP; 6.5 Ci/mmol, Perkin Elmer). Reactions are allowed to proceed for

60 min at room temperature before quenching. Next, reactions are stopped by the addition of 400 μg/per well SPA beads (RPNQ0150, Perkin Elmer) and a potent non-selective PDE inhibitor to quench the reaction. Bead bound radioactivity (product) is quantified 12 h later a Microbeta counter (Perkin Elmer). Data is normalized to % inhibition using standard methods (Campbell et al., 2004), and IC_{50} values were plotted using PRISM (GraphPad Software) using the 4 parameter logistic equation (Campbell et al., 2004). Data for potency values are expressed as the geometric mean and arithmetic standard deviation.

Rat Telemetry Studies

Male Sprague Dawley (Taconic Biosciences) rats, Spontaneous Hypertensive rats (Charles River Laboratories, United States), and Dahl Salt Sensitive rats (Medical College of Wisconsin) were implanted with transmitters (HD S10; Data Science International) for collection of BP and heart rate (HR) data. The transmitters are capable of transmitting a BP signal via a pressure catheter inserted into the abdominal aorta. Initially, a baseline was established and recorded. Each rat was then removed from its recording cage and was dosed by p.o. gavage with vehicle or compound and the animals were then returned to the recording cage. Data sampling for BP and HR was carried out in intervals at selected time points for the duration of the experiment.

Rat Ear Temperature

Male Sprague Dawley rats at 6 to 7 weeks were dosed orally by p.o. gavage with different doses of BTTQ formulated in 1% hydroxyethlycellulose (Dow Corning, Midland, MI, United States) (w/v), 0.25% polysorbate 80 (Sigma-Aldrich, St. Louis, MO, United States) (v/v), and 0.05% antifoam (v/v; Dow Corning, Midland, MI, United States) in purified water. Following dosing, ear temperature was measured by using a k-type thermocouple probe digital thermometer (Cole Parmer) every hour for 6 h and then at 24 h. Blood samples for plasma exposure measurement were obtained at the same time. Blood was collected via a tail snip directly into a 20-μL EDTA-coated capillary and immediately spotted onto a Whatman DMPK-C DBS card (GE Healthcare Bio-Sciences). Tail snips were performed by removing approximately 1 mm of the tail by using a scalpel. Blood flow was initiated by gentle squeezing of the tail. No analgesia or anesthesia was used during blood collections. A single sample and spot were collected per time point. The DBS cards were allowed to dry for approximately 2 h at room temperature, after which the cards were placed in a zip-top bag, stored, and shipped at ambient temperature.

Studies in Isolated Vascular Segments (Myography Study)

For studies of the mesenteric arteries, rats were anesthetized using 5% isoflurane gas followed by euthanasia by secondary method. Small mesenteric arteries (∼300-μm internal diameter, 350-μm external diameter) supplying the small intestine were carefully excised under a dissecting microscope (Leica; Buffalo, NY, United States) and immersed in a cold physiological salt solution having the following ionic composition (in mM): NaCl (119.0), KCl (4.7), $CaCl_2$ (1.6), NaH_2PO_4 (1.18), $MgSO_4$ (1.17), $NaHCO_3$ (24.0), D-glucose (5.5), and EDTA (0.03). The arteries were cannulated at the proximal and distal ends using glass micropipettes. The vessels were equilibrated with a 21% O_2, 5% CO_2, 74% N_2 gas mixture at 37°C in the physiological salt solution for 30 min. The intraluminal pressure was maintained at 80 mmHg to approximate *in vivo* conditions, and the internal diameter of the artery was measured using television microscopy. Responses to vasodilator stimuli (different BTTQ concentrations) were determined in arteries precontracted with 10 μM phenylephrine (PE) and expressed as % increase from basal (PE-precontracted) diameter. Responses of the mesenteric arteries to the endothelium-dependent vasodilator agonist acetylcholine (ACh) were evaluated in SS rats fed a high salt diet (4% NaCl) for 3 weeks and treated with BTTQ (3 mg/kg) p.o. gavage twice daily or vehicle.

Western Blot

Heart, aorta, and mesenteric artery samples collected from SS rats were pulse sonicated in Laemmli buffer with a protease inhibitor cocktail (Roche, Basel, Switzerland). The homogenates were centrifuged at 1000 *g* for 15 min at +4°C and sediment was discarded. The resulting supernatant was separated on SDS-PAGE, then transferred onto nitrocellulose membrane (Millipore, Bedford, MA, United States) and probed with PDE1 antibody (1:500, Thermoscintific Fisher, Invitrogen, Cat# PA5-87915), and subsequently visualized by enhanced chemiluminescence (Amersham Biosciences, Inc., Piscataway, NJ, United States).

Statistical Analysis

All data in this manuscript were presented as mean ± SEM with a significance level of $p < 0.05$, and n represents the number of individual animals. The significance of differences in concentration-response curves in the ear temperature and, myograft study were calculated using *t*-test, compare to the vehicle group. The EC_{50} was calculated using GraphPad Prism 8.3 using a 4-parameter logistic non-linear curve fit model. Single-dose rat telemetry data for normal and SHR rats and repeat-dose telemetry data in Dahls salt-sensitive rats were analyzed by two-way repeated measures ANOVA. Treatment group main effects were compared by Tukey's HSD method. All telemetry data were analyzed with GraphPad Prism 8.3.

RESULTS

Identification of a Selective PDE1 Inhibitor

In effort to generate a selective PDE1 inhibitor we synthesized the compound 1-[1,1′-**bi**(cyclopropyl)-1-yl]-5-(cyclopropylmethyl)-6,7,8,9-**t**etrahydro[1,2,4]**t**riazolo[4,3-A]**q**uinoxaline-4(5H)-one that we refer to hereafter as BTTQ. We tested BTTQ against all human and some rat recombinant PDE enzymes using a radioactivity-based enzyme activity assay. BTTQ inhibited all

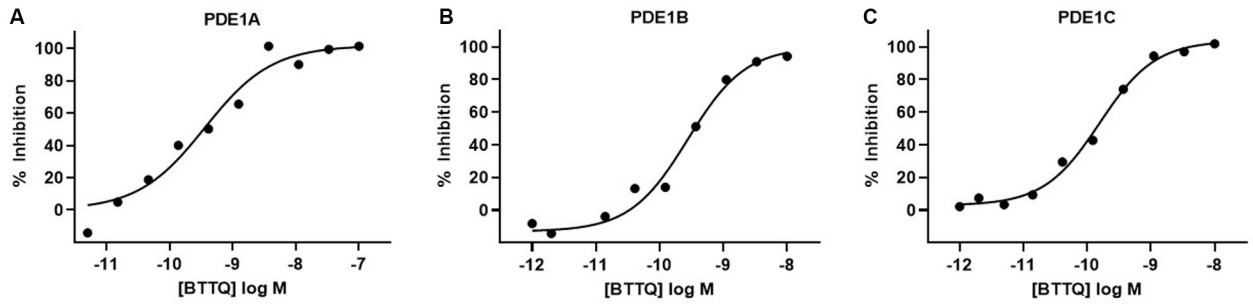

FIGURE 1 | Inhibition of PDE1 enzyme activity by BTTQ. The compound was pre-incubated with different recombinant PDE1 isoforms for 30 min before the addition of the substrate. After incubating at room temperature for 60 min, reactions were stopped by the addition of SPA beads. cAMP level was measured after 12 h. IC_{50} values of PDE1A **(A)**, PDE1B **(B)**, and PDE1C **(C)** were calculated by plotting the normalized data vs. log [compound] and fitting the data using a four-parameter logistic equation.

three isoforms of PDE1 with very comparable half-maximal inhibitory concentrations (IC_{50}) (1, 0.5, and 0.2 nM for PDE1A, PDE1B, and PDE1C, respectively; **Figures 1A–C**), while other PDEs were only affected at high μM concentrations (**Table 1**). To ensure that BTTQ retains inhibition against rat PDE enzymes, we also tested rat PDE1B and PDE3A, which had respective IC_{50} values of 1 nM and inactive.

Inhibition of PDE1 Caused Vasodilation in Normal Rats

To assess the role of PDE1 inhibition on vasodilation, normal Sprague Dawley (SD) rats were administered orally, a single dose of BTTQ at 0.03, 0.1, 0.3, 1, or 3 mg/kg and ear temperature was measured. The ear temperature method was used to test if vasodilation caused by PDE1 inhibition would increase the blood flow in the rat ear arteriole that would subsequently increase the surface temperature. Indeed, there was a significant rapid increase of ear temperature observed as high as 14% at the highest dose of 3 mg/kg within 1 h compared to the vehicle control, as shown in **Figure 2A**. A significant dose-dependent increase in ear temperature was observed at 0.1, 0.3, and 1 mg/kg. The dose-dependent increase in ear temperature stayed significant for up to 3 h and returned to baseline for all doses at 6 h. The pharmacokinetic analysis revealed a dose-dependent increase in plasma concentration of BTTQ that maintained for several hours after oral administration (**Figure 2C** and **Supplementary Table 2**) with a half-life of almost 4 h. The calculated percent target engagement based on the unbound drug concentration and with hill slope of 1 demonstrated about 65% target engagement (TE) at the lowest dose at 1 h and saturated after 0.3 mg/kg (**Table 2**). At this level of target engagement, the median effective dose (ED_{50}) was 0.14 mg/kg as calculated using four parametric logistic equation (**Figure 2B**).

TABLE 1 | Inhibition of PDE enzyme activity by BTTQ.

BTTQ	IC_{50} nM (SD, *n*)
Human PDE enzymes	
PDE1A	1.0 (0.8, *n* = 14)
PDE1B	0.45 (0.2, *n* = 4)
PDE1C	0.14 (0.3, *n* = 3)
PDE2A	>10,000 (*n* = 2)
PDE3A	>100,000 (*n* = 8)
PDE4D	12,000 (1000, *n* = 3)
PDE5A	>10,000 (*n* = 3)
PDE6A/6B	>10,000 (*n* = 4)
PDE7B	1600 (800, *n* = 2)
PDE8A	>10,000 (*n* = 2)
PDE9A	>10,000 (*n* = 2)
PDE10A	>10,000 (*n* = 2)
PDE11A	2,400 (800, *n* = 2)
Rat PDE enzymes	
PDE1B	1.0 (*n* = 1)
PDE3A	>100,000 (*n* = 1)

PDE1 Inhibition Lowered Blood Pressure in Normal Sprague Dawley, Spontaneously Hypertensive, and Dahl Salt Sensitive Rats

To evaluate the hemodynamic effect of PDE1 inhibition in normal animals, BTTQ was administered in freely moving Sprague Dawley (SD) rats. They were dosed at 1 and 3 mg/kg twice daily via oral gavage, and the data was captured every hour for 24 h with telemetry. As shown in **Figure 3A**, there was a significant reduction in the mean arterial pressure (MAP), with a concomitant increase in heart rate (**Figure 3B**) compared to the vehicle-treated group. An immediate decrease of about 5 mmHg in MAP has been observed in both groups within 1 h of the first dose compared to the vehicle. In general, the BP-lowering effect sustained longer in the high dose group and returned to baseline post 7 h of the second dose. A dose-dependent increase in heart rate was observed, which showed a trend to return to baseline within the time of measurement.

The significant hemodynamic effect of PDE1 inhibition, as seen in the normal rats suggested that inhibition of PDE1 might be beneficial in the context of hypertension. In order to test this, SHR rats were dosed orally with 0.03, 0.1, 0.3, 1, and 3 mg/kg twice daily, and cardiovascular parameters were recorded for

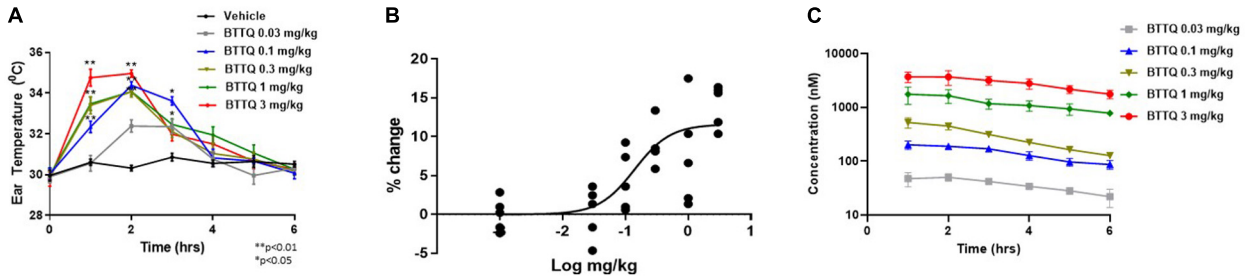

FIGURE 2 | Effect of BTTQ on ear temperature in rats. Sprague Dawley rats were orally dosed with 0.03, 0.1, 0.3, 1, or 3 mg/kg of BTTQ and the temperature of the pinnae was measured with a K-probe thermometer every hour for 6 h after dosing. Ear temperature was plotted against time **(A)**, and median effective dose (ED_{50}) was calculated using four parametric logistic equation during 1 h time point **(B)**. Data are given as mean ± SEM ($N = 5$). Data represent the mean of group average with $n = 5$ and the p-value calculated using one-way ANOVA compared to the vehicle group. **(C)** Pharmacokinetic profile of BTTQ. Plasma concentrations of BTTQ were determined after a single oral administration of 0.03, 0.1, 0.3, 1, and 3 mg/kg of the compound to Sprague Dawley rats. Data are given as mean ± SEM ($N = 5$). *$p < 0.05$, one way anova; **$p < 0.005$, one way anova.

TABLE 2 | Target engagement by BTTQ.

Dose	IC_{50}	Unbound compound concentration (nM)	% TE
0.03	1.37	2.52	64.78
0.1		10.6	88.55
0.3		27.7	95.29
1		92.5	98.54
3		197	99.31

24 h with telemetry. As shown in **Figure 4A**, a dose-dependent decrease in the MAP was observed. The lowest dose of 0.03 mg/kg did not show any effect in both BP and HR in SHR. The magnitude of BP-lowering effect was much greater in SHR rats compared to normal rats when compared at the same dose level. A dose-dependent increase in heart rate was also evident in SHR rats (**Figure 4B**) with a relatively greater magnitude compared to SD rats within the same dose level.

To test the anti-hypertensive effect of the PDE1 inhibitor over a longer duration in a model of salt-induced hypertension, Dahl SS rats were dosed orally with BTTQ (3 mg/kg twice daily) for 21 days while keeping them on a high salt (4%) diet. There was a profound reduction in the MAP in the PDE1 inhibitor group compared to the vehicle-treated group (**Figure 5A**), which was accompanied by elevation of heart rate (**Figure 5B**).

In clinic, ACE inhibitors are used as a standard of care for hypertensive patients. In order to evaluate the additive effect of PDE1 inhibitor with ACE inhibitor, SHR rats were orally dosed (twice daily) either with 3 mg/kg enalapril alone or in combination with 0.3 mg/kg of BTTQ and cardiovascular parameters were recorded for 24 h. As expected, enalapril lowered the MAP by 13% without affecting the heart rate (**Figure 6**). The co-administration of PDE1 on top of enalapril similarly lowered MAP by almost 30% (**Figure 6A**) with a significant increase in heart rate, which kept elevated for a long period of time (**Figure 6B**). Effects of BTTQ on systolic and diastolic blood pressure in SD, SHR, and Dahl SS rats are shown on **Supplementary Figures 1–4**.

Myography Studies in Isolated Vascular Segments

The expression of PDE1 in the wall of mesenteric artery isolated from SS rat, was confirmed using western blot technique which also revealed the abundance of PDE1 in other parts of the cardiovascular system, i.e., heart, and aorta (**Supplementary Figure 5**). The third-order mesenteric arteries from Dahl SS rats were constricted at the beginning of the experiment using 10 μM of phenylephrine, then escalating doses of PDE1 inhibitor or vehicle were added, and the inner diameter was measured after stabilization. Experiments reveal concentration-dependent relaxation in mesenteric arteries with PDE1 inhibitor compared to the vehicle treatment that reached about 92% of the initial fully relaxed diameter with 1 mM. On the contrary, the vehicle did not show a significant relaxing effect (**Figure 7**). The same set up was used to test the effect of serial concentration of acetylcholine to induce vasorelaxation on pre-constricted mesenteric artery using 10 μM of phenylephrine from Dahl SS rats that have treated through oral gavage with PDE1 inhibitor and kept on a high salt diet for 21 days, however, no significant difference between the two groups was observed (**Supplementary Figure 6**).

DISCUSSION

In this manuscript, we presented a novel, potent PDE1 inhibitor BTTQ highly selective for PDE1 over all other PDES but equipotent for all isoforms of PDE1 (A, B, and C). This compound possesses ADME characteristics allowing its use *in vivo*. BTTQ demonstrated BP-lowering effects in both normotensive rats and animals with hypertension of different genesis (SHR rat, a high renin model, and Dahl SS rat, a low renin model of salt-induced hypertension) suggesting the pattern of activity independent of primary mechanisms of hypertension. Moreover, additional BP lowering could be achieved when BTTQ was administered on top of ACE inhibitor lisinopril, a current standard of care in the treatment of hypertension. These anti-hypertensive effects are likely associated with vasodilatory properties of BTTQ that we have demonstrated *in vitro*, using

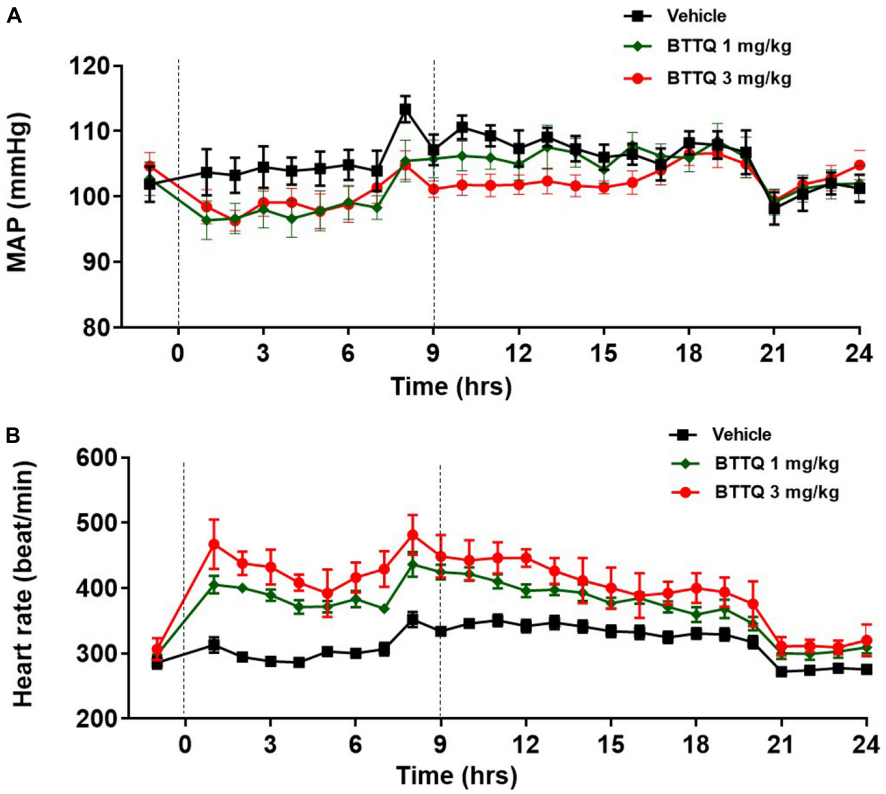

FIGURE 3 | Effect of BTTQ on the blood pressure and heart rate of SD rats. SD rats were dosed twice daily, and **(A)** mean arterial pressure (MAP), and **(B)** heart rate were recorded for 24 h with telemetry. Dotted line represents the timing of doses. All the data represented as mean ± SEM. The main effect of BTTQ treated animals is significantly different from vehicle, $p < 0.0001$ for high dose group.

isolated mesenteric arteries, and *in vivo*, using novel Pk/Pd model. Administration of BTTQ was associated with increased heart rate in both models of hypertension as well as in the normotensive rats.

PDE1 attracted interest in the context of arterial hypertension when an association of PDE1A single nucleotide polymorphism with diastolic and mean blood pressure was described in human genetics study (Tragante et al., 2014). Importantly, this association was further confirmed by a different research group in an independent cohort of patients (Bautista Nino et al., 2015). However, mechanistic experimental studies lagged behind due to the lack of potent and selective PDE1 inhibitors suitable for *in vivo* use in the animal models of disease. In a seminal conceptual study, Giachini et al. (2011) postulated the role of PDE1 in Angiotensin II-induced hypertension and vascular contraction. In this study, the authors used vinprocetin, a natural product with low potency and poor selectivity. Only relatively recently, Khammy et al. (2017) followed up with confirmatory data supported by potent and selective PDE1 inhibitors. Based on PDE gene expression data and using compounds with different affinity to PDE1 isoforms, they concluded that PDE1A inhibition was primarily responsible for this pharmacological effect.

Our current data obtained using a structurally unrelated compound further supports the critical involvement of PDE1 into the regulation of blood pressure via demonstration of therapeutic benefits in two independent rodent models of hypertension. While SHR rats share important mechanistic features with Angiotensin II infusion model, it is, arguably, more representative of human disease (Doggrell and Brown, 1998). Another animal model used in the current investigation, Dahl salt-sensitive hypertension, capitalizes on different mechanisms of blood pressure regulation (Rapp, 1982) and commonly used to study salt-induced hypertension (Palygin et al., 2017; Fehrenbach et al., 2019; Lerman et al., 2019). Our current data obtained using a structurally unrelated compound further supports the critical involvement of PDE1 into the regulation of blood pressure via demonstration of therapeutic benefits in two independent rodent models of hypertension. While SHR rats share important mechanistic features with Angiotensin II infusion model, it is, arguably, more representative of human disease (Doggrell and Brown, 1998). Another animal model used in the current investigation, Dahl salt-sensitive hypertension, capitalizes on different mechanisms of blood pressure regulation (Rapp, 1982) and commonly used to study salt-induced hypertension (Palygin et al., 2017; Fehrenbach et al., 2019; Lerman et al., 2019). Several studies have shown expression of PDE1 in the vascular wall (e.g., aorta, femoral, and mesenteric artery) of different rat strains, e.g., Wistar (Khammy et al., 2017; Laursen et al., 2017), Sprague Dawley (Giachini et al., 2011), and SHR rats (McMahon et al., 1989; Pontes et al., 2012). We also have confirmed the expression of the PDE1 in the mesenteric artery as well as other parts in the cardiovascular system (i.e., heart and aorta) of Dahl salt sensitive

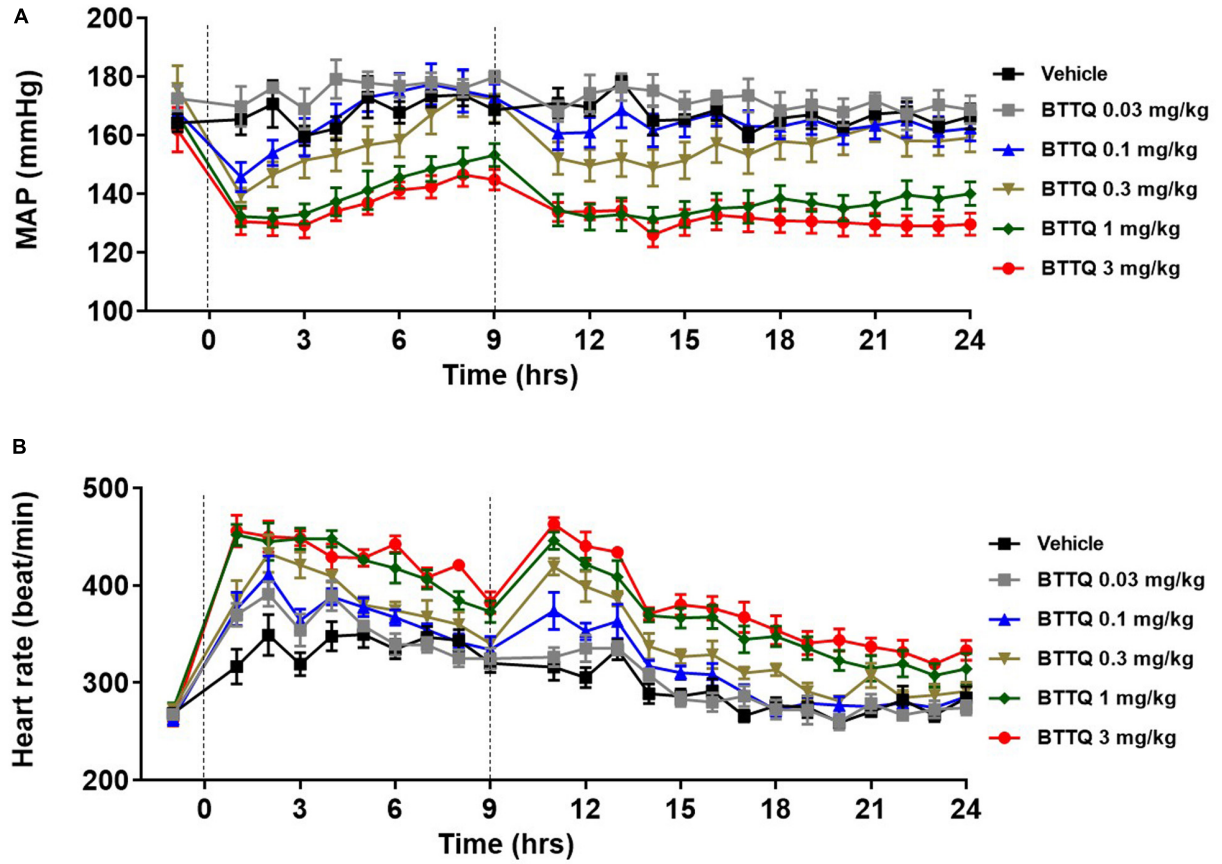

FIGURE 4 | Effect of BTTQ on the blood pressure and heart rate of SHR rats. SHR rats were dosed twice daily, and **(A)** mean arterial pressure (MAP), and **(B)** heart rate were recorded for 24 h with telemetry. Dotted line represents the timing of doses. All the data represented as mean ± SEM. The main effect of BTTQ treated animals is significantly different from the vehicle, $p < 0.0001$ for high dose group.

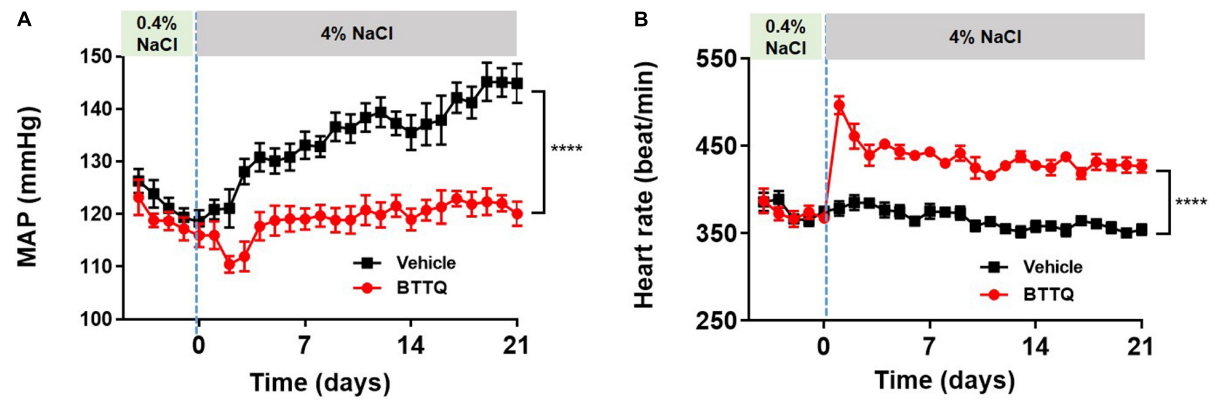

FIGURE 5 | Effect of BTTQ on the blood pressure and heart rate of Dahl SS rats. SS rats were dosed twice daily with BTTQ (3 mg/kg) through oral gavage. **(A)** Mean arterial pressure (MAP) and **(B)** heart rate were recorded with telemetry for 5 days on a normal salt diet (0.4% NaCl) and 21 days after switching the animals to a high salt diet (4% NaCl). Data represent mean ± SEM. ****p-value < 0.0001.

rats using western blot (**Supplementary Figure 5**). The fact that BTTQ was equally efficacious in both models, suggesting that PDE1 inhibition acts at the downstream signaling common for BP control regardless of the factors that initiated hypertension.

PDE1 is likely to be involved in multiple mechanisms regulating BP. Our data strongly suggest that peripheral vasodilation could play a critical role. First, we demonstrated direct dose-dependent relaxation of pre-constricted mesenteric

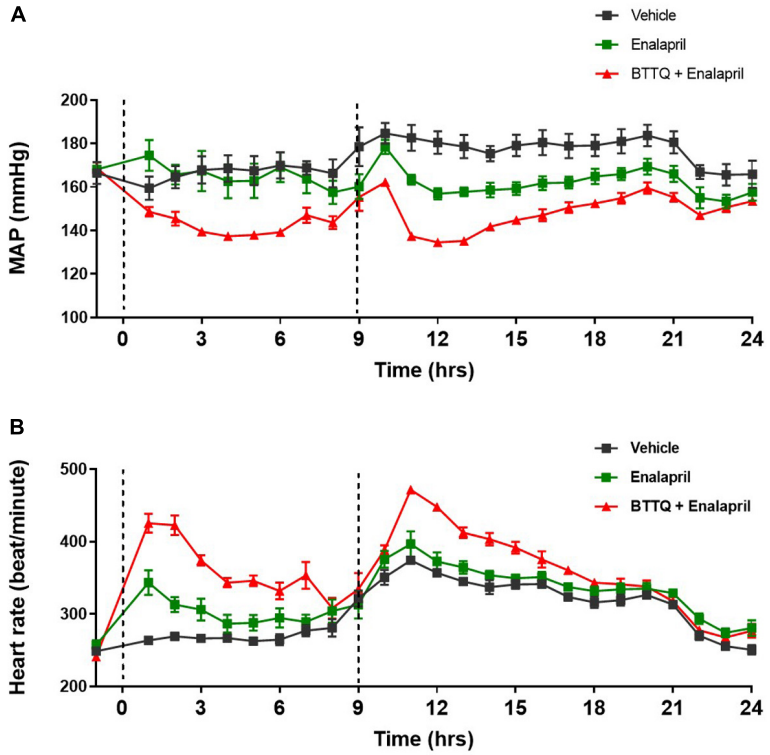

FIGURE 6 | Effect of combined BTTQ and enalapril therapy on the blood pressure and heart rate of SHR rats. SHR rats were dosed twice daily, and **(A)** mean arterial pressure (MAP), and **(B)** heart rate were recorded for 24 h with telemetry. Dotted line represents the timing of doses. All the data represented as mean ± SEM. The main effect of BTTQ + Enalapril treated animals is significantly different from enalapril alone, $p = 0.004$.

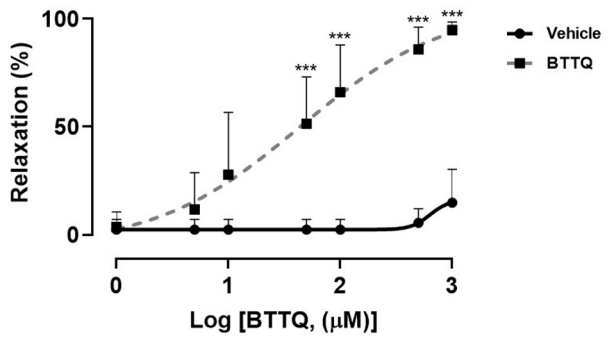

FIGURE 7 | Concentration-response curve showing the percent of relaxation of pre-constricted third-order mesenteric artery from Dahl SS rats that were on a normal diet (0.4% NaCl) in response to varying concentrations of BTTQ. Data represent mean ± SEM. ***p-value < 0.001.

arteries. Second, BTTQ increased rat ear temperature in a dose-dependent manner. This change in temperature is likely a result of increased local blood flow driven by vasodilation. Importantly, plasma levels of the compound and, hence, tissue exposure, were comparable with compound concentrations *in vitro* that induced vasodilation and exceeded the IC_{50} for PDE1A. Given that diameter of small arteries and arterioles is directly related to peripheral vascular resistance, and the latter, together with the pumping capacity of the heart and blood volume, ultimately defines BP (Mayet and Hughes, 2003), we surmise that vasodilation could be the main mechanism of the anti-hypertensive effects of PDE1 inhibitors.

Since PDE1A is the major isoform expressed in arterial SMC (Giachini et al., 2011; Khammy et al., 2017), it is highly likely that BP lowering activity of BTTQ is primarily driven by its inhibition of PDE1A. The preferred substrate of PDE1A is cGMP that is produced in vascular SMCs by nitric oxide-induced soluble guanylate cyclase or natriuretic peptide-activated particulate guanylate cyclase (Francis et al., 2010). Downstream, cGMP signaling is associated with activation of protein kinase G, ultimately leading to SMC relaxation. When PDE1 is activated, it degrades cGMP and hence impedes vasorelaxation. Interestingly, PDE1 is the only PDE activated by calcium (Maurice et al., 2014). Calcium signaling is enhanced in arterial hypertension (Pinterova et al., 2011). Therefore, it is reasonable to suggest that PDE1A activation serves as one of the major mechanisms associated with increased peripheral vascular resistance, and its inhibition would have significant therapeutic benefit. Importantly, the potential role of PDE1 in the development of Autosomal Dominant Polycystic Kidney Disease (ADPKD) was shown. It was reported that calcium- and calmodulin-dependent PDEs (PDE1A and PDE1C) and PDE3A modulate the development of PKD, possibly through the regulation of compartmentalized cAMP pools that

control cell proliferation and CFTR-driven fluid secretion (Ye et al., 2016). Pde1a mutant mice had a mild renal cystic disease and a urine concentrating defect on a wild-type genetic background and aggravated renal cystic disease on a $Pkd2^{WS25/-}$ background (Wang et al., 2017). Based on these observations it was proposed that PDE1A plays an important role in the renal pathogenesis of ADPKD and in the regulation of BP.

PDE1 inhibition, however, could also be responsible for an observed increase in heart rate. Tachycardia is not unique to BTTQ. It is likely to be the class effect since structurally unrelated PDE1 inhibitors increased heart rate in different species of experimental animals (Hashimoto et al., 2018). The precise mechanism of PDE1-induced tachycardia needs to be further investigated. However, it likely has both extracardiac and intracardiac components. The former could be a result of baroreflex, activation of sympathetic signaling induced by BP lowering (Lanfranchi and Somers, 2002) that, to some degree, is germane to any peripheral vasodilator (Pettinger and Mitchell, 1988). The latter is likely to be specifically associated with inhibition of PDE1A. Lukyanenko et al. (2016) reported that PDE1 is expressed in the rabbit sinoatrial node. While cGMP is a preferred substrate of this enzyme, PDE1 is also capable of binding to (albeit with lower affinity) and degrading cAMP. cAMP, in turn, can stimulate calcium signaling resulting in increased pacemaker activity (Lukyanenko et al., 2016). It is still unknown whether this mechanism is involved in tachycardia in the rat, and, most critically, is translatable to the human.

In general, cross-species translation remains an issue given a significant difference in the patterns of PDE1 expression in the heart. Recent studies by Hashimoto et al. (2018) demonstrated that PDE1 inhibition with ITI-214, a PDE1 inhibitor with similar potency and selectivity (Li et al., 2016), was simultaneously associated with positive inotropic effects (most likely driven by inhibition of PDE1C in cardiomyocytes) and peripheral vasodilation (most likely driven by inhibition of PDE1A in vascular SMCs). This "ino-dilation" provides intriguing prospects for PDE1 inhibitors in patients with heart failure. ITI-214 has recently completed the second dose cohort (single dose of 30 mg administered orally) a proof-of-mechanism study in patients with chronic heart failure (ClinicalTrials.gov Identifier: NCT03387215). In addition, ITI-214 has also finished Phase II clinical trial for Parkinson's disease (ClinicalTrials.gov Identifier: NCT03257046).

Despite significant improvement in patient care, resistant arterial hypertension remains an unmet medical need (Hashimoto et al., 2018). Blood pressure-lowering effects of PDE1 inhibitor BTTQ in two mechanistically distinct animal models of hypertension and activity on top of standard of care, demonstrated in the current study, suggest a potential benefit of PDE1 inhibitors for this patient population. Vasodilatory properties/reduction of peripheral vascular resistance could also be instrumental for the treatment of other diseases beyond arterial hypertension (chronic kidney disease, improvement of brain circulation, etc.).

DATA AVAILABILITY STATEMENT

All datasets generated for this study are included in the article/**Supplementary Material**.

ETHICS STATEMENT

The animal study was reviewed and approved by Eli Lilly and Company's Animal Care and Use Committees or by IACUC at the Medical College of Wisconsin.

AUTHOR CONTRIBUTIONS

AD and SK designed the study, interpreted and analyzed the data, and drafted the manuscript. JB, LP, XZ, MT, and TM performed the experiments and made the analyses. JH reviewed the statistical analysis of the data. MR, FW, AS, MK, and SA revisited it critically for important intellectual content design and manuscript preparation. CJ, KR, and MW contributed to the chemical synthesis of the BTTQ. MR conceived the project. All authors provided approval for the publication of the final manuscript.

FUNDING

This research was partially supported by the National Heart, Lung, and Blood Institute grant R35 HL135749 (to AS), and Department of Veteran Affairs I01 BX004024 (to AS).

ACKNOWLEDGMENTS

The authors would like to thank Juanjo Carrillo, Maria Cuadrado, and Enrique Jambrina for initial PDE enzymology studies. Thanks to Yuewei Qian and the LEM reagents group for the cloning and purification of PDE enzymes. They also would like to thank Mike Genin and Qing Shi for their valuable suggestions.

SUPPLEMENTARY MATERIAL

The Supplementary Material for this article can be found online at: https://www.frontiersin.org/articles/10.3389/fphys.2020.543727/full#supplementary-material

REFERENCES

Bautista Nino, P. K., Durik, M., Danser, A. H., De Vries, R., Musterd-Bhaggoe, U. M., Meima, M. E., et al. (2015). Phosphodiesterase 1 regulation is a key mechanism in vascular aging. *Clin. Sci.* 129, 1061–1075. doi: 10.1042/cs20140753

Bellamy, T. C., and Garthwaite, J. (2001). "cAMP-specific" phosphodiesterase contributes to cGMP degradation in cerebellar cells exposed

to nitric oxide. *Mol. Pharmacol.* 59, 54–61. doi: 10.1124/mol.59.1.54

Campbell, R. M., Dymshitz, J., Eastwood, B. J., Emkey, R., Greenen, D. P., Heerding, J. M., et al. (2004). "Data standardization for results management," in *Assay Guidance Manual*, eds G. S. Sittampalam, A. Grossman, K. Brimacombe, M. Arkin, D. Auld, C. P. Austin, et al. (Bethesda, MD: Eli Lilly & Company and the National Center for Advancing Translational Sciences).

Carey, R. M., Calhoun, D. A., Bakris, G. L., Brook, R. D., Daugherty, S. L., Dennison-Himmelfarb, C. R., et al. (2018). Resistant hypertension: detection, evaluation, and management: a scientific statement from the american heart association. *Hypertension* 72, e53–e90.

Corbin, J. D. (2004). Mechanisms of action of PDE5 inhibition in erectile dysfunction. *Int. J. Impot. Res.* 16(Suppl. 1), S4–S7.

Doggrell, S. A., and Brown, L. (1998). Rat models of hypertension, cardiac hypertrophy and failure. *Cardiovasc. Res.* 39, 89–105. doi: 10.1016/s0008-6363(98)00076-5

Fehrenbach, D. J., Abais-Battad, J. M., Dasinger, J. H., Lund, H., and Mattson, D. L. (2019). Salt-sensitive increase in macrophages in the kidneys of Dahl SS rats. *Am. J. Physiol. Renal Physiol.* 317, F361–F374.

Francis, S. H., Busch, J. L., Corbin, J. D., and Sibley, D. (2010). cGMP-dependent protein kinases and cGMP phosphodiesterases in nitric oxide and cGMP action. *Pharmacol. Rev.* 62, 525–563. doi: 10.1124/pr.110.002907

Giachini, F. R., Lima, V. V., Carneiro, F. S., Tostes, R. C., and Webb, R. C. (2011). Decreased cGMP level contributes to increased contraction in arteries from hypertensive rats: role of phosphodiesterase 1. *Hypertension* 57, 655–663. doi: 10.1161/hypertensionaha.110.164327

Hashimoto, T., Kim, G. E., Tunin, R. S., Adesiyun, T., Hsu, S., Nakagawa, R., et al. (2018). Acute enhancement of cardiac function by phosphodiesterase Type 1 inhibition. *Circulation* 138, 1974–1987. doi: 10.1161/circulationaha.117.030490

Khammy, M. M., Dalsgaard, T., Larsen, P. H., Christoffersen, C. T., Clausen, D., Rasmussen, L. K., et al. (2017). PDE1A inhibition elicits cGMP-dependent relaxation of rat mesenteric arteries. *Br. J. Pharmacol.* 174, 4186–4198. doi: 10.1111/bph.14034

Kitt, J., Fox, R., Tucker, K. L., and Mcmanus, R. J. (2019). New approaches in hypertension management: a review of current and developing technologies and their potential impact on hypertension care. *Curr. Hypertens. Rep.* 21:44.

Lanfranchi, P. A., and Somers, V. K. (2002). Arterial baroreflex function and cardiovascular variability: interactions and implications. *Am. J. Physiol. Regul. Integr. Comp. Physiol.* 283, R815–R826.

Laursen, M., Beck, L., Kehler, J., Christoffersen, C. T., Bundgaard, C., Mogensen, S., et al. (2017). Novel selective PDE type 1 inhibitors cause vasodilatation and lower blood pressure in rats. *Br. J. Pharmacol.* 174, 2563–2575. doi: 10.1111/bph.13868

Lerman, L. O., Kurtz, T. W., Touyz, R. M., Ellison, D. H., Chade, A. R., Crowley, S. D., et al. (2019). Animal models of hypertension: a scientific statement from the american heart association. *Hypertension* 73, e87–e120.

Li, P., Zheng, H., Zhao, J., Zhang, L., Yao, W., Zhu, H., et al. (2016). Discovery of potent and selective inhibitors of phosphodiesterase 1 for the treatment of cognitive impairment associated with neurodegenerative and neuropsychiatric diseases. *J. Med. Chem.* 59, 1149–1164. doi: 10.1021/acs.jmedchem.5b01751

Lukyanenko, Y. O., Younes, A., Lyashkov, A. E., Tarasov, K. V., Riordon, D. R., Lee, J., et al. (2016). Ca(2+)/calmodulin-activated phosphodiesterase 1A is highly expressed in rabbit cardiac sinoatrial nodal cells and regulates pacemaker function. *J. Mol. Cell Cardiol.* 98, 73–82. doi: 10.1016/j.yjmcc.2016.06.064

Maurice, D. H., Ke, H., Ahmad, F., Wang, Y., Chung, J., and Manganiello, V. C. (2014). Advances in targeting cyclic nucleotide phosphodiesterases. *Nat. Rev. Drug Discov.* 13, 290–314.

Mayet, J., and Hughes, A. (2003). Cardiac and vascular pathophysiology in hypertension. *Heart* 89, 1104–1109. doi: 10.1136/heart.89.9.1104

McMahon, E. G., Palomo, M. A., Mehta, P., and Olins, G. M. (1989). Depressor and natriuretic effects of M&B 22,948, a guanosine cyclic 3',5'-monophosphate-selective phosphodiesterase inhibitor. *J. Pharmacol. Exp. Ther.* 251, 1000–1005.

Muñoz-Durango, N., Fuentes, C. A., Castillo, A. E., González-Gómez, L. M., Vecchiola, A., Fardella, C. E., et al. (2016). Role of the renin-angiotensin-aldosterone system beyond blood pressure regulation: molecular and cellular mechanisms involved in end-organ damage during arterial hypertension. *Int. J. Mol. Sci.* 17:797. doi: 10.3390/ijms17070797

Palygin, O., Levchenko, V., Ilatovskaya, D. V., Pavlov, T. S., Pochynyuk, O. M., Jacob, H. J., et al. (2017). Essential role of Kir5.1 channels in renal salt handling and blood pressure control. *JCI Insight* 2:e92331.

Pettinger, W. A., and Mitchell, H. C. (1988). Side effects of vasodilator therapy. *Hypertension* 11, II34–II36.

Pinterova, M., Kunes, J., and Zicha, J. (2011). Altered neural and vascular mechanisms in hypertension. *Physiol. Res.* 60, 381–402. doi: 10.33549/physiolres.932189

Pontes, L. B., Antunes, F., Sudo, R. T., Raimundo, J. M., Lima, L. M., Barreiro, E. J., et al. (2012). Vasodilatory activity and antihypertensive profile mediated by inhibition of phosphodiesterase type 1 induced by a novel sulfonamide compound. *Fund. Clin. Pharmacol.* 26, 690–700. doi: 10.1111/j.1472-8206.2011.00999.x

Rapp, J. P. (1982). Dahl salt-susceptible and salt-resistant rats. A review. *Hypertension* 4, 753–763. doi: 10.1161/01.hyp.4.6.753

Tragante, V., Barnes, M. R., Ganesh, S. K., Lanktree, M. B., Guo, W., Franceschini, N., et al. (2014). Gene-centric meta-analysis in 87,736 individuals of European ancestry identifies multiple blood-pressure-related loci. *Am. J. Hum. Genet.* 94, 349–360.

Turko, I. V., Ballard, S. A., Francis, S. H., and Corbin, J. D. (1999). Inhibition of cyclic GMP-binding cyclic GMP-specific phosphodiesterase (Type 5) by sildenafil and related compounds. *Mol. Pharmacol.* 56, 124–130. doi: 10.1124/mol.56.1.124

Wang, X., Yamada, S., Lariviere, W. B., Ye, H., Bakeberg, J. L., and Irazabal, M. V. (2017). Generation and phenotypic characterization of Pde1a mutant mice. *PLoS One* 12:e0181087. doi: 10.1371/journal.pone.0181087

Ye, H., Wang, X., Sussman, C. R., Hopp, K., Irazabal, M. V., Bakeberg, J. L., et al. (2016). Modulation of polycystic kidney disease severity by phosphodiesterase 1 and 3 subfamilies. *J Am Soc Nephrol* 27, 1312–1320. doi: 10.1681/asn.2015010057

Conflict of Interest: MR, JB, CJ, TM, and MW were employed by the company Eli Lilly and Company.

The remaining authors declare that the research was conducted in the absence of any commercial or financial relationships that could be construed as a potential conflict of interest.

frontiers in Physiology

ORIGINAL RESEARCH
published: 18 September 2020
doi: 10.3389/fphys.2020.566403

Treatment With Gemfibrozil Prevents the Progression of Chronic Kidney Disease in Obese Dahl Salt-Sensitive Rats

*Corbin A. Shields[1], Bibek Poudel[1], Kasi C. McPherson[1], Andrea K. Brown[1], Ubong S. Ekperikpe[1], Evan Browning[1], Lamari Sutton[1], Denise C. Cornelius[1,2] and Jan M. Williams[1]**

[1] Department of Experimental Therapeutics and Pharmacology, University of Mississippi Medical Center, Jackson, MS, United States, [2] Department of Emergency Medicine, University of Mississippi Medical Center, Jackson, MS, United States

Recently, we reported that Dahl salt-sensitive leptin receptor mutant (SS^{LepR}mutant) rats exhibit dyslipidemia and renal lipid accumulation independent of hyperglycemia that progresses to chronic kidney disease (CKD). Therefore, in the current study, we examined the effects of gemfibrozil, a lipid-lowering drug (200 mg/kg/day, orally), on the progression of renal injury in SS and SS^{LepR}mutant rats for 4 weeks starting at 12 weeks of age. Plasma triglyceride levels were markedly elevated in the SS^{LepR}mutant strain compared to SS rats (1193 ± 243 and 98 ± 16 mg/day, respectively). Gemfibrozil treatment only reduced plasma triglycerides in the SS^{LepR}mutant strain (410 ± 79 mg/dL). MAP was significantly higher in the SS^{LepR}mutant strain vs. SS rats at the end of the study (198 ± 7 vs. 165 ± 7 mmHg, respectively). Administration of gemfibrozil only lowered MAP in SS^{LepR}mutant rats (163 ± 8 mmHg). During the course of the study, proteinuria increased to 125 ± 22 mg/day in SS rats. However, proteinuria did not change in the SS^{LepR}mutant strain and remained near baseline (693 ± 58 mg/day). Interestingly, treatment with gemfibrozil increased the progression of proteinuria by 77% in the SS^{LepR}mutant strain without affecting proteinuria in SS rats. The renal injury in the SS^{LepR}mutant strain progressed to CKD. Moreover, the kidneys from SS^{LepR}mutant rats displayed significant glomerular injury with mesangial expansion and increased renal lipid accumulation and fibrosis compared to SS rats. Treatment with gemfibrozil significantly reduced glomerular injury and lipid accumulation and improved renal function. These data indicate that reducing plasma triglyceride levels with gemfibrozil inhibits hypertension and CKD associated with obesity in SS^{LepR}mutant rats.

Keywords: obesity, renal injury, SS rat, SS^{LepR}mutant rat, lipid accumulation, gemfibrozil

OPEN ACCESS

Edited by:
Jennifer Sullivan, Augusta University, United States

Reviewed by:
Tengis Pavlov, Henry Ford Health System, United States
Alexander Staruschenko, Medical College of Wisconsin, United States

***Correspondence:**
Jan M. Williams
jmwilliams5@umc.edu

Specialty section:
This article was submitted to Renal and Epithelial Physiology, a section of the journal Frontiers in Physiology

Received: *27 May 2020*
Accepted: *27 August 2020*
Published: *18 September 2020*

Citation:
Shields CA, Poudel B, McPherson KC, Brown AK, Ekperikpe US, Browning E, Sutton L, Cornelius DC and Williams JM (2020) Treatment With Gemfibrozil Prevents the Progression of Chronic Kidney Disease in Obese Dahl Salt-Sensitive Rats. Front. Physiol. 11:566403. doi: 10.3389/fphys.2020.566403

INTRODUCTION

The incidence of obesity has increased considerably within the last decade and is now considered an independent risk factor for chronic kidney disease (CKD) (Chagnac et al., 2000; Bosma et al., 2004; Ejerblad et al., 2006; Hsu et al., 2006; Jacobs et al., 2010). One of the hallmark characteristics of obesity is dyslipidemia

(National Cholesterol Education Program Expert Panel on Detection Evaluation, and Treatment of High Blood Cholesterol in Aults, 2002; Huang, 2009). Moreover, the presence of dyslipidemia has been associated with a greater risk for the development of CKD (Kasiske et al., 1993; Guijarro and Keane, 1996; Keane, 2000). In support of this finding, preclinical studies have demonstrated similar results, in which glomerular injury and tubulointerstitial damage were markedly increased in the setting of dyslipidemia (McPherson et al., 2016, 2020). We have previously reported that the obese Dahl salt-sensitive leptin receptor mutant (SS^{LepR}mutant) rat develops dyslipidemia, progressive proteinuria, and glomerular injury as early as 6 weeks of age independent of hyperglycemia and elevations in arterial pressure (McPherson et al., 2016, 2020). Moreover, the kidneys from SS^{LepR}mutant rats displayed lipid accumulation, which is one of the most common characteristics of renal disease associated with obesity at this same time period (McPherson et al., 2020). Previous studies have provided evidence that renal lipid accumulation leads to structural and functional changes in glomeruli and tubules that lead to proteinuria and renal dysfunction (Foster et al., 2011; Straub et al., 2013; de Vries et al., 2014; DeZwaan-McCabe et al., 2017; Praga and Morales, 2017; Jonker et al., 2018). Additionally, lipid accumulation in the kidney contributes to oxidative stress, inflammation, and fibrosis (Yang et al., 2017), in which all of these processes contribute to the development of CKD. Recently, we observed that plasma triglyceride levels were substantially higher in the SS^{LepR}mutant strain compared to their lean wild-type counterparts (McPherson et al., 2016, 2020), which was linked to alterations in various lipid transporters that may have led to significant renal lipid accumulation in the SS^{LepR}mutant strain during the development of CKD (McPherson et al., 2020). However, it remains to be determined whether the increased triglyceride levels contribute to the progression of renal disease in the SS^{LepR}mutant strain.

Lipid-lowering drugs are commonly administered to patients suffering from various forms of CKD with dyslipidemia (Kasiske, 1998). However, the link between dyslipidemia and the progression of renal disease has been inconsistent and determining the role of dyslipidemia as a mediator of CKD remains unclear (Samuelsson et al., 1997; Hadjadj et al., 2004; Dalrymple and Kaysen, 2008; Rahman et al., 2008; Kaysen, 2009; Navaneethan et al., 2009; Chawla et al., 2010). While the statins are more effective in reducing plasma cholesterol concentration, the fibrates are more successful in decreasing the levels of triglycerides. However, one of the major disadvantages of fibrates is that this class of drugs can lead to a reduction in renal function by potentially inhibiting the synthesis of vasodilatory prostaglandins (Wilson et al., 1995; Ledwith et al., 1997). One of the fibrates in particular, gemfibrozil, appears to be free of this renal dysfunction effect (Broeders et al., 2000). Therefore, the objective of the current study was to examine the effects of gemfibrozil treatment on the progression of renal injury and CKD in SS^{LepR}mutant rats. We hypothesized that treatment with gemfibrozil would decrease plasma triglyceride levels, reduce renal lipid accumulation, and prevent the progression of CKD in the obese SS^{LepR}mutant strain.

MATERIALS AND METHODS

General

Experiments were performed on a total of 54 female and male SS and SS^{LepR}mutant rats at 12 weeks of age. SS and SS^{LepR}mutant strains were obtained from our in-house colony of heterozygous SS^{LepR}mutant rats, which were created using zinc-finger nuclease technology as previously described (McPherson et al., 2016). Genotyping was performed by the Molecular and Genomics Facility at the University of Mississippi Medical Center. The SS^{LepR}mutant rat develops renal injury associated with obesity without hyperglycemia (McPherson et al., 2016, 2020). We pooled a small number of female SS and SS^{LepR}mutant rats with the male rats in the current study, since the female rats display a similar susceptibility to renal injury as their male counterparts from our colony, which is highlighted in **Table 1**. Food and water were provided *ad libitum* throughout the study. Rats were maintained on a 1% NaCl diet (TD8640; Harlan Laboratories, Madison, WI, United States) at wean. The rats were housed in the Laboratory Animal Facility at the University of Mississippi Medical Center was approved by the American Association for the Accreditation of Laboratory Animal Care, and all protocols were approved by the University of Mississippi Medical Center Institutional Animal Care and Use Committee.

Protocol 1: Comparison of body weight, blood glucose, arterial pressure, and proteinuria in female and male SS and SS^{LepR}mutant rats. Experiments were performed on 12–14 week-old female and male SS and SS^{LepR}mutant rats. The rats were weighed and placed in metabolic cages for an overnight urine collection to determine proteinuria using the Bradford method (Bio-Rad Laboratories; Hercules, CA, United States), and a blood sample was collected from the tail vein for the measurement of blood glucose levels (glucometer from Bayer HealthCare; Mishawaka, IN, United States). Mean arterial pressure (MAP) was measured in conscious animals via the tail-cuff method (MC4000 BP Analysis System, Hatteras Instruments, Cary, NC, United States). One week prior to measuring MAP the rats were trained and adapted to restraint for 15–25 min for 3 sequential days, and MAP was measured at the same time of day. These experiments were performed to justify that female SS^{LepR}mutant

TABLE 1 | Comparison of metabolic and cardiovascular parameters in female and male Dahl salt-sensitive (SS) and SS leptin receptor mutant (SS^{LepR}mutant) rats between 12 and 14 weeks of age.

Metabolic parameters	SS		SS^{LepR}mutant	
	Female	Male	Female	Male
Body weight (g)	210 ± 3	347 ± 5$^{\#}$	392 ± 4†	471 ± 15$^{\dagger\#}$
Glucose (mg/dL)	96 ± 4	102 ± 6	104 ± 4	100 ± 4
MAP (mmHg)	135 ± 5	133 ± 6	132 ± 17	147 ± 13
Proteinuria (mg/day)	41 ± 6	94 ± 19	500 ± 60†	552 ± 53†

Values are means ± SE. † *P <0.05 vs. SS rats within the same sex and* $^{\#}$*P <0.05 vs. female rats within the same strain (n = 6–17 per group in each parameter).*

rats had a comparable susceptibility to renal injury as the male SS^{LepR}mutant rats.

Protocol 2: Effects of Gemfibrozil on the progression of renal injury in SS and SS^{LepR}mutant rats. Experiments were performed on 12 week-old SS and SS^{LepR}mutant rats. The measurement of proteinuria and blood glucose levels as described in Protocol 1. After collecting baseline data, SS and SS^{LepR}mutant rats were separated into four groups: (1) SS and (2) SS^{LepR}mutant rats were treated with vehicle – powdered food (TD8640) and (3) SS and (4) SS^{LepR}mutant rats were treated with gemfibrozil (200 mg/kg/day, orally in the powdered food) for 4 weeks. Every 2 weeks rats were placed in metabolic cages until the rats reached 16 weeks of age, and proteinuria and blood glucose levels were measured at each time period. During the final week of the study, rats were placed under anesthesia, and a catheter was inserted in the carotid artery for the measurement of MAP. After a 24 h recovery period, catheters were connected to pressure transducers (MLT0699; ADInstruments, Colorado Springs, CO, United States) coupled to a computerized data PowerLab acquisition system (ADInstruments, Colorado Springs, CO, United States). MAP was recorded continuously for 30 min after a 30 min equilibration period. After arterial pressure measurements, a final blood sample was taken from the abdominal aorta to measure plasma triglyceride and total cholesterol concentrations (Cayman Chemical Company, Ann Arbor, MI, United States) and insulin (Mercodia Rat Insulin ELISA, Uppsala, Sweden). Next, both kidneys were weighed and each kidney was placed in individual flasks containing a 10% buffered formalin fixation solution for histology.

Renal Histopathology and Lipid Accumulation

Measurement of Glomerular Injury and Renal Fibrosis

Paraffin kidney sections were prepared from the right kidneys collected from SS and SS^{LepR}mutant rats treated with and without gemfibrozil. Kidney sections were cut into 3 μm sections and stained with Periodic acid-Schiff (PAS) and Masson's Trichrome. To determine glomerular injury, 30 glomeruli per PAS section were scored in a blinded fashion on a 0–4 scale with 0 representing a normal glomerulus, 1 representing a 25% of loss, 2 representing a 50% loss, 3 representing a 75% loss, and 4 representing >75% loss of capillaries in the tuft. To determine the degree of renal fibrosis, 5–10 representative images per section was captured using a SeBa microscope equipped with a color camera (Laxco Inc., North Creek, Washington, United States) and analyzed for the percentage of the image stained blue (primarily collagen) in the Masson's trichrome-stained sections using NIS-Elements D 3.0 software.

Measurement of Renal Lipid Accumulation and Low-Density Lipoprotein (LDL)

To determine renal lipid accumulation via oil-red-O staining, the left kidney was cut in half, removed from the 10% buffered formalin solution, and washed in 0.1% PBS for 5 h. The other half was placed back into the 10% buffered formalin solution for later use. The kidneys were then placed in 30% sucrose overnight or until the kidneys sunk to the bottom of the container. Kidneys were then cut into 10 μm sections and stored at −80°C overnight. On the next day, the frozen sections were thawed and allowed to air dry for 20 min before fixation in 40% formalin and washed with H_2O. Then, the sections were stained in Oil-red-O solution (EKI; Joilet, IL, United States) for 10 min and washed with H_2O. The sections then were counterstained with Harris hematoxylin containing acetic acid (Stat Lab; McKinney, TX, United States) for 1 min and washed again with H_2O. Finally, the sections were incubated in ammonia water to cause the blue counterstain and washed a final time with H_2O before mounting with an aqueous mounting medium (Thermo Fisher Scientific, Waltham, MA, United States). Images were obtained using the same microscope as mentioned above and analyzed for the percentage of the image stained red using the NIS-Elements D 3.0 software.

To measure renal LDL accumulation, paraffin-embedded sections (3 μm) were deparaffinized with xylene, followed by dehydration utilizing a series of ethanol with decreasing concentrations keeping the sections at 60°C for 30 min. Then, the sections were incubated in a citrate buffer (pH-6.0) solution for 20 min using a microwave oven to retrieve the LDL receptor in the kidney section. The sections were washed 3 times with DPBS containing Ca^{2+} and Mg^{2+} (Sigma-Aldrich, St. Louis, MO, United States) for 5 min and incubated in 10% blocking goat serum solution for 2 h at room temperature. After removal of the blocking solution, the sections were incubated with FITC-labeled BODIPY FL LDL (Life Technologies Corporation, Carlsbad, CA, United States) overnight at 4°C. Then, the sections were washed three times with DPBS containing Ca^{2+} and Mg^{2+} for 5 min and incubated with 0.001% Evans blue for 10 min to quench auto-fluorescence. Next, the sections were washed three times with DPBS containing Ca^{2+} and Mg^{2+} for 5 min. The slides were then applied with a drop of an anti-fade mounting medium with DAPI (H-1200, Vector Laboratories, Inc., Burlingame, CA, United States) and cover slipped. Images were obtained using a Nikon Eclipse 55i microscope equipped with a Nikon DS-Fi1 color camera (Nikon, Melville, NY, United States).

Statistical Analysis

Statistical analysis was performed using GraphPad Prism 8 (GraphPad Software, San Diego, CA, United States). The significance of the difference in mean values for a single time point was determined by an one-way ANOVA followed by the Tukey's multiple comparisons test. Temporal changes in metabolic and cardiovascular parameters were compared between and within strains using a two-way ANOVA followed by the Holm-Sidak test. A p-value <0.05 was considered significantly different. The data are presented as mean ± SEM.

RESULTS

Sex Differences in Female and Male SS and SS^{LepR}Mutant Rats

The comparison of metabolic and cardiovascular parameters in female and male SS and SS^{LepR}mutant rats is presented in **Table 1**. When examining body weight, both male SS and SS^{LepR}mutant rats had a significantly higher body weight when

compared to their female counterparts (210 ± 3 vs. 347 ± 5 and 392 ± 4 vs. 471 ± 15 g, respectively). We did not observe any sex or strain differences in blood glucose levels in SS and SS^{LepR}mutant rats. Similar to blood glucose, MAP was not different among the groups. Proteinuria had a tendency to be elevated in male SS rats compared to the values seen in female SS rats (94 ± 19 vs. 41 ± 6 mg/day), but it did not reach statistical significance. While we did not observe any significant differences in proteinuria between female and male SS^{LepR}mutant rats (500 ± 60 vs. 552 ± 53 mg/day, respectively), proteinuria was markedly elevated in the SS^{LepR}mutant strain compared to their SS littermates.

Metabolic Parameters

The efficacy of gemfibrozil on plasma cholesterol and triglyceride levels in SS and SS^{LepR}mutant rats is presented in **Figure 1**. In **Figure 1A**, cholesterol was significantly elevated in SS^{LepR}mutant rats compared to SS rats (67 ± 8 and 27 ± 3 mg/day, respectively), and chronic treatment with gemfibrozil did not have an effect on cholesterol levels in both strains. Plasma triglyceride levels were significantly elevated in the obese SS^{LepR}mutant rats compared to the values measured in the lean SS rats (1193 ± 256 and 89 ± 16 mg/day, respectively) (**Figure 1B**). Chronic treatment with gemfibrozil markedly reduced the levels of plasma triglycerides in SS^{LepR}mutant rats by more than 50% while not having any effect in SS rats (410 ± 79 and 32 ± 9 mg/day, respectively).

Comparison of body weight, blood glucose, and plasma insulin levels in SS and SS^{LepR}mutant rats are presented in **Figure 2**. Body weight was markedly increased in the SS^{LepR}mutant strain (485 ± 17 g) compared to the values measured in SS rats (303 ± 20 g) (**Figure 2A**). Chronic treatment with gemfibrozil had no effect on body weight in both strains. A hallmark characteristic of the SS^{LepR}Mutant strain is the development of insulin resistance and obesity in the absence of hyperglycemia. In the current study, we did not observe any differences in blood glucose levels among the groups by the end of the study (**Figure 2B**). When examining plasma insulin levels at the end of the study, we found plasma insulin levels to be higher and more variable in the SS^{LepR}mutant strain vs. the levels measured in SS rats (1.34 ± 0.42 and 0.47 ± 0.07 ng/mL, respectively), but the difference did not reach statistical significance (**Figure 2C**). This may be due to apoptosis of the insulin producing cells of the pancreas in the SS^{LepR}mutant strain. Similar to body weight and blood glucose levels, treatment with gemfibrozil had no significant effect on plasma insulin levels in either strain.

Cardiovascular and Renal Injury Parameters

Comparison of MAP and temporal changes in proteinuria in SS and SS^{LepR}mutant rats are presented in **Figure 3**. At the end of the study, MAP was markedly elevated in SS^{LepR}mutant rats when compared to SS rats (198 ± 7 and 165 ± 7 mmHg, respectively) (**Figure 3A**). Administration of gemfibrozil significantly lowered MAP in SS^{LepR}mutant rats (163 ± 8 mmHg) while not having any effect in SS rats (160 ± 5 mmHg). During the course of the study, proteinuria increased from 96 ± 13 to 125 ± 25 mg/day in SS rats but showed a trend to decrease from 783 ± 113 to 693 ± 58 mg/day in the SS^{LepR}mutant strain (**Figure 3B**). Interestingly, treatment with gemfibrozil increased the progression of proteinuria by 77% in the SS^{LepR}mutant strain (1224 ± 139 mg/day) without affecting proteinuria in SS rats (127 ± 13 mg/day).

The effects of gemfibrozil on the degree of renal injury in SS and SS^{LepR}mutant rats are presented in **Figure 4**. The kidneys from vehicle-treated SS^{LepR}mutant rats exhibited more mesangial expansion and glomerular injury compared to SS rats (**Figures 4A,B**). In contrast, kidneys from the

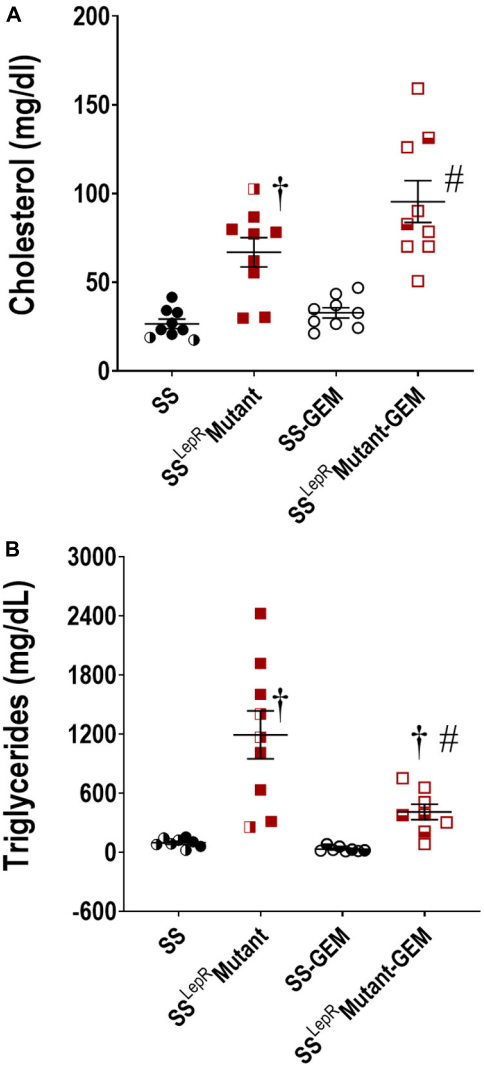

FIGURE 1 | Efficacy of gemfibrozil treatment on plasma cholesterol **(A)** and triglyceride **(B)** levels in wild-type Dahl salt-sensitive (SS) rats and the obese SS leptin receptor mutant (SS^{LepR}mutant) strain. Numbers of rats studied (n = 7–9 per group). Female rats in each group are represented by partially filled symbols. Values are means ± SE. $^{\dagger}p$ <0.05 vs. SS rats within the same treatment, and $^{\#}p$ <0.05 vs. vehicle-treated rats within the same strain.

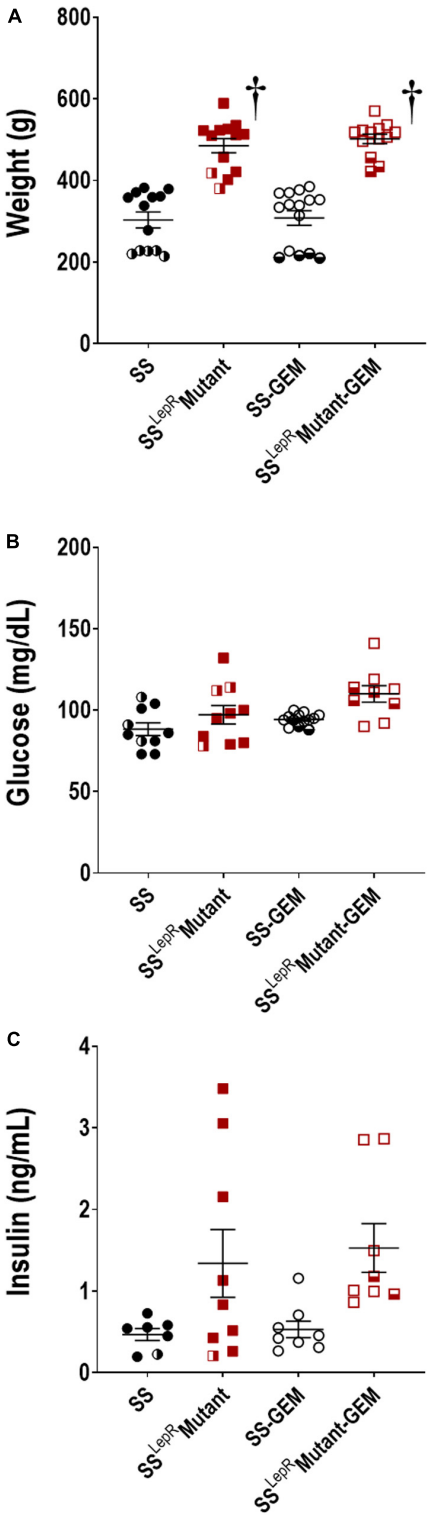

FIGURE 2 | Comparison of metabolic parameters in wild-type Dahl salt-sensitive (SS) rats and the obese SS leptin receptor mutant (SS^{LepR}mutant) strain treated with gemfibrozil: body weight **(A)**, blood glucose **(B)**, and plasma insulin **(C)**. Numbers of rats studied (n = 7–15 per group). Female rats in each group are represented by partially filled symbols. Values are means ± SE. $^{\dagger}p$ <0.05 vs. SS rats within the same treatment.

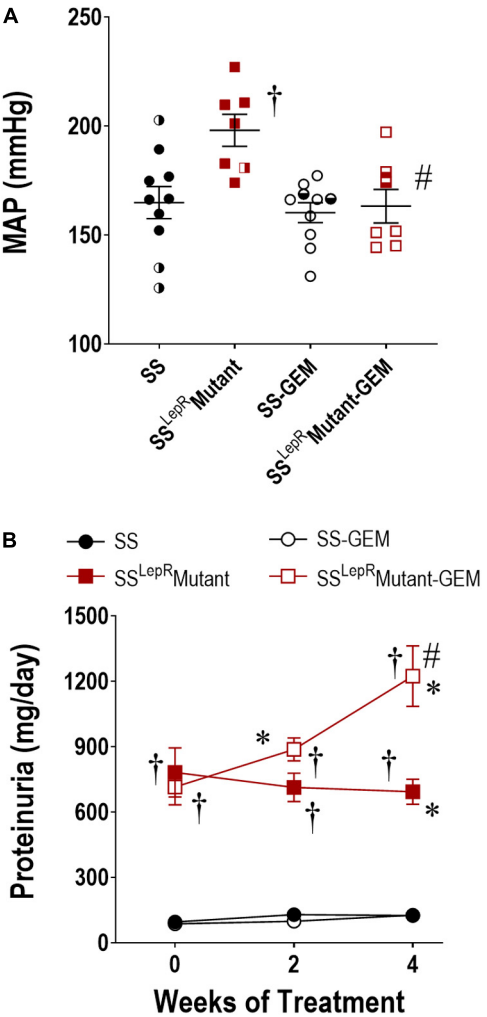

FIGURE 3 | Effects of gemfibrozil treatment on mean arterial pressure (MAP) **(A)** and proteinuria **(B)** in wild-type Dahl salt-sensitive (SS) rats and the obese SS leptin receptor mutant (SS^{LepR}mutant) strain. Numbers of rats studied (n = 7–12 per group). Female rats in each group are represented by partially filled symbols. Values are means ± SE. $^{*}p$ <0.05 vs. same strain at baseline, $^{\dagger}p$ <0.05 vs. SS rats within the same treatment, and $^{\#}p$ <0.05 vs. vehicle-treated rats within the same strain.

SS^{LepR}mutant strain treated with gemfibrozil displayed reduced expansion of the mesangial matrix and glomerular injury. When examining renal fibrosis by thresholding for blue staining, fibrosis (% of blue staining) was significantly elevated in vehicle-treated SS^{LepR}mutant rats when compared to the values measured in SS rats (**Figures 4C,D**). However, chronic treatment with gemfibrozil did not reduce renal fibrosis in the SS^{LepR}mutant strain. When evaluating renal function, we observed that Pcr levels were considerably higher in SS^{LepR}mutant rats vs. the values measured in SS rats (1.35 ± 0.21 vs. 0.62 ± 0.02 mg/dL, respectively) (**Figure 4E**). Moreover, administration of gemfibrozil improved renal function and markedly reduced Pcr levels in the SS^{LepR}mutant strain

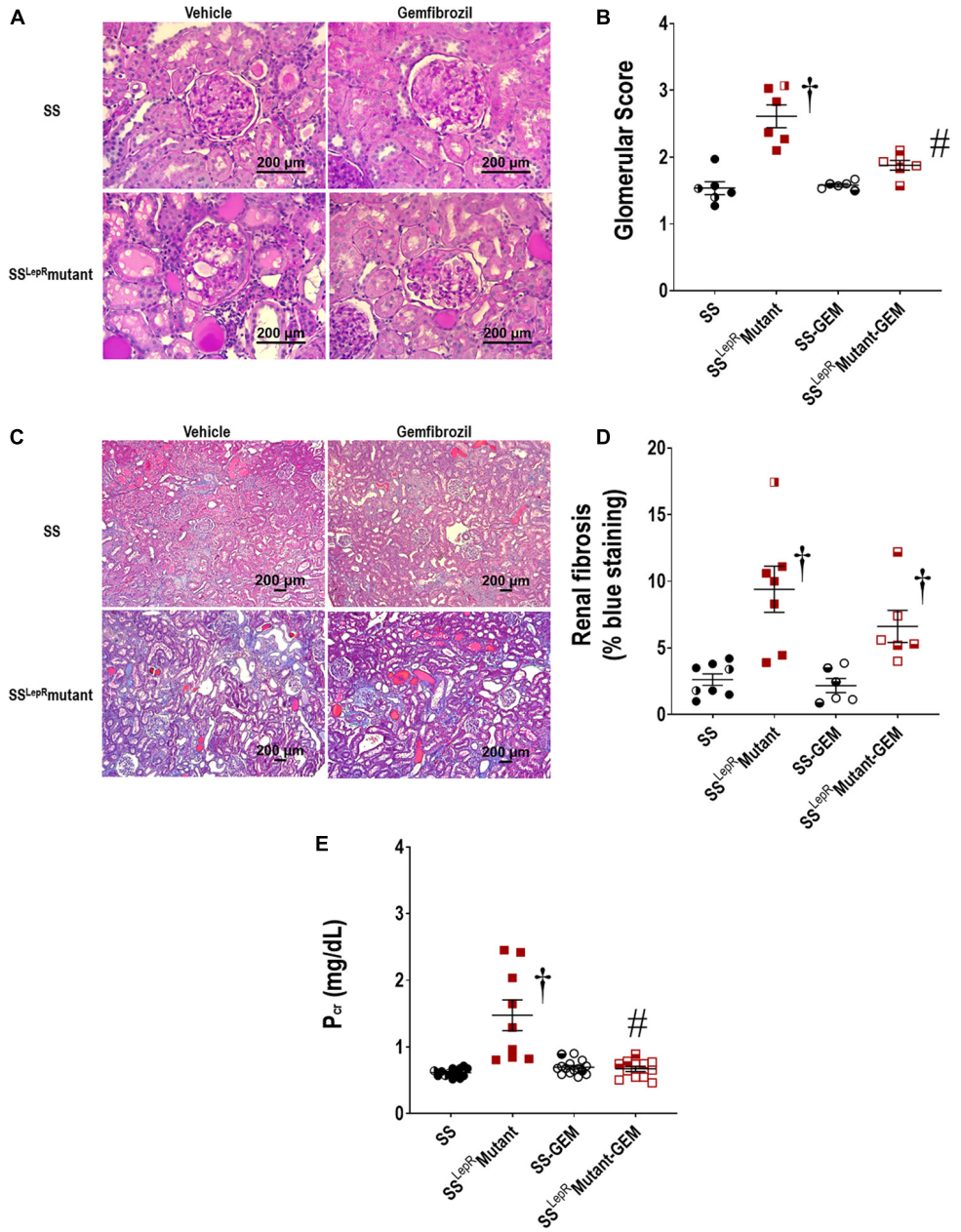

FIGURE 4 | Effects of gemfibrozil treatment on renal histopathology and renal function in wild-type Dahl salt-sensitive (SS) rats and the obese SS leptin receptor mutant (SS^{LepR}mutant) strain. Representative images of renal histopathology: Glomerular injury – Periodic acid-Schiff staining **(A)** and glomerular injury score **(B)**; Fibrosis – Masson's Trichrome staining **(C)** and renal fibrosis (% blue staining) **(D)**. Measurement of renal function by plasma creatinine levels among the groups is represented in **(E)**. Numbers of rats studied (n = 6–12 per group). Female rats in each group are represented by partially filled symbols. Values are means ± SE. $^{\dagger}p$ <0.05 vs. SS rats within the same treatment, and $^{\#}p$ <0.05 vs. vehicle-treated rats within the same strain.

without affecting the levels in SS rats (0.73 ± 0.07 vs. 0.70 ± 0.03 mg/dL, respectively).

Renal Lipid Accumulation

The effects of gemfibrozil on renal lipid accumulation via oil-red-O staining and FITC-labeled BODIPY FL LDL are presented in **Figures 5**, **6**. We observed noticeably more oil-red-O staining in glomeruli, tubules, and interstitial space in vehicle-treated SS^{LepR}mutant rats compared to SS rats suggesting significantly higher lipid accumulation in the kidneys of SS^{LepR}mutant rats (**Figures 5A,B**). Chronic treatment with gemfibrozil decreased oil-red-O staining in SS^{LepR}mutant rats. When assessing LDL accumulation by FITC-labeled BODIPY FL, we found similar results as with the oil-red-O staining, but LDL accumulation was more localized to the interstitial space in the vehicle-treated

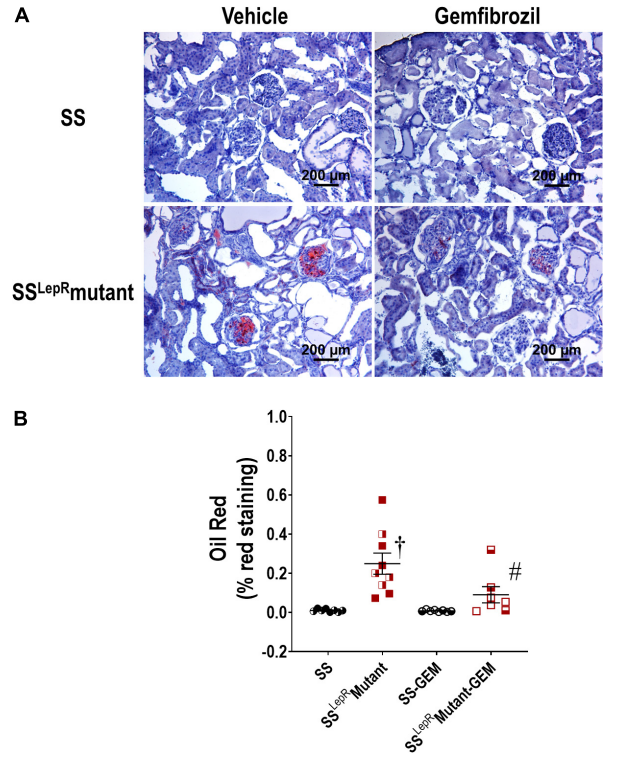

FIGURE 5 | Effects of gemfibrozil on renal lipid accumulation. Representative images of renal lipid accumulation by oil-red-O staining **(A)** and quantification of % red staining **(B)** in the kidneys from wild-type Dahl salt-sensitive (SS) rats and the obese SS leptin receptor mutant (SS^{LepR}mutant) strain. Female rats in each group are represented by partially filled symbols. Values are means ± SE. $^{\dagger}p$ <0.05 vs. SS rats within the same treatment, and $^{\#}p$ <0.05 vs. vehicle-treated rats within the same strain.

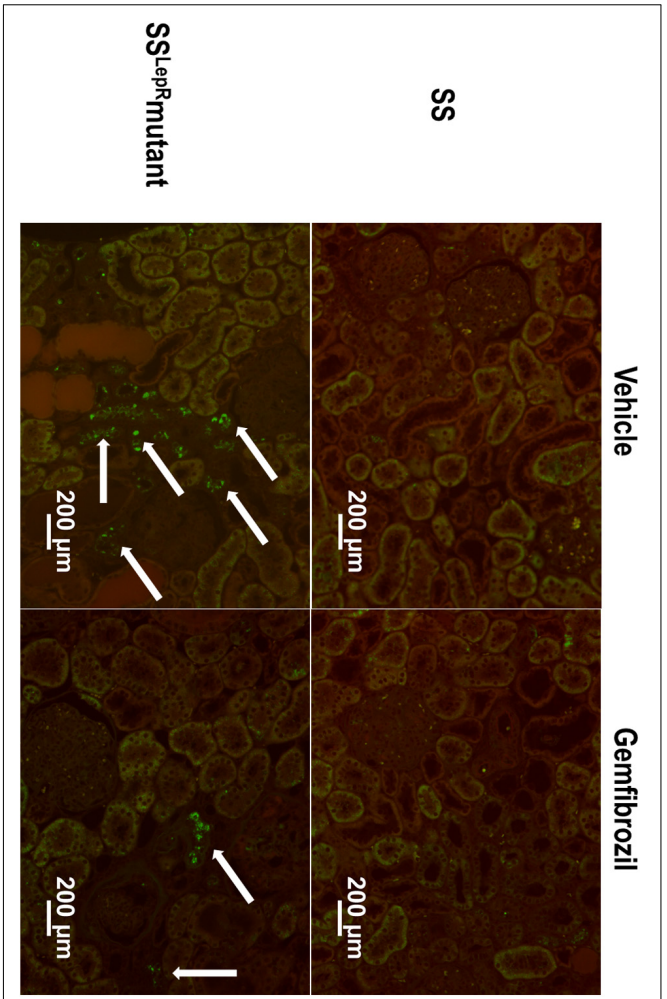

FIGURE 6 | Effects of gemfibrozil on renal low-density lipoprotein (LDL) accumulation. Representative images of renal LDL accumulation by FITC-labeled BODIPY FL LDL staining (indicated by white arrows) in the kidneys from wild-type Dahl salt-sensitive (SS) rats and the obese SS leptin receptor mutant (SS^{LepR}mutant) strain.

SS^{LepR}mutant strain vs. SS rats (**Figure 6**). Moreover, treatment with gemfibrozil appeared to reduce LDL accumulation in SS^{LepR}mutant rats.

DISCUSSION

One of the major characteristics of obesity is dyslipidemia, which has been linked to the development of CKD (Kasiske et al., 1993; Guijarro and Keane, 1996; Keane, 2000). However, the relationship between dyslipidemia and the progression of renal disease has been conflicting (Samuelsson et al., 1997; Hadjadj et al., 2004; Dalrymple and Kaysen, 2008; Rahman et al., 2008; Kaysen, 2009; Navaneethan et al., 2009; Chawla et al., 2010) and needs further investigation. Recently, we reported that the development of CKD in the SS^{LepR}mutant strain was associated with dyslipidemia and renal lipid accumulation (McPherson et al., 2016, 2020). In the current study, we examined the effects of gemfibrozil, a lipid-lowering drug, on the progression of renal injury in SS^{LepR}mutant rats during the progression of renal injury. Treatment with gemfibrozil had no effect on body weight, blood glucose, or plasma insulin levels in both strains. Plasma triglyceride levels were markedly elevated in the SS^{LepR}mutant strain compared to SS rats, and chronic treatment with gemfibrozil reduced plasma triglycerides by more than 50% in the SS^{LepR}mutant strain. Arterial pressure was significantly elevated in the SS^{LepR}mutant strain vs. SS rats, and administration of gemfibrozil prevented the increase in arterial pressure observed in SS^{LepR}mutant rats. We observed a trend for proteinuria to decrease in the SS^{LepR}mutant strain over the course of the study, which was accompanied with significant glomerular injury and renal lipid accumulation (i.e., oil-red-O staining and LDL fluorescence) and fibrosis. Moreover, the concentration of Pcr was significantly elevated in the SS^{LepR}mutant rats compared to the values measured in their lean SS control counterparts suggesting that the SS^{LepR}mutant rats developed CKD. Chronic treatment with gemfibrozil markedly increased proteinuria, reduced glomerular injury, and improved renal function in SS^{LepR}mutant rats.

These data indicate that reducing plasma triglyceride levels with gemfibrozil reduces renal lipid accumulation and inhibits the progression of hypertension and CKD associated with obesity in SS^{LepR}mutant rats.

Fibrates are agonists for the nuclear transcription receptor, PPAR-α, and are often used to effectively reduce plasma triglyceride levels by increasing the lipolysis of lipoprotein triglyceride via lipoprotein lipase (Heller and Harvengt, 1983; Keech et al., 2005; Remick et al., 2008). Additionally, fibrates are the most commonly prescribed drug for patients suffering from hypertriglyceridemia. In the current study, we chose to use gemfibrozil since it has less of an effect on stimulating a decline in renal function in patients susceptible to the development of CKD (Broeders et al., 2000). We observed that plasma triglyceride levels were markedly elevated in the SS^{LepR}mutant strain vs. the values measured in SS rats, and treatment with gemfibrozil significantly decreased plasma triglyceride levels by more than half in the SS^{LepR}mutant strain. Treatment with gemfibrozil was specific in lowering triglyceride levels because it did not have an effect on plasma cholesterol levels. These data suggest that the dose of gemfibrozil used in the current study was effective in reducing triglyceride levels in our rodent model of obesity with severe renal disease.

Obesity has been associated with elevated proteinuria in humans as well as animals (Bagby, 2004; Chen et al., 2004; Kurella et al., 2005; Kanauchi et al., 2006; Ninomiya and Kiyohara, 2007; Wahba and Mak, 2007; McPherson et al., 2016, 2019, 2020; Kovesdy et al., 2017). In the current study, proteinuria was already markedly elevated at baseline in SS^{LepR}mutant rats compared to SS rats and had a tendency to decrease over the course of study. This result is not at all surprising, since we have previously observed that proteinuria declines after 14 weeks of age in the SS^{LepR}mutant strain, which is more than likely due to a decline of renal function (McPherson et al., 2016). The impact of dylipidemia on the progression of proteinuria and decline in renal function is unclear but undoubtedly involves inflammation, oxidative stress, and lipid accumulation (D'Agati et al., 2016; Yang et al., 2017; Gai et al., 2019). While we did not measure inflammation and oxidative stress in the current study, lipid accumulation was significantly higher in glomeruli, tubules, and interstitium of obese SS^{LepR}mutant rats compared to their lean counterparts. Various cells in the glomerulus (i.e., podocytes and mesangial cells) are sensitive to lipid accumulation, and once lipids affect these cells, they contribute to structural and functional changes that lead to the development glomerulosclerosis and proteinuria (Straub et al., 2013; de Vries et al., 2014), which eventually leads to decreased renal function and CKD. Interestingly, treatment with gemfibrozil for 4 weeks significantly increased proteinuria and reduced glomerular injury and renal fibrosis in SS^{LepR}mutant rats without having any effect in SS rats, and this was associated with reduced renal lipid accumulation. We hypothesize that the increase in proteinuria is due to improved renal function observed in gemfibrozil-treated SS^{LepR}mutant rats. In support of our hypothesis, Wilson et al. demonstrated that treatment with fenofibrate markedly increased proteinuria but reduced mesangial expansion and glomerulosclerosis in SS rats fed a high salt diet with pre-existing renal injury (Wilson et al., 1998). Taken together, these data provide direct evidence that reducing hypertriglyceridemia and renal lipid accumulation improves renal function during the progression of renal injury associated with obesity.

Previous studies have demonstrated that a major side effect of fibrates is decreased renal function (Broeders et al., 2000; Tonelli et al., 2004). This may be attributed to the potential inhibitory effects of fibrates on the production of vasodilatory prostaglandins in the kidney that regulate renal blood flow and glomerular filtration rate (Wilson et al., 1995; Ledwith et al., 1997). In the current study, we used gemfibrozil, which appears to be free from these renal dysfunction effects (Yoshinari et al., 1998; Broeders et al., 2000). We observed that chronic treatment with gemfibrozil did not impair but rather improved renal function in our model of obesity susceptible to CKD. Our results are very similar to what has been demonstrated in clinical studies (Broeders et al., 2000; Tonelli et al., 2004). Broeders et al. conducted a study that examined the effects of four main fibrates (i.e., fenofibrate, bezafibrate, ciprofibrate, and gemfibrozil) on renal function in patients with pre-existing renal dysfunction and found that all the fibrates except for gemfibrozil impaired renal function (Broeders et al., 2000; Tonelli et al., 2004). These results further suggest that gemfibrozil does not worsen renal function in patients or animals that are susceptible to CKD.

One of the major findings in the current study is chronic treatment with gemfibrozil significantly reduced arterial pressure in the obese SS^{LepR}mutant strain during the progression of renal injury. The arterial pressure lowering effect of fibrates in various animals of models of hypertension and renal disease has been well-documented (Wilson et al., 1998; Cruz et al., 2011; Lee et al., 2011; Li et al., 2014; Weng et al., 2014). However, studies examining the effects of fibrates on arterial pressure in animal models with either established hypertension and/or renal disease are limited. Roman and colleagues reported that administration of fenofibrate decreased arterial pressure in SS rats fed high salt diet with established hypertension and renal disease (Wilson et al., 1998). The exact mechanism by which fibrates lower arterial pressure is not completely understood but involves various pathways such as anti-lipidemic (Jonkers et al., 2001; Kim and Kim, 2020), anti-inflammatory (Feingold and Grunfeld, 2000; Diep et al., 2004; Ruscica et al., 2018), nitric oxide (Newaz et al., 2005; Ibarra-Lara et al., 2010; Esenboga et al., 2019; Xu et al., 2019), and 20-HETE (Roman et al., 1993; Wilson et al., 1998). In the current study, we cannot exclude the impact of any of these pathways on reducing arterial pressure in response to gemfibrozil treatment. However, we hypothesis that the arterial pressure lowering effect of gemfibrozil is due to improving renal function in the obese SS^{LepR}mutant strain. Moreover, to our knowledge, the current study is one of few studies demonstrating that treatment with a fibrate is beneficial in lowering arterial pressure and preventing the progression of CKD associated with obesity.

Overall, the results of the current study support the hypothesis that treatment with gemfibrozil reduces progression of renal injury in obese SS^{LepR}mutant rats predisposed to the

development of CKD. Yet, there are a few limitations that should be noted. One limitation is that we did not fully investigate the impact of sex in the current study. Previous studies have demonstrated that there are sex differences in the development of hypertension and renal injury in SS rats on either a high salt or high fat diet (Hinojosa-Laborde et al., 2000; Bayorh et al., 2001; Gerhold et al., 2007; Podesser et al., 2007; Turbeville et al., 2020; Zhang et al., 2020). In contrast to those previous studies, we did not feed our rats a typical high salt diet (4–8% NaCl diet) (Mohammed-Ali et al., 2017), but we will admit that the degree of proteinuria may be elevated in male vs. female SS rats on a lower salt diet containing 1% NaCl. However, other studies have shown no differences in the development of hypertension and renal injury between females and males in the SS strain on high salt diet (Hinojosa-Laborde et al., 2000; Murphy et al., 2012). In the current study, the susceptibility to hypertension and renal injury were similar in female and male SS^{LepR}mutant rats, which suggests that inhibiting leptin signaling may temper sex differences in the SS rats. Another limitation is the measurement of arterial pressure by the chronic carotid catheter method, which was performed on the day after surgery and involves stress on the animals due being placed in constrainers for a given amount of time, instead of using telemetry. However, we were still able to observed differences in arterial pressure among the groups. If telemetry was used, temporal changes in arterial pressure could have been measured throughout the study rather than at the end. An additional limitation of the study is that we did not examine whether treatment with gemfibrozil had effects on lipid transporters in the kidneys. We recently reported that the progression of renal injury in the SS^{LepR}mutant strain is associated with alterations in various lipid transporters that contribute to lipid accumulation (McPherson et al., 2020). Since the vehicle-treated SS^{LepR}mutant rats developed progressive renal injury and CKD, we believed that the renal tissue from this group would be necrotic and not be reliable to use for the comparison of gene/protein expression of the lipid transporters to the other groups in the study. An additional limitation is that we did not test whether treatment with gemfibrozil would slow the progression of renal injury and improve renal function in SS^{LepR}mutant rats with established impaired renal function, which may have produced different results. Future studies will be designed to consider these limitations.

Clinical Translational Perspective

Over the last few decades, there has been a growing need to understand the development and progression of renal injury in obese patients in the absence of hyperglycemia (Wesson et al., 1985; Praga et al., 2000; Praga, 2002; Chen et al., 2006; Kramer et al., 2006). The obese SS^{LepR}mutant strain represents an ideal model to study the role of dyslipidemia during the progression of CKD associated with obesity without the complications of hyperglycemia. Lipid-lowering drugs such as fibrates are commonly administered to patients suffering from dyslipidemia. However, examining the role of dyslipidemia as a mediator of CKD has yielded inconsistent results and still remains unclear. However, data from the current study have provided strong evidence that fibrates are advantageous for treating patients whom are suffering from dyslipidemia and susceptible to CKD. Over the course of the study, we observed that reducing plasma triglyceride levels with gemfibrozil leads to a decrease in renal lipid accumulation and prevention of renal injury and hypertension associated with obesity in SS^{LepR}mutant rats. These results also support previous studies that demonstrate gemfibrozil does not further impair renal function in patients that are predisposed to the development of CKD (Broeders et al., 2000; Tonelli et al., 2004). This is contradictory to the other fibrates in this class of drugs, which have been shown to cause a reduction in renal function (Tannock, 2000; Kidney Disease Outcomes Quality Initiative Group, 2003; Harper and Jacobson, 2008). Overall, more studies are needed to test the roles of dyslipidemia and renal lipid accumulation in the progression of renal disease to be able develop novel therapeutic targets to prevent this devastating disease in obese patients.

DATA AVAILABILITY STATEMENT

The raw data supporting the conclusions of this article will be made available by the authors, without undue reservation, to any qualified researcher.

ETHICS STATEMENT

The animal study was reviewed and approved by the University of Mississippi Medical Center Institutional Animal Care and Use Committee.

AUTHOR CONTRIBUTIONS

JW and CS provided conception and prepared the figures. CS, BP, KM, AB, UE, EB, LS, DC, and JW drafted, edited, and revised the manuscript, and approved the final version of the manuscript. All authors contributed to the article and approved the submitted version.

FUNDING

This work was financially supported by the National Institutes of Diabetes and Digestive and Kidney Diseases of the National Institutes of Health (NIH/NIDDK, DK109133) awarded to JW, the National Heart, Lung and Blood Institute of the National Institutes of Health (NIH/NHLBI, HL130456 and HL151407) awarded to DC. The work performed through the UMMC Molecular and Genomics Facility was supported, in part, by funds from the NIGMS, including the Mississippi INBRE (P20GM103476), Obesity, Cardiorenal and Metabolic Diseases- COBRE (P20GM104357), and the Mississippi Center of Excellence in Perinatal Research (MS-CEPR)-COBRE (P20GM121334). The content was solely the responsibility of the authors and does not necessarily represent the official views of the National Institutes of Health.

REFERENCES

Bagby, S. P. (2004). Obesity-initiated metabolic syndrome and the kidney: a recipe for chronic kidney disease? *J. Am. Soc. Nephrol.* 15, 2775–2791. doi: 10.1097/01.asn.0000141965.28037.ee

Bayorh, M. A., Bayorh, M. A., Socci, R. R., Eatman, D., Wang, M., and Thierry-Palmer, M. (2001). The role of gender in salt-induced hypertension. *Clin. Exp. Hypertens.* 23, 241–255. doi: 10.1081/ceh-100102663

Bosma, R. J., van der Heide, J. J., Oosterop, E. J., de Jong, P. E., and Navis, G. (2004). Body mass index is associated with altered renal hemodynamics in non-obese healthy subjects. *Kidney Int.* 65, 259–265. doi: 10.1111/j.1523-1755.2004.00351.x

Broeders, N., Knoop, C., Antoine, M., Tielemans, C., and Abramowicz, D. (2000). Fibrate-induced increase in blood urea and creatinine: is gemfibrozil the only innocuous agent? *Nephrol. Dial Transplant.* 15, 1993–1999. doi: 10.1093/ndt/15.12.1993

Chagnac, A., Weinstein, T., Korzets, A., Ramadan, E., Hirsch, J., and Gafter, U. (2000). Glomerular hemodynamics in severe obesity. *Am. J. Physiol. Renal Physiol.* 278, F817–F822.

Chawla, V., Greene, T., Beck, G. J., Kusek, J. W., Collins, A. J., Sarnak, M. J., et al. (2010). Hyperlipidemia and long-term outcomes in nondiabetic chronic kidney disease. *Clin. J. Am. Soc. Nephrol.* 5, 1582–1587. doi: 10.2215/cjn.01450210

Chen, H. M., Liu, Z. H., Zeng, C. H., Li, S. J., Wang, Q. W., and Li, L. S. (2006). Podocyte lesions in patients with obesity-related glomerulopathy. *Am. J. Kidney Dis.* 48, 772–779. doi: 10.1053/j.ajkd.2006.07.025

Chen, J., Muntner, P., Hamm, L. L., Jones, D. W., Batuman, V., Fonseca, V., et al. (2004). The metabolic syndrome and chronic kidney disease in U.S. adults. *Ann. Intern. Med.* 140, 167–174.

Cruz, A., Rodriguez-Gomez, I., Perez-Abud, R., Vargas, M. A., Wangensteen, R., Quesada, A., et al. (2011). Effects of clofibrate on salt loading-induced hypertension in rats. *J. Biomed. Biotechnol.* 2011:469481.

D'Agati, V. D., Chagnac, A., de Vries, A. P., Levi, M., Porrini, E., Herman-Edelstein, M., et al. (2016). Obesity-related glomerulopathy: clinical and pathologic characteristics and pathogenesis. *Nat. Rev. Nephrol.* 12, 453–471. doi: 10.1038/nrneph.2016.75

Dalrymple, L. S., and Kaysen, G. A. (2008). The effect of lipoproteins on the development and progression of renal disease. *Am. J. Nephrol.* 28, 723–731. doi: 10.1159/000127980

de Vries, A. P., Ruggenenti, P., Ruan, X. Z., Praga, M., Cruzado, J. M., Bajema, I. M., et al. (2014). Fatty kidney: emerging role of ectopic lipid in obesity-related renal disease. *Lancet Diabetes Endocrinol.* 2, 417–426. doi: 10.1016/s2213-8587(14)70065-8

DeZwaan-McCabe, D., Sheldon, R. D., Gorecki, M. C., Guo, D. F., Gansemer, E. R., Kaufman, R. J., et al. (2017). ER stress inhibits liver fatty acid oxidation while unmitigated stress leads to anorexia-induced lipolysis and both liver and kidney steatosis. *Cell Rep.* 19, 1794–1806. doi: 10.1016/j.celrep.2017.05.020

Diep, Q. N., Benkirane, K., Amiri, F., Cohn, J. S., Endemann, D., and Schiffrin, E. L. (2004). PPAR alpha activator fenofibrate inhibits myocardial inflammation and fibrosis in angiotensin II-infused rats. *J. Mol. Cell Cardiol.* 36, 295–304. doi: 10.1016/j.yjmcc.2003.11.004

Ejerblad, E., Fored, C. M., Lindblad, P., Fryzek, J., McLaughlin, J. K., and Nyren, O. (2006). Obesity and risk for chronic renal failure. *J. Am. Soc. Nephrol.* 17, 1695–1702.

Esenboga, K., Cicek, O. F., Oktay, A. A., Ayral, P. A., and Gurlek, A. (2019). Effect of fenofibrate on serum nitric oxide levels in patients with hypertriglyceridemia. *Adv. Clin. Exp. Med.* 28, 931–936. doi: 10.17219/acem/94161

Feingold, K. R., Grunfeld, C. (2000). *The Effect of Inflammation and Infection on Lipids and Lipoproteins*. K. R. Feingold, B. Anawalt, A. Boyce, G. Chrousos, K. Dungan, A. Grossman, et al., eds Endotext: South Dartmouth, MA.

Foster, M. C., Hwang, S. J., Porter, S. A., Massaro, J. M., Hoffmann, U., and Fox, C. S. (2011). Fatty kidney, hypertension, and chronic kidney disease: the framingham heart study. *Hypertension* 58, 784–790. doi: 10.1161/hypertensionaha.111.175315

Gai, Z., Wang, T., Visentin, M., Kullak-Ublick, G. A., Fu, X., and Wang, Z. (2019). Lipid accumulation and chronic kidney disease. *Nutrients* 11:722. doi: 10.3390/nu11040722

Gerhold, D., Bagchi, A., Lu, M., Figueroa, D., Keenan, K., Holder, D., et al. (2007). Androgens drive divergent responses to salt stress in male versus female rat kidneys. *Genomics* 89, 731–744. doi: 10.1016/j.ygeno.2007.01.009

Guijarro, C., and Keane, W. F. (1996). Effects of lipids on the pathogenesis of progressive renal failure: role of 3-hydroxy-3-methylglutaryl coenzyme A reductase inhibitors in the prevention of glomerulosclerosis. *Miner. Electrolyte Metab.* 22, 147–152.

Hadjadj, S., Duly-Bouhanick, B., Bekherraz, A., BrIdoux, F., Gallois, Y., Mauco, G., et al. (2004). Serum triglycerides are a predictive factor for the development and the progression of renal and retinal complications in patients with type 1 diabetes. *Diabetes Metab.* 30, 43–51. doi: 10.1016/s1262-3636(07)70088-5

Harper, C. R., and Jacobson, T. A. (2008). Managing dyslipidemia in chronic kidney disease. *J. Am. Coll. Cardiol.* 51, 2375–2384.

Heller, F., and Harvengt, C. (1983). Effects of clofibrate, bezafibrate, fenofibrate and probucol on plasma lipolytic enzymes in normolipaemic subjects. *Eur. J. Clin. Pharmacol.* 25, 57–63. doi: 10.1007/bf00544015

Hinojosa-Laborde, C., Lange, D. L., and Haywood, J. R. (2000). Role of female sex hormones in the development and reversal of dahl hypertension. *Hypertension* 35(1 Pt 2), 484–489. doi: 10.1161/01.hyp.35.1.484

Hsu, C. Y., McCulloch, C. E., Iribarren, C., Darbinian, J., and Go, A. S. (2006). Body mass index and risk for end-stage renal disease. *Ann. Intern. Med.* 144, 21–28. doi: 10.7326/0003-4819-144-1-200601030-00006

Huang, P. L. (2009). A comprehensive definition for metabolic syndrome. *Dis. Model. Mech.* 2, 231–237. doi: 10.1242/dmm.001180

Ibarra-Lara, L., Cervantes-Perez, L. G., Perez-Severiano, F., Del Valle, L., Rubio-Ruiz, E., Soria-Castro, E., et al. (2010). PPARalpha stimulation exerts a blood pressure lowering effect through different mechanisms in a time-dependent manner. *Eur. J. Pharmacol.* 627, 185–193. doi: 10.1016/j.ejphar.2009.10.039

Jacobs, E. J., Newton, C. C., Wang, Y., Patel, A. V., McCullough, M. L., Campbell, P. T., et al. (2010). Waist circumference and all-cause mortality in a large US cohort. *Arch. Intern. Med.* 170, 1293–1301. doi: 10.1001/archinternmed.2010.201

Jonker, J. T., de Heer, P., Engelse, M. A., van Rossenberg, E. H., Klessens, C. Q. F., Baelde, H. J., et al. (2018). Metabolic imaging of fatty kidney in diabesity: validation and dietary intervention. *Nephrol. Dial. Transplant.* 33, 224–230. doi: 10.1093/ndt/gfx243

Jonkers, I. J., de Man, F. H., van der Laarse, A., Frolich, M., Gevers Leuven, J. A., Kamper, A. M., et al. (2001). Bezafibrate reduces heart rate and blood pressure in patients with hypertriglyceridemia. *J. Hypertens.* 19, 749–755. doi: 10.1097/00004872-200104000-00012

Kanauchi, M., Kanauchi, K., Kimura, K., Inoue, T., and Saito, Y. (2006). Associations of chronic kidney disease with the metabolic syndrome in non-diabetic elderly. *Nephrol. Dial. Transplant.* 21, 3608–3609. doi: 10.1093/ndt/gfl435

Kasiske, B. L. (1998). Hyperlipidemia in patients with chronic renal disease. *Am. J. Kidney Dis.* 32(5 Suppl. 3), S142–S156.

Kasiske, B. L., O'Donnell, M. P., Kim, Y., and Keane, W. F. (1993). Treatment of hyperlipidemia in chronic progressive renal disease. *Curr. Opin. Nephrol. Hypertens.* 2, 602–608. doi: 10.1097/00041552-199307000-00011

Kaysen, G. A. (2009). Lipid and lipoprotein metabolism in chronic kidney disease. *J. Ren. Nutr.* 19, 73–77. doi: 10.1053/j.jrn.2008.10.011

Keane, W. F. (2000). The role of lipids in renal disease: future challenges. *Kidney Int. Suppl.* 75, S27–S31.

Keech, A., Simes, R. J., Barter, P., Best, J., Scott, R., Taskinen, M. R., et al. (2005). Effects of long-term fenofibrate therapy on cardiovascular events in 9795 people with type 2 diabetes mellitus (the FIELD study): randomised controlled trial. *Lancet* 366, 1849–1861. doi: 10.1016/s0140-6736(05)67667-2

Kidney Disease Outcomes Quality Initiative Group (2003). K/DOQI clinical practice guidelines for management of dyslipidemias in patients with kidney disease. *Am. J. Kidney Dis.* 41(4 Suppl. 3), S1–S91.

Kim, N. H., and Kim, S. G. (2020). Fibrates revisited: potential role in cardiovascular risk reduction. *Diabetes Metab. J.* 44, 213–221. doi: 10.4093/dmj.2020.0001

Kovesdy, C. P., Furth, S. L., Zoccali, C., World Kidney, Day Steering, and Committee. (2017). Obesity and kidney disease: hidden consequences of the epidemic. *Indian J. Nephrol.* 27, 85–92.

Kramer, H. J., Saranathan, A., Luke, A., Durazo-Arvizu, R. A., Guichan, C., Hou, S., et al. (2006). Increasing body mass index and obesity in the incident ESRD population. *J. Am. Soc. Nephrol.* 17, 1453–1459. doi: 10.1681/asn.2005111241

Kurella, M., Lo, J. C., and Chertow, G. M. (2005). Metabolic syndrome and the risk for chronic kidney disease among nondiabetic adults. *J. Am. Soc. Nephrol.* 16, 2134–2140. doi: 10.1681/asn.2005010106

Ledwith, B. J., Pauley, C. J., Wagner, L. K., Rokos, C. L., Alberts, D. W., and Manam, S. (1997). Induction of cyclooxygenase-2 expression by peroxisome proliferators and non-tetradecanoylphorbol 12,13-myristate-type tumor promoters in immortalized mouse liver cells. *J. Biol. Chem.* 272, 3707–3714. doi: 10.1074/jbc.272.6.3707

Lee, D. L., Wilson, J. L., Duan, R., Hudson, T., and El-Marakby, A. (2011). Peroxisome proliferator-activated receptor-alpha activation decreases mean arterial pressure, plasma Interleukin-6, and COX-2 while increasing renal CYP4A expression in an acute model of DOCA-Salt hypertension. *PPAR Res.* 2011:502631.

Li, J., Stier, C. T., Chander, P. N., Manthati, V. L., Falck, J. R., and Carroll, M. A. (2014). Pharmacological manipulation of arachidonic acid-epoxygenase results in divergent effects on renal damage. *Front. Pharmacol.* 5:187. doi: 10.3389/fphar.2014.00187

McPherson, K. C., Shields, C. A., Poudel, B., Fizer, B., Pennington, A., Szabo-Johnson, A., et al. (2019). Impact of obesity as an independent risk factor for the development of renal injury: implications from rat models of obesity. *Am. J. Physiol. Renal Physiol.* 316, F316–F327.

McPherson, K. C., Shields, C. A., Poudel, B., Johnson, A. C., Taylor, L., Stubbs, C., et al. (2020). Altered renal hemodynamics is associated with glomerular lipid accumulation in obese Dahl salt-sensitive leptin receptor mutant rats. *Am. J. Physiol. Renal Physiol.* 318, F911–F921.

McPherson, K. C., Taylor, L., Johnson, A. C., Didion, S. P., Geurts, A. M., Garrett, M. R., et al. (2016). Early development of podocyte injury independently of hyperglycemia and elevations in arterial pressure in nondiabetic obese Dahl SS leptin receptor mutant rats. *Am. J. Physiol. Renal Physiol.* 311, F793–F804.

Mohammed-Ali, Z., Carlisle, R. E., Nademi, S., and Dickhout, J. G. (2017). "Animal models of kidney disease," in *Animal Models for the Study of Human Disease*, ed. P. Michael Conn (Cambridge, MA: Academic Press), 379–417. doi: 10.1016/b978-0-12-809468-6.00016-4

Murphy, S. R., Dahly-Vernon, A. J., Dunn, K. M., Chen, C. C., Ledbetter, S. R., Williams, J. M., et al. (2012). Renoprotective effects of anti-TGF-beta antibody and antihypertensive therapies in Dahl S rats. *Am. J. Physiol. Regul. Integr. Comp. Physiol.* 303, R57–R69.

National Cholesterol Education Program Expert Panel on Detection Evaluation, and Treatment of High Blood Cholesterol in Aults (2002). Third report of the National Cholesterol Education Program (NCEP) expert panel on detection, evaluation, and treatment of high blood cholesterol in adults (Adult Treatment Panel III) final report. *Circulation* 106, 3143–3421. doi: 10.1161/circ.106.25.3143

Navaneethan, S. D., Pansini, F., Perkovic, V., Manno, C., Pellegrini, F., Johnson, D. W., et al. (2009). HMG CoA reductase inhibitors (statins) for people with chronic kidney disease not requiring dialysis. *Cochrane Database Syst. Rev.* 133:CD007784.

Newaz, M., Blanton, A., Fidelis, P., and Oyekan, A. (2005). NAD(P)H oxidase/nitric oxide interactions in peroxisome proliferator activated receptor (PPAR)alpha-mediated cardiovascular effects. *Mutat. Res.* 579, 163–171. doi: 10.1016/j.mrfmmm.2005.02.024

Ninomiya, T., and Kiyohara, Y. (2007). Albuminuria and chronic kidney disease in association with the metabolic syndrome. *J. Cardiometab. Syndrome* 2, 104–107. doi: 10.1111/j.1559-4564.2007.05734.x

Podesser, B. K., Jain, M., Ngoy, S., Apstein, C. S., and Eberli, F. R. (2007). Unveiling gender differences in demand ischemia: a study in a rat model of genetic hypertension. *Eur. J. Cardiothorac. Surg.* 31, 298–304. doi: 10.1016/j.ejcts.2006.10.041

Praga, M. (2002). Obesity–a neglected culprit in renal disease. *Nephrol. Dial. Transplant.* 17, 1157–1159. doi: 10.1093/ndt/17.7.1157

Praga, M., Hernandez, E., Herrero, J. C., Morales, E., Revilla, Y., Diaz-Gonzalez, R., et al. (2000). Influence of obesity on the appearance of proteinuria and renal insufficiency after unilateral nephrectomy. *Kidney Int.* 58, 2111–2118. doi: 10.1111/j.1523-1755.2000.00384.x

Praga, M., and Morales, E. (2017). The fatty kidney: obesity and renal disease. *Nephron* 136, 273–276. doi: 10.1159/000447674

Rahman, M., Baimbridge, C., Davis, B. R., Barzilay, J., Basile, J. N., Henriquez, M. A., et al. (2008). Progression of kidney disease in moderately hypercholesterolemic, hypertensive patients randomized to pravastatin versus usual care: a report from the Antihypertensive and Lipid-Lowering Treatment to Prevent Heart Attack Trial (ALLHAT). *Am. J. Kidney Dis.* 52, 412–424. doi: 10.1053/j.ajkd.2008.05.027

Remick, J., Weintraub, H., Setton, R., Offenbacher, J., Fisher, E., and Schwartzbard, A. (2008). Fibrate therapy: an update. *Cardiol. Rev.* 16, 129–141. doi: 10.1097/crd.0b013e31816b43d3

Roman, R. J., Ma, Y. H., Frohlich, B., and Markham, B. (1993). Clofibrate prevents the development of hypertension in Dahl salt-sensitive rats. *Hypertension* 21(6 Pt 2), 985–988. doi: 10.1161/01.hyp.21.6.985

Ruscica, M., Ferri, N., Macchi, C., Corsini, A., and Sirtori, C. R. (2018). Lipid lowering drugs and inflammatory changes: an impact on cardiovascular outcomes? *Ann. Med.* 50, 461–484. doi: 10.1080/07853890.2018.1498118

Samuelsson, O., Mulec, H., Knight-Gibson, C., Attman, P. O., Kron, B., Larsson, R., et al. (1997). Lipoprotein abnormalities are associated with increased rate of progression of human chronic renal insufficiency. *Nephrol. Dial. Transplant.* 12, 1908–1915. doi: 10.1093/ndt/12.9.1908

Straub, B. K., Gyoengyoesi, B., Koenig, M., Hashani, M., Pawella, L. M., Herpel, E., et al. (2013). Adipophilin/perilipin-2 as a lipid droplet-specific marker for metabolically active cells and diseases associated with metabolic dysregulation. *Histopathology* 62, 617–631. doi: 10.1111/his.12038

Tannock L. (2000). *Dyslipidemia in Chronic Kidney Disease*. K. R. Feingold, B. Anawalt, A. Boyce, G. Chrousos, K. Dungan, A. Grossman, et al., eds (Endotext: South Dartmouth, MA).

Tonelli, M., Collins, D., Robins, S., Bloomfield, H., and Curhan, G. C. (2004). Effect of gemfibrozil on change in renal function in men with moderate chronic renal insufficiency and coronary disease. *Am. J. Kidney Dis.* 44, 832–839. doi: 10.1016/s0272-6386(04)01082-0

Turbeville, H. R., Johnson, A. C., Garrett, M. R., Dent, E. L., and Sasser, J. M. (2020). Nitric oxide and oxidative stress pathways do not contribute to sex differences in renal injury and function in Dahl SS/Jr rats. *Physiol. Rep.* 8:e14440.

Wahba, I. M., and Mak, R. H. (2007). Obesity and obesity-initiated metabolic syndrome: mechanistic links to chronic kidney disease. *Clin. J. Am. Soc. Nephrol.* 2, 550–562. doi: 10.2215/cjn.04071206

Weng, H., Ji, X., Endo, K., and Iwai, N. (2014). Pex11a deficiency is associated with a reduced abundance of functional peroxisomes and aggravated renal interstitial lesions. *Hypertension* 64, 1054–1060. doi: 10.1161/hypertensionaha.114.04094

Wesson, D. E., Kurtzman, N. A., and Frommer, J. P. (1985). Massive obesity and nephrotic proteinuria with a normal renal biopsy. *Nephron* 40, 235–237. doi: 10.1159/000183467

Wilson, M. W., Lay, L. T., Chow, C. K., Tai, H. H., Robertson, L. W., and Glauert, H. P. (1995). Altered hepatic eicosanoid concentrations in rats treated with the peroxisome proliferators ciprofibrate and perfluorodecanoic acid. *Arch. Toxicol.* 69, 491–497. doi: 10.1007/s002040050203

Wilson, T. W., Alonso-Galicia, M., and Roman, R. J. (1998). Effects of lipid-lowering agents in the Dahl salt-sensitive rat. *Hypertension* 31(1 Pt 2), 225–231. doi: 10.1161/01.hyp.31.1.225

Xu, N., Wang, Q., Jiang, S., Wang, Q., Hu, W., Zhou, S., et al. (2019). Fenofibrate improves vascular endothelial function and contractility in diabetic mice. *Redox. Biol.* 20, 87–97. doi: 10.1016/j.redox.2018.09.024

Yang, P., Xiao, Y., Luo, X., Zhao, Y., Zhao, L., Wang, Y., et al. (2017). Inflammatory stress promotes the development of obesity-related chronic kidney disease via CD36 in mice. *J. Lipid Res.* 58, 1417–1427. doi: 10.1194/jlr.m076216

Yoshinari, M., Asano, T., Kaori, S., Shi, A. H., Wakisaka, M., Iwase, M., et al. (1998). Effect of gemfibrozil on serum levels of prostacyclin and precursor fatty acids in hyperlipidemic patients with Type 2 diabetes. *Diabetes Res. Clin. Pract.* 42, 149–154. doi: 10.1016/s0168-8227(98)00107-7

Zhang, J., Zhu, J., Wei, J., Jiang, S., Xu, L., Qu, L., et al. (2020). New mechanism for the sex differences in salt-sensitive hypertension. *Hypertension* 75, 449–457. doi: 10.1161/hypertensionaha.119.13822

Conflict of Interest: The authors declare that the research was conducted in the absence of any commercial or financial relationships that could be construed as a potential conflict of interest.

frontiers in Physiology

MINI REVIEW
published: 09 November 2020
doi: 10.3389/fphys.2020.566871

Role of α2-Adrenoceptors in Hypertension: Focus on Renal Sympathetic Neurotransmitter Release, Inflammation, and Sodium Homeostasis

*Lydia Hering, Masudur Rahman, Sebastian A. Potthoff, Lars C. Rump and Johannes Stegbauer**

Department of Nephrology, Medical Faculty, University Hospital Düsseldorf, Heinrich-Heine-University Düsseldorf, Düsseldorf, Germany

OPEN ACCESS

Edited by:
Jennifer Sullivan, Augusta University, United States

Reviewed by:
Adriana Castello Costa Girardi, University of São Paulo, Brazil
Ulla Kopp, The University of Iowa, United States

***Correspondence:**
Johannes Stegbauer
lydia.hering@med.uni-duesseldorf.de

Specialty section:
This article was submitted to Renal and Epithelial Physiology, a section of the journal Frontiers in Physiology

Received: *28 May 2020*
Accepted: *19 October 2020*
Published: *09 November 2020*

Citation:
Hering L, Rahman M, Potthoff SA, Rump LC and Stegbauer J (2020) Role of α2-Adrenoceptors in Hypertension: Focus on Renal Sympathetic Neurotransmitter Release, Inflammation, and Sodium Homeostasis. Front. Physiol. 11:566871. doi: 10.3389/fphys.2020.566871

The kidney is extensively innervated by sympathetic nerves playing an important role in the regulation of blood pressure homeostasis. Sympathetic nerve activity is ultimately controlled by the central nervous system (CNS). Norepinephrine, the main sympathetic neurotransmitter, is released at prejunctional neuroeffector junctions in the kidney and modulates renin release, renal vascular resistance, sodium and water handling, and immune cell response. Under physiological conditions, renal sympathetic nerve activity (RSNA) is modulated by peripheral mechanisms such as the renorenal reflex, a complex interaction between efferent sympathetic nerves, central mechanism, and afferent sensory nerves. RSNA is increased in hypertension and, therefore, critical for the perpetuation of hypertension and the development of hypertensive kidney disease. Renal sympathetic neurotransmission is not only regulated by RSNA but also by prejunctional α2-adrenoceptors. Prejunctional α2-adrenoceptors serve as autoreceptors which, when activated by norepinephrine, inhibit the subsequent release of norepinephrine induced by a sympathetic nerve impulse. Deletion of α2-adrenoceptors aggravates hypertension ultimately by modulating renal pressor response and sodium handling. α2-adrenoceptors are also expressed in the vasculature, renal tubules, and immune cells and exert thereby effects related to vascular tone, sodium excretion, and inflammation. In the present review, we highlight the role of α2-adrenoceptors on renal sympathetic neurotransmission and its impact on hypertension. Moreover, we focus on physiological and pathophysiological functions mediated by non-adrenergic α2-adrenoceptors. In detail, we discuss the effects of sympathetic norepinephrine release and α2-adrenoceptor activation on renal sodium transporters, on renal vascular tone, and on immune cells in the context of hypertension and kidney disease.

Keywords: renal sympathetic nervous system, hypertension, α2-adrenoceptors, sodium transporters, renal vasculature resistance, renal sympathetic neurotransmission, immune cells, macrophages

INTRODUCTION

Hypertension is the second common cause for end stage renal disease (ESRD) and one of the major risk factors for morbidity and mortality worldwide (GBD 2016 Risk Factors Collaborators, 2017). The kidney is a master regulator of blood pressure homeostasis by regulating vascular tone, as well as sodium and water handling. Renal dysfunction, such as an increase in sodium and water retention, renin release, or renal vascular resistance, causes hypertension and, subsequently in the long-term run chronic kidney damage. The kidney is extensively innervated by sympathetic nerves, which are playing an important role in the regulation of blood pressure homeostasis (Dibona and Kopp, 1997; Dibona, 2000; Grassi et al., 2015). Renal nerves follow the renal arteries and innervate not only the vasculature but also the juxtaglomerular apparatus and the basement membrane of epithelial cells within the nephron. Therefore, it is not surprising that the main neurotransmitter neuropeptide Y (NPY), ATP, and norepinephrine, released at neuroeffector junctions in the kidney, mediate several physiological effects within the kidney. Sympathetic norepinephrine release induces renal vasoconstriction and stimulates renin release as well as tubular sodium and water reabsorption in the kidney. In hypertensive patients, renal sympathetic nerve activity (RSNA) is increased (Schlaich et al., 2009; Grassi et al., 2015). Thus, increased RSNA results in a reduction of renal blood flow and glomerular filtration rate (GFR), an increase in renal vascular resistance and tubular sodium and water reabsorption, and an increased release of renin, contributing to the development and maintenance of hypertension. Studies performed in patients with therapy resistant hypertension show a robust reduction in blood pressure after renal denervation, highlighting a critical crosstalk between the sympathetic nervous system and the kidney in hypertension (Schlaich et al., 2009; Kandzari et al., 2018; Vonend et al., 2018; Steinberg et al., 2020). In addition, evidence emerges that hypertension is at least in part an immune-mediated inflammatory disease. In this regard, several studies have shown a close interaction between the sympathetic nervous system and immune cell response in hypertension. Thus, reduction in RSNA by renal denervation reduces pro-inflammatory markers and immune cell migration in humans and mice (Xiao et al., 2015; Zaldivia et al., 2017).

To understand the role of RSNA in the development of hypertensive kidney disease, it is essential to know how RSNA affects mechanisms in the kidney controlling blood pressure homeostasis. The amount of neurotransmitter released from renal prejunctional nerve endings is not only controlled by the RSNA but also by prejunctional alpha2-adrenergic receptors (α2-adrenoceptors). Prejunctional α2-adrenoceptors serve as autoreceptors which, when activated by norepinephrine released from sympathetic nerve endings, inhibit the subsequent release of norepinephrine induced by a sympathetic nerve impulse (**Figures 1, 2**). Recent studies have highlighted the critical role of α2-adrenoceptors in the development of hypertension and kidney disease (Kim and Padanilam, 2013; Hering et al., 2020). However, α2-adrenergic receptors are not only expressed prejunctional on sympathetic nerves but also on non-adrenergic cells like immune cells, vascular smooth muscle cells (VSMCs), and renal epithelial cells. Activation of α2-adrenoceptors on these cells mediates a variety of effects, including inflammatory and fibrotic responses (Kim and Padanilam, 2013, 2015) and changes in renal vasoconstriction and VSMC turnover (Bohmann et al., 1995; Jackson et al., 2001, 2005), as well as altering sodium balance (Nord et al., 1987; Mansley et al., 2015) which may also influence blood pressure and kidney damage.

In the present review, we will highlight the role of α2-adrenoceptors on RSNA and its impact on hypertension. Moreover, we will focus on physiological and pathophysiological effects which were mediated by non-adrenergic α2-adrenoceptors with special respect to renal epithelial cells and immune cells.

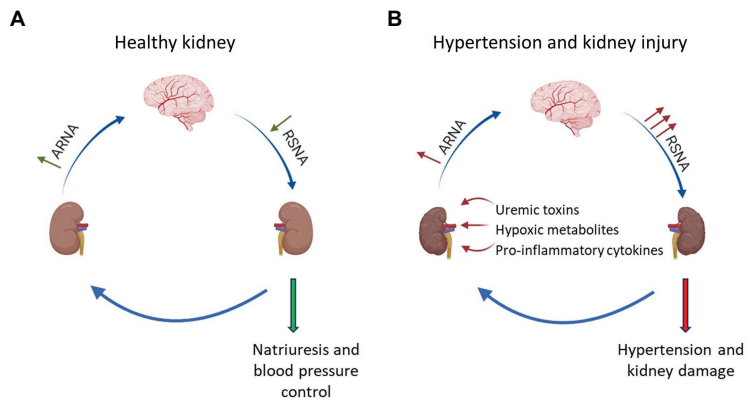

FIGURE 1 | Interaction between afferent renal nerves and renal sympathetic nerve activity in healthy and injured kidneys. **(A)** In healthy kidneys, increased renal sympathetic nerve activity (RSNA) leads to an activation of α1-adrenoceptors expressed in the renal pelvis, which increases afferent renal nerve activity (ARNA). Subsequently, inhibitory neurons within the brainstem and hypothalamus decrease RSNA *via* a negative feedback mechanism leading to natriuresis. **(B)** In hypertension or kidney injury, accumulation of pro-inflammatory cytokines, uremic toxins, or ischemic metabolites activate afferent renal nerves. Under these conditions, the negative feedback mechanism is dysregulated and increased ARNA results in a further activation of renal sympathetic nerves causing the progression of hypertension and hypertensive kidney disease.

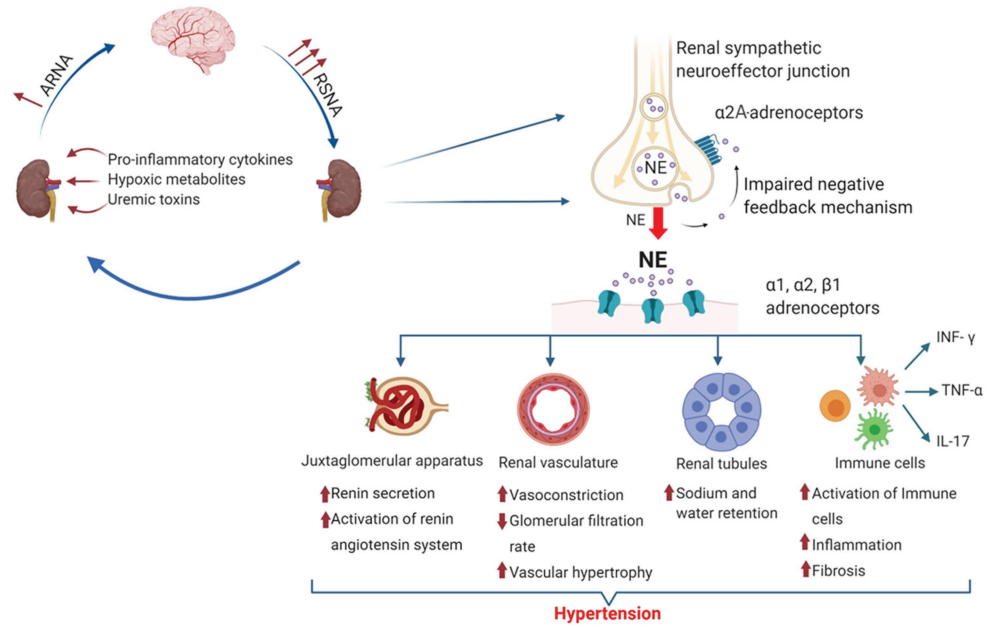

FIGURE 2 | Mechanisms causing hypertension by increased renal sympathetic norepinephrine release. The amount of norepinephrine released by prejunctional renal sympathetic nerves is controlled by RSNA and prejunctional α2A-adrenoceptors. Norepinephrine activates different adrenoceptors and exerts various physiological and pathophysiological effects leading to hypertension and chronic kidney disease (CKD). Thereby, norepinephrine activates the renin-angiotensin system (RAS) by stimulating renin release from the juxtaglomerular apparatus *via* β2-adrenergic receptor activation. Activation of α1- and α2-adrenoceptors causes vasoconstriction and increases renal vascular resistance, leading to vascular hypertrophy and a reduced glomerular filtration rate (GFR). In renal tubules, NE induced α1-, α2-, and β1-adrenergic receptor activation modulates the activity of different sodium transporters such as sodium hydrogen exchanger 3 (NHE3), Na^+-Cl^- Co-transporter (NCC), and epithelial sodium channel (ENaC) leading to decreased sodium excretion. In addition, norepinephrine modulates immune cell function and phenotype, leading to an increased infiltration into the kidney and an increased release of various pro-inflammatory cytokines such as interferon gamma (INF-γ), tumor necrosis factor alpha (TNF-α), and interleukin-17 (IL-17) aggravating the development of hypertension and renal fibrosis.

Most of the mechanisms described in the present review are based on animal studies.

CENTRAL EFFECTS AND POLYMORPHISM OF α2-ADRENOCEPTORS IN HYPERTENSION

While this review focuses on physiological and pathophysiological effects mediated by the prejunctional and non-adrenergic α2-adrenoceptors expressed in the kidney and on immune cells, it should be noted that all three α2-adrenoceptor subtypes are widely distributed throughout the central nervous system (CNS) that is ultimately regulating sympathetic nerve activity. Central acting α2-adrenoceptor agonists such as clonidine, guanabenz, and moxonidine are effective in the treatment of hypertension (Kanagy, 2005). These sympatholytic agents cross the blood-brain barrier and interact with central α2-adrenoceptors, leading to a reduction in sympathetic nerve activity and an increase in vagal activity. This change in sympathetic tone causes lower cardiac output and heart rate, reduced renin release, and subsequently a reduction in vascular resistance leading to blood pressure reduction (Dibona and Kopp, 1997; Hein, 2006; Schlaich et al., 2012; Sata et al., 2018). In addition, sympatholytic treatment induced by moxonidine has been shown to attenuate the progression of chronic kidney disease (CKD) in hypertensive patients and rats with advanced renal failure (Amann et al., 2000; Vonend et al., 2003). Whether these effects are in part mediated by non-central effects of α2-adrencoeptor activation is still not fully understood.

Several studies have investigated the association of hypertension and polymorphism of human ADRA2 gene. Genes of α2-adrenocepotor subtypes ADRA2A (α2A-adrenoceptors), ADRA2B (α2B-adrenoceptors), and ADRA2C (α2C-adrenoceptors) are located on chromosomes 10, 2, and 4, respectively. The ADRA2A 1780 C > T (rs553668) genotype is associated with an exercise-dependent aggravation of systolic as well as diastolic blood pressures in women (Nunes et al., 2014). In addition, the described polymorphism is associated with increased platelet aggregation and a marked decrease in sodium excretion. Both findings are common in essential hypertension (Freeman et al., 1995). Moreover, the −1291 C > G (rs1800544) substitution in the ADRA2A promoter region is responsible for reduced presynaptic autoinhibition of α2A-adrenoceptors, resulting in excessive norepinephrine concentration and, therefore, in an increased vascular resistance (Kelsey et al., 2012). Deletion polymorphisms or different variants of ADRA2B and ADRA2C are known to be related to endothelial dysfunction, heart failure, and hypertension (Heinonen et al., 2002; Small et al., 2002; von Wowern et al., 2004; Matsunaga et al., 2007).

In conclusion, there is substantial evidence that genetic variability in ADRA2A and ADRA2B genes influences α2-adrenoceptor function, leading to hypertension due to modulating vascular resistance, endothelial function, and sodium homeostasis in different cohorts.

MECHANISMS REGULATING RENAL SYMPATHETIC NERVE ACTIVITY

The regulation of RSNA is complex and involves central and peripheral mechanism. In general, the nerve activity of sympathetic premotor nuclei in the brainstem and hypothalamus [the rostral ventrolateral medulla (RVLM) and rostral ventromedial medulla (RVMM) as well as the paraventricular nucleus (PVN)] regulates RSNA. While the exact regulatory system of these central mechanisms is not the focus of the current review (Zheng and Patel, 2017), it is noteworthy that central nerve activity in the RVLM, RVMM, and PVN is modulated by neurotransmitters, local factors such as reactive oxygen species, cytokines, and angiotensin II (Ang II), as well as mechano- and chemo-sensitive renal afferent nerves which project to the RVLM *via* the nucleus tractus solitarius (NTS) and PVN. According to physiological or pathophysiological conditions, afferent renal nerve activity (ARNA) can either activate or inhibit sympathetic premotor activity and thereby RSNA *via* a positive or negative feedback mechanism (Dibona, 2000; Pyner, 2014; Zheng and Patel, 2017).

Under physiological conditions, RSNA is controlled by the renorenal reflex, which is considered as a negative feedback loop to maintain efferent RSNA (ERSNA) at low-levels, and thereby controlling natriuresis and blood pressure. This interaction between efferent sympathetic nerves and afferent sensory nerves is complex. Increased RSNA increases ARNA by activating mechanoceptors and chemoceptors, which in turn lowers efferent RSNA *via* inhibitory neurons which project to the RVLM (Dibona and Kopp, 1997; Kopp et al., 2007, 2011a). Norepinephrine acting on adrenoceptors located in the renal pelvis mediates the ERSNA-ARNA interaction. Activation of α1-adrenoceptors leads to an increase in ARNA whereas activation of α2-adrenoceptors decreases ARNA (Kopp et al., 2007). In this regard, Kopp et al. (2011b) showed that low sodium diet reduces ARNA *via* α2-adrenoceptor activation leading to an increase in RSNA and consequently to sodium reabsorption. In contrast, in spontaneous hypertensive rats (SHRs), this mechanism seems to be dysregulated. Thus, ARNA is reduced in SHRs due to an overactivation of α2-adrenoceptors in renal pelvic tissue. These studies suggest a direct role of renal pelvic α2-adrenoceptors in decreasing the responsiveness of ARNA to increased RSNA and thereby in the development of hypertension (Kopp et al., 2007, 2011a). In contrast, a recent study performed in α2A-adrenoceptor deficient mice showed that deletion of α2A-adrenoceptors accelerates Ang II-dependent hypertension rather than decreases blood pressure (Hering et al., 2020). This study suggests that the renorenal reflex mediated by α2-adrenoceptors is dysregulated or does not seem to play an important role in this experimental model of hypertension.

In hypertension as well as acute or chronic kidney damage, stimulation of renal nociceptive afferent nerves mediate an increase in sympathetic nerve activity leading to a further activation of RSNA and subsequently to a progression of hypertension and hypertensive kidney disease. Thus, several other factors such as pro-inflammatory cytokines (Banek et al., 2019), uremic toxins (Campese and Kogosov, 1995), and hypoxia (Dibona and Kopp, 1997; Soukhova-O'hare et al., 2006; Saha et al., 2019) can activate the chemo- and mechano-sensitive afferent nerves leading to an increased RSNA. Activation of afferent nerves under pathophysiological conditions such as acute kidney injury induced by a phenol injection into the kidney causes hypertension by increasing RSNA *via* afferent renal nerve stimulation (Ye et al., 2002a,b; Leong et al., 2006). The importance of an increased ARNA in the development and maintenance of hypertension in acute kidney disease or CKD is supported by several studies. For instance, in hypertensive rats treated with deoxycorticosterone acetate (DOCA) salt, increased ARNA seems to perpetuate hypertension as selective ablation of the afferent renal nerves reduces blood pressure (Banek et al., 2016). Additionally, in patients with kidney failure treated with dialysis, increased sympathetic nerve activity and thereby hypertension could only be reduced by a bilateral removal of the kidneys (Converse et al., 1992).

In summary, renal pelvic α1- and α2-adrenoceptors affect the renorenal reflex that regulates RSNA activity *via* ARNA under physiological conditions. In hypertension or kidney injury, ARNA is activated by other factors leading to an increase in RSNA *via* a positive feedback mechanism. Therefore, it seems plausible that in patients with hypertension increased RSNA is in part the consequence of increased ARNA and an important pathophysiological mechanism for the development of treatment resistant hypertension.

CELLULAR DISTRIBUTION OF α2-ADRENOCEPTORS IN THE KIDNEY

There are three different subtypes of α2-adrenoceptors (α2A-, α2B-, and α2C-adrenoceptors; Trendelenburg et al., 2001). The cellular distribution of these subtypes varies, but several *in vivo* and *in vitro* studies confirmed that the α2A-adrenoceptor is the predominant subtype involved in the regulation of renal and cardiac sympathetic neurotransmitter release (Hein et al., 1999; Vonend et al., 2007; Hoch et al., 2011). Based on early results from radioligand binding studies which were confirmed and expanded by deep sequencing analysis of microdissected rat renal tubules (Muntz et al., 1986; Nord et al., 1987; Lee et al., 2015), the cellular distribution of α2-adrenoceptor subtypes along the nephron is now well-described and summarized in **Figure 3** and **Table 1**. α2B-adrenoceptors are expressed in the proximal tubule whereas the α2A-adrenoceptors are located on the connecting tubule, collecting duct and the renal pelvis (Dibona and Kopp, 1997; Kopp et al., 2007; Lee et al., 2015; **Table 1**). In the glomerulus, only α2B-adrenoceptors seem to be expressed. However, the exact cellular localization is not known (Lee et al., 2015). In VSMCs, all three subtypes

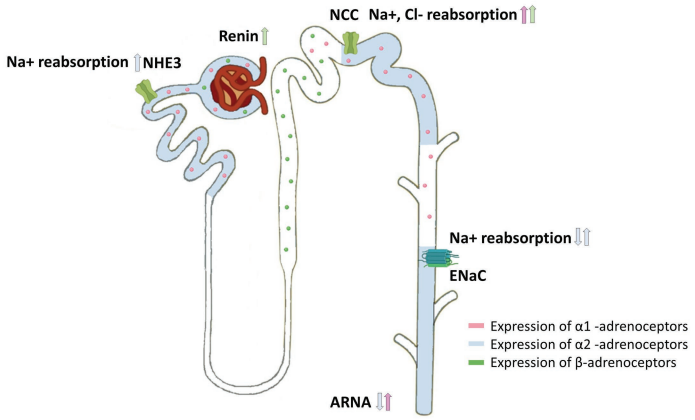

FIGURE 3 | Cellular distribution of adrenoceptors in the nephron and their effects on sodium transporters. Expression of α1-adrenoceptors (pink), α2-adrenoceptors (blue), and β-adrenoceptors (green) along the nephron showing the influence of renal sympathetic neurotransmission on sodium handling. Norepinephrine modulates sodium handling in the proximal (Na+/H+ 1 and 3 Exchange) and distal tubule (NCC and ENaC) by activating α1-adrenoceptors, α2-adrenoceptors, or β-adrenoceptors. Furthermore, α2-adrenoceptor activation within the renal pelvis decreases ARNA, whereas α1-adrenoceptor activation increases ARNA. β-adrenergic receptor activation induces renin release.

TABLE 1 | Gene expression levels of α1-, α2-, and β-adrenoceptor subtypes along a microdissected rat nephron are summarized.

	ADRA1			ADRA2			ADRB		
	A	*B*	*D*	*A*	*B*	*C*	1	2	3
Glomerulus		+			+		+++	+	
Proximal tubule		+			+++				
Henle/thick ascending limb							+++		
Distal convoluted tubule							+++		
Connecting tubule			#	+			++		
Cortical collecting duct			++	+					
Outer medullary collecting duct			+						
Inner medullary collecting duct				++					

Values are expressed as median reads per kilobase million (RPKM) with (+) being the lowest expression and (+++) being the highest expression of adrenoceptors (adapted from Lee et al. 2015). In a functional study, α1D-adrenoceptor expression (#) was found in non-microdissected renal cortex mRNA and linked to NCC regulation (Frame et al., 2019). +, represents lowest expression; +++, represents highest expression.

are expressed and involved in maintaining vascular tone. However, the distribution of the α2-adrenoceptor subtypes varies based on vascular bed and size of the vessels and species. High amount of α2A-adrenoceptor is expressed in large arteries like the aorta, whereas α2B-adrenoceptor is mostly distributed in small arteries and veins contributing to vasoconstriction (Faber et al., 2001; Kanagy, 2005). In addition, most immune cells express α2-adrenoceptors, with α2A- and α2B-adrenoceptors being the predominant subtypes. Thus, α2A- and α2B-adrenoceptors were detected on macrophages, T-cells, and natural killer cells from rodents and humans (Elenkov et al., 2000; Flierl et al., 2007; Scanzano and Cosentino, 2015; Harwani, 2018).

Taken together, α2-adrenoceptor subtypes are expressed along the nephron, on VSMC and on immune cells. When examining the physiological relevance of α2-adrenoceptors, one has to consider, that physiological activity of α2-adrenoceptors is at least in part dependent on their density (Duzic et al., 1992).

EFFECTS OF α2-ADRENOCEPTORS IN THE KIDNEY

The effects of α2-adrenoceptor function in renal physiology can be divided into two categories. First, prejunctional α2A- and α2C-adrenoceptors regulate renal sympathetic neurotransmitter release *via* an autoinhibitory feedback mechanism (Philipp et al., 2002). Activation of prejunctional α-adrenoceptors regulates not only the release of norepinephrine but also the release of ATP, neuropeptide Y (NPY; Burnstock, 1996; Lundberg, 1996; Oberhauser et al., 1999), and thereby modifies renin release, vascular tone, water and sodium handling, as well as the development of renal inflammation and fibrosis by activating different receptors (Dibona and Kopp, 1997; Amann et al., 2000; Bradley et al., 2003; Mcdonough, 2010; Sumi et al., 2010; Kim and Padanilam, 2013).

Second, norepinephrine (in part prejunctional released) activates α2-adrenoceptors expressed on non-adrenergic cells such as renal epithelial cells, VSMCs, or immune cells.

This α2-adrenoceptor activation modifies vascular tone, sodium handling, tubulo-interstitial fibrosis, and inflammation within the kidney (Starke et al., 1975; Gilsbach et al., 2009, 2011; Hoch et al., 2011; Kim and Padanilam, 2013; Jang et al., 2019; Hering et al., 2020; **Figure 2**).

Although the effects of prejunctional released ATP and NPY are not the focus of this review, their effects on renal physiological and pathophysiological mechanisms are important. NPY and ATP, released from sympathetic neurons upon α1- and α2-adrenoceptor signaling (Bradley et al., 2003; Vonend et al., 2007; Sumi et al., 2010), are described to play a role in hypertension (Thulin and Erlinge, 1995) and renal failure (Bald et al., 1997). Additionally to the pleiotropic effects of ATP on its P2 (purinergic type 2) receptors in the kidney (Solini et al., 2015), ATP can also be sequentially hydrolyzed by CD93 to ADP and AMP with AMP being further converted to adenosine by CD73. Alterations in the balance of nucleotides to nucleosides have major impacts on renal function, the development of hypertension, renal fibrosis, and inflammation (for a better overview, please refer to Kishore et al., 2018; Perry et al., 2019).

α2-Adrenoceptors in Renal Vasculature

Norepinephrine induced renal pressor response is predominantly mediated by α1-adrenoceptors. However, subpressor concentrations of Ang II revealed a role of α2-adrenoceptors in the renal vasoconstrictor response to norepinephrine (Bohmann et al., 1995). Moreover, α2-adrenoceptor activation potentiates Ang II-induced renal pressor response *in vivo* and *in vitro* of SHRs mainly through an α2-adrenoceptor-mediated RhoA-dependent mechanism (Jackson et al., 2001, 2005).

Beside a direct effect on renal vascular resistance, activation of both α1- and α2B-adrenoceptors by chronic renal sympathetic overactivity induces a phenotypic switch of VSMC into proliferative VSMC, leading to hypertrophy, renal vascular stiffness, and reduced renal blood flow (Wang et al., 2004; Huhtinen and Scheinin, 2008). This phenotypic switch is mediated by norepinephrine-induced reactive oxygen species *via* p38 MAPK activation (Kalyankrishna and Malik, 2003; Bleeke et al., 2004). However, the exact mechanism of how increased RSNA induces the development of preglomerular arteriolopathy is still not known. As proof that RSNA is involved in regulating renal pressor response, renal denervation reduced renal sympathetic neurotransmission results in a significant decrease of renal vascular resistance and a significant increase of renal plasma flow as well as GFR in SHR compared to non-denervated SHRs (Tomoda et al., 1997).

Summing up, α2- and α1-adrenoceptors are directly involved in renal vasoconstriction and indirectly by causing a phenotypic switch toward proliferative VSMC.

Effects of Renal Sympathetic Norepinephrine Release and Epithelial α2-Adrenoceptors on Sodium Homeostasis in Hypertension

Changes in renal vascular resistance and renal blood flow have been shown to influence sodium excretion (Sparks et al., 2015). RSNA affects natriuresis in several animal models and patients with resistant hypertension (Katayama et al., 2013; Poss et al., 2015; Hering et al., 2020). Renal sympathetic nerves also innervate renal tubules. As shown in **Figure 3**, α1-adrenoceptors, α2-adrenoceptors, and β1-adrenergic receptors are expressed along the nephron (Dibona and Kopp, 1997; Lee et al., 2015; Sata et al., 2018; Kiuchi et al., 2019). During chronic Ang II infusion, sodium and volume excretion was significantly reduced in α2A-adrenoceptor deficient mice compared to wildtype mice (Hering et al., 2020). This impaired natriuretic response was in part caused by an increased abundance of the cleaved epithelial sodium channel (ENaC)-alpha and -gamma subtypes, both markers for ENaC activation (Nguyen et al., 2013; Veiras et al., 2020). The role of α2-adrenoceptors in controlling natriuresis is still not fully understood, as it is hard to distinguish between α2-adrenoceptor-mediated effects and effects mediated by an increased renal sympathetic norepinephrine release. In general, it is widely accepted that increased sympathetic norepinephrine release increases ENaC expression and activation (Mansley et al., 2015; Hering et al., 2020). In contrast, renal denervation has been shown to reduce ENaC and aquaporin2 expression in a mouse model of heart failure, suggesting that the amount of renal norepinephrine release is relevant for the regulation of ENaC expression (Zheng et al., 2019). Besides that, several reports demonstrate an interaction between α2-adrenoceptor activation and regulation of ENaC abundance and activation. Thus, α2-adrenoceptor activation inhibits vasopressin-induced cAMP generation (Chabardes et al., 1984; Krothapalli and Suki, 1984), which in turn decreases vasopressin induced ENaC activation (Roos et al., 2013). In contrast, activation of basolateral α2-adrenoceptors on principal cells increases ENaC activity *in vitro* (Mansley et al., 2015). Thus, only selective deletion of α2A-adrenoceptors from the collecting duct will show evidence about the impact of α2-adrenoceptors on ENaC function.

In addition, sympathetic norepinephrine influences the expression and activation of the Na^+Cl^- co-transporter (NCC) and, thereby, sodium excretion in the distal nephron and the development of hypertension. Norepinephrine stimulates NCC expression through an activation of basolateral Kir4.1/Kir5.1 potassium channel *via* beta-adrenergic receptor activation (Duan et al., 2019). Activation of α1-adrenoceptors inhibits the suppression of NCC during high salt intake *via* a WNK/SPAK/OxSR1-dependent signaling pathway in rat kidneys (Frame et al., 2019). Dephosphorylation of NCC by the protein phosphatase 1 can be inhibited through a protein kinase A-dependent activation of the protein phosphatase 1 inhibitor *via* β1-adrenergic receptor activation (Penton et al., 2019).

In proximal tubules, acute increase in sympathetic norepinephrine has been shown to stimulate sodium hydrogen exchanger 1 and 3 and, thereby, sodium reabsorption most likely by activating α2-adrenoceptors (Nord et al., 1987; Leong et al., 2006; Healy et al., 2014; Lee et al., 2015). In this context, short term stimulation of renal nerves has been shown to activate sodium hydrogen exchanger 3 (NHE3)-mediated sodium reabsorption and the intrarenal renin-angiotensin system (RAS). As this effect was blocked by losartan, a selective Ang II type

1 receptor blocker, the authors suggested that this mechanism is in part mediated *via* an intrarenal RAS activation induced by ERSA (Pontes et al., 2015). NHE3 function is negatively correlated to its phosphorylation status at the PKA site (serine 552) that effects subcellular trafficking and, therefore, its activity (Kocinsky et al., 2005). Ang II treatment decreased cAMP/PKA signaling and, therefore, the phosphorylation at serin 552 leading to increased NHE3 activity (Crajoinas et al., 2016). In contrast, increased sympathetic norepinephrine release in long-term Ang II-dependent hypertension suppresses NHE3 abundance (Nguyen et al., 2013; Hering et al., 2020; Veiras et al., 2020). This suppression of NHE3 is a compensatory natriuretic mechanism of the kidney to regulate blood pressure in chronic hypertension and override the stimulatory effect of Ang II on NHE3 (Mcdonough, 2010; Mcdonough and Nguyen, 2015).

This section highlights the effect of renal sympathetic norepinephrine release on renal sodium transport. The amount of prejunctional released norepinephrine regulates sodium homeostasis in the kidney. There is strong evidence that α2-adrenoceptors play a role in regulating ENaC function, whereas α1- and β-adrenoceptors are involved in the regulation of NCC.

ROLE OF RENAL SYMPATHETIC NEUROTRANSMISSION AND α2-ADRENOCEPTOR SIGNALING ON IMMUNE CELL FUNCTION IN HYPERTENSION

Although renal sympathetic overactivity plays an important role in the progression of hypertensive kidney disease, its role in the development of fibrosis and inflammation leading to CKD is not fully understood (Veelken et al., 2008; Jang et al., 2019). The therapeutic strategy of renal denervation preventing renal failure may also be at least in part due to its protective anti-inflammatory effect attenuating renal inflammation and fibrosis (Veelken et al., 2008; Kim and Padanilam, 2013). Animal studies show robust evidence that the sympathetic nervous system interacts with the immune system and, thereby, modulates the inflammatory response in the target organ, leading to fibrosis und progression of the underlying disease (Andersson and Tracey, 2012; Carnevale et al., 2016).

In lymphoid organs, sympathetic neurons release norepinephrine which has a direct effect on immune cells by modulating T-cell polarization, lymphocyte trafficking, and proliferation as well as cytokine production *via* adrenoceptor activation. Moreover, immune cell trafficking depends also on regional blood flow which is under tight control of the local sympathetic nerve activity (Elenkov et al., 2000). Although all three adrenoceptor subtypes are expressed within the immune system, β-adrenergic receptor-mediated effects are studied most extensively with special interest for the β2-adrenoceptor subtype due to its anti-inflammatory effects (Elenkov et al., 2000). The role of α2-adrenoceptors on immune cells is still not well-examined but comes into the focus of research (Elenkov et al., 2000; Flierl et al., 2007; Kim and Padanilam, 2013).

A very recent study showed that increased sympathetic nerve activity caused by experimental hypertension increases T-cell homing of effector memory T-cells in the bone marrow *via* β2-adrenergic receptor activation (Xiao et al., 2020). When hypertensive stimuli persist, these effector memory T-cells infiltrate into the vasculature and the kidney and release cytokines like interferon gamma (INF-γ), interleukin-17 (IL-17), and tumor necrosis factor alpha (TNF-α), which aggravate hypertension (Madhur et al., 2010). INF-γ, TNF-α, and IL-17 accelerate vascular damage and water reabsorption by affecting different sodium transporters along the distal nephron (Sriramula et al., 2008; Kamat et al., 2015; Wu et al., 2016). In addition, increased RSNA in low-dose Ang II-dependent hypertension activates antigen presenting cells and, subsequently, T-cells infiltrating hypertensive kidneys. Reduction in RSNA by renal denervation significantly reduced T-cell and macrophage infiltration, attenuated renal fibrosis, and improved renal function (Xiao et al., 2015). These results clearly demonstrate that renal sympathetic nerves mediate renal inflammation and T-cell activation in hypertension. However, there is conflicting evidence concerning the distinctive contribution of renal afferent and efferent nerves on the described anti-inflammatory effects of RDN. Xiao et al. (2015) could not find a contribution of afferent nerves on Ang II-induced hypertension and renal inflammation, whereas Banek showed evidence that renal afferent nerves modulate at least in part renal inflammation in DOCA-salt hypertension (Banek et al., 2016, 2019). In another study, performed in global α2A-deficent mice chronically infused with a high dose of Ang II, increased renal sympathetic norepinephrine release impairs renal function and aggravates hypertension as well as renal fibrosis without affecting the amount of infiltrating immune cells (Hering et al., 2020). At first glance, these results seem to be conflicting as several studies have shown that increased RSNA activates a pro-inflammatory immune cell response leading to immune cell infiltration and an aggravation of renal fibrosis and hypertension (Kim and Padanilam, 2013, 2015; Xiao et al., 2015; Banek et al., 2019). However, α2-adrenoceptors also seem to regulate immune cell function, and activation of α2-adrenoceptors seems to induce a pro-inflammatory immune response (Scanzano and Cosentino, 2015). Thus, inhibition of α2-adrenoceptor on alveolar macrophages reduces the release of several cytokines like TNF-α, IL-6, or IL-1β (Flierl et al., 2007), whereas activation of α2-adrenoceptors on macrophages has been shown to increase TNF-α production (Spengler et al., 1994). In addition, inhibition of renal a2-adrenoceptors reduces renal inflammation and infiltration of neutrophils and macrophages in obstructed murine kidneys, whereas direct infusion of norepinephrine in denervated kidneys induced a fibrotic response similar to innervated non-infused kidneys. These results suggest an important role of norepinephrine signaling through renal α2-adrenoceptors in fibrogenesis and mediating inflammation (Kim and Padanilam, 2013). In line with these observations, a recent study could show that α2A-adrenoceptor deficiency reduced lung injury in mice and

decreased lung inflammation by reducing immune cell infiltration as well as decreasing pro-inflammatory cytokines (Cong et al., 2020).

Activation of α1- and α2-adrenoceptors seems to induce polarization toward the inflammatory M1 phenotype (Grisanti et al., 2011; Harwani, 2018), and activated macrophages have been shown to accelerate hypertension (Wenzel et al., 2011). In contrast to the innate immune system, adrenoceptor functions on T-cells are less well described and conflicting. On one side, activation of β2-adrenergic receptors activates the homing of $CD8^+$ effector memory T-cells and an upregulation of CCL19 and CCL21 in hypertension. On the other side, activation of β2-adrenergic receptors in experimental autoimmune disease or *in vitro* reduces the T-cell response to sympathetic norepinephrine and decreases the release of INF-γ and TNF-α from $CD8^+$ T-cells (Estrada et al., 2016; Araujo et al., 2019). Although α2-adrenoceptors are expressed on T-cells, their role in T-cell function in general and particularly in hypertension is not well understood. Early studies have shown that reduced peripheral blood T-cell mitogenesis is caused by activation of peripheral α2-adrenoceptors (Felsner et al., 1995). Activation of α2-adrenoceptors expressed on dendritic cells reduces induction of T-cell proliferation (Araujo et al., 2019). In patients undergoing surgery, activation of α2-adrenoceptors shifted the Th1/Th2 and the Treg/Th17 cytokine balance toward a Th1 and Th17 response, respectively, suggesting a pro-inflammatory rather than an anti-inflammatory effect on human T-cells (Lee et al., 2018).

In conclusion, increased sympathetic norepinephrine release seems to activate T-cell response through a complex interaction with the innate immune system leading to an aggravation of hypertension and CKD. The role of adrenergic receptors in modulating the immune response in hypertensive kidney damage needs further investigation but seems to be an interesting therapeutic approach, as selective agonists and antagonists of α- and β-adrenergic receptors are already in clinical practice.

CONCLUSION AND LIMITATION

Renal sympathetic nerve activity plays a major role in blood pressure homeostasis. Regulation of RSNA describes a complex interaction between afferent nerve activity and central mechanism. Under physiological conditions, RSNA is controlled by afferent renal mechano- and chemo-sensitive nerves by the renorenal reflex *via* a negative feedback mechanism. Thereby, ARNA is regulated in part by α1- or α2-adrenoceptors located in the renal pelvis. During hypertension or kidney damage, this negative feedback mechanism is disturbed. Activation of afferent renal nerves induced by several factors including uremic toxin, pro-inflammatory cytokines, and hypoxia injury increases RSNA and is therefore an important factor for the development of resistant hypertension and kidney disease.

Increased sympathetic nerve activity results in an elevated release of sympathetic neurotransmitter. Prejunctional α2-adrenoceptors control renal sympathetic neurotransmission *via* a negative feedback mechanism. Deletion or pharmacological inhibition of α2-adrenoceptors accelerates hypertension and kidney injury through multiple mechanisms. First, increased sympathetic neurotransmission particularly norepinephrine release increases renin release, renal vascular tone, sodium reabsorption, and inflammation through an activation of α- and β-adrenoceptors in the kidney and on immune cells. Second, non-adrenergic α2-adrenoceptor activation on renal epithelial cells, VSMCs, or immune cells directly modulates vascular tone, sodium balance, and immune cell response in the kidney. Based on this complex interaction between the well-studied function of prejunctional α2-adrenoceptors and the multiple effects of adrenoceptors activation on non-adrenergic cells in the kidney and on immune cells, the exact physiological and pathophysiological role of α2-adrenoceptor is still not fully understood and needs further studies in where α2-adrenoceptor function can be examined cell specific.

AUTHOR CONTRIBUTIONS

All authors listed have made a substantial, direct and intellectual contribution to the work, and approved it for publication.

FUNDING

This study was supported through a research grant of the German Research Foundation (DFG) to JS (STE 2042/1-1).

REFERENCES

Amann, K., Rump, L. C., Simonaviciene, A., Oberhauser, V., Wessels, S., Orth, S. R., et al. (2000). Effects of low dose sympathetic inhibition on glomerulosclerosis and albuminuria in subtotally nephrectomized rats. *J. Am. Soc. Nephrol.* 11, 1469–1478.

Andersson, U., and Tracey, K. J. (2012). Neural reflexes in inflammation and immunity. *J. Exp. Med.* 209, 1057–1068. doi: 10.1084/jem.20120571

Araujo, L. P., Maricato, J. T., Guereschi, M. G., Takenaka, M. C., Nascimento, V. M., De Melo, F. M., et al. (2019). The sympathetic nervous system mitigates CNS autoimmunity via beta2-adrenergic receptor signaling in immune cells. *Cell Rep.* 28, 3120.e5–3130.e5. doi: 10.1016/j.celrep.2019.08.042

Bald, M., Gerigk, M., and Rascher, W. (1997). Elevated plasma concentrations of neuropeptide Y in children and adults with chronic and terminal renal failure. *Am. J. Kidney Dis.* 30, 23–27. doi: 10.1016/s0272-6386(97)90560-6

Banek, C. T., Gauthier, M. M., Van Helden, D. A., Fink, G. D., and Osborn, J. W. (2019). Renal inflammation in DOCA-salt hypertension. *Hypertension* 73, 1079–1086. doi: 10.1161/HYPERTENSIONAHA.119.12762

Banek, C. T., Knuepfer, M. M., Foss, J. D., Fiege, J. K., Asirvatham-Jeyaraj, N., Van Helden, D., et al. (2016). Resting afferent renal nerve discharge and renal inflammation: elucidating the role of afferent and efferent renal nerves in deoxycorticosterone acetate salt hypertension. *Hypertension* 68, 1415–1423. doi: 10.1161/HYPERTENSIONAHA.116.07850

Bleeke, T., Zhang, H., Madamanchi, N., Patterson, C., and Faber, J. E. (2004). Catecholamine-induced vascular wall growth is dependent on generation of reactive oxygen species. *Circ. Res.* 94, 37–45. doi: 10.1161/01.RES.0000109412.80157.7D

Bohmann, C., Rist, W., Schollmeyer, P., and Rump, L. C. (1995). Low concentrations of angiotensin II unmask vasoconstrictory alpha 2-adrenoceptors in isolated perfused kidneys of spontaneously hypertensive rats. *Cardiovasc. Res.* 30, 857–865.

Bradley, E., Law, A., Bell, D., and Johnson, C. D. (2003). Effects of varying impulse number on cotransmitter contributions to sympathetic vasoconstriction in rat tail artery. *Am. J. Physiol. Heart Circ. Physiol.* 284, H2007–H2014. doi: 10.1152/ajpheart.01061.2002

Burnstock, G. (1996). Development and perspectives of the purinoceptor concept. *J. Auton. Pharmacol.* 16, 295–302. doi: 10.1111/j.1474-8673.1996.tb00039.x

Campese, V. M., and Kogosov, E. (1995). Renal afferent denervation prevents hypertension in rats with chronic renal failure. *Hypertension* 25, 878–882. doi: 10.1161/01.hyp.25.4.878

Carnevale, D., Perrotta, M., Pallante, F., Fardella, V., Iacobucci, R., Fardella, S., et al. (2016). A cholinergic-sympathetic pathway primes immunity in hypertension and mediates brain-to-spleen communication. *Nat. Commun.* 7:13035. doi: 10.1038/ncomms13035

Chabardes, D., Montegut, M., Imbert-Teboul, M., and Morel, F. (1984). Inhibition of alpha 2-adrenergic agonists on AVP-induced cAMP accumulation in isolated collecting tubule of the rat kidney. *Mol. Cell. Endocrinol.* 37, 263–275. doi: 10.1016/0303-7207(84)90096-0

Cong, Z., Li, D., Lv, X., Yang, C., Zhang, Q., Wu, C., et al. (2020). alpha2A-adrenoceptor deficiency attenuates lipopolysaccharide-induced lung injury by increasing norepinephrine levels and inhibiting alveolar macrophage activation in acute respiratory distress syndrome. *Clin. Sci.* 134, 1957–1971. doi: 10.1042/CS20200586

Converse, R. L. Jr., Jacobsen, T. N., Toto, R. D., Jost, C. M., Cosentino, F., Fouad-Tarazi, F., et al. (1992). Sympathetic overactivity in patients with chronic renal failure. *N. Engl. J. Med.* 327, 1912–1918. doi: 10.1056/NEJM199212313272704

Crajoinas, R. O., Polidoro, J. Z., Carneiro De Morais, C. P., Castelo-Branco, R. C., and Girardi, A. C. (2016). Angiotensin II counteracts the effects of cAMP/PKA on NHE3 activity and phosphorylation in proximal tubule cells. *Am. J. Physiol. Cell Physiol.* 311, C768–C776. doi: 10.1152/ajpcell.00191.2016

Dibona, G. F. (2000). Neural control of the kidney: functionally specific renal sympathetic nerve fibers. *Am. J. Physiol. Regul. Integr. Comp. Physiol.* 279, R1517–R1524. doi: 10.1152/ajpregu.2000.279.5.R1517

Dibona, G. F., and Kopp, U. C. (1997). Neural control of renal function. *Physiol. Rev.* 77, 75–197. doi: 10.1152/physrev.1997.77.1.75

Duan, X. P., Gu, L., Xiao, Y., Gao, Z. X., Wu, P., Zhang, Y. H., et al. (2019). Norepinephrine-induced stimulation of Kir4.1/Kir5.1 is required for the activation of NaCl transporter in distal convoluted tubule. *Hypertension* 73, 112–120. doi: 10.1161/HYPERTENSIONAHA.118.11621

Duzic, E., Coupry, I., Downing, S., and Lanier, S. M. (1992). Factors determining the specificity of signal transduction by guanine nucleotide-binding protein-coupled receptors. I. Coupling of alpha 2-adrenergic receptor subtypes to distinct G-proteins. *J. Biol. Chem.* 267, 9844–9851.

Elenkov, I. J., Wilder, R. L., Chrousos, G. P., and Vizi, E. S. (2000). The sympathetic nerve—an integrative interface between two supersystems: the brain and the immune system. *Pharmacol. Rev.* 52, 595–638.

Estrada, L. D., Agac, D., and Farrar, J. D. (2016). Sympathetic neural signaling via the beta2-adrenergic receptor suppresses T-cell receptor-mediated human and mouse CD8(+) T-cell effector function. *Eur. J. Immunol.* 46, 1948–1958. doi: 10.1002/eji.201646395

Faber, J. E., Yang, N., and Xin, X. (2001). Expression of alpha-adrenoceptor subtypes by smooth muscle cells and adventitial fibroblasts in rat aorta and in cell culture. *J. Pharmacol. Exp. Ther.* 298, 441–452.

Felsner, P., Hofer, D., Rinner, I., Porta, S., Korsatko, W., and Schauenstein, K. (1995). Adrenergic suppression of peripheral blood T cell reactivity in the rat is due to activation of peripheral alpha 2-receptors. *J. Neuroimmunol.* 57, 27–34. doi: 10.1016/0165-5728(94)00158-k

Flierl, M. A., Rittirsch, D., Nadeau, B. A., Chen, A. J., Sarma, J. V., Zetoune, F. S., et al. (2007). Phagocyte-derived catecholamines enhance acute inflammatory injury. *Nature* 449, 721–725. doi: 10.1038/nature06185

Frame, A. A., Puleo, F., Kim, K., Walsh, K. R., Faudoa, E., Hoover, R. S., et al. (2019). Sympathetic regulation of NCC in norepinephrine-evoked salt-sensitive hypertension in Sprague-Dawley rats. *Am. J. Physiol. Renal Physiol.* 317, F1623–F1636. doi: 10.1152/ajprenal.00264.2019

Freeman, K., Farrow, S., Schmaier, A., Freedman, R., Schork, T., and Lockette, W. (1995). Genetic polymorphism of the alpha 2-adrenergic receptor is associated with increased platelet aggregation, baroreceptor sensitivity, and salt excretion in normotensive humans. *Am. J. Hypertens.* 8, 863–869. doi: 10.1016/0895-7061(95)00155-I

GBD 2016 Risk Factors Collaborators (2017). Global, regional, and national comparative risk assessment of 84 behavioural, environmental and occupational, and metabolic risks or clusters of risks, 1990-2016: a systematic analysis for the global burden of disease study 2016. *Lancet* 390, 1345–1422. doi: 10.1016/S0140-6736(17)32366-8

Gilsbach, R., Albarran-Juarez, J., and Hein, L. (2011). Pre- versus post-synaptic signaling by alpha(2)-adrenoceptors. *Curr. Top. Membr.* 67, 139–160. doi: 10.1016/B978-0-12-384921-2.00007-0

Gilsbach, R., Roser, C., Beetz, N., Brede, M., Hadamek, K., Haubold, M., et al. (2009). Genetic dissection of alpha2-adrenoceptor functions in adrenergic versus nonadrenergic cells. *Mol. Pharmacol.* 75, 1160–1170. doi: 10.1124/mol.109.054544

Grassi, G., Mark, A., and Esler, M. (2015). The sympathetic nervous system alterations in human hypertension. *Circ. Res.* 116, 976–990. doi: 10.1161/CIRCRESAHA.116.303604

Grisanti, L. A., Perez, D. M., and Porter, J. E. (2011). Modulation of immune cell function by alpha(1)-adrenergic receptor activation. *Curr. Top. Membr.* 67, 113–138. doi: 10.1016/B978-0-12-384921-2.00006-9

Harwani, S. C. (2018). Macrophages under pressure: the role of macrophage polarization in hypertension. *Transl. Res.* 191, 45–63. doi: 10.1016/j.trsl.2017.10.011

Healy, V., Thompson, C., and Johns, E. J. (2014). The adrenergic regulation of proximal tubular Na^+/H^+ exchanger 3 in the rat. *Acta Physiol.* 210, 678–689. doi: 10.1111/apha.12181

Hein, L. (2006). Adrenoceptors and signal transduction in neurons. *Cell Tissue Res.* 326, 541–551. doi: 10.1007/s00441-006-0285-2

Hein, L., Altman, J. D., and Kobilka, B. K. (1999). Two functionally distinct alpha2-adrenergic receptors regulate sympathetic neurotransmission. *Nature* 402, 181–184. doi: 10.1038/46040

Heinonen, P., Jartti, L., Jarvisalo, M. J., Pesonen, U., Kaprio, J. A., Ronnemaa, T., et al. (2002). Deletion polymorphism in the alpha2B-adrenergic receptor gene is associated with flow-mediated dilatation of the brachial artery. *Clin. Sci.* 103, 517–524. doi: 10.1042/cs1030517

Hering, L., Rahman, M., Hoch, H., Marko, L., Yang, G., Reil, A., et al. (2020). Alpha2A-adrenoceptors modulate renal sympathetic neurotransmission and protect against hypertensive kidney disease. *J. Am. Soc. Nephrol.* 31, 783–798. doi: 10.1681/ASN.2019060599

Hoch, H., Stegbauer, J., Potthoff, S. A., Hein, L., Quack, I., Rump, L. C., et al. (2011). Regulation of renal sympathetic neurotransmission by renal alpha(2A)-adrenoceptors is impaired in chronic renal failure. *Br. J. Pharmacol.* 163, 438–446. doi: 10.1111/j.1476-5381.2011.01223.x

Huhtinen, A., and Scheinin, M. (2008). Expression and characterization of the human alpha 2B-adrenoceptor in a vascular smooth muscle cell line. *Eur. J. Pharmacol.* 587, 48–56. doi: 10.1016/j.ejphar.2008.03.049

Jackson, E. K., Andresen, B. T., Seasholtz, T. M., Zhu, C., and Romero, G. G. (2005). Enhanced activation of RhoA by angiotensin II in SHR preglomerular microvascular smooth muscle cells. *J. Cardiovasc. Pharmacol.* 45, 283–285. doi: 10.1097/01.fjc.0000155383.83927.9f

Jackson, E. K., Herzer, W. A., Kost, C. K. Jr., and Vyas, S. J. (2001). Enhanced interaction between renovascular alpha(2)-adrenoceptors and angiotensin II receptors in genetic hypertension. *Hypertension* 38, 353–360. doi: 10.1161/01.hyp.38.3.353

Jang, H. S., Kim, J., and Padanilam, B. J. (2019). Renal sympathetic nerve activation via alpha2-adrenergic receptors in chronic kidney disease progression. *Kidney Res. Clin. Pract.* 38, 6–14. doi: 10.23876/j.krcp.18.0143

Kalyankrishna, S., and Malik, K. U. (2003). Norepinephrine-induced stimulation of p38 mitogen-activated protein kinase is mediated by arachidonic acid metabolites generated by activation of cytosolic phospholipase a(2) in vascular smooth muscle cells. *J. Pharmacol. Exp. Ther.* 304, 761–772. doi: 10.1124/jpet.102.040949

Kamat, N. V., Thabet, S. R., Xiao, L., Saleh, M. A., Kirabo, A., Madhur, M. S., et al. (2015). Renal transporter activation during angiotensin-II hypertension is blunted in interferon-gamma−/− and interleukin-17A−/− mice. *Hypertension* 65, 569–576. doi: 10.1161/HYPERTENSIONAHA.114.04975

Kanagy, N. L. (2005). Alpha(2)-adrenergic receptor signalling in hypertension. *Clin. Sci.* 109, 431–437. doi: 10.1042/CS20050101

Kandzari, D. E., Bohm, M., Mahfoud, F., Townsend, R. R., Weber, M. A., Pocock, S., et al. (2018). Effect of renal denervation on blood pressure in the presence of antihypertensive drugs: 6-month efficacy and safety results

from the SPYRAL HTN-ON MED proof-of-concept randomised trial. *Lancet* 391, 2346–2355. doi: 10.1016/S0140-6736(18)30951-6

Katayama, T., Sueta, D., Kataoka, K., Hasegawa, Y., Koibuchi, N., Toyama, K., et al. (2013). Long-term renal denervation normalizes disrupted blood pressure circadian rhythm and ameliorates cardiovascular injury in a rat model of metabolic syndrome. *J. Am. Heart Assoc.* 2:e000197. doi: 10.1161/JAHA.113.000197

Kelsey, R. M., Alpert, B. S., Dahmer, M. K., Krushkal, J., and Quasney, M. W. (2012). Alpha-adrenergic receptor gene polymorphisms and cardiovascular reactivity to stress in black adolescents and young adults. *Psychophysiology* 49, 401–412. doi: 10.1111/j.1469-8986.2011.01319.x

Kim, J., and Padanilam, B. J. (2013). Renal nerves drive interstitial fibrogenesis in obstructive nephropathy. *J. Am. Soc. Nephrol.* 24, 229–242. doi: 10.1681/ASN.2012070678

Kim, J., and Padanilam, B. J. (2015). Renal denervation prevents long-term sequelae of ischemic renal injury. *Kidney Int.* 87, 350–358. doi: 10.1038/ki.2014.300

Kishore, B. K., Robson, S. C., and Dwyer, K. M. (2018). CD39-adenosinergic axis in renal pathophysiology and therapeutics. *Purinergic Signal* 14, 109–120. doi: 10.1007/s11302-017-9596-x

Kiuchi, M. G., Ho, J. K., Nolde, J. M., Gavidia, L. M. L., Carnagarin, R., Matthews, V. B., et al. (2019). Sympathetic activation in hypertensive chronic kidney disease—a stimulus for cardiac arrhythmias and sudden cardiac death? *Front. Physiol.* 10:1546. doi: 10.3389/fphys.2019.01546

Kocinsky, H. S., Girardi, A. C., Biemesderfer, D., Nguyen, T., Mentone, S., Orlowski, J., et al. (2005). Use of phospho-specific antibodies to determine the phosphorylation of endogenous Na+/H+ exchanger NHE3 at PKA consensus sites. *Am. J. Physiol. Renal Physiol.* 289, F249–F258. doi: 10.1152/ajprenal.00082.2004

Kopp, U. C., Cicha, M. Z., and Smith, L. A. (2011a). Impaired interaction between efferent and afferent renal nerve activity in SHR involves increased activation of alpha2-adrenoceptors. *Hypertension* 57, 640–647. doi: 10.1161/HYPERTENSIONAHA.110.166595

Kopp, U. C., Cicha, M. Z., Smith, L. A., Mulder, J., and Hokfelt, T. (2007). Renal sympathetic nerve activity modulates afferent renal nerve activity by PGE2-dependent activation of alpha1- and alpha2-adrenoceptors on renal sensory nerve fibers. *Am. J. Physiol. Regul. Integr. Comp. Physiol.* 293, R1561–R1572. doi: 10.1152/ajpregu.00485.2007

Kopp, U. C., Cicha, M. Z., Smith, L. A., Ruohonen, S., Scheinin, M., Fritz, N., et al. (2011b). Dietary sodium modulates the interaction between efferent and afferent renal nerve activity by altering activation of alpha2-adrenoceptors on renal sensory nerves. *Am. J. Physiol. Regul. Integr. Comp. Physiol.* 300, R298–R310. doi: 10.1152/ajpregu.00469.2010

Krothapalli, R. K., and Suki, W. N. (1984). Functional characterization of the alpha adrenergic receptor modulating the hydroosmotic effect of vasopressin on the rabbit cortical collecting tubule. *J. Clin. Invest.* 73, 740–749. doi: 10.1172/JCI111267

Lee, J. W., Chou, C. L., and Knepper, M. A. (2015). Deep sequencing in microdissected renal tubules identifies nephron segment-specific transcriptomes. *J. Am. Soc. Nephrol.* 26, 2669–2677. doi: 10.1681/ASN.2014111067

Lee, J. M., Han, H. J., Choi, W. K., Yoo, S., Baek, S., and Lee, J. (2018). Immunomodulatory effects of intraoperative dexmedetomidine on T helper 1, T helper 2, T helper 17 and regulatory T cells cytokine levels and their balance: a prospective, randomised, double-blind, dose-response clinical study. *BMC Anesthesiol.* 18:164. doi: 10.1186/s12871-018-0625-2

Leong, P. K., Yang, L. E., Landon, C. S., Mcdonough, A. A., and Yip, K. P. (2006). Phenol injury-induced hypertension stimulates proximal tubule Na^+/H^+ exchanger activity. *Am. J. Physiol. Renal Physiol.* 290, F1543–F1550. doi: 10.1152/ajprenal.00392.2005

Lundberg, J. M. (1996). Pharmacology of cotransmission in the autonomic nervous system: integrative aspects on amines, neuropeptides, adenosine triphosphate, amino acids and nitric oxide. *Pharmacol. Rev.* 48, 113–178.

Madhur, M. S., Lob, H. E., Mccann, L. A., Iwakura, Y., Blinder, Y., Guzik, T. J., et al. (2010). Interleukin 17 promotes angiotensin II-induced hypertension and vascular dysfunction. *Hypertension* 55, 500–507. doi: 10.1161/HYPERTENSIONAHA.109.145094

Mansley, M. K., Neuhuber, W., Korbmacher, C., and Bertog, M. (2015). Norepinephrine stimulates the epithelial Na^+ channel in cortical collecting duct cells via alpha2-adrenoceptors. *Am. J. Physiol. Renal Physiol.* 308, F450–F458. doi: 10.1152/ajprenal.00548.2014

Matsunaga, T., Yasuda, K., Adachi, T., Gu, N., Yamamura, T., Moritani, T., et al. (2007). Alpha-adrenoceptor gene variants and autonomic nervous system function in a young healthy Japanese population. *J. Hum. Genet.* 52:28. doi: 10.1007/s10038-006-0076-3

Mcdonough, A. A. (2010). Mechanisms of proximal tubule sodium transport regulation that link extracellular fluid volume and blood pressure. *Am. J. Physiol. Regul. Integr. Comp. Physiol.* 298, R851–R861. doi: 10.1152/ajpregu.00002.2010

Mcdonough, A. A., and Nguyen, M. T. (2015). Maintaining balance under pressure: integrated regulation of renal transporters during hypertension. *Hypertension* 66, 450–455. doi: 10.1161/HYPERTENSIONAHA.115.04593

Muntz, K. H., Meyer, L., Gadol, S., and Calianos, T. A. (1986). Alpha-2 adrenergic receptor localization in the rat heart and kidney using autoradiography and tritiated rauwolscine. *J. Pharmacol. Exp. Ther.* 236, 542–547.

Nguyen, M. T., Lee, D. H., Delpire, E., and Mcdonough, A. A. (2013). Differential regulation of Na+ transporters along nephron during ANG II-dependent hypertension: distal stimulation counteracted by proximal inhibition. *Am. J. Physiol. Renal Physiol.* 305, F510–F519. doi: 10.1152/ajprenal.00183.2013

Nord, E. P., Howard, M. J., Hafezi, A., Moradeshagi, P., Vaystub, S., and Insel, P. A. (1987). Alpha 2 adrenergic agonists stimulate Na+-H+ antiport activity in the rabbit renal proximal tubule. *J. Clin. Invest.* 80, 1755–1762. doi: 10.1172/JCI113268

Nunes, R. A., Barroso, L. P., Pereira Ada, C., Krieger, J. E., and Mansur, A. J. (2014). Gender-related associations of genetic polymorphisms of alpha-adrenergic receptors, endothelial nitric oxide synthase and bradykinin B2 receptor with treadmill exercise test responses. *Open Heart* 1:e000132. doi: 10.1136/openhrt-2014-000132

Oberhauser, V., Vonend, O., and Rump, L. C. (1999). Neuropeptide Y and ATP interact to control renovascular resistance in the rat. *J. Am. Soc. Nephrol.* 10, 1179–1185.

Penton, D., Moser, S., Wengi, A., Czogalla, J., Rosenbaek, L. L., Rigendinger, F., et al. (2019). Protein phosphatase 1 inhibitor-1 mediates the cAMP-dependent stimulation of the renal NaCl cotransporter. *J. Am. Soc. Nephrol.* 30, 737–750. doi: 10.1681/ASN.2018050540

Perry, H. M., Gorldt, N., Sung, S. J., Huang, L., Rudnicka, K. P., Encarnacion, I. M., et al. (2019). Perivascular $CD73^+$ cells attenuate inflammation and interstitial fibrosis in the kidney microenvironment. *Am. J. Physiol. Renal Physiol.* 317, F658–F669. doi: 10.1152/ajprenal.00243.2019

Philipp, M., Brede, M., and Hein, L. (2002). Physiological significance of alpha(2)-adrenergic receptor subtype diversity: one receptor is not enough. *Am. J. Physiol. Regul. Integr. Comp. Physiol.* 283, R287–R295. doi: 10.1152/ajpregu.00123.2002

Pontes, R. B., Crajoinas, R. O., Nishi, E. E., Oliveira-Sales, E. B., Girardi, A. C., Campos, R. R., et al. (2015). Renal nerve stimulation leads to the activation of the Na^+/H^+ exchanger isoform 3 via angiotensin II type I receptor. *Am. J. Physiol. Renal Physiol.* 308, F848–F856. doi: 10.1152/ajprenal.00515.2014

Poss, J., Ewen, S., Schmieder, R. E., Muhler, S., Vonend, O., Ott, C., et al. (2015). Effects of renal sympathetic denervation on urinary sodium excretion in patients with resistant hypertension. *Clin. Res. Cardiol.* 104, 672–678. doi: 10.1007/s00392-015-0832-5

Pyner, S. (2014). The paraventricular nucleus and heart failure. *Exp. Physiol.* 99, 332–339. doi: 10.1113/expphysiol.2013.072678

Roos, K. P., Bugaj, V., Mironova, E., Stockand, J. D., Ramkumar, N., Rees, S., et al. (2013). Adenylyl cyclase VI mediates vasopressin-stimulated ENaC activity. *J. Am. Soc. Nephrol.* 24, 218–227. doi: 10.1681/ASN.2012050449

Saha, M., Menuet, C., Sun, Q. J., Burke, P. G. R., Hildreth, C. M., Allen, A. M., et al. (2019). Respiratory sympathetic modulation is augmented in chronic kidney disease. *Respir. Physiol. Neurobiol.* 262, 57–66. doi: 10.1016/j.resp.2019.02.001

Sata, Y., Head, G. A., Denton, K., May, C. N., and Schlaich, M. P. (2018). Role of the sympathetic nervous system and its modulation in renal hypertension. *Front. Med.* 5:82. doi: 10.3389/fmed.2018.00082

Scanzano, A., and Cosentino, M. (2015). Adrenergic regulation of innate immunity: a review. *Front. Pharmacol.* 6:171. doi: 10.3389/fphar.2015.00171

Schlaich, M. P., Hering, D., Sobotka, P., Krum, H., Lambert, G. W., Lambert, E., et al. (2012). Effects of renal denervation on sympathetic activation, blood pressure, and glucose metabolism in patients with resistant hypertension. *Front. Physiol.* 3:10. doi: 10.3389/fphys.2012.00010

Schlaich, M. P., Sobotka, P. A., Krum, H., Lambert, E., and Esler, M. D. (2009). Renal sympathetic-nerve ablation for uncontrolled hypertension. *N. Engl. J. Med.* 361, 932–934. doi: 10.1056/NEJMc0904179

Small, K. M., Wagoner, L. E., Levin, A. M., Kardia, S. L., and Liggett, S. B. (2002). Synergistic polymorphisms of beta1- and alpha2C-adrenergic receptors and the risk of congestive heart failure. *N. Engl. J. Med.* 347, 1135–1142. doi: 10.1056/NEJMoa020803

Solini, A., Usuelli, V., and Fiorina, P. (2015). The dark side of extracellular ATP in kidney diseases. *J. Am. Soc. Nephrol.* 26, 1007–1016. doi: 10.1681/ASN.2014070721

Soukhova-O'hare, G. K., Roberts, A. M., and Gozal, D. (2006). Impaired control of renal sympathetic nerve activity following neonatal intermittent hypoxia in rats. *Neurosci. Lett.* 399, 181–185. doi: 10.1016/j.neulet.2006.01.054

Sparks, M. A., Stegbauer, J., Chen, D., Gomez, J. A., Griffiths, R. C., Azad, H. A., et al. (2015). Vascular type 1A angiotensin II receptors control BP by regulating renal blood flow and urinary sodium excretion. *J. Am. Soc. Nephrol.* 26, 2953–2962. doi: 10.1681/ASN.2014080816

Spengler, R. N., Chensue, S. W., Giacherio, D. A., Blenk, N., and Kunkel, S. L. (1994). Endogenous norepinephrine regulates tumor necrosis factor-alpha production from macrophages in vitro. *J. Immunol.* 152, 3024–3031.

Sriramula, S., Haque, M., Majid, D. S., and Francis, J. (2008). Involvement of tumor necrosis factor-alpha in angiotensin II-mediated effects on salt appetite, hypertension, and cardiac hypertrophy. *Hypertension* 51, 1345–1351. doi: 10.1161/HYPERTENSIONAHA.107.102152

Starke, K., Endo, T., and Taube, H. D. (1975). Pre- and postsynaptic components in effect of drugs with alpha adrenoceptor affinity. *Nature* 254, 440–441. doi: 10.1038/254440a0

Steinberg, J. S., Shabanov, V., Ponomarev, D., Losik, D., Ivanickiy, E., Kropotkin, E., et al. (2020). Effect of renal denervation and catheter ablation vs catheter ablation alone on atrial fibrillation recurrence among patients with paroxysmal atrial fibrillation and hypertension: the ERADICATE-AF randomized clinical trial. *JAMA* 323, 248–255. doi: 10.1001/jama.2019.21187

Sumi, Y., Woehrle, T., Chen, Y., Yao, Y., Li, A., and Junger, W. G. (2010). Adrenergic receptor activation involves ATP release and feedback through purinergic receptors. *Am. J. Physiol. Cell Physiol.* 299, C1118–C1126. doi: 10.1152/ajpcell.00122.2010

Thulin, T., and Erlinge, D. (1995). Neuropeptide Y and hypertension. *Nutrition* 11, 495–497.

Tomoda, F., Bergstrom, G., Evans, R. G., and Anderson, W. P. (1997). Evidence for decreased structurally determined preglomerular resistance in the young spontaneously hypertensive rat after 4 weeks of renal denervation. *J. Hypertens.* 15, 1187–1195. doi: 10.1097/00004872-199715100-00018

Trendelenburg, A. U., Klebroff, W., Hein, L., and Starke, K. (2001). A study of presynaptic alpha2-autoreceptors in alpha2A/D-, alpha2B- and alpha2C-adrenoceptor-deficient mice. *Naunyn Schmiedeberg's Arch. Pharmacol.* 364, 117–130. doi: 10.1007/s002100100423

Veelken, R., Vogel, E. M., Hilgers, K., Amann, K., Hartner, A., Sass, G., et al. (2008). Autonomic renal denervation ameliorates experimental glomerulonephritis. *J. Am. Soc. Nephrol.* 19, 1371–1378. doi: 10.1681/ASN.2007050552

Veiras, L. C., Mcfarlin, B. E., Ralph, D. L., Buncha, V., Prescott, J., Shirvani, B. S., et al. (2020). Electrolyte and transporter responses to angiotensin II induced hypertension in female and male rats and mice. *Acta Physiol.* 229:e13448. doi: 10.1111/apha.13448

von Wowern, F., Bengtsson, K., Lindblad, U., Rastam, L., and Melander, O. (2004). Functional variant in the (alpha)2B adrenoceptor gene, a positional candidate on chromosome 2, associates with hypertension. *Hypertension* 43, 592–597. doi: 10.1161/01.HYP.0000116224.51189.80

Vonend, O., Habbel, S., Stegbauer, J., Roth, J., Hein, L., and Rump, L. C. (2007). Alpha(2A)-adrenoceptors regulate sympathetic transmitter release in mice kidneys. *Br. J. Pharmacol.* 150, 121–127. doi: 10.1038/sj.bjp.0706961

Vonend, O., Marsalek, P., Russ, H., Wulkow, R., Oberhauser, V., and Rump, L. C. (2003). Moxonidine treatment of hypertensive patients with advanced renal failure. *J. Hypertens.* 21, 1709–1717. doi: 10.1097/00004872-200309000-00021

Vonend, O., Martin, O., Rump, L. C., Kroepil, P., and Stegbauer, J. (2018). Erythrocyte salt sedimentation assay does not predict response to renal denervation. *Front. Med.* 5:51. doi: 10.3389/fmed.2018.00051

Wang, Y., Hou, R., Li, P., Li, J., Yan, J., Yin, F., et al. (2004). Gene expression profiles in response to the activation of adrenoceptors in A7r5 aortic smooth muscle cells. *Clin. Exp. Pharmacol. Physiol.* 31, 602–607. doi: 10.1111/j.1440-1681.2004.04058.x

Wenzel, P., Knorr, M., Kossmann, S., Stratmann, J., Hausding, M., Schuhmacher, S., et al. (2011). Lysozyme M-positive monocytes mediate angiotensin II-induced arterial hypertension and vascular dysfunction. *Circulation* 124, 1370–1381. doi: 10.1161/CIRCULATIONAHA.111.034470

Wu, J., Saleh, M. A., Kirabo, A., Itani, H. A., Montaniel, K. R., Xiao, L., et al. (2016). Immune activation caused by vascular oxidation promotes fibrosis and hypertension. *J. Clin. Invest.* 126, 50–67. doi: 10.1172/JCI80761

Xiao, L., Do Carmo, L., Foss, J. D., Chen, W., and Harrison, D. G. (2020). Sympathetic enhancement of memory T cell homing and hypertension sensitization. *Circ. Res.* 126, 708–721. doi: 10.1161/CIRCRESAHA.119.314758

Xiao, L., Kirabo, A., Wu, J., Saleh, M. A., Zhu, L., Wang, F., et al. (2015). Renal denervation prevents immune cell activation and renal inflammation in angiotensin II-induced hypertension. *Circ. Res.* 117, 547–557. doi: 10.1161/CIRCRESAHA.115.306010

Ye, S., Zhong, H., Duong, V. N., and Campese, V. M. (2002a). Losartan reduces central and peripheral sympathetic nerve activity in a rat model of neurogenic hypertension. *Hypertension* 39, 1101–1106. doi: 10.1161/01.hyp.0000018590.26853.c7

Ye, S., Zhong, H., Yanamadala, V., and Campese, V. M. (2002b). Renal injury caused by intrarenal injection of phenol increases afferent and efferent renal sympathetic nerve activity. *Am. J. Hypertens.* 15, 717–724. doi: 10.1016/s0895-7061(02)02959-x

Zaldivia, M. T., Rivera, J., Hering, D., Marusic, P., Sata, Y., Lim, B., et al. (2017). Renal denervation reduces monocyte activation and monocyte-platelet aggregate formation: an anti-inflammatory effect relevant for cardiovascular risk. *Hypertension* 69, 323–331. doi: 10.1161/HYPERTENSIONAHA.116.08373

Zheng, H., Liu, X., Katsurada, K., and Patel, K. P. (2019). Renal denervation improves sodium excretion in rats with chronic heart failure: effects on expression of renal ENaC and AQP2. *Am. J. Physiol. Heart Circ. Physiol.* 317, H958–H968. doi: 10.1152/ajpheart.00299.2019

Zheng, H., and Patel, K. P. (2017). Integration of renal sensory afferents at the level of the paraventricular nucleus dictating sympathetic outflow. *Auton. Neurosci.* 204, 57–64. doi: 10.1016/j.autneu.2016.08.008

Conflict of Interest: The authors declare that the research was conducted in the absence of any commercial or financial relationships that could be construed as a potential conflict of interest.

Advantages of publishing in Frontiers

OPEN ACCESS
Articles are free to read for greatest visibility and readership

FAST PUBLICATION
Around 90 days from submission to decision

HIGH QUALITY PEER-REVIEW
Rigorous, collaborative, and constructive peer-review

TRANSPARENT PEER-REVIEW
Editors and reviewers acknowledged by name on published articles

Frontiers
Avenue du Tribunal-Fédéral 34
1005 Lausanne | Switzerland

Visit us: www.frontiersin.org
Contact us: frontiersin.org/about/contact

REPRODUCIBILITY OF RESEARCH
Support open data and methods to enhance research reproducibility

DIGITAL PUBLISHING
Articles designed for optimal readership across devices

FOLLOW US
@frontiersin

IMPACT METRICS
Advanced article metrics track visibility across digital media

EXTENSIVE PROMOTION
Marketing and promotion of impactful research

LOOP RESEARCH NETWORK
Our network increases your article's readership